SAN-20500-1(Vol.2)

CONCEPTUAL DESIGN OF ADVANCED CENTRAL RECEIVER POWER SYSTEMS

Volume 2. Final Technical Report

By
A. S. Brower
J. F. Doyle
E. E. Gerrels
A. C. Ku
B. D. Pomeroy
J. M. Roberts
R. M. Salemme

June 29, 1979

Work Performed Under Contract No. EM-78-C-03-1725

General Electric Company
Schenectady, New York

U.S. Department of Energy

Solar Energy

SAN-20500-1(Vol.2)
Distribution Category UC-62d

CONCEPTUAL DESIGN OF ADVANCED CENTRAL RECEIVER POWER SYSTEMS

Volume II

U.S. Department of Energy

Contract No. DE-AC03-78ET20500

Final Technical Report

June 29, 1979

GENERAL ELECTRIC

ACKNOWLEDGMENTS

This report has been prepared by General Electric Corporate Research and Development for the Department of Energy. The principal authors are:

A.S. Brower, GE
J.F. Doyle, Kaiser Engineers
E.E. Gerrels, GE
A.C. Ku, GE
B.D. Pomeroy, GE
J.M. Roberts, GE
R.M. Salemme, GE

B.D. Pomeroy was Technical Manager for this study, R.M. Salemme was Deputy Program Manager, and G.R. Fox was Program Manager.

Other General Electric components participating in this program were the Energy Systems Programs Department, the Advanced Reactor Systems Department, the Electric Utility Systems Engineering Department, and the Medium Steam Turbine Department. Kaiser Engineers, Foster Wheeler Development Corporation, and the University of Houston Energy Laboratory were subcontractors.

This report is based upon work performed by the authors and the following technical contributors:

J.C. Amos, GE
G. Carli, Foster Wheeler
D.H. Hall, GE
V. Kadambi, GE
F.V. Kahle, Kaiser Engineers
W.L. Kuhre, Kaiser Engineers
R.G. Livingston, GE
F.W. Lipps, Univ. of Houston
W.D. Marsh, GE
T.V. Narayanan, Foster Wheeler
J.J. Reilly, GE
C.N. Spalaris, GE
L.L. Vant Hull, Univ. of Houston
M.D. Walzel, Univ. of Houston

The authors would also like to thank the following people for their assistance and advice:

S.C. Bialy, GE
E. Brooks, GE
D.H. Brown, GE
K. Chen, GE
R.N. Clayton, GE
A.V. Curinga, GE
K.J. Daniel, GE
J.A. Elsner, GE
F.N. Mazandarany, GE
G. Oganowski, GE
F. Tippets, GE

TABLE OF CONTENTS

Volume I, Part 1

TABLE OF CONTENTS (Cont'd)

TABLE OF CONTENTS (Cont'd)

Volume II

TABLE OF CONTENTS (Cont'd)

Volume III

TABLE OF CONTENTS (Cont'd)

Volume IV

TABLE OF CONTENTS (Cont'd)

Volume V

TABLE OF CONTENTS (Cont'd)

LIST OF ILLUSTRATIONS

Volume II

LIST OF ILLUSTRATIONS (Cont'd)

LIST OF ILLUSTRATIONS (Cont'd)

LIST OF TABLES

Volume II

LIST OF TABLES (Cont'd)

Section 5

CONCEPTUAL DESIGN OF COMMERCIAL PLANT

5.1 INTRODUCTION

The plant configuration selected as a result of the parametric analysis was analyzed in more detail to provide better estimates of performance and cost. Cost estimation was performed in Task 5; the methodology and results are reported in Section 6. The plant description and performance estimate given in this section are the final output of Task 4, the conceptual design analysis.

The analysis procedure used by the General Electric team is shown in Figure 5.1-1. The first step was to establish the steam cycle heat balance; this provided information needed to design the steam generators and set the thermal power required at the tower base (solar multiple = 1.5).

The right hand path in Figure 5.1-1 shows this information being used to design the heliostat field. Field optimization also required data on cost and performance for the receiver subsystem, so that costs for alternative field arrangements can be evaluated with respect to increments in receiver cost due to changing tower height or receiver size. Ideally, the receiver model used should be the final result of Tasks 4 and 5; however, this information was not available at the time the field design was performed, so the Task 2 model was used.

Field optimization generated the flux plot required to design the absorber. An iteration is involved here since the loss estimates changed somewhat from Task 2 to Task 4. The procedure was to calculate losses on the basis of the given flux plot, then to scale (trim) this flux plot to achieve the incident power required to close the energy balance. The heliostat field was also trimmed to account for these changes.

Storage design was carried out in parallel with the field optimization. The steam generator analysis provided the data required to establish the volume of tankage and pump sizes required.

When the field optimization and storage design were completed, the plant layout and analysis of equipment in the balance of plant was begun. This work was performed by Kaiser Engineers and involved equipment arrangement considerations and specifications for the conventional plant equipment such as feedwater heaters and cooling towers.

Finally, the master control subsystem was designed to integrate the other subsystem control strategies. This involved some iteration on subsystem control concepts, especially in the area of receiver flow control.

These analyses are described in the sections which follow.

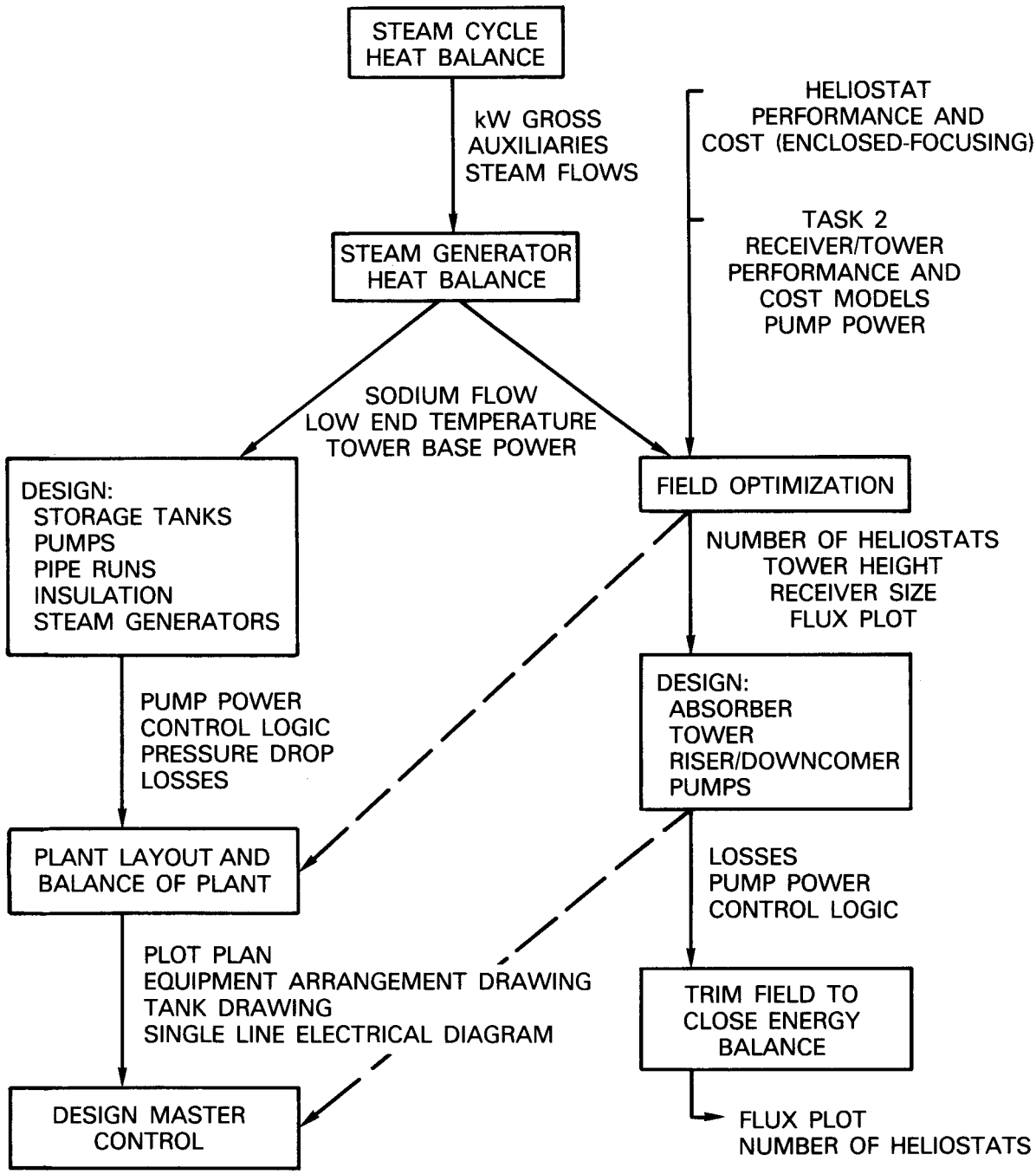

Figure 5.1-1. Task 4 Analysis - Logic Flow

5.2 COLLECTOR SUBSYSTEM

Based on the results of the Task 2 study, the concept of the GE focusing, enclosed heliostat in a 360° field was chosen for the conceptual design. Field design input data used, including heliostat specifications and receiver cost and performance models, are the same as those used in the Task 2 study (see Section 3.2.1). The results of the field design are presented in this section.

An optimized field/receiver which delivers 372 MW_t net power at the design point (summer solstice noon, 950 watts/m^2) was designed. A sketch of this field is shown in Figure 5.2-1. Packing density for each computational cell, defined as the ratio of reflective surface area to land area, is indicated in the figure.

In computing the flux impinging on the receiver, the heliostats were aimed at points on the midline (half-height) of the cylindrical receiver at 45° intervals, i.e., at points in the north, northeast, east, southeast, south, southwest, west, and northwest directions on the midline of the cylinder. This resulted in flux peaks at these locations. The computed circumferential variation of flux at the midline of the receiver is illustrated in Figure 5.2-2(a). If the heliostats had been aimed at points on the receiver midline which have the shortest distances from the individual heliostats, as would be done in a real plant, the receiver flux variation would have been smooth. A least squares curve fit was done on the uneven computed receiver flux distribution to arrive at the smoothed distribution used in the receiver design, shown as dashed lines in Figure 5.2-2(a). Axial variations of flux on the north and the south panels, for both the computed and the smoothed versions, are shown in Figure 5.2-2(b). The smoothed version was selected to have symmetry both about the receiver north/south centerline and the midline even though the original flux plot is slightly asymetrical. Tabulated values of the smoothed version of the receiver flux used in the receiver design are given in Figure 5.2-3.

The field efficiency is defined as

$$\text{field efficiency} = \frac{\text{power impinging on receiver}}{\text{total reflector surface area} \times \text{normal solar flux}}$$

The variation of field efficiency with time for the summer and winter solstices and the equinox are shown in Figure 5.2-4.

Table 5.2-1 summarizes the annual performance of the collector subsystem and also describes the University of Houston's sun model used in estimating the annual energy incident on the receiver. Note that this sun model does not match the design point insolation of 950 watt/m^2 at summer solstice noon, and therefore the incident power of 437.354 MW_t does not coincide with the design value of 414.14 MW_t.

TOWER HEIGHT = 190 m

RECEIVER SIZE = 16 m (H) x 16 m (D)

NUMBER OF HELIOSTATS = 20415

LAND AREA = 5.64 km^2

ANNUAL POWER IMPINGING ON RECEIVER = 1.3334 E6 MW_tH

SUMMER SOLSTICE NOON NET POWER = 372 MW_t

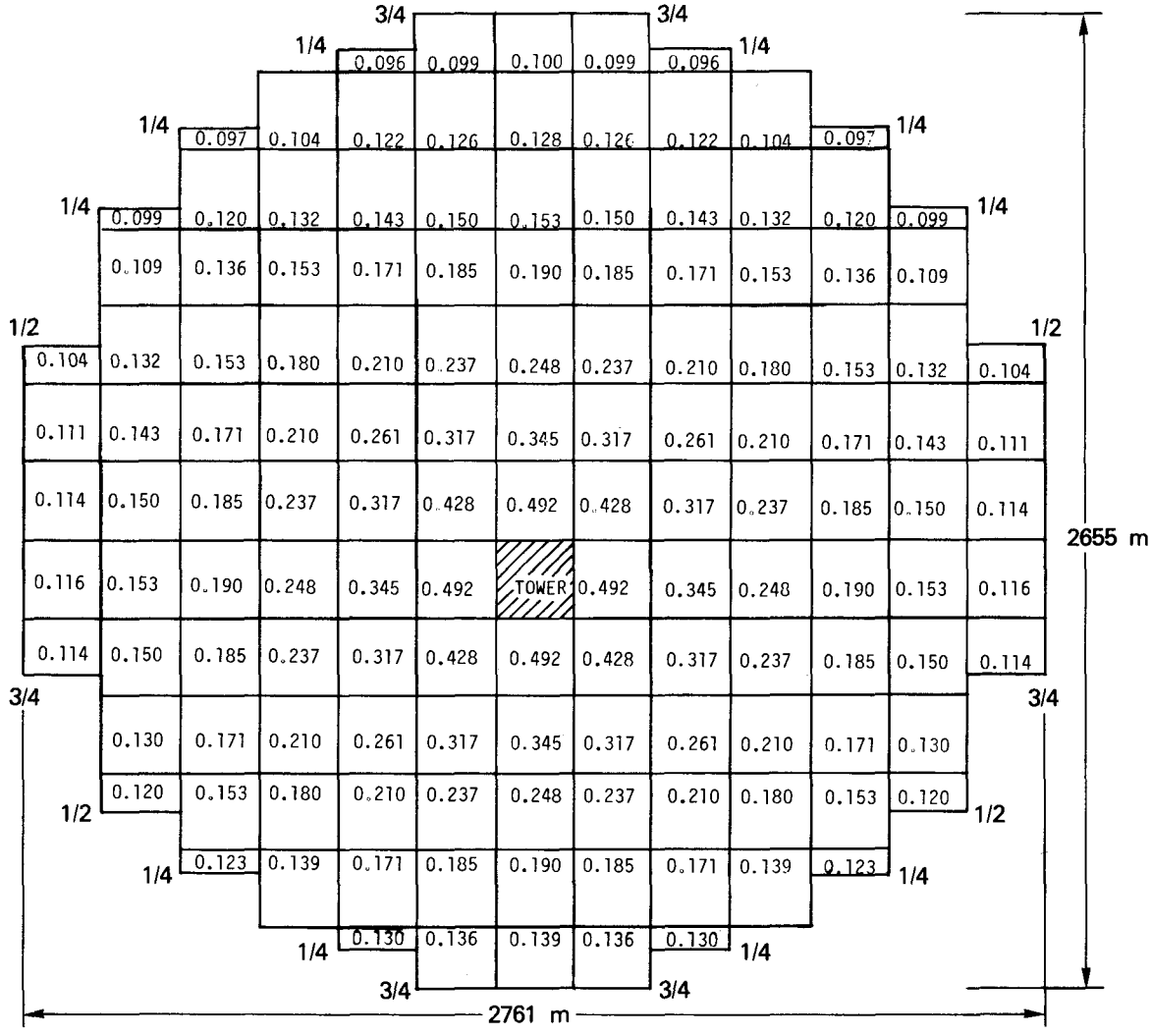

NOTE:
NUMBERS IN CELLS INDICATE HELIOSTAT PACKING DENSITIES.
CELL SIZE: 212.43 m SQUARE, EXCEPT WHERE NOTED WITH A FRACTION, e.g., 1/2 = 212.43 x 106.22

Figure 5.2-1. Heliostat Field Sketch

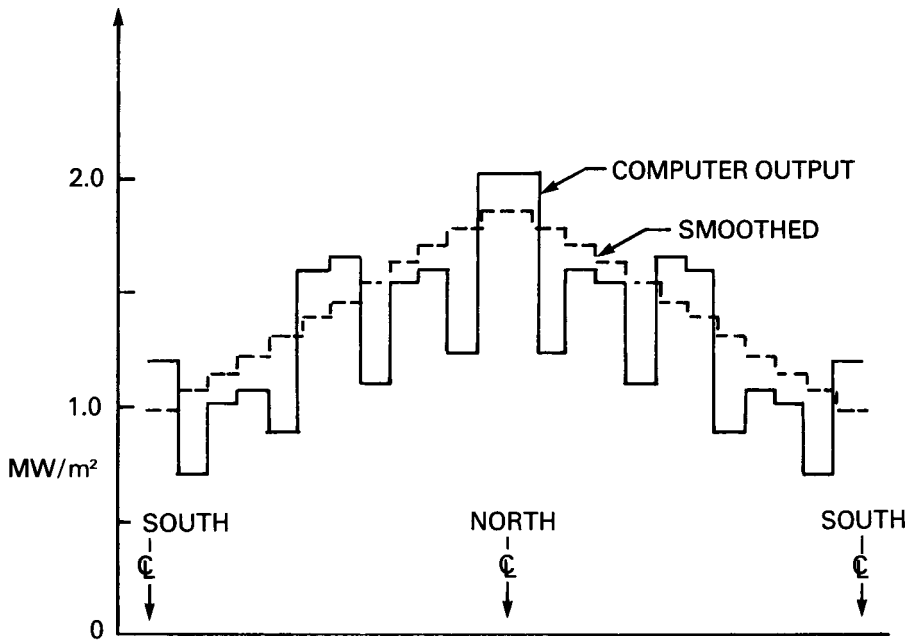

(a) CIRCUMFERENTIAL VARIATION OF FLUX AT RECEIVER MIDLINE

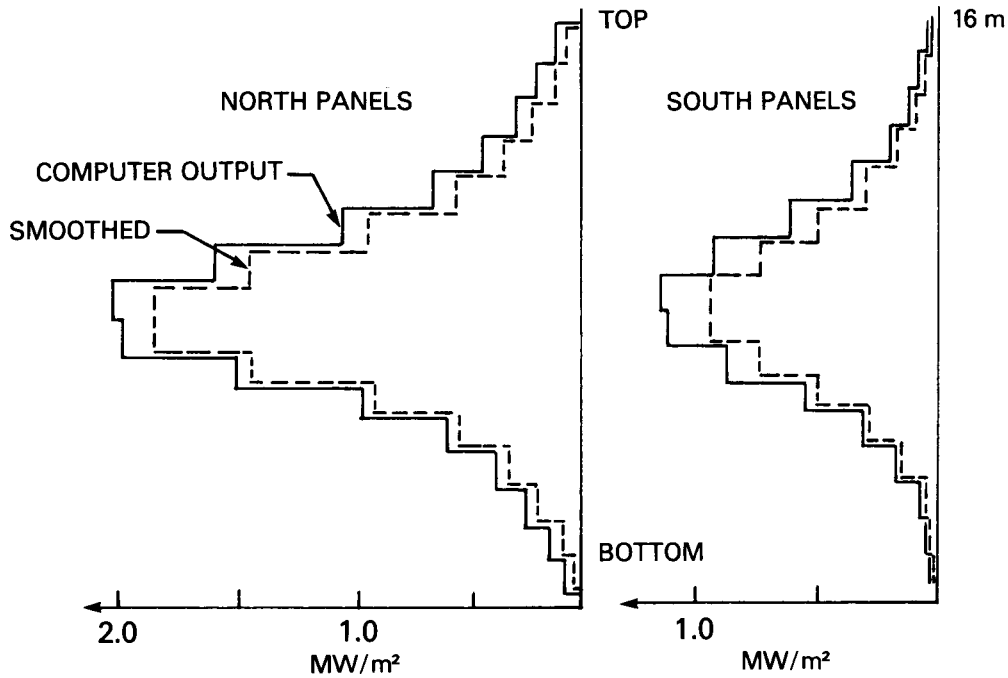

(b) AXIAL VARIATION OF FLUX

Figure 5.2-2. Receiver Flux Variations at Summer Solstice Noon

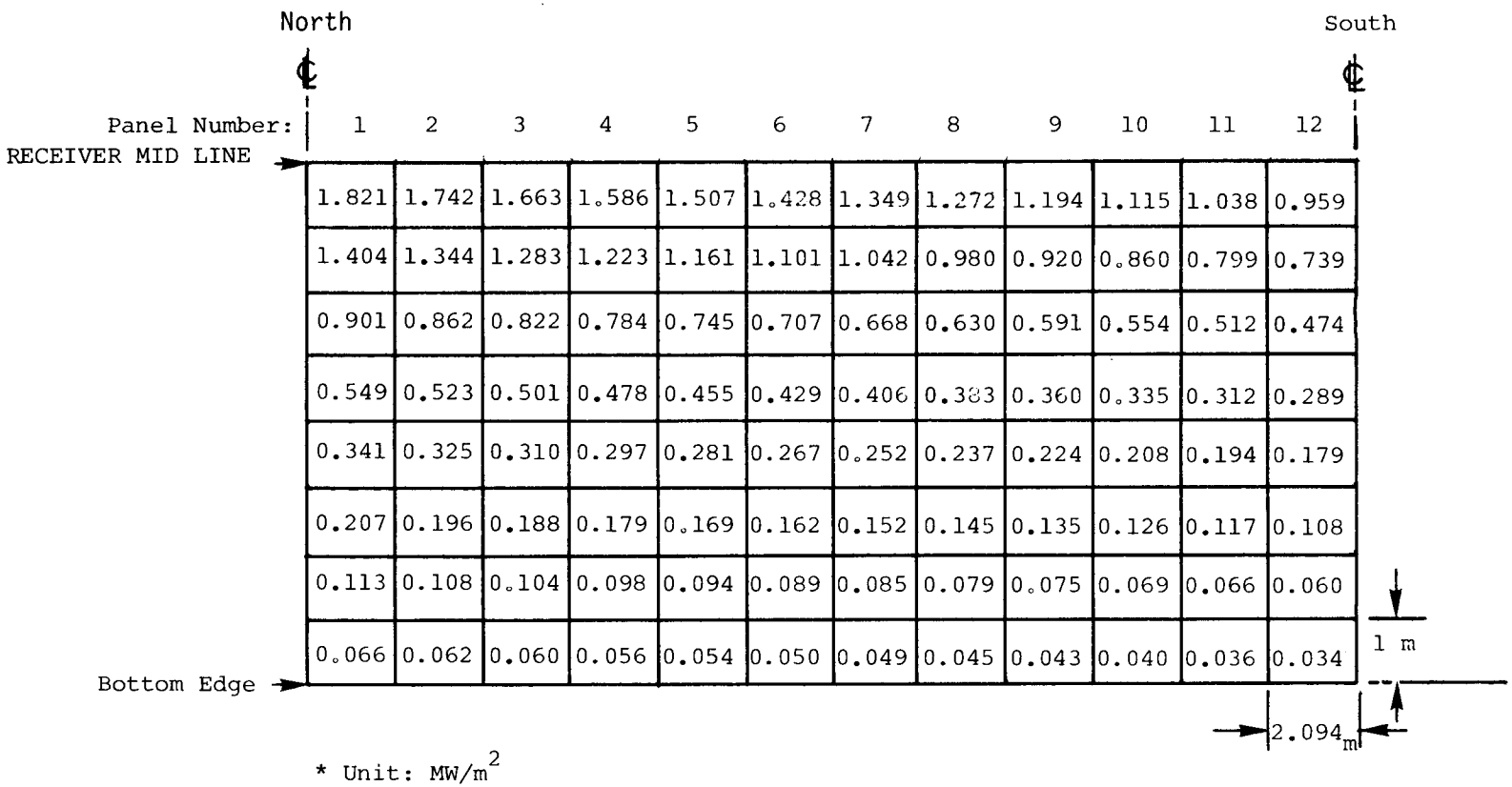

* Unit: MW/m^2

Figure 5.2-3. Design Point Incident Flux on Lower Quadrant of Receiver, Smoothed by Least Square Fit. (This plot is for the summer solstice at noon and a normal solar flux of 950 W/m^2. Total incident thermal power is 414.14 MW_t.)

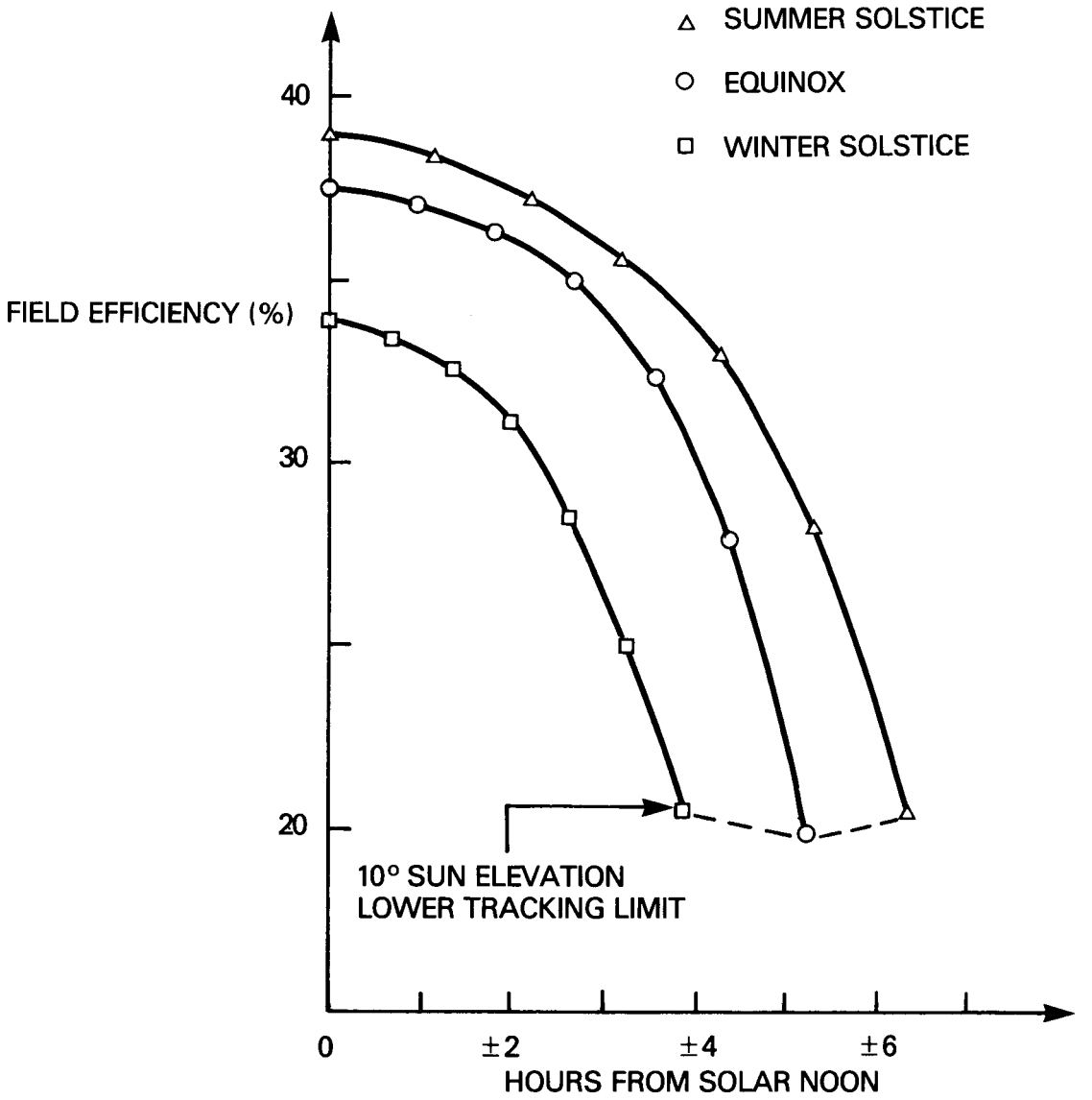

Figure 5.2-4. Field Efficiency Variations

Table 5.2-1

ANNUAL PERFORMANCE SUMMARY

Days From Vernal Equinox	Hours From Noon	Elevation Degrees	Azimuth Degrees	Normal Insolation Watts/m^2	Thermal Power Incident on Receiver MW_t	Field Efficiency
92	0	78.44	0	1003.24	437.354	0.3883
	1.05	72.12	-53.93	999.42	429.882	0.3831
	2.09	60.43	-75.52	987.27	411.488	0.3712
	3.14	47.73	-87.23	964.26	385.620	0.3562
	4.18	34.89	-95.95	924.22	342.027	0.3296
	5.23	22.24	-103.79	850.29	267.528	0.2802
	6.28	10.	-111.69	673.39	152.629	0.2019
122	0	75.25	0	1002.11	434.965	0.3866
	1.02	70.01	-46.45	998.32	427.907	0.3818
	2.04	59.31	-69.40	986.26	410.664	0.3709
	3.06	47.15	-82.33	963.43	384.893	0.3558
	4.08	34.63	-91.71	923.69	342.951	0.3307
	5.10	22.17	-99.84	850.21	268.296	0.2811
	6.12	10.	-107.79	673.77	152.884	0.2021
152	0	66.79	0	1003.90	429.343	0.3809
	0.96	63.39	-32.74	1000.15	423.928	0.3775
	1.91	55.17	-55.27	988.21	408.466	0.3682
	2.87	44.73	-69.96	965.59	384.244	0.3544
	3.82	33.39	-80.63	926.25	341.770	0.3287
	4.78	21.70	-89.41	853.56	267.607	0.2793
	5.73	10.	-97.45	679.57	149.366	0.1958
182	0	55.25	0	1002.88	419.325	0.3724
	0.87	53.20	-22.04	999.13	414.526	0.3695
	1.73	47.64	-40.55	987.21	401.078	0.3619
	2.60	39.75	-54.88	964.70	377.510	0.3486
	3.46	30.48	-66.05	925.73	334.648	0.3220
	4.33	20.45	-75.21	854.52	266.435	0.2777
	5.20	10.	-83.22	689.57	153.139	0.1978
212	0	43.65	0	993.61	403.155	0.3614
	0.77	42.38	-15.37	989.84	398.467	0.3586
	1.54	38.77	-29.48	977.91	384.402	0.3501
	2.30	33.27	-41.69	955.52	358.380	0.3341
	3.07	26.38	-52.01	917.22	317.344	0.3082
	3.84	18.52	-60.80	848.97	257.030	0.2697
	4.61	10.	-68.45	701.44	166.011	0.2108
242	0	35.01	0	977.87	379.363	0.3456
	0.68	34.16	-11.62	974.12	373.518	0.3415
	1.36	31.69	-22.68	962.30	359.477	0.3327
	2.04	27.79	-32.78	940.30	336.130	0.3184
	2.72	22.71	-41.80	903.28	296.228	0.2921
	3.41	16.71	-49.76	839.44	240.860	0.2556
	4.09	10.	-56.82	712.10	165.819	0.2074
272	0	31.57	0	970.34	366.685	0.3366
	0.64	30.86	-10.29	966.62	360.146	0.3319
	1.28	28.79	-20.17	954.91	347.353	0.3240
	1.92	25.49	-29.37	933.22	324.529	0.3097
	2.56	21.13	-37.72	897.05	287.793	0.2858
	3.21	15.91	-45.23	835.81	235.523	0.2489
	3.85	10.	-51.95	718.69	164.320	0.2037

Total Annual Incident Energy: 1.3334E6 $MW_t h$

5.3 RECEIVER SUBSYSTEM

5.3.1 ABSORBER

Figure 5.3.1 is an overall description of the sodium-cooled absorber concept. The active absorber surface is 16 meters in diameter by 16 meters in height, and is comprised of 24 separate panels.

The panels are of a three header design. Cold sodium is pumped into the center header and flows in both directions toward the outlet headers at either end. This design has the advantage of reducing tube wall temperatures in the high flux region which improves resistance of the tubes to thermal stress damage and reduces receiver losses. A brief summary of the panel design data is given in Table 5.3-1.

Each panel has an electromagnetic (EM) pump to control sodium flow in response to incident flux variations. The pumps are located inside the absorber as shown in Figure 5.3-1 and are connected to an air duct which provides cooling air for the stator windings. About 15 percent of the electrical input to these pumps is carried off by the cooling air and discharged through an air vent in the roof of the absorber. As discussed in Section 4, "Selection of Preferred Plant Concept," the EM pumps are an expensive flow control device with respect to control valves, but the pumps are more reliable than valves. It is anticipated that the increased cost will be justified by the lower incidence of outages.

Cold sodium enters the absorber through a riser and inlet header, as shown in Figure 5.3-1. Hot sodium is collected in two outlet headers which connect to the downcomer. All headers and piping connections have been designed to be self-draining to avoid blockage by frozen sodium after a system dump. In addition, all piping is designed to minimize trapping of gas bubbles during filling with sodium. Since it is not possible to eliminate all bubbles in this way, the system will also be partially evacuated during filling.

A cylindrical insulating curtain covers the absorber panels when there is no solar input to reduce thermal cycling damage and heat losses. At sunrise, this curtain is rolled back to the position shown in Figure 5.3-1.

The receiver subsystem flow control is described in detail in Section 5.6. The basic control concept is illustrated in Figure 5.3-2; it consists of the EM pumps and controls on the downcomer throttle valve. If solar input to the panels increases, the outlet sodium temperature (T_E) would start to rise and the EM pumps would increase flow to bring T_E back to its setpoint (nominally 1100 F). Increasing flow through the panels would unbalance the pressure differential (DP), causing the throttle valve to open and increase flow in the riser/downcomer until DP is returned to its setpoint valve (DP = 0 psi). This arrangement was selected to give the EM pumps the greatest possible leverage on controlling panel flows by eliminating variations in the differential pressure at the top of the riser/downcomer. From the view of the EM pumps, the DP points should look as though they are connected to two equal pressure tanks full of sodium. From the view of the main receiver pump and throttle valve, the riser and downcomer should look as though they are directly joined at DP with no absorber in the loop.

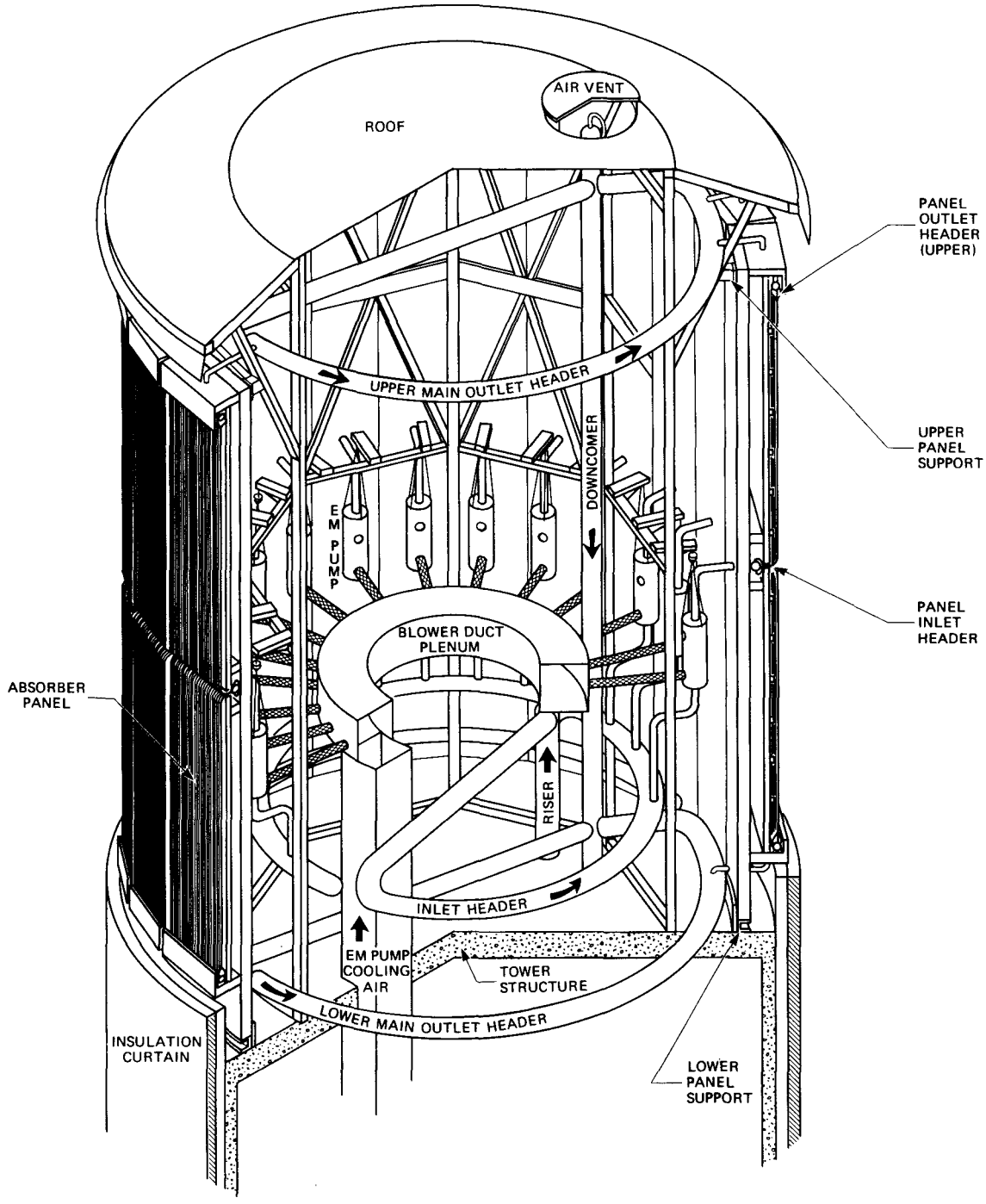

Figure 5.3-1. Sodium-Cooled Absorber

Table 5.3-1

ADVANCED CENTRAL RECEIVER
ABSORBER PANEL DESIGN DATA

TUBE OUTSIDE DIAM. (inches)	0.750
TUBE WALL THICKNESS (inches)	0.050
ACTIVE TUBE LENGTH (ft)	52.50
TOTAL TUBE LENGTH (ft)	56.50
NUMBER OF TUBES/PANEL	108.0
PANEL WIDTH (ft)	6.872
PANEL LENGTH (ft)	58.50
NUMBER OF PANELS	24
INLET HEADER - O.D. (in)	16
INLET HEADER - WALL THICKNESS (in)	0.312
OUTLET HEADERS - O.D. (in)	12
OUTLET HEADERS - WALL THICKNESS (in)	0.250
SODIUM TEMP. - PANEL INLET (°F)	613
SODIUM TEMP. - PANEL OUTLET* (°F)	1100
PEAK HEAT FLUX - (MW/m^2)	1.821
AVERAGE HEAT FLUX - (MW/m^2)	.515
DESIGN PRESSURE - PSIG	120

*Sodium flow to each panel is controlled to meet outlet temperature specified

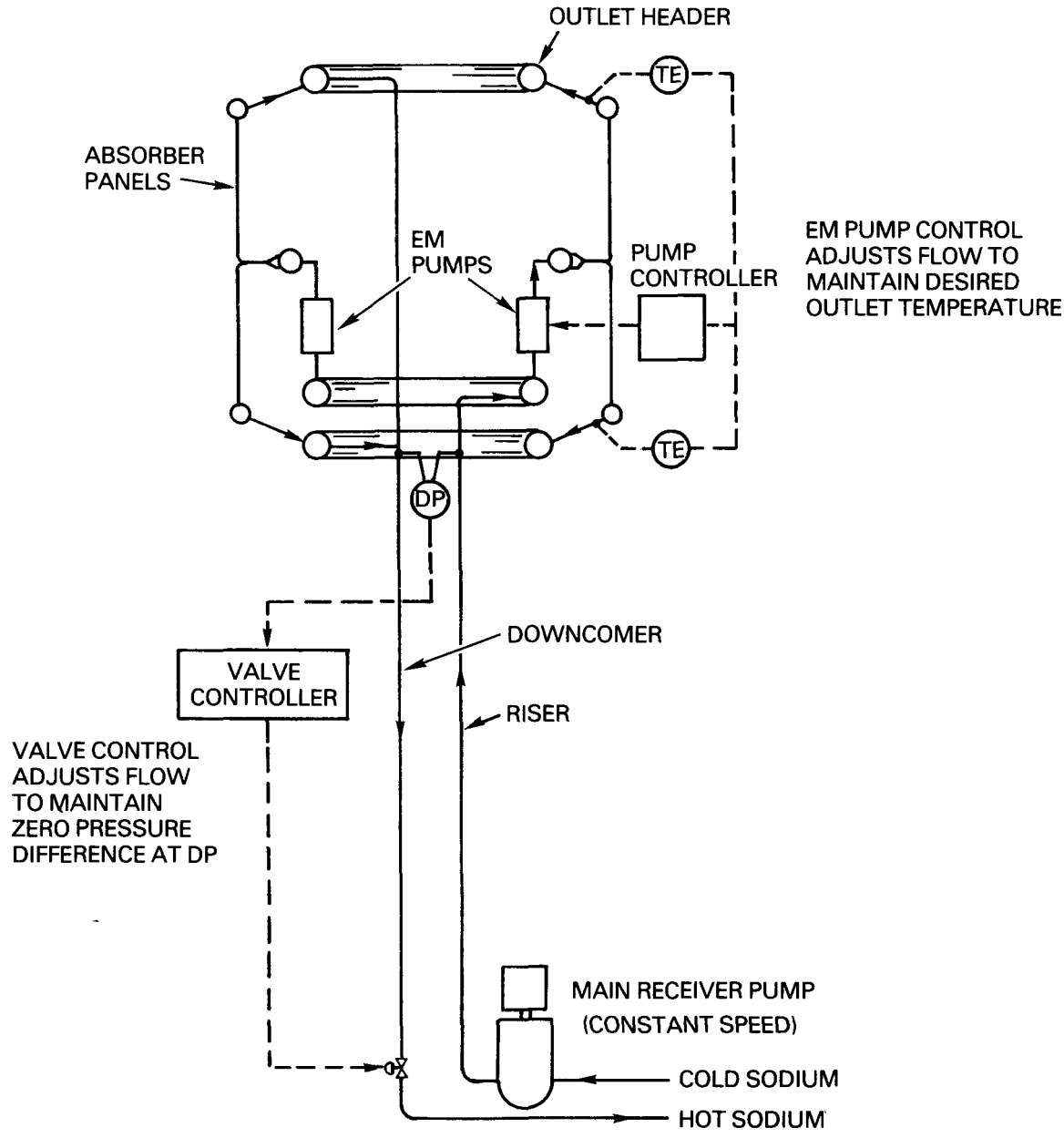

Figure 5.3-2. Receiver Flow Control

The following sections describe details of the absorber panel design, fabrication, installation and maintenance.

Absorber Panel Concept

Each of the 24 identical panels consists of two tube bundles, one inlet and two outlet headers, a support structure, and insulation.

The tube bundles contain 108 tubes fabricated of high strength Incoloy 800H seamless tubing. Each tube is 0.75 inch (OD) by 0.65 inch (ID). The top and bottom tube bundles are identical except for the tube bends connecting the tube bundles to the inlet header. The surfaces of the tubes that are exposed to solar radiation are coated with Pyromark black paint to provide high solar absorptivity for the absorber panels. Fiberfrax thermal insulation is attached to the back of the tube bundles by heat-resistant studs welded to transverse strips that are brazed to the back of the tube bundle.

All three headers are made of Incoloy 800H. As shown in Figure 5.3-3, the inlet header is located near the middle of the panel behind the Fiberfrax insulation. Thus it is protected from the high solar fluxes. To ensure complete draining of the tube bends, the centerline of this header is located 2.67 feet below the middle of the absorber panel. The inlet header is supported at three locations; the middle support is welded to the header so that the header can expand or contract sideways. Because the length of the inlet header is less than the width of the tube bundle, at least eight tubes at each side of the tube bundle will have to be bent in and doubled over.

The two outlet headers are located at each end of the absorber panel, one at the top and one at the bottom of the panel. These headers are protected by a radiation shield coated with Pyromark 2500 white paint (see Figure 5.3-3).

Along with providing support to the panel assembly for shipment, handling, and installation, the panel support structure also provides an interface with the main receiver structure and allowances for thermal expansion. Details of this structure are shown in Figure 5.3-3. It consists of a strong-back or main support structure made of two 12-inch by 3-inch channels and a secondary structure of three 4-inch I-beams fixed to the strongback.

As shown in Section E-E of Figure 5.3-3, the tube bundles are supported at the middle by a clamp arrangement to minimize flux leakage and are allowed to grow freely downward, upward, and sideways during thermal expansion and contraction.

The mountings for thermal expansion are shown in Figures 5.3-4, 5.3-5, and 5.3-6. At several axial locations along the panel, there are transverse strips brazed to the back of the tubes. Small clips are welded to these transverse strips. The clips permit lateral expansion of the panel by sliding along a T-shaped beam. Because the center clip is welded to the beam to hold the panel at the center, the panel expands from the center outward in both directions.

The center-roller mountings provide lateral support to the panel while the two side-roller mountings hold the panel close to the support structure. The outlet headers are supported by similar thermal-expansion mountings, as shown in Figure 5.3-6.

It should be noted that these provisions for thermal expansion are only intended to be an example of one possible technique. The subject of expansion accommodation deserves considerably more thought than was possible in the present study.

A typical mounting arrangement for installation of the panels is shown in Figure 5.3-7. The headers and strong-back have been designed to fit into the cylindrical receiver geometry, and half-cylinder reflective shields have been placed behind the gaps between panels to prevent flux leakage. As with the thermal expansion equipment, these shields were selected for costing purposes and deserve further consideration in Phase II.

The panel tube size of 0.75-inch OD was selected by running a hot panel analysis with variable tube sizes. (Tube walls were chosen to be 0.050-inch thick, based on welding and corrosion considerations.) The results of this analysis are summarized in Table 5.3-2, showing maximum wall temperature and friction pressure loss for a series of tube sizes from 0.500-inch to 0.875-inch OD. Since the small EM pumps used with these panels have low efficiency (about 25 percent), it is desirable to minimize the pressure loss; however, high tube temperature reduces tube resistance to creep and fatigue damage. A tube 0.75-inch in diameter was selected as a good compromise.

Preliminary estimates of tube wall temperatures indicate several advantages for the three header panel concept.

Figure 5.3-8 shows temperature profiles for sodium and the tube wall in the hot and cold panels at full-rated power. The two extremes in temperature are therefore represented on this plot. Note that by bringing the cold sodium into the middle of the panel, the temperatures are kept low in the region of the peak heat flux. As a result, the peak metal temperatures are only a few degrees higher than the outlet sodium temperature. This has obvious advantages from the viewpoint of materials strength, and also helps reduce receiver losses. Since the temperature profiles for the hot and cold panels are similar, it is expected that changes in overall flux level can be accommodated easily so long as the flux distribution is unchanged.

Figure 5.3-9 illustrates the way fairly large flow maldistributions between panels or panel halves can be accommodated. In most heat exchange equipment, a reduction in flow reduces heat transfer performance and divergence occurs between coolant and metal temperatures. This is not true of the absorber however. Figure 5.3-9 shows a convergence such that large flow reductions are required before the metal temperatures rise appreciably. This is directly related to the three header design because, as flow is reduced, the maximum temperature points tend to be more toward the center of the panel. Since this moves them closer to the lowest fluid temperature, the peak metal temperature rises more slowly than in a two header panel.

At the full solar power condition the panels on the side of the cylindrical receiver are subjected to large flux gradients across the width of the panel. The tube at the north edge of the panel runs hot and the tube at the south

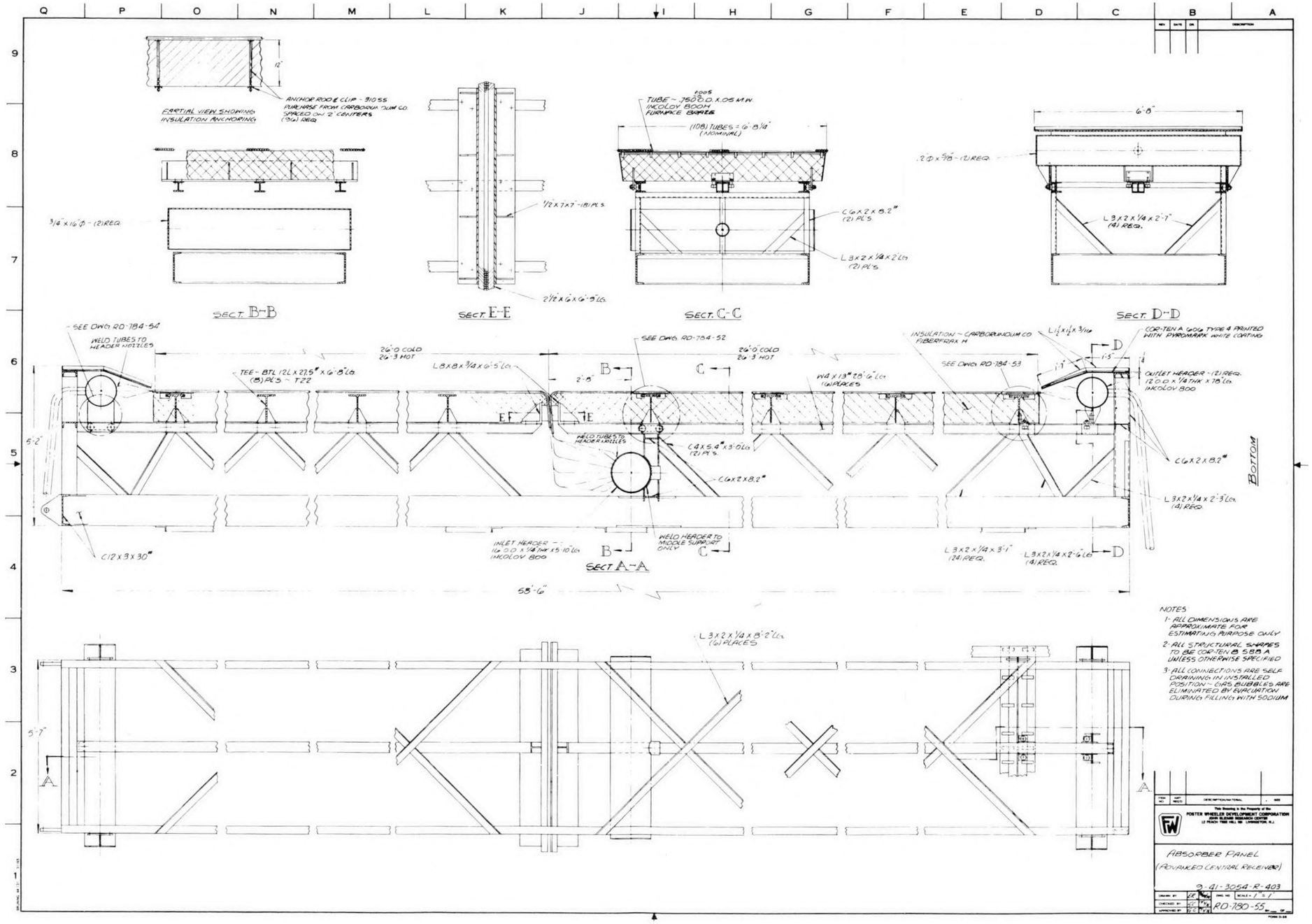

Figure 5.3-3. Absorber Panel

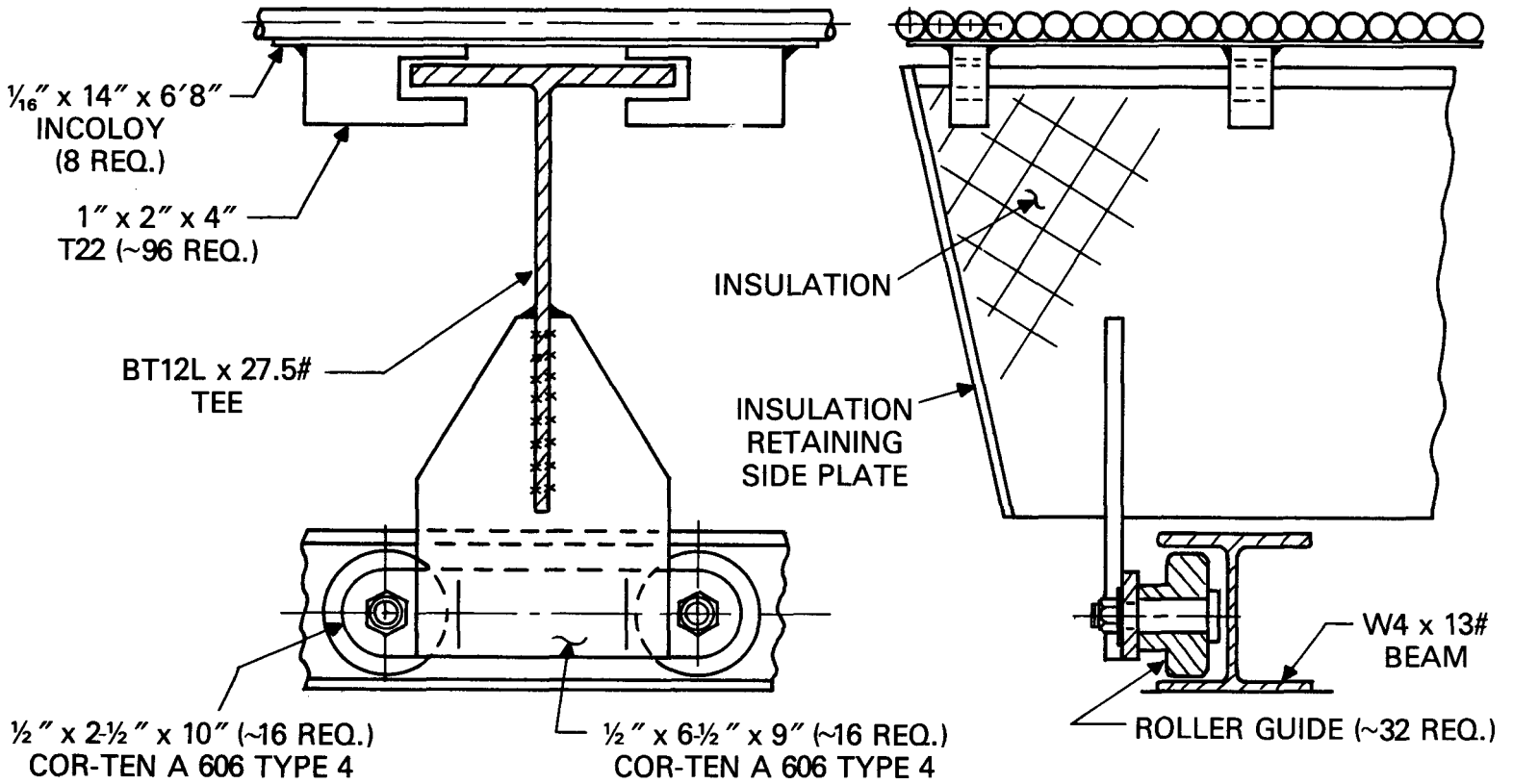

NOTES:
ALL DIMENSIONS APPROXIMATE;
FOR ESTIMATING ONLY

Figure 5.3-4. Panel Expansion Mounting (Sides)

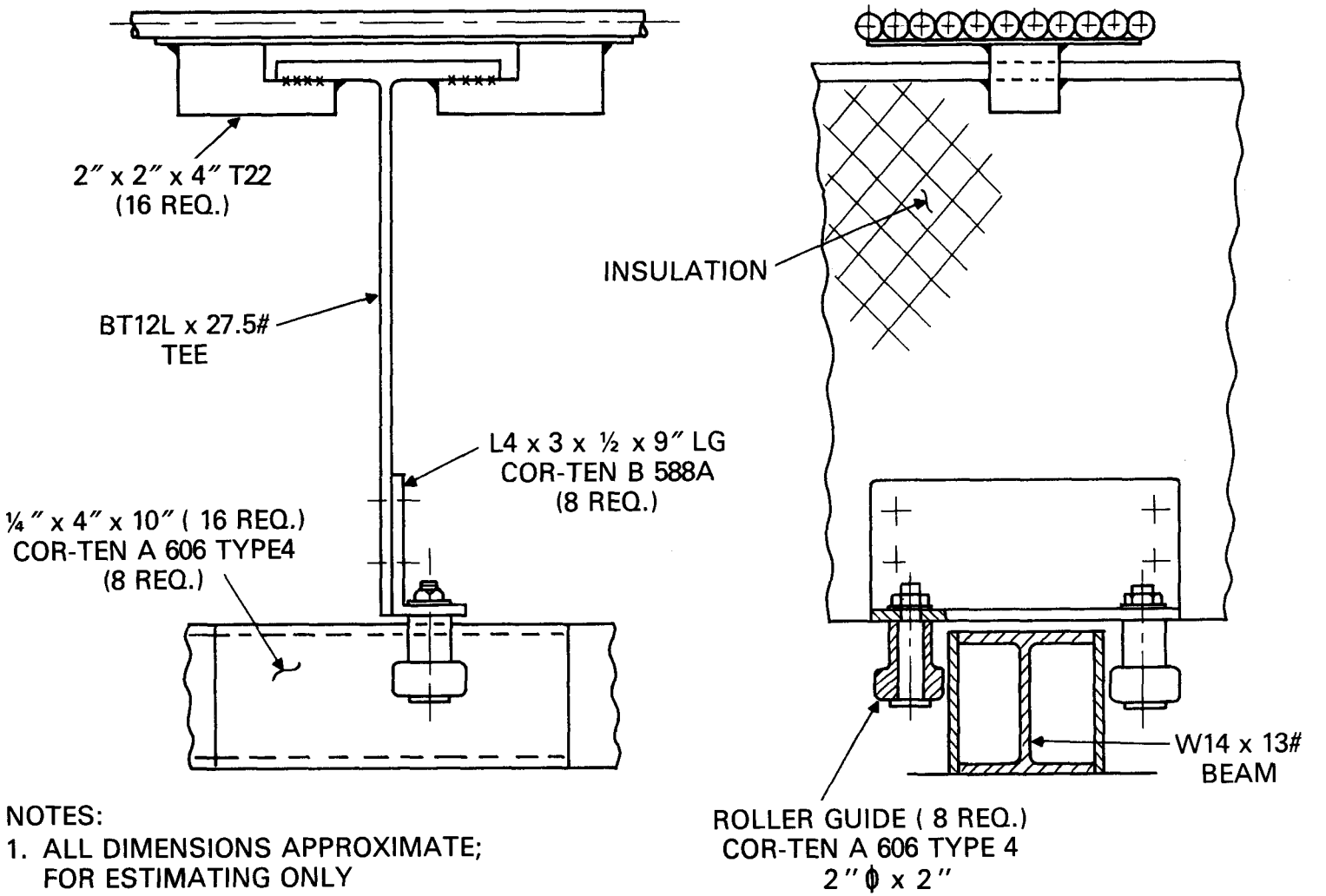

Figure 5.3-5. Panel Expansion Mounting (Middle)

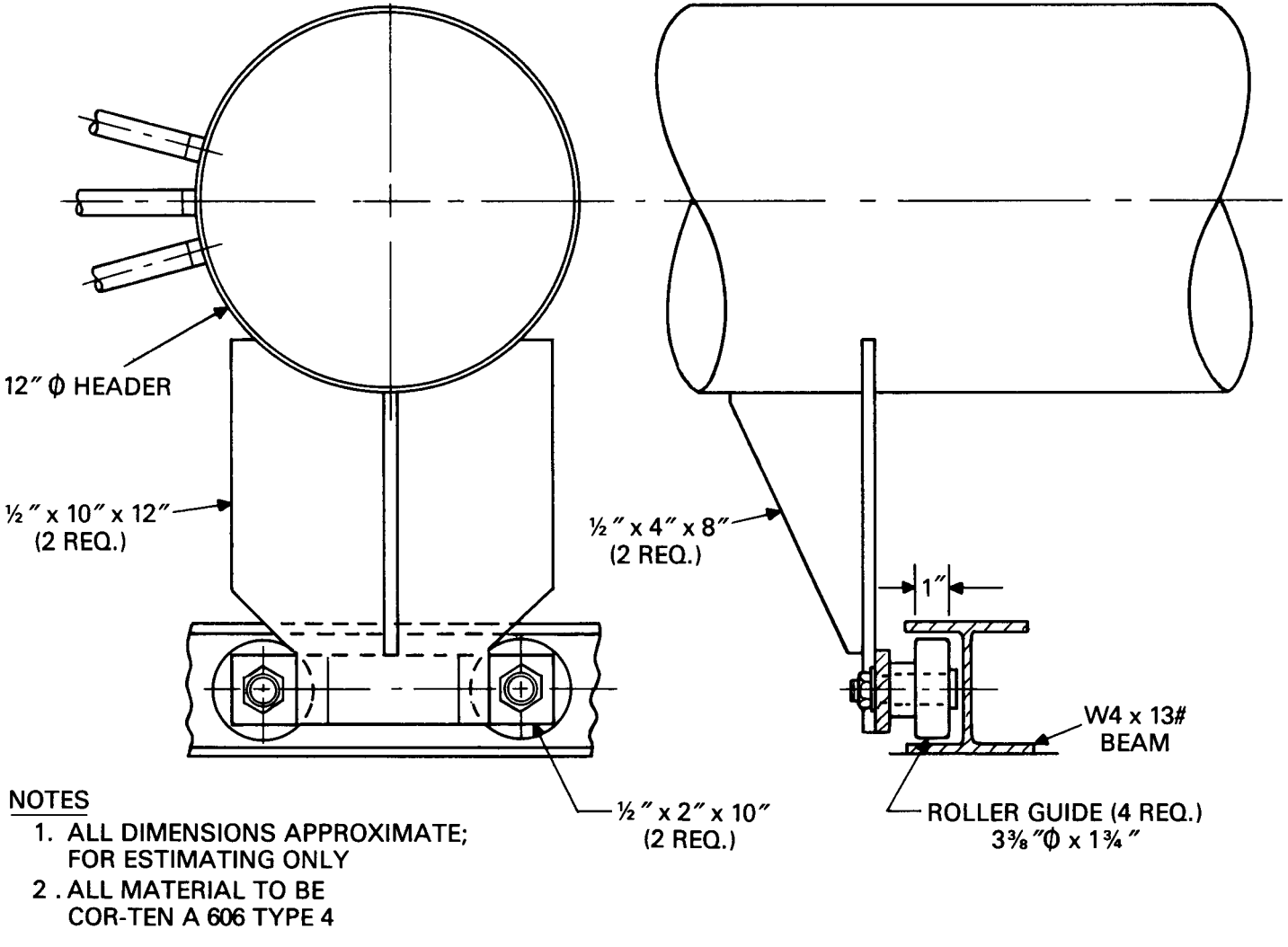

Figure 5.3-6. Outlet Header Expansion Mounting

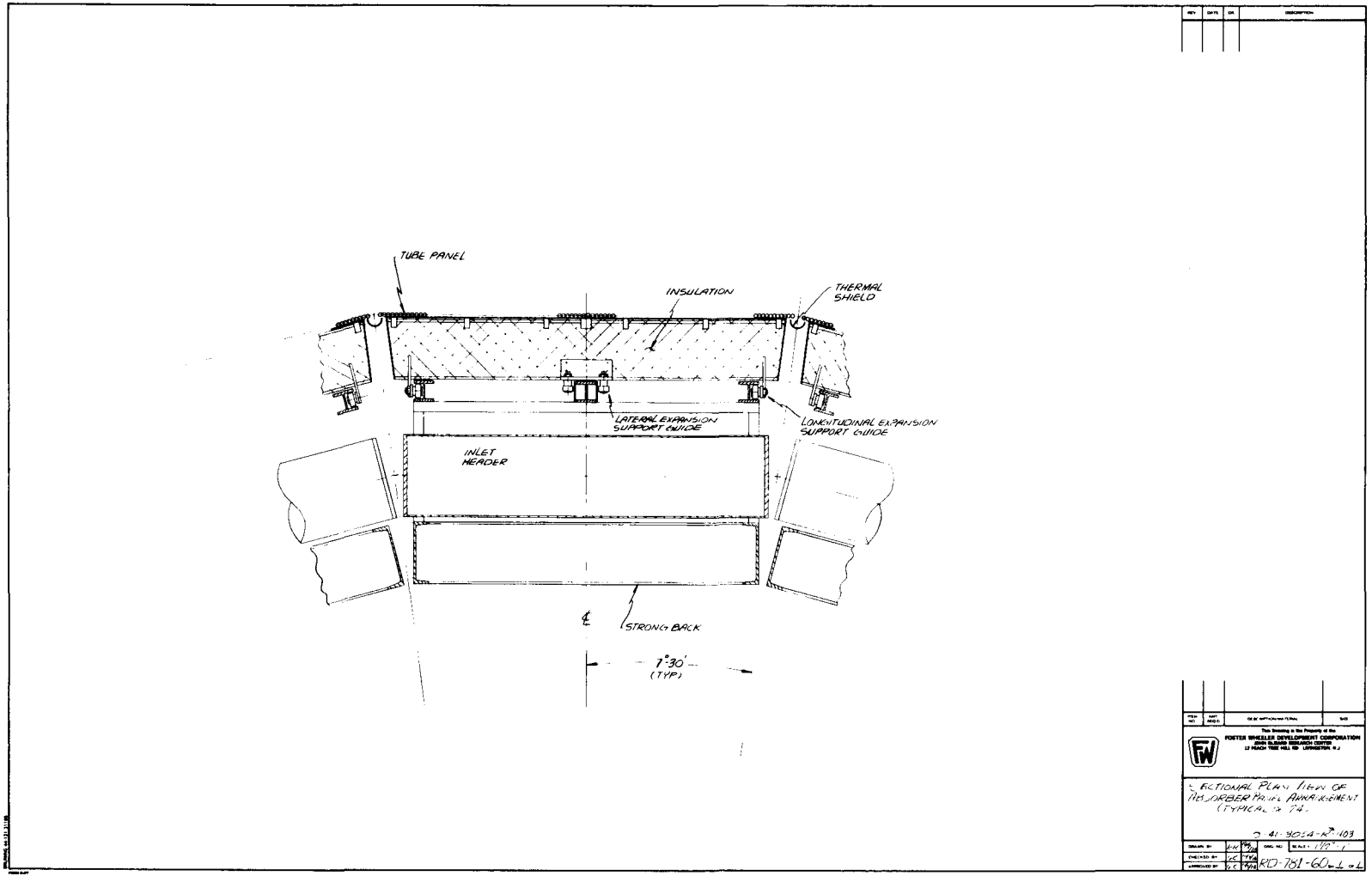

Figure 5.3-7. Sectional Plan View of Absorber Panel Arrangement

Table 5.3-2

HOT ABSORBER PANEL STUDY

TUBE O.D. (inches)	TUBE WALL (inches)	TMAX* WALL (°F)	ΔP FRICTION PSI	
0.875	.050	1160.0	0.65	
0.750	"	1143.4	1.18	← DESIGN SELECTION
0.625	"	1136.4	2.43	
0.5625	"	1132.9	3.73	
0.500	"	1129.9	6.13	

*These temperatures are based on preliminary calculations and may not agree precisely with the final temperatures presented in Section 5.3.2

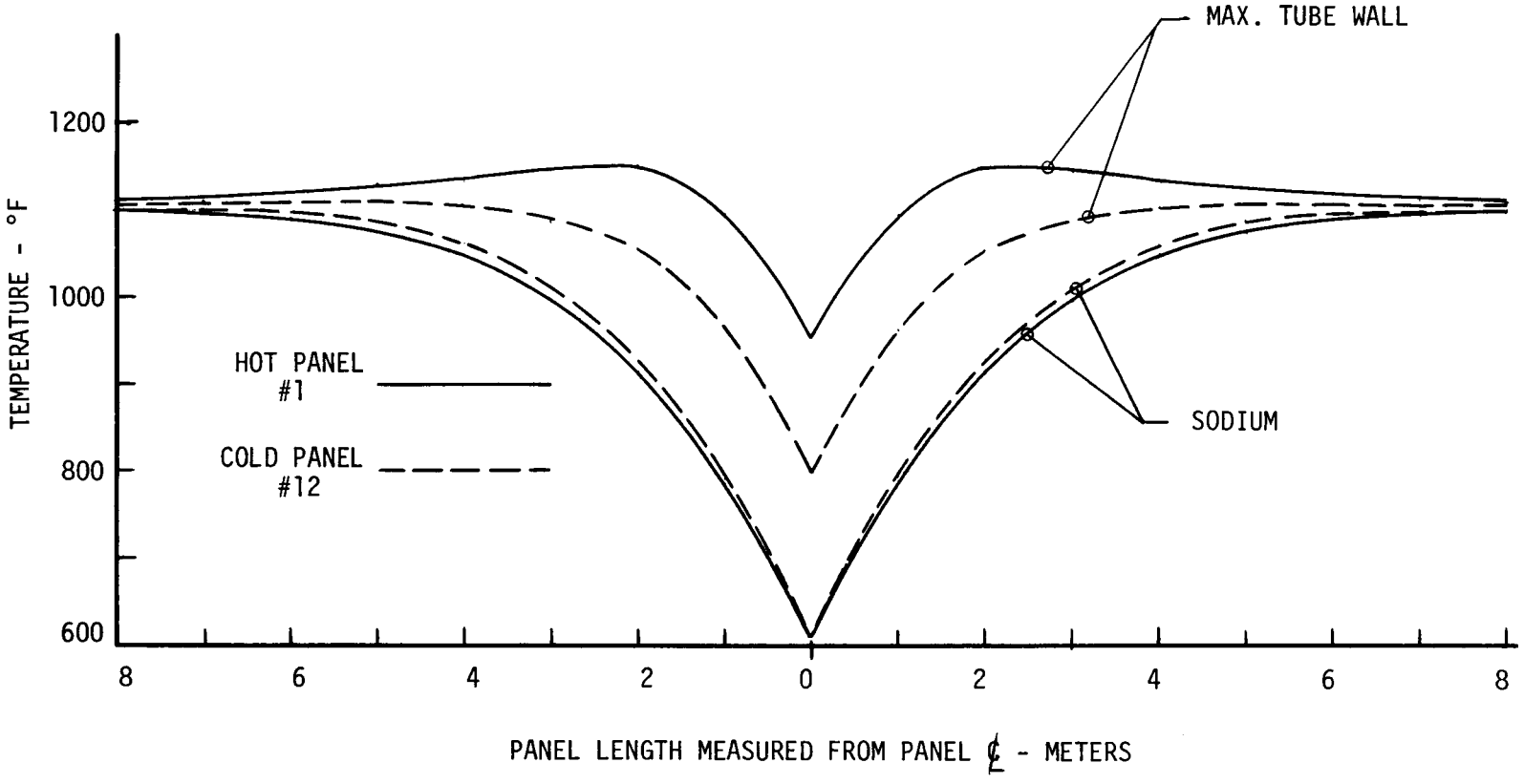

Figure 5.3-8. Absorber Panel Temperature Distribution

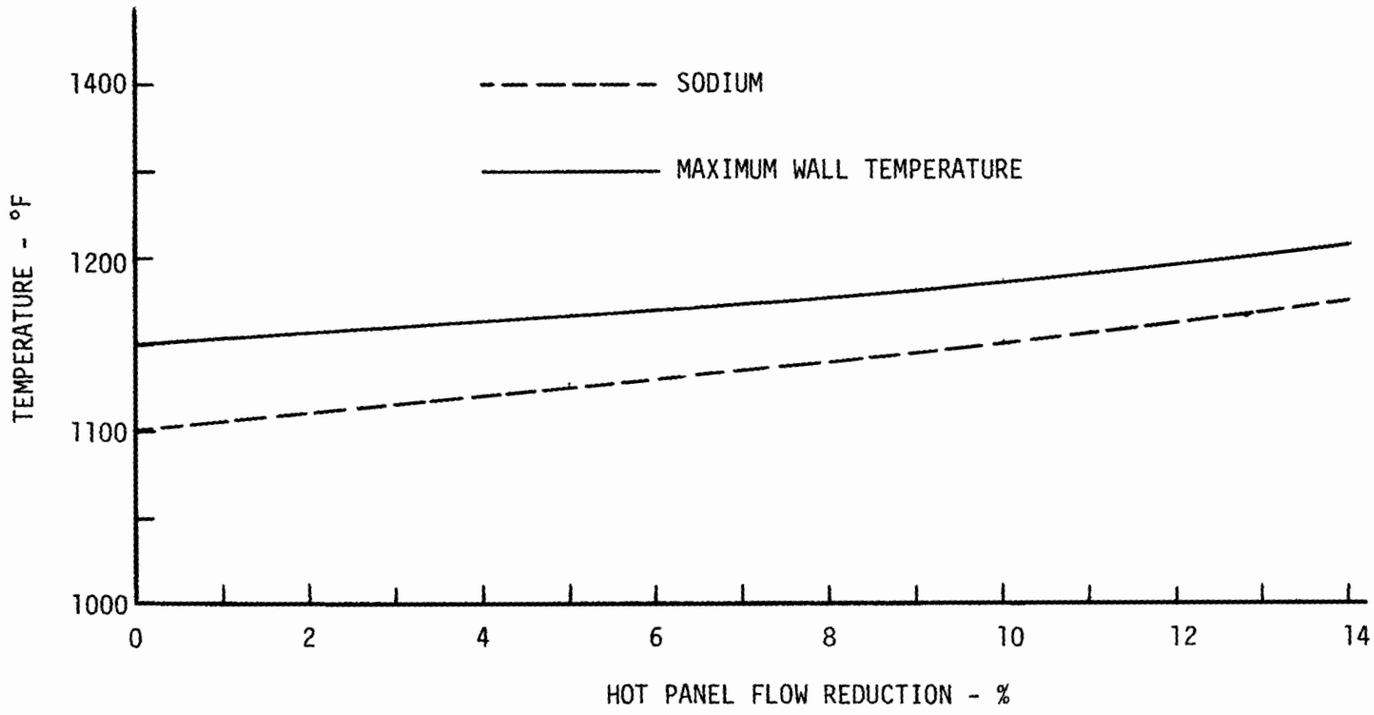

Figure 5.3-9. Hot Panel Flow Sensitivity Study

edge of the panel runs cold. The effect of this flux gradient is shown in Figure 5.3-10. Again the three header design limits the spread in operating temperatures between the two edge tubes to reasonable values.

Using three headers instead of two also reduces thermal expansion movement at the ends of the panels. Figure 5.3-11 illustrates how the panel expansions are accommodated in the receiver piping system without imposing large stresses between the piping and the panels at the connecting interface. The upper and lower receiver outlet headers are allowed to expand vertically from a piping anchor placed in the connecting line (see Figure 5.3-11). The panels are anchored at the center header to the supporting strong-back in the panel assembly. The two panel outlet headers are also allowed to expand vertically. The vertical expansions in the absorber panels are thus matched by similar vertical expansions in the receiver piping, which reduces stresses at the interfaces.

The three header concept has some disadvantages with respect to panel flow control. These disadvantages are:

- A shift in the flux distribution (eccentricity) may cause instability in the flow control which operates on a fluid outlet temperature set-point. It may be necessary to trim the flux distribution through the field controller to prevent this.
- There tends to be more flow in the lower half of the panel than in the upper half because of gravity heads. This will require a variable orifice on the lower outlet nozzle to equalize flow.
- There is the possibility of hot fluid streaming upward (backflow) at low loads because the lower half panel flow opposes natural convection.

Preliminary calculations (Appendix M) indicate that these concerns do not negate the three header concept, but they will require careful design to avoid operating problems.

Absorptive Coatings

Pyromark* high temperature black paint has been specified as the absorptive coating for this conceptual design, based on successful experience with this material in Subsystem Research Experiments for the first generation water/steam receivers (Ref. 5.3-9). These tests seem to indicate that absorptivities of 95 percent can be maintained under severe environmental conditions.

This selection leaves room for improvement, however. The reflection and radiation losses represent a significant penalty in additional heliostat costs.

A brief survey of alternative coatings was made to see if any new technology has become available within the last two years which might be an improvement over Pyromark paint.

One possibility is plasma-sprayed ceramic powders, consisting of oxides of chromium, cobalt, nickel, or titanium. Metco (Westbury, New York) is able to produce intensely black coatings on almost any metal substrate (including

*Trademark of Tempil Division, Big Three Industries Inc., South Plainfield, New Jersey.

Incoloy 800H) by this technique. Since these coatings are formed of many small particles in a rough surface the total absorptivity is potentially better than that of Pyromark paint. It is possible that this surface would also have a lower emissivity since ceramics typically range from 0.5 to 0.9 at 1000 F. One problem with these coatings is their low thermal conductivity. Chrome oxide conductivity is 1.0 Btu/hr/ft/^{o}F at 1000 ^{o}F. A 0.002 inch layer of chrome oxide would support a temperature rise of about 100 F at a flux of 2 MW/m^2. This adds to tube wall temperature rise and increases absorber losses. Another potential problem is the difference in expansion coefficients between the coating and substrate material. Metco has agreed to supply General Electric with samples of these coatings for evaluation.

Selective coatings, based on semiconductor behavior in layered structures, appear to be still in an early stage of development (Ref. 5.3-10). At low temperatures, these materials work quite well, but at higher temperatures (1000 F) the semiconducting behavior is more difficult to attain, and environmental durability may be a problem. These films typically have poorer absorptivities in the visible range than Pyromark paint, which makes them less desirable at high concentrations.

An intriguing absorptive surface concept was disclosed last year in a Government-owned patent (Ref. 5.3-11). The surface is prepared by etching away the metallic substrate to form a very fine-grained roughness which greatly enhances absorption. Test results quoted in the disclosure indicate that absorptivities as high as 98 percent were measured on specimens prepared on molybdenum and nickel substrates. The process is claimed to be applicable to "nickel, iron, molybdenum, titanium, zirconium, copper...and their alloys." The nickel sample also displayed low thermal emission characteristics (ε= 0.10 for wavelengths greater than 2 μm). This selective surface has the advantage of being integral with the substrate material, thus eliminating thermal expansion mismatch and the temperature rise associated with ceramic coatings. Of the candidate coatings investigated, this surface seems to offer the best hope of improving receiver performance beyond that available with Pyromark paint.

Panel Stress Analysis

To ensure the structural integrity and cyclic life of the receiver panels, thermal and elastic stress analyses of the tubes were performed. Since time did not permit full analysis of the absorber, only the highest temperature segment (1150 F) of the absorber was examined. Preliminary calculations indicated that this occurred at a local flux of 1.614 MW/m^2 on the two most northerly panels. The analytical model, the computer program, evaluation criteria, and results of the stress analysis are described below.

Analytical Model. The receiver tube is assumed to be a long, thick, cylindrical shell. The ends of the tube are welded to headers which are supported in such a way that axial expansion of the tube is allowed. Hence in the thermal stress analysis, a generalized plane strain model is assumed. The heat flux is assumed to have a cosine distribution (i.e., $q = q_o \cos \theta$) on the sun side of the tube, and the rear side is assumed to be insulated. Because of symmetry, only half a tube is considered. This half is divided into 114 nodes as shown in Figure 5.3-12.

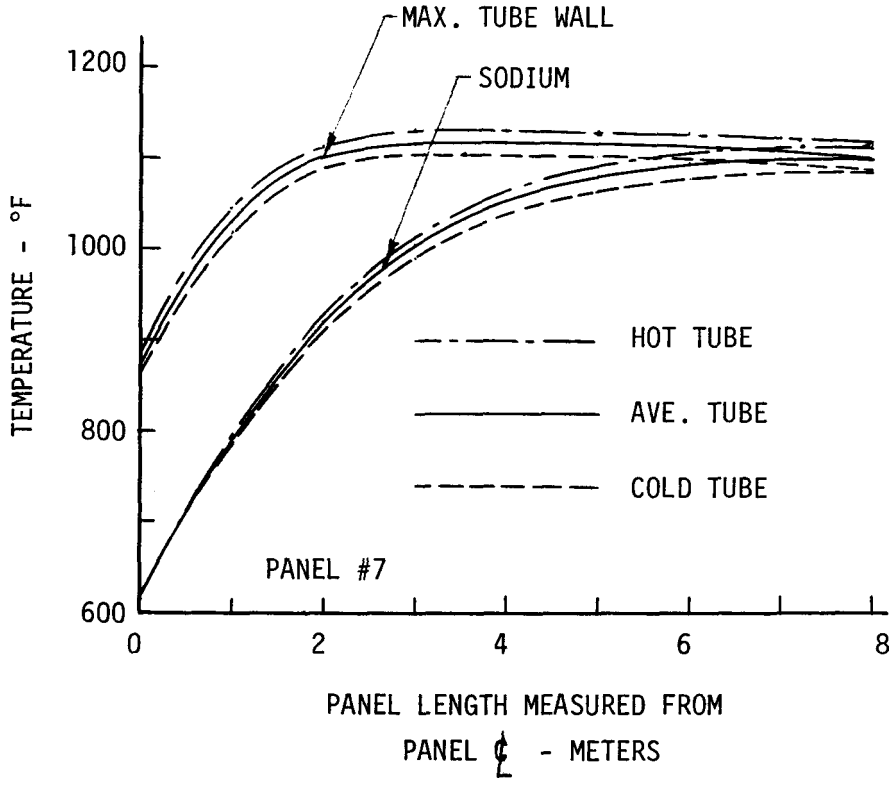

Figure 5.3-10. Temperature Distribution in the Absorber Panel with Maximum Flux Maldistribution

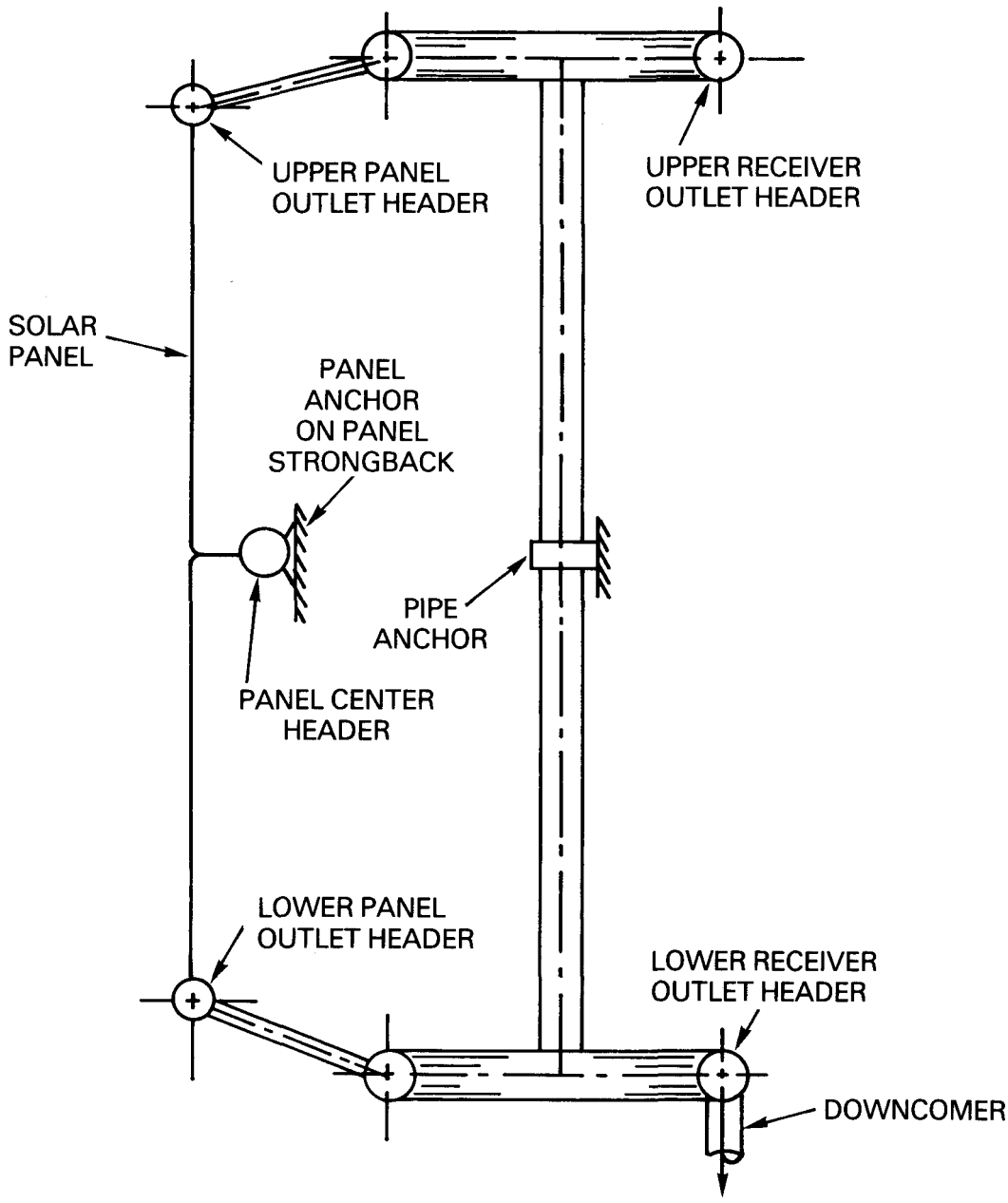

Figure 5.3-11. Absorber Panels-Provision for Thermal Expansion

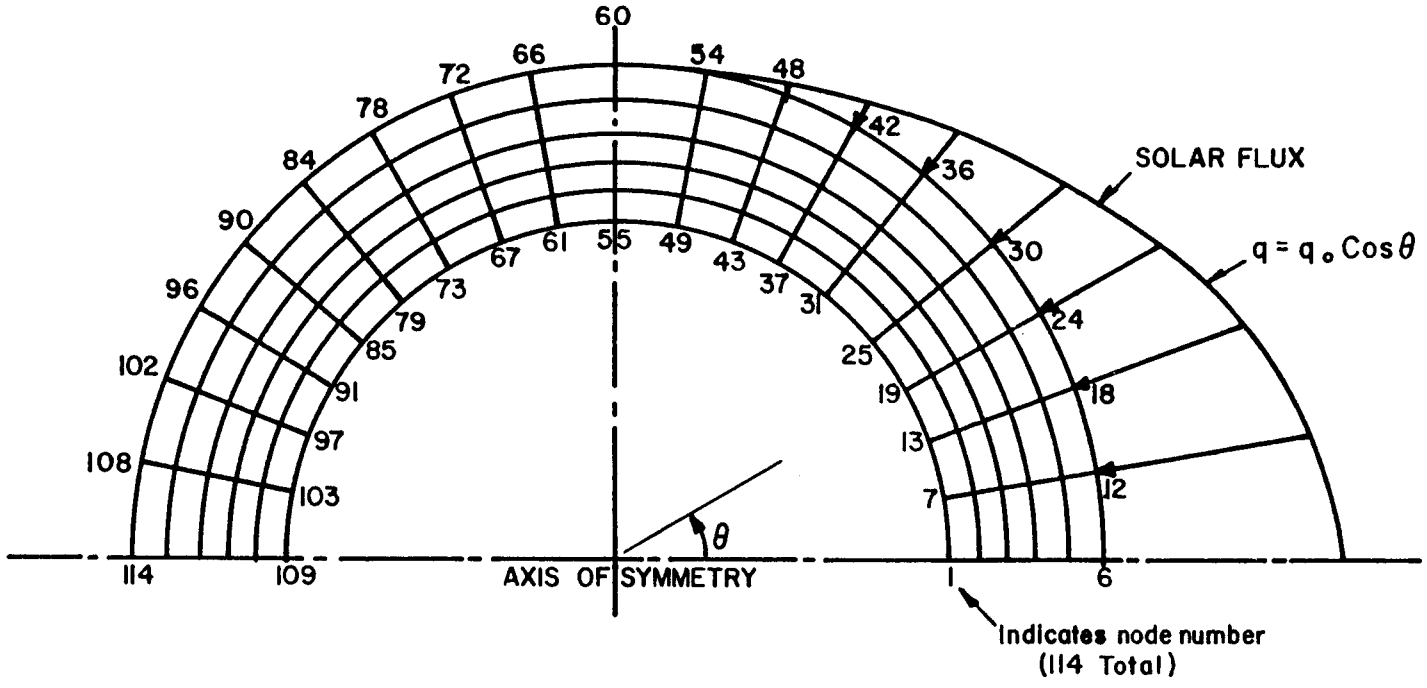

Figure 5.3-12. Tube Model

Computer Program. A specialized in-house computer program called NONSYM (Refs. 5.3-1, 5.3-2), developed by Foster Wheeler Development Corporation, was used in this analysis. This program is now capable of thermal and stress analysis of tubes subjected to nonaxisymmetric radiant heating. The tube material can be elastic or elastic-plastic undergoing creep. Elastic spring suports are permissible. This program, verified extensively with exact solutions as well as with finite-element solution, is very accurate and much cheaper than the general-purpose, finite-element programs.

Evaluation Criteria. Since the sodium pressure inside the receiver tube is low 35 pounds/square inch), the hoop stresses are very low, and ductile rupture is not a predominant failure mode. Hence the minimum tube thickness is determined from welding considerations rather than pressure stresses. The solar receiver is subjected to startup and shutdown cycles resulting from diurnal solar flux variations and cloud covers. Thus fatigue and creep-fatigue interactions are important failure modes. One set of possible criteria for the creep-fatigue evaluation of the tubes is that of the ASME Code Case 1592 (Elevated Temperature Design of Class 1 Nuclear Components). These criteria are consistent with the high reliability and integrity required in nuclear components. Consequently, these criteria may be too conservative for solar applications and may result in severe economic penalties. As a result, the following criteria, a combination of Section I, Section VIII - Division 2, and Code Case 1592, were used in this study (Ref. 5.3-3):

- Limit the primary stress (P_m) to the allowable stress S given in Section I. (S is identical to S_o in Code Case 1592.)
- Limit the primary and secondary stress ($P_L + P_B + Q$) to $\leq 3\ S_m$. This is an extension of the shakedown limit given in Section VIII - Division 2 to the elevated temperature region.
- Use the inelastic fatigue curves of Code Case 1592 as the fatigue criteria. The elastic fatigue curves are very conservative. The creep damage is ignored, which is justified at least in regions where the stresses are predominantly compressive. In solar tubes the stress state in those regions where the temperature is the highest is compressive.

In the present design the third criterion governs.

Analysis and Results. The values of the various parameters at the critical point are given below:

Heat flux (q_o) = 1.614 MW/m^2

Film coefficient (h_i) = 6025 $Btu/hr \cdot ft^2 \cdot F$

Sodium temperature (T_f) = 784 F

Tube OD (r_o) = 0.75 in.

Tube thickness (t) = 0.05 in.

Material properties of Incoloy 800H at 1150 F:

Modulus of elasticity (E) = 22.7 x 10^6 lb/in^2

Poisson's ratio (ν) = 0.372

Coefficient of thermal expansion (α) = 10.8 x 10^{-6}/°F

Thermal conductivity (k) = 14.0 Btu/hr·ft·°F

Yield stress = 15.4 ksi

Allowable stress S_o = 11.2 ksi

Allowable stress S_m = 13.9 ksi

The model used is shown in Figure 5.3-12. Temperature and stress profiles of the tube are given in Figures 5.3-13 and 5.3-14. The stresses shown in Figure 5.3-14 are the axial stress σ_z.

The effective elastic strain range is 1.998 x 10^{-3}. Corresponding to this strain range, from Figure T-1420-1C of Code Case 1592-10, the fatigue life of the tube is 20,000 cycles. It should be noted that in nuclear designs Figure T-1420-1C is usually used in conjunction with inelastic analysis. In the present case, inelastic analysis was not done. However, previous analyses have shown that for strain-controlled thermal cycling, such as the case under consideration, the inelastic strain range is approximately equal to the elastic strain range.

If the only source of thermal cycling were the diurnal variations of insolation, the panels would be cycled once each day or about 11,000 cycles in 30 years. However, cloud-induced transients could increase this to perhaps 50,000 cycles. Thus, the north panels analyzed above may have to be replaced once or twice during the life of the plant to ensure reliability. The cost of each panel is about $100,000. The other panels do not endure the same stress levels and would have longer lives. It should also be noted that the final absorber loss calculations (Section 5.3.2) show peak temperatures of 1107 F rather than 1150 F, and indicate that this peak occurs in a much lower flux region (0.341 MW/m^2). Obviously, this issue requires a more thorough analysis than has been possible in this study; however, these results do seem to indicate that the present design concept is not inconsistent with the goal of 30-year plant life.

Panel Fabrication Procedure

The absorber panel manufacturing plan which defines the major steps of the manufacturing process, is shown schematically in Figure 5.3-15. The operations required are listed in Table 5.3-3. The absorber panels will be complete rail-shippable assemblies ready for installation in the receiver.

After inspection, the stock tubes are trimmed to size and shaped to a configuration appropriate for each tube. The tubes are cleaned and then assembled into panels in a fixture that will hold the tubes in close contact for brazing. The braze alloy is then applied, after which the tube bundles are placed in a retort and introduced into a furnace for brazing at 1900 to 1950 F for 30 minutes. After removal from the furnace, the panels are inspected for gaps between tubes.

Concurrently, the headers are fabricated. Holes are drilled in them, end caps are machined and welded in place, studs are fabricated and welded to the headers, and tube-to-header welds are made. At this point the tube bundles are pressure-tested.

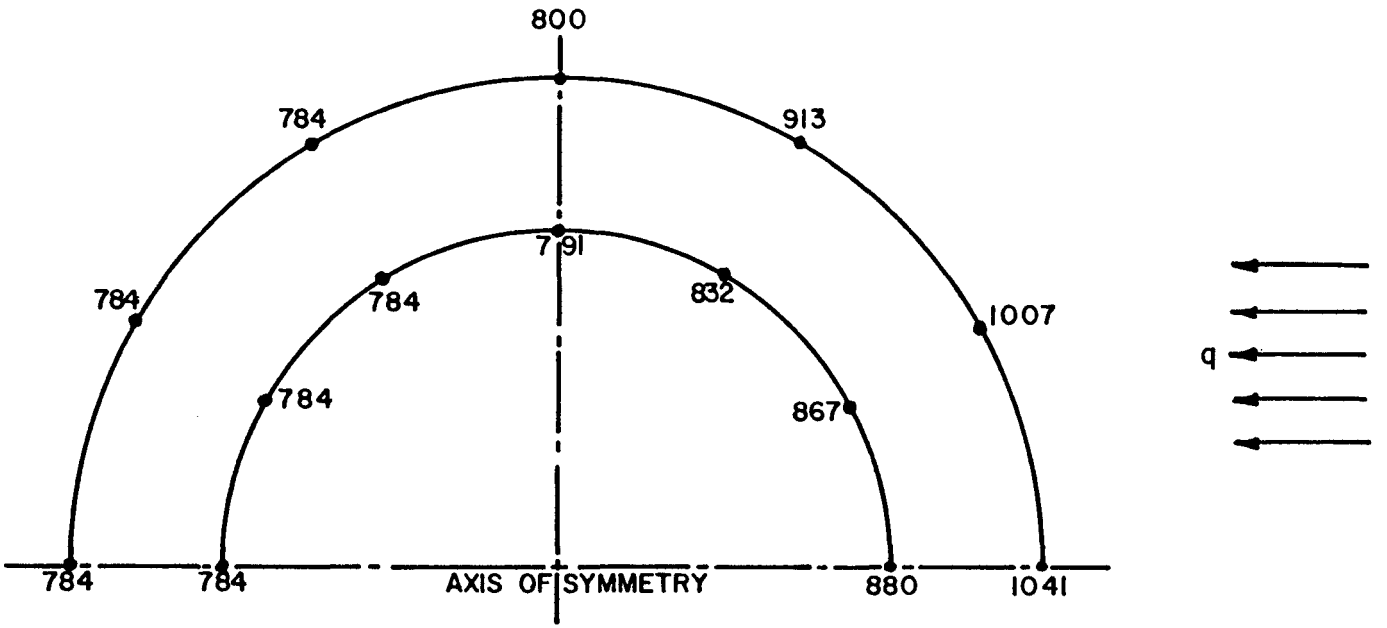

Figure 5.3-13. Temperature Distribution in the Tube (°F)

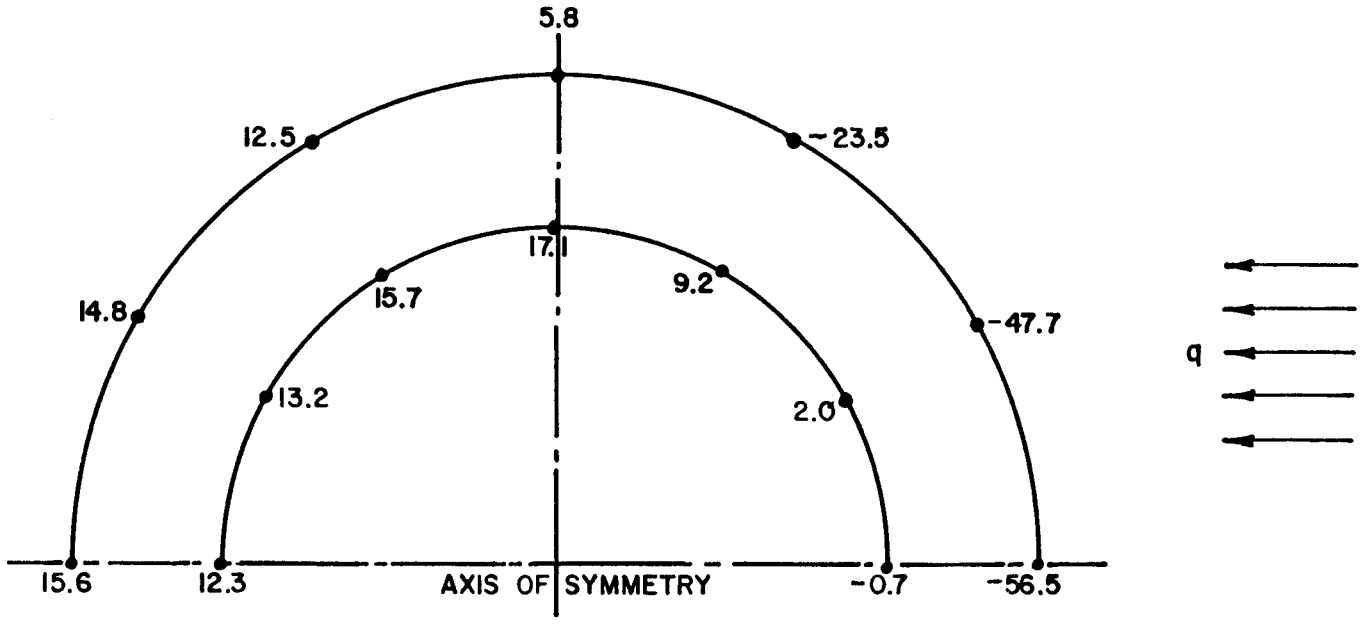

Figure 5.3-14. Axial Stress Distribution (stresses in ksi)

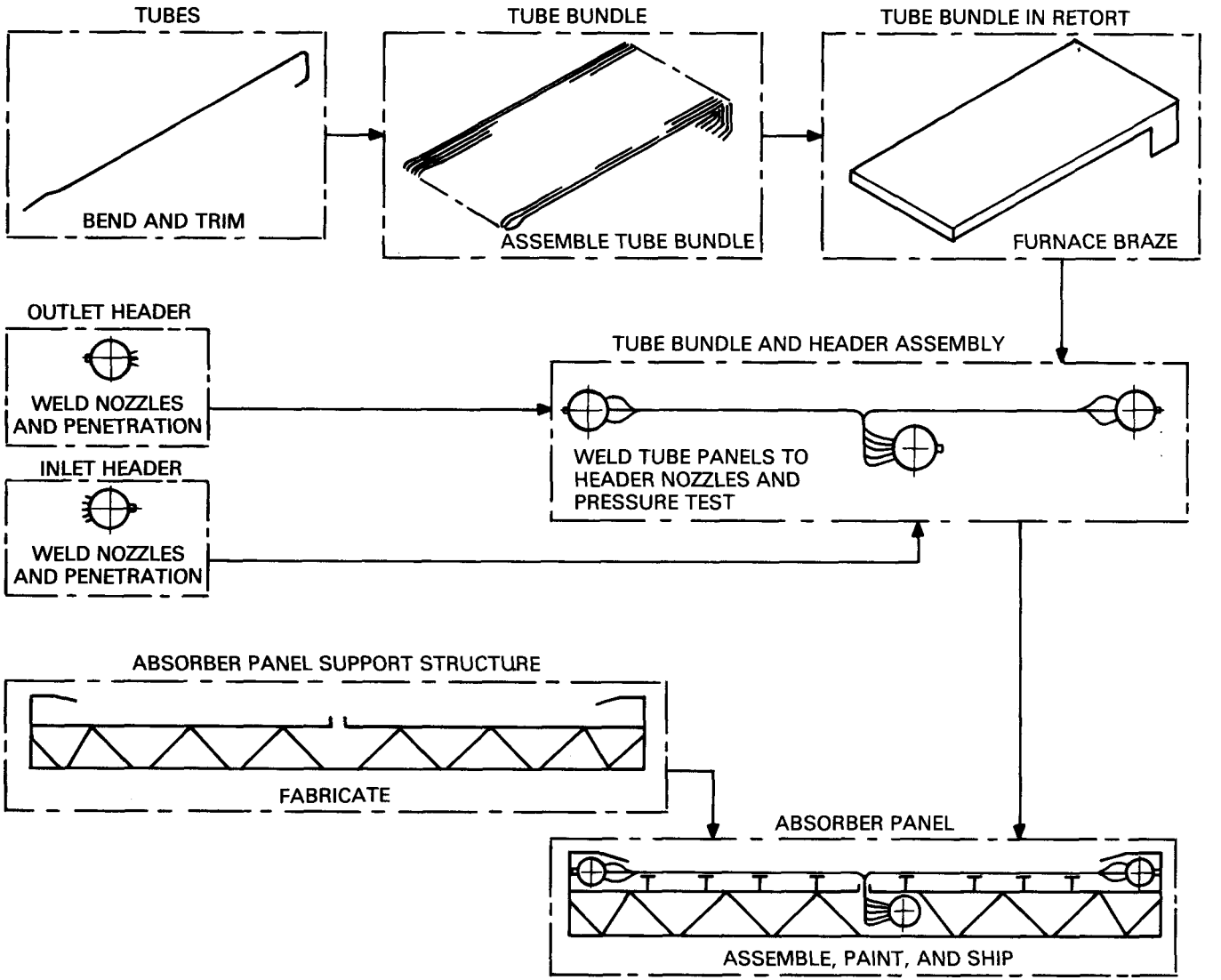

Figure 5.3-15. Basic Fabrication Sequence

Table 5.3-3

MANUFACTURING OPERATIONS

1. Inspect, cut to size, and machine end tubes
2. Bend tubes
3. Set up tube bundle in fixture
4. Apply braze alloy
5. Furnace braze tube bundles
6. Fabricate inlet header
7. Fabricate outlet headers
8. Weld tubes to headers
9. Stress relieve
10. Pressure test
11. Fabricate support structure
12. Fabricate roller-mounting devices
13. Attach tube bundle to support structure
14. Install insulation
15. Paint
16. Prepare for shipment
17. Load on railroad car

The next step involves attachment of the backup structure. The clips are welded to strips that have been brazed to the back side of the tubes and the T-beams are inserted in the clips. Simultaneously, the support structure and the roller-mounting devices are assembled. The panels are secured to the support structure via the roller-mounting devices, which are bolted to the I-beams and to the headers.

The 12-inch Fiberfrax insulation is then installed, and Pyromark paint, which does not require heat for drying, is applied.

Table 5.3-4 provides a list of materials required for fabrication of the absorber panel.

Furnace brazing within a retort using a nickel-base Nicrobraz 50 or 51 has been selected for making the longitudinal ligaments between tubes. The assembly produced by furnace brazing at 1900 to 1950 F will be strong and free of distortion and will involve less overall labor and risk than assembly by other techniques. Local repair between tubes, if needed, can be accomplished by local torch heating or other means, such as metallizing, to cover gaps.

Straightness of the long Incoloy 800H tubes may be a concern because, before brazing, the solar receiver panels must be assembled to ensure surface-to-surface contact of most of the tubes. Since the tubes are thin-walled (0.75-inch OD by 0.050-inch wall), the use of a clamping fixture will keep the gaps within tolerance. Small, controlled amounts of braze alloy can be applied semiautomatically with an air-powered, caulking-gun-type applicator. The braze alloy, prepackaged like a paste, contains a binder so that loss of powder during handling is eliminated.

Two minor problems have come to light. First, the aluminum content of Incoloy 800H is detrimental to wetting because of preferential oxidation of aluminum which forms Al_2O_3 on the surface. The braze alloys selected are not as sensitive to the aluminum effect as are older alloys such as Ni-Si-B, and most likely the interference by aluminum will not be significant. If it should interfere with the flow of the liquid braze, there is a simple thin-film flux that can be applied to the tube before brazing. The second problem is the probability of gaps between the tubes that are larger than the limit for bridging by the braze alloy. The gap problem is very easily overcome by the use of a minor application of granular stainless-steel powder before application of the braze alloy (Figure 5.3-16). However, even if found after brazing, the gap can easily be repaired.

Thermal analysis has shown that gaps filled in this way can be as wide as 0.010 inch without experiencing significant over-heating even in the highest flux parts of the panel.

The braze is retained in the cusp between the tubes and flows through the joint. When pure, dry hydrogen is used (with an adequate nitrogen gas purge before and after brazing), the braze alloy always penetrates joint surfaces that are in metal-to-metal contact.

Table 5.3-4

LIST OF MATERIALS

Material	lb
Incoloy 800H	3,316
T22	1,794
COR-TEN	9,601
FIBERFRAX	1,732
TOTAL	16,443

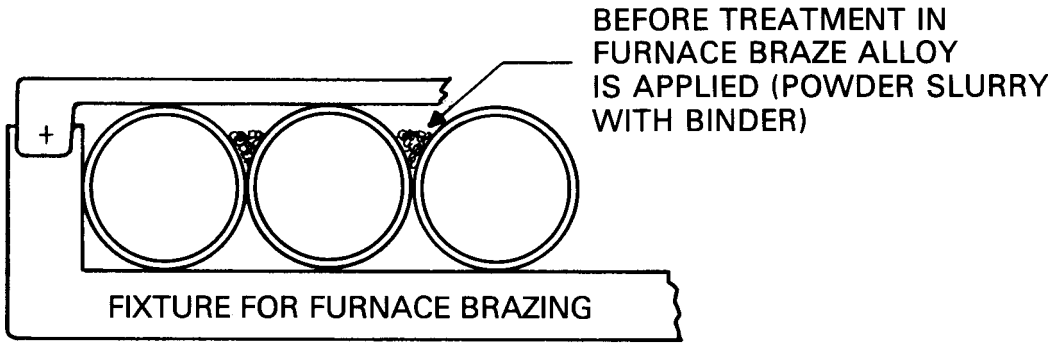

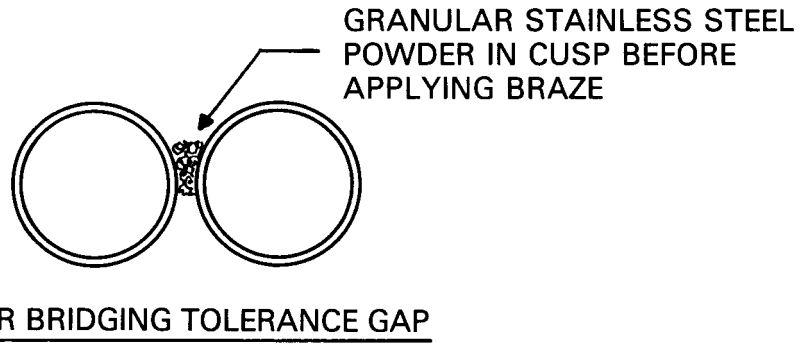

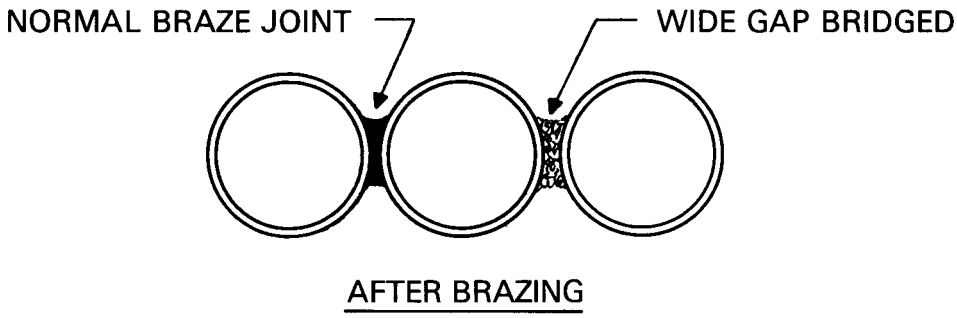

NOTE:
NICROBRAZ #50 & 51 DO NOT REQUIRE
ANY MEASURABLE GAP TO FLOW
DESIRE GAP: 0 TO 0.004″ BETWEEN TUBES

Figure 5.3-16. Brazing of Tube Bundle

Nicrobraz 50 or 51 is preferred because it minimizes diffusion into the tube alloy while providing good high-temperature strength and low-temperature ductility. The alloy has also proved adequate for sodium systems where many tubes must be simultaneously joined into a tubesheet. The resulting joints are tight, strong, and resistant to sodium.

The main factors determining the success of furnace brazing are surface cleanliness, fixtures that prevent movement during the furnace cycle, and good control of the gas purity and dew point of the H_2 during brazing. Vacuum brazing eliminates the problems relative to the H_2 gas system. Although we know of no available furnace large enough for the job (approximately a 7 foot by 30 foot heated zone at 1950 F), such a furnace could be designed.

In production, the use of the big Foster Wheeler Mountaintop normalizing furnace with two, or possibly four, retorts on the car heating simultaneously is possible. The heating cycle is short. After holding above 1900 F for 30 minutes, the retorts are furnace-cooled to 1600 F; then the retorts (purged with N_2 gas) can be withdrawn from the furnace.

Installation and Maintenance

The panels are lifted to the top of the tower by helicopter. Each panel weighs 16,443 pounds including insulation and strong-back. Installation of the absorber panels is performed sequentially as follows:

- Lift absorber panel to top of the tower
- Install absorber panel in place
- Bolt strong-back panel structure to receiver structure
- Weld inlet and outlet piping.

Thus the only operations required are welding of the inlet and outlet pipes and bolting of the absorber strong-back structure to the receiver structure.

Only three preventive maintenance operations are expected for the absorber panel assembly: painting, roller lubrication, and visual inspection. Scaffolding and a sprayer will be used to facilitate repainting of the exposed tube surface. Industrial experience with Pyromark paint indicates many years of maintenance-free service.

A complete panel will be replaced when damaged tubes and leaks must be repaired. The installation procedure in reverse will be used to remove a defective panel. The panels can be repaired on site or returned to the factory for repairs, depending upon the extent of the damage. Obviously, the inlet and outlet pipes will be cut and the bolts securing the panel strong-back structure to the main receiver structure will have to be removed.

The electromagnetic pumps operate at almost constant temperature and have no moving parts. These will probably not require any maintenance beyond inspection of the external insulation and lubrication of the cooling air blower.

5.3.2 ABSORBER LOSSES

A single quadrant of the absorber was analyzed to estimate reflection, radiation, and convection losses. This implies an assumption that the receiver flux plot is symmetrical about both the belt line and vertical north/south center lines. This is not precisely true, but the approximation is good enough for the conceptual design analysis since losses are not very sensitive to the flux distribution.

The quadrant is divided into 96 nodes as shown in the flux plot (Figure 5.3-17). Cold sodium enters each half panel at the top of node 1 and exits to the downcomer at the bottom of node 8.

The flow rate of sodium in each half panel was determined by the following equation:

$$W_j = \Delta x \Delta y \sum_{i=1}^{8} q_{sij}\, \eta_{ij} \left[C_N(T_H - T_C)\right]^{-1} \qquad (5.3\text{-}1)$$

where:

W_j = flow rate of sodium in panel j (lb/hr)

C_N = average specific heat of sodium (Btu/lb, ^oF)

T_H = sodium outlet temperature (^oF)

T_C = sodium inlet temperature (^oF)

Δx = width of panel = 2.0944 m

Δy = length of one node = 1.0 m

q_{sij} = incident solar flux in node i of panel j (Btu/hr/ft^2)

η_{ij} = efficiency of node i in panel j

The efficiencies η_{ij} are unknown at the start of the analysis. An initial value of 90 percent is assumed for all nodes and the calculation through the equations below is repeated until convergence is obtained (about five iterations in most cases).

Sodium temperature is computed for each node by

$$T_{Nij} = T_{Ni-1,j} + q_{sij}\, \eta_{ij}\, \Delta x \Delta y / W_j\, C_N \qquad (5.3\text{-}2)$$

where:

T_{Nij} = temperature of sodium at outlet of node i of panel j ($T_{Noj} \equiv T_C$)

$$\overline{T}_{Nij} = (T_{Ni-1,j} + T_{Nij})/2 \qquad (5.3\text{-}3)$$

where:

$\overline{T}_{Nij}$ = average temperature of sodium in node i of panel j

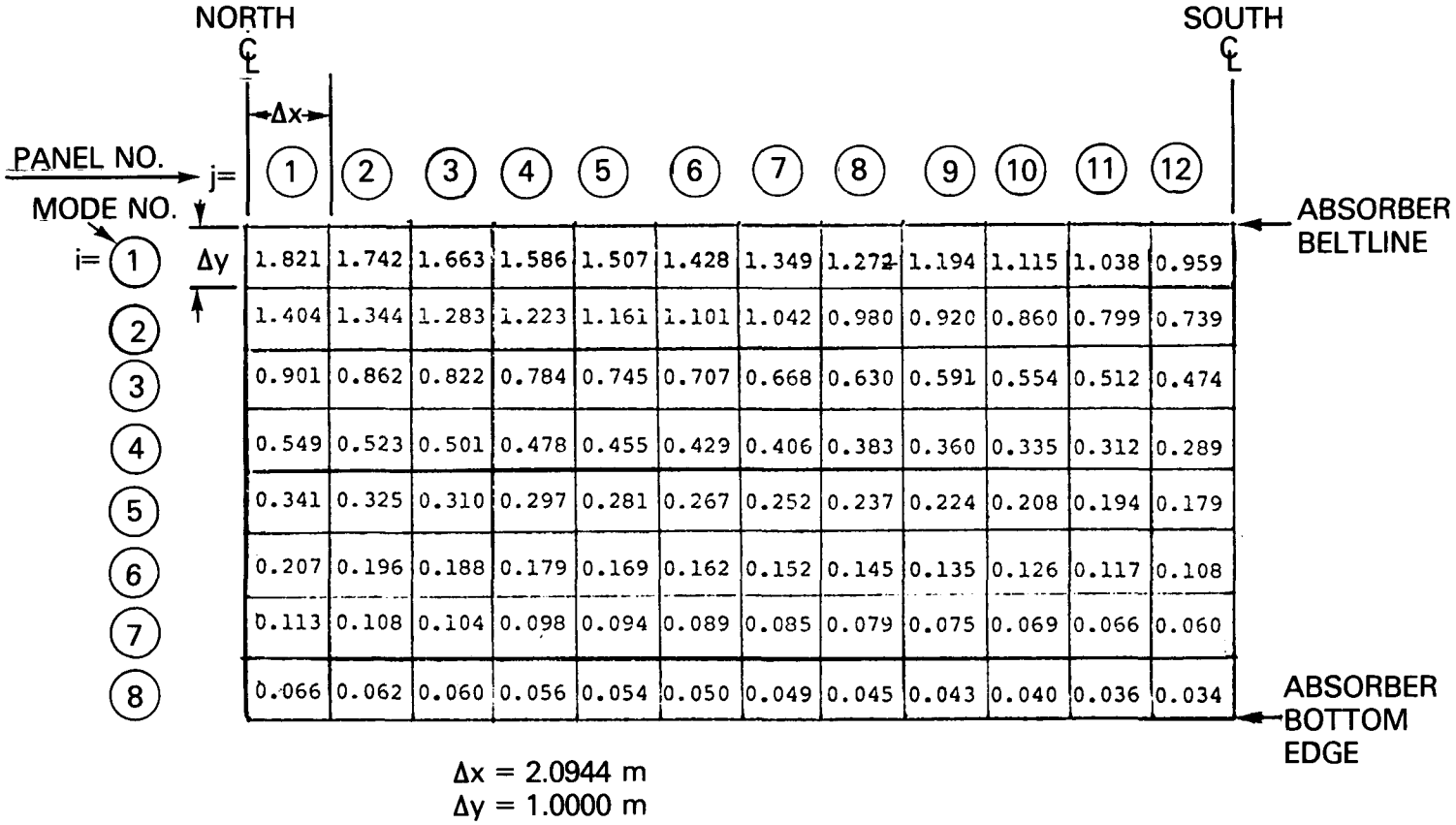

i \ j	1	2	3	4	5	6	7	8	9	10	11	12
1	1.821	1.742	1.663	1.586	1.507	1.428	1.349	1.272	1.194	1.115	1.038	0.959
2	1.404	1.344	1.283	1.223	1.161	1.101	1.042	0.980	0.920	0.860	0.799	0.739
3	0.901	0.862	0.822	0.784	0.745	0.707	0.668	0.630	0.591	0.554	0.512	0.474
4	0.549	0.523	0.501	0.478	0.455	0.429	0.406	0.383	0.360	0.335	0.312	0.289
5	0.341	0.325	0.310	0.297	0.281	0.267	0.252	0.237	0.224	0.208	0.194	0.179
6	0.207	0.196	0.188	0.179	0.169	0.162	0.152	0.145	0.135	0.126	0.117	0.108
7	0.113	0.108	0.104	0.098	0.094	0.089	0.085	0.079	0.075	0.069	0.066	0.060
8	0.066	0.062	0.060	0.056	0.054	0.050	0.049	0.045	0.043	0.040	0.036	0.034

Figure 5.3-17. Incident Solar Flux (q_{Sij}) in MW/m^2 at Design Point

The outer tube temperature is computed in two ways.

$$T_{Tij} = \overline{T}_{Nij} + \left(\frac{2}{\pi}\right) q_{sij}\, \eta_{ij}/U_{ij} \qquad (5.3\text{-}4)$$

$$T^*_{Tij} = \overline{T}_{Nij} + q_{sij}\, \eta_{ij}/U_{ij} \qquad (5.3\text{-}5)$$

where: T_{Tij} = average outer temperature of tube

T^*_{Tij} = maximum outer temperature of tube

U_{ij} = total tube conductance (Btu/hr-ft^2-^{o}F)

Equation (5.3-4) gives an average tube temperature based on the assumption that the flux is uniformly distributed around the front face of the tube. Equation (5.3-5) gives an upper limit on tube temperature for the crown of the tube where the incident flux is parallel to the tube radius. The temperature in Equation (5.3-5) is an extreme case which could only occur if there were no circumferential conduction in the tube wall.

The tube wall conductance is given by

$$U_{ij} = \left[\frac{1}{h_{Nij}}\left(\frac{D}{d}\right) + \left(\frac{D}{2K_{Tij}}\right) \ln\left(\frac{D}{d}\right)\right]^{-1} \qquad (5.3\text{-}6)$$

where: h_{Nij} = sodium heat transfer coefficient (Btu/hr/ft^2/^{o}F)

D = outside tube diameter (0.75 in.)

d = inside tube diameter (0.65 in.)

K_{Tij} = thermal conductivity of tube material (Btu/hr/ft/^{o}F)

The thermal conductivity for Incoloy 800H was estimated from data for Incoloy 802 (Ref. 5.3-4). Equation (5.3-7) is a least squares fit of this data from 600 F to 1200 F.

$$K_{Tij} = 6.70 + 0.004705\left[\frac{\overline{T}_{Nij}+T_{Tij}}{2}\right] \qquad (5.3\text{-}7)$$

In the iteration scheme, T_{Tij} is given an initial value of 1100 F.

Heat transfer coefficients for sodium were estimated using Lyon's correlation (Ref. 5.3-5) as follows:

$$h_{Nij} = K_{Nij}\,(7.0 + .025\, P_{eij}{}^{0.8})/d \qquad (5.3\text{-}8)$$

where: K_{Nij} = thermal conductivity of sodium (Btu/hr/ft/^{o}F)

P_{eij} = Peclet number = $4W_{ij}\, C_N/(\pi d\, K_{Nij}\, N)$

N = number of tubes in panel (108)

The thermal conductivity of sodium was computed from a least squares fit of data from (Ref. 5.3-6) from 600 F to 1200 F.

$$K_{Nij} = 125.3 - 12.74 \ln(\overline{T}_{Nij}) \qquad (5.3\text{-}9)$$

The radiative losses from each node are computed as follows:

$$Q_{Rij} = \sigma\varepsilon \, \Delta x \Delta y \left[(T_{Tij}+460)^4 - (T_A+460)^4\right] \qquad (5.3\text{-}10)$$

where:

Q_{Rij} = radiative loss in node i of panel j (Btu/hr)

σ = Stephen Boltzman constant = 0.1714E-8 Btu/hr/ft^2/^{o}R^4

ε = emissivity of Pyromark paint = 0.90

T_A = air temperature (^{o}F)

This assumes that the half tube array emits as a flat plate with an area equal to the face area, not the actual metal area. There will probably be some enhancement of this loss due to the cavities formed between tubes. These cavities would also improve the absorptivity slightly. However, neither effect has been accounted for here. In the future it may be possible to improve absorber performance by intentionally making the surface optically "complicated" on a scale small enough that the added surface area would not add to the convection loss (cavities smaller than boundary layer).

The radiation sink temperature (sky temperature) has been taken to be equal to the air temperature because water vapor and carbon dioxide tend to make the air mass opaque to thermal wavelengths except near the zenith where the effective sky temperature may be much lower (e.g., -50 F).

Convection losses were also estimated on the basis of the face area as follows:

$$Q_{Cij} = h_T \, \Delta x \Delta y \, (T_{Tij} - T_A) \qquad (5.3\text{-}11)$$

where:

Q_{Cij} = convective loss from node i of panel j (Btu/hr)

h_T = air side convective heat transfer coefficient (Btu/hr/ft^2/^{o}F)

The effect of surface roughness on these losses was accounted for in the value of h_T using the data by Achenbach (Ref. 5.3-7), and the effect of mixed free and forced convection was estimated by a combining rule developed by Churchill and Usagi (Ref. 5.3-8). These calculations and further discussion of the theoretical and physical aspects of this problem are given in Appendix N.

Losses through insulation on the backs of the panels have been neglected in this analysis. An initial estimate indicated that these would be about 0.05 percent of the incident power.

Once Equations (5.3-10) and (5.3-11) have been used to estimate the losses, it is possible to compute the node efficiencies, repeat the calculations, and converge a solution. Node efficiencies are given by,

$$\eta_{ij} = \alpha - (Q_{Rij}+Q_{Cij})/(q_{sij}\ \Delta x\Delta y) \qquad (5.3\text{-}12)$$

where: α = absorptivity of Pyromark paint (0.95)

A computer program was written to perform these calculations; it is described in Appendix O. Table 5.3-5 lists the input data used for the design point calculations. Note that the inlet and outlet sodium temperatures were determined by setting the sodium temperature at the inlet to the steam generators at exactly 1100 F and then working backwards through the system, accounting for insulation losses and pump inputs, to determine the thermal power and sodium temperatures in the absorber. This is explained in Section 5.8.

The absorber performance estimated on this basis is summarized in Table 5.3-6. The detailed results are given in Appendix O.

Receiver efficiency deteriorates when the incident flux is reduced. To estimate the magnitude of this effect, several runs were made with scaled flux plots, i.e. Figure 5.3-17 multiplied by a constant factor. The results are plotted in Figure 5.3-18 down to 30 percent of full rated power.* This figure shows that the overall receiver efficiency is quite high even at reduced power. However, closer examination of these results has revealed a potential problem at low loads.

Figure 5.3-19 is a plot of the node efficiencies at the design point for the north and south panels and one intermediate panel. In the high flux regions of the panels (nodes 1 through 5) the efficiency is high, but it drops off rapidly in nodes 6 through 8. On panel 12 the efficiency goes negative in node 8, indicating that this node is losing more heat than it absorbs from the sun. At 30 percent load this problem occurs in the outlet nodes of all the panels as shown in Figure 5.3-20.

To maintain the desired sodium outlet temperature under these conditions, the control system would cut back flow until the temperature setpoint was achieved. Since the outer ends of the panel are losing heat, the sodium temperature at the center of the panel would have to rise above the desired outlet temperature and could cause materials problems. This is illustrated in Figure 5.3-21. From 100 percent power down to 30 percent power, the tube wall temperature rise is not a problem, but at 20 percent power the southern panels (11 and 12) may experience temperatures in excess of 1300 F. There are two possible solutions to this problem. Receiver operation can be limited to power levels greater than 30 percent of peak without losing a significant amount of energy during the year. Alternately, the receiver can be fitted with a segmented insulating curtain to cover the nonproductive parts of the absorber at low loads.

---

*Diurnal variation of power is typically 100 percent at noon down to 35-40 percent at the 10^{0} elevation field cutoff point.

Table 5.3-5

DESIGN POINT INPUT DATA TO ABSORBER LOSS CALCULATION

Incident Flux:	q_{Sij} (see flux plot, Figure 5.3-17)
Sodium Properties:	C_N = 0.304 Btu/lb/^oF
	T_H = 1097.22 F (see Section 5.8)
	T_C = 612.95 F (see Section 5.8)
	K_{Nij} = Equation (5.3-9)
Panel Properties:	Δx = 2.0944 m
	Δy = 1.0000 m
	D = 0.75 in.
	d = 0.65 in.
	N = 108 tubes/panel
	K_{Tij} = Equation (5.3-7)
	ε = 0.90, α = 0.95 } Pyromark Paint
	h_{Nij} = 2.0 Btu/hr/ft^2/^oF (Appendix N)
Ambient:	T_A = 83 F
	Wind Speed = 17.9 ft/sec

Table 5.3-6

RECEIVER LOSS SUMMARY AT THE DESIGN POINT*

Incident Power	414.14 MW_t
Losses:	
Reflection	-20.71
Radiation	-19.60
Convection	-4.83
Net Power to Sodium	369.00 MW_t
Receiver Efficiency	89.1%
Sodium Flow rate	8.5679 x 10^6 lb/hr

Panel No.	Flow (lb/hr)	Incident MW_t	Radiation MW_t	Convection MW_t	Efficiency
1	474851.	22.628	0.841	0.204	0.9038
2	452795.	21.623	0.837	0.204	0.9019
3	431586.	20.655	0.832	0.203	0.8999
4	410449.	19.692	0.827	0.203	0.8977
5	388861.	18.707	0.822	0.202	0.8952
6	367449.	17.731	0.818	0.202	0.8925
7	346319.	16.768	0.813	0.201	0.8895
8	324987.	15.796	0.809	0.201	0.8861
9	303940.	14.837	0.805	0.200	0.8823
10	282316.	13.852	0.801	0.200	0.8777
11	260880.	12.876	0.798	0.199	0.8726
12	239525.	11.905	0.795	0.199	0.8665

*Summer solstice noon with a normal solar intensity of 950 MW/m^2

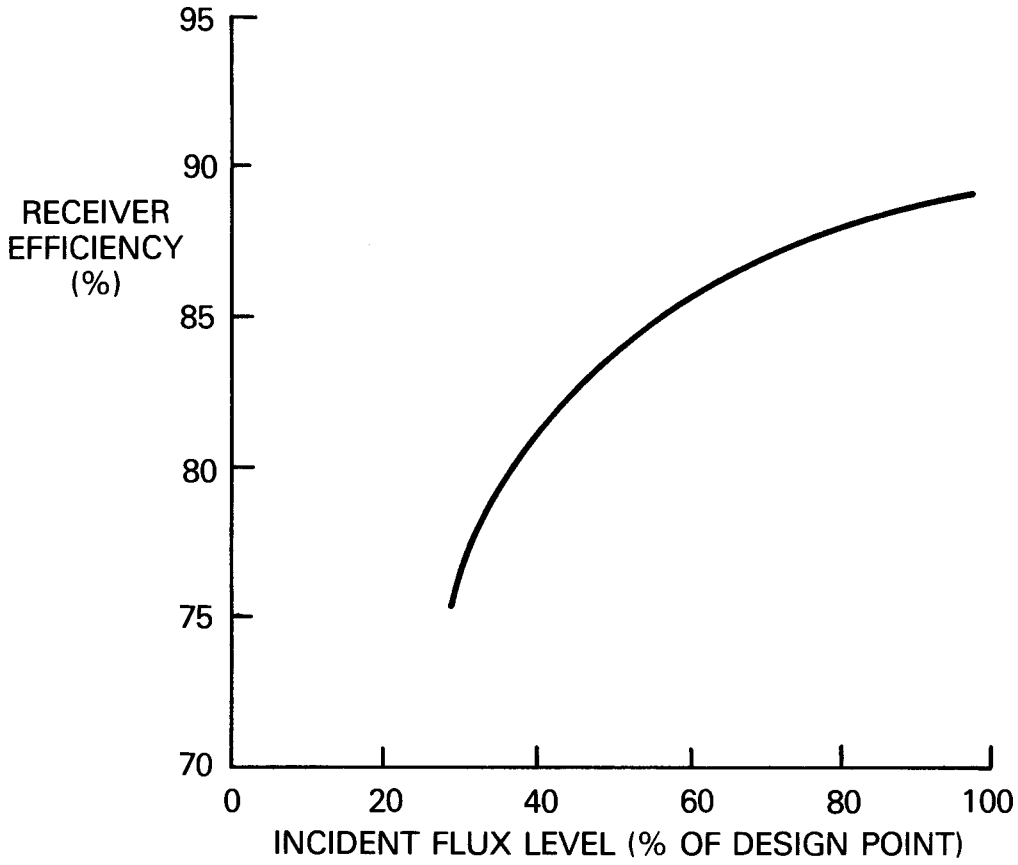

Figure 5.3-18. Variation of Absorber Efficiency with Incident Flux Level (air temperature = 83 F)

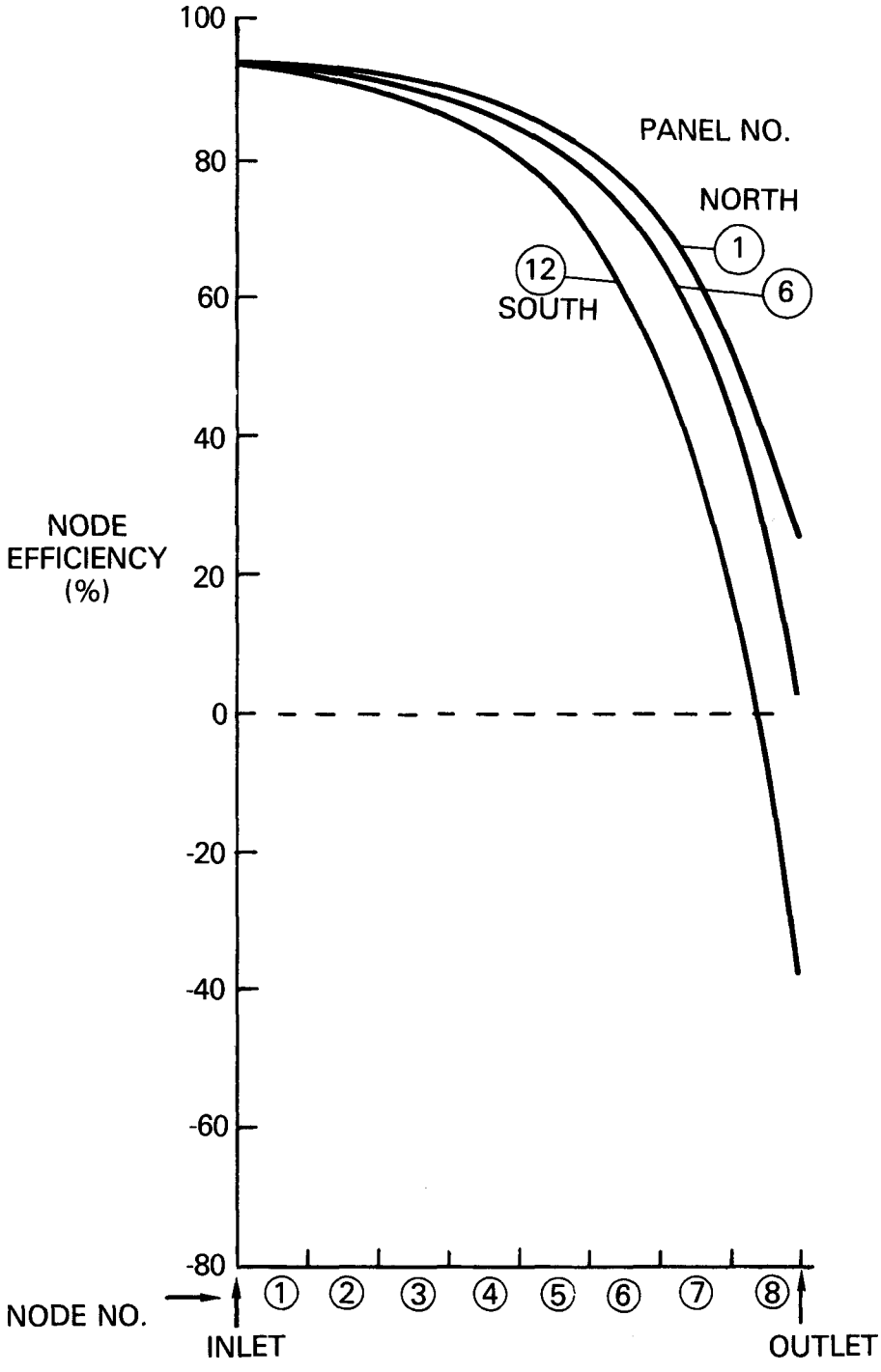

Figure 5.3-19. Variation of Efficiency on Absorber Surface (100 percent power)

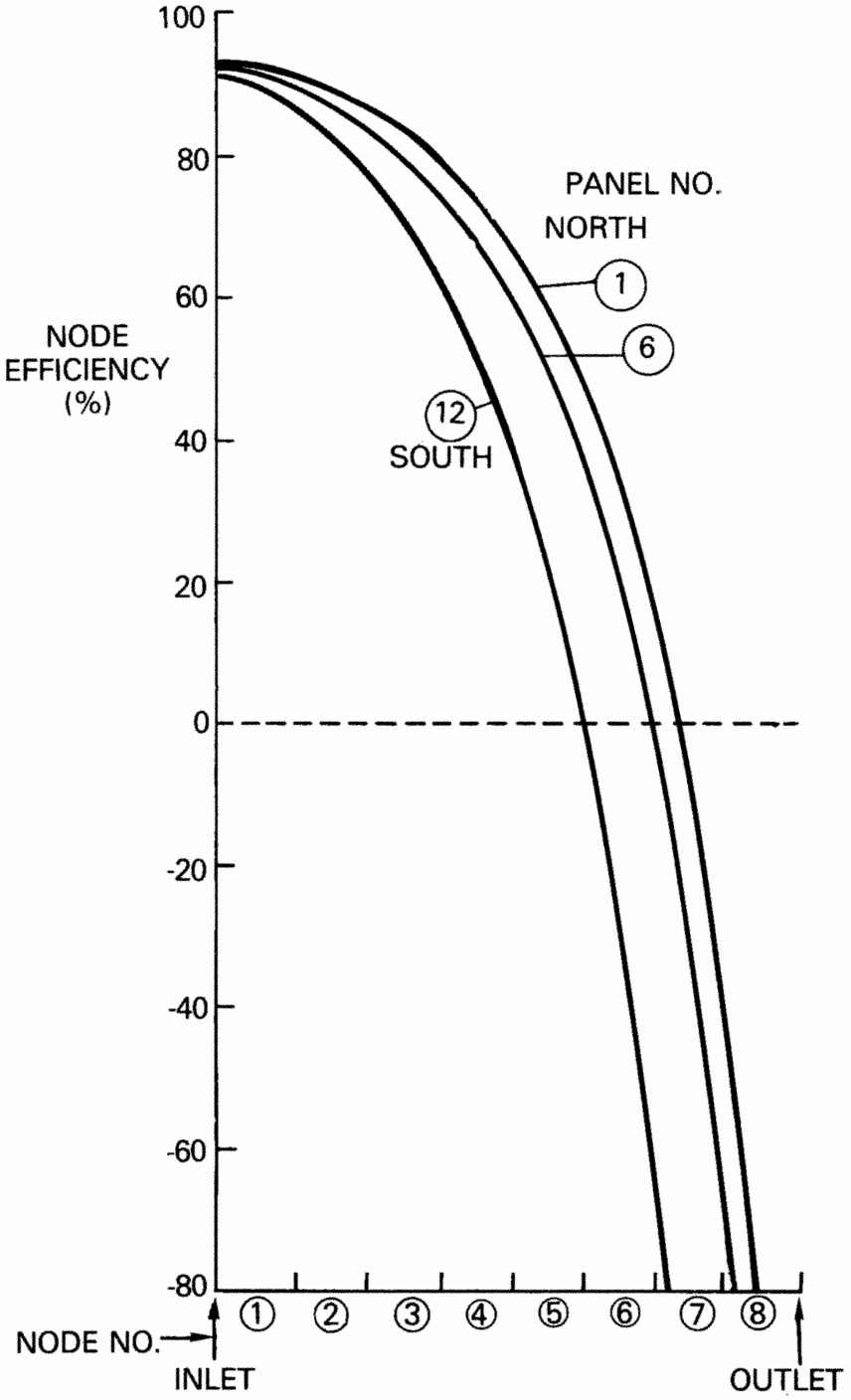

Figure 5.3-20. Variation of Efficiency on Absorber Surface (30 percent power)

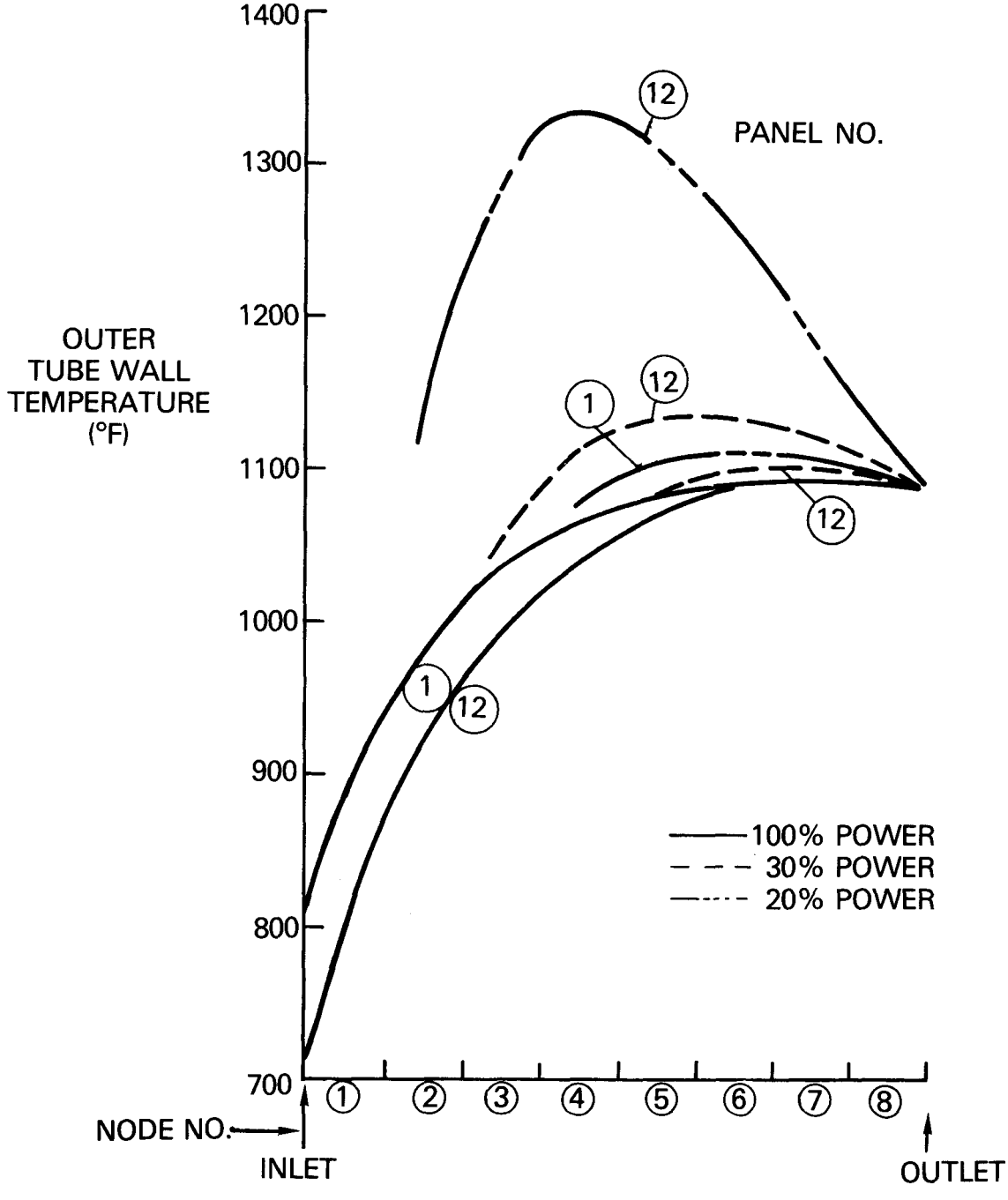

Figure 5.3-21. Variation of Temperature on Absorber Surface

5.3.3 TOWER AND RISER/DOWNCOMER

Tower

The tower design was established based upon the criterion that height of the tower from ground level to the top of receiver is 202.3 meters. For reasons outlined in Section 3.3.3, a slip formed reinforced concrete tower was chosen. Design criteria for seismic, wind speed, soil pressure, and importance factor are as given in Section 3.3.3.

Figure 5.3-22 shows the tower with foundation, elevator shaft, downcomer/riser pipes, hoist room, pump room, receiver, insulating curtain, and maintenance platforms. The top of the tower is constructed as a cylinder rather than tapered section. This allows the insulating curtain, which is raised at night, to be moved on guides over the top section of the tower.

The curtain will be cantilevered such that roughly one-third of the length of the curtain can act as support while the curtain is in the raised position. In the lowered position, the curtain acts as protection during sunlight hours for the upper concrete section of the tower from sunbeams which may be caused by erroneously positioned heliostats. The curtain could be raised in a number of ways including:

- Hydraulic cylinders
- Cable lift with electric motor drive
- Screwjack drive

Further work would need to be done to determine the optimum choice of curtain drive with regard for cost, reliability, and other factors.

Receiver Construction

Receiver assembly could best be done on site by use of helicopter for lifting panels into position. This saves the cost of a crane on top of the receiver. Additional tower or receiver design and cost required to accommodate the crane is also eliminated.

Garlick Enterprises (San Francisco) was contacted regarding helicopter rental. Garlick indicated that a Sikorsky Sky Crane S-64 could handle up to 22,000 pounds (during winter) and 20,000 pounds (during summer). This should easily accommodate the 24 total receiver panels of 16,443 pounds each. Garlick indicated a budget price of approximately $40,000 for the total receiver travel lifts. It is expected that the receiver panels will constitute the heaviest lift compared with other components.

Riser/Downcomer Piping

For reasons explained in Section 3.3, the helical configuration of riser/downcomer was chosen over use of bellows to accommodate thermal expansion. Other methods of allowance for thermal expansion such as expansion loops were also explored but not chosen for Task 4.

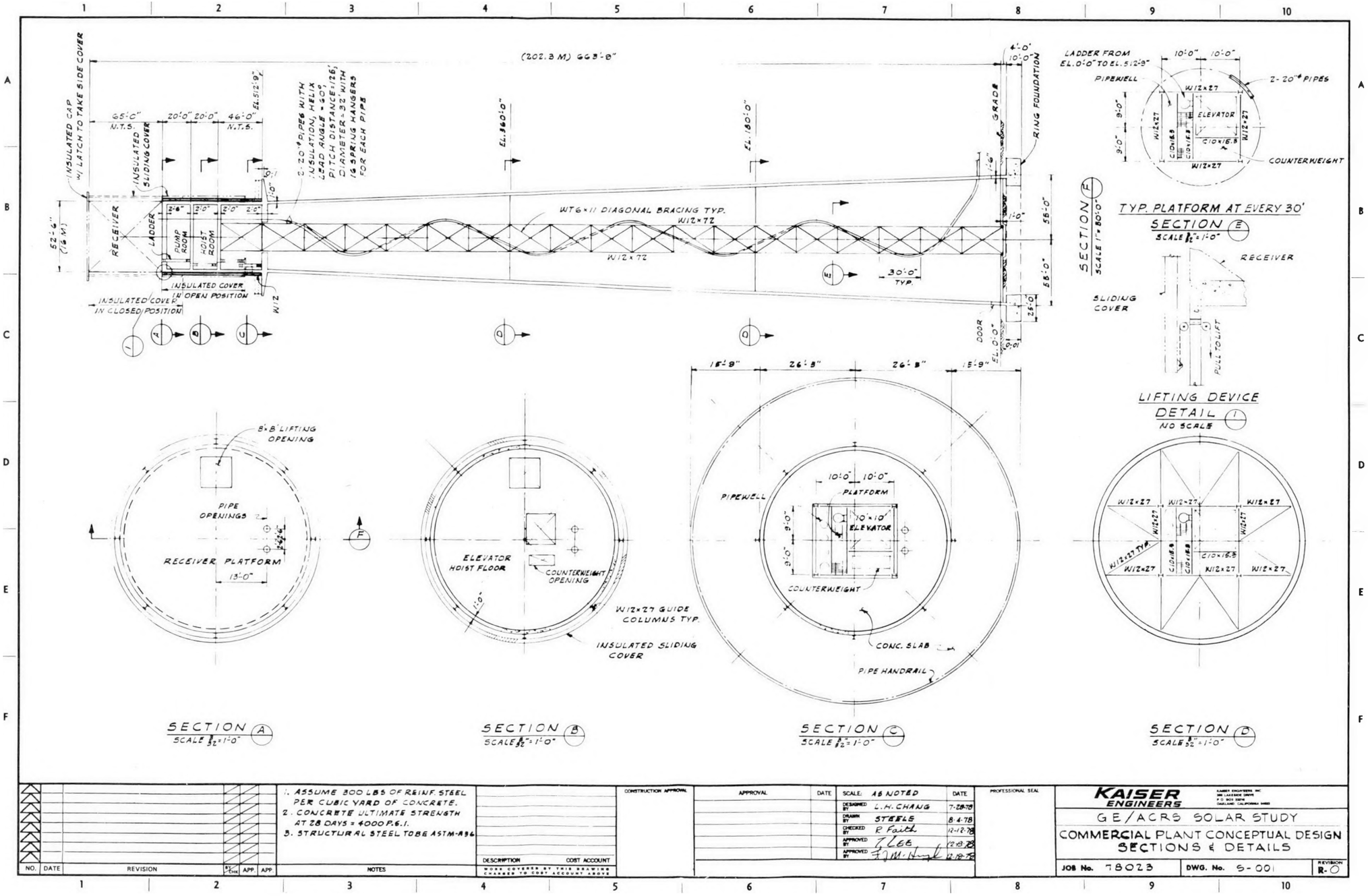

Figure 5.3-22. Receiver Tower Conceptual Design - Sections and Details

The riser/downcomer pipes consist of a helix with a lead angle of 60 degrees, pitch distance of 125 feet, and diameter of 23 feet. The helical pipes spiral around the central elevator shaft as shown in Figure 5.3-22. A cylindrical helix is chosen because it can be analyzed from a thermal expansion and stress viewpoint as a cylindrical spring. The conical helical configuration shown in Figures 3.3-14, 3.3-15, and 3.3-16 is more difficult to analyze from a stress and expansion viewpoint and is more difficult to support due to the larger diameter and tapered wall sections of the tower.

Sufficient steel bracing is required to support the weight of the piping from the central elevator shaft. The piping is hung from the elevator structural steel by 16 spring hangers for each pipe. A typical hanger is shown in Figure 5.3-23.

The pipe size is 20-inch diameter for both downcomer and riser pipes. Hot leg material operates at 1100 F and is fabricated from 316 stainless steel. Cold leg material operates at 612 F and is fabricated from carbon steel. The total length of pipe (in cold condition) is 562 feet for both riser and downcomer.

Although the helical pipe configuration is chosen for conceptual design purposes, alternative expansion methods should be analyzed in Phase 2 with regard to cost, reliability, and other factors. Alternative methods could include:

- Nonstandard bellows allowing for greater axial expansion and better cost effectiveness, e.g., Pathway Bellows X-press design
- Expansion loops
- Conical helix supported from inside tower walls

The helical shape can be achieved with existing manufacturing facilities. Pacific Pipe Company of Oakland, California, has an incremental bending machine which can form helix shapes in pipes up to 60 inches in diameter. The bending is performed with pressurized water inside of the pipe.

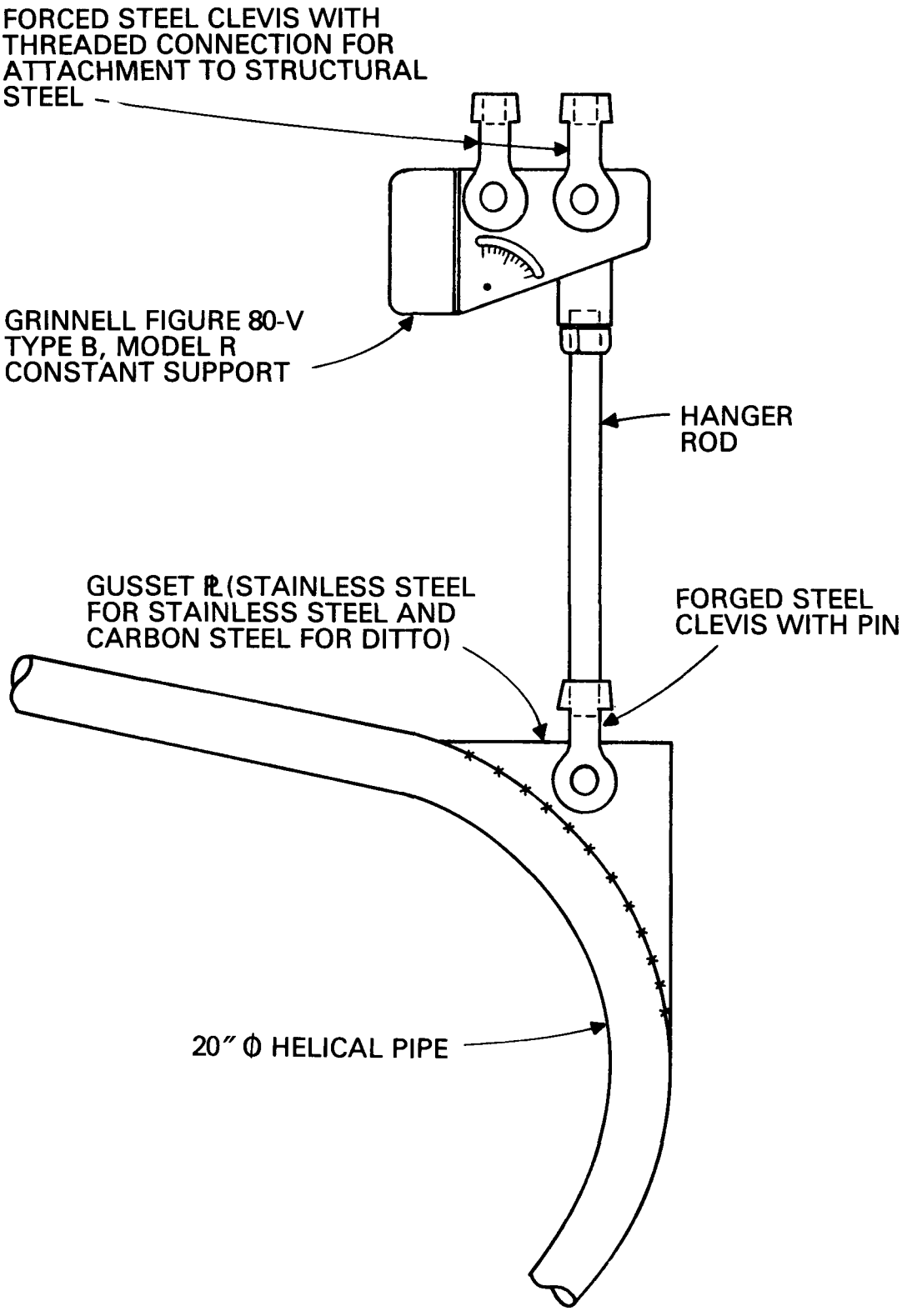

Figure 5.3-23. Pipe Hanger

5.3.4 PUMPS AND PIPING SELECTION

It is necessary to examine the system pressure drops in considerable detail to determine the most critical operating modes in order to specify the pumps for this plant. This analysis and the final pump specifications are presented in this section.

Storage Tank Pressures

Presented below is an analysis of the pressures in the hot and cold storage tanks as a function of tank levels. The analysis addresses the case with one hot tank and one cold tank joined by a pressure equalization line. A six tank analysis would be identical since the tanks are in tandem. The analytical model used for the analysis is shown in Figure 5.3-24.

The mass of gas is assumed trapped in the tops of the tanks and moves from one tank to the other as the sodium is displaced by ΔV_C in the cold tank and ΔV_H in the hot tank. It is further assumed that the gas in the tanks is always in thermal equilibrium with the sodium in the tank (T_C and T_H respectively for the cold and hot tanks). Since the mass of gas is held constant

$$V_{ch}\rho_C + V_{Hh}\rho_H = W_T = \text{constant} \qquad (5.3\text{-}13)$$

where: ρ_C = density of gas in cold tank

ρ_H = density of gas in hot tank

W_T = total weight of gas

But from the gas law:

$$\rho_C = P_C/RT_C \text{ and } \rho_H = P_H/RT_H \qquad (5.3\text{-}14)$$

Introducing Equation (5.3-14) into Equation (5.3-13) and noting that $P_C = P_H = P_g$ as a result of the pressure equalization line:

$$P_g = RW_T/(V_{ch}/T_c + V_{Hh}/T_H) \qquad (5.3\text{-}15)$$

The initial conditions in the tanks are cold tank empty (V_{CO}) and hot tank full (V_{HO}) from which the initial gas pressure can be derived using Equation (5.3-15).

$$P_{go} = RW_T/(V_{CO}/T_C + V_{HO}/T_H) \qquad (5.3\text{-}16)$$

As sodium is displaced from one tank over to the other, mass is conserved:

$$\Delta V_c\rho_{NC} = \Delta V_H\rho_{NH} \qquad (5.3\text{-}17)$$

where: ρ_{NC} = density of sodium in cold tank

ρ_{NH} = density of sodium in hot tank

From Figure 5.3-24, note that $V_{ch} = V_{CO} - \Delta V_c$ and $V_{Hh} = V_{HO} + \Delta V_H$ from which Equation (5.3-15) becomes:

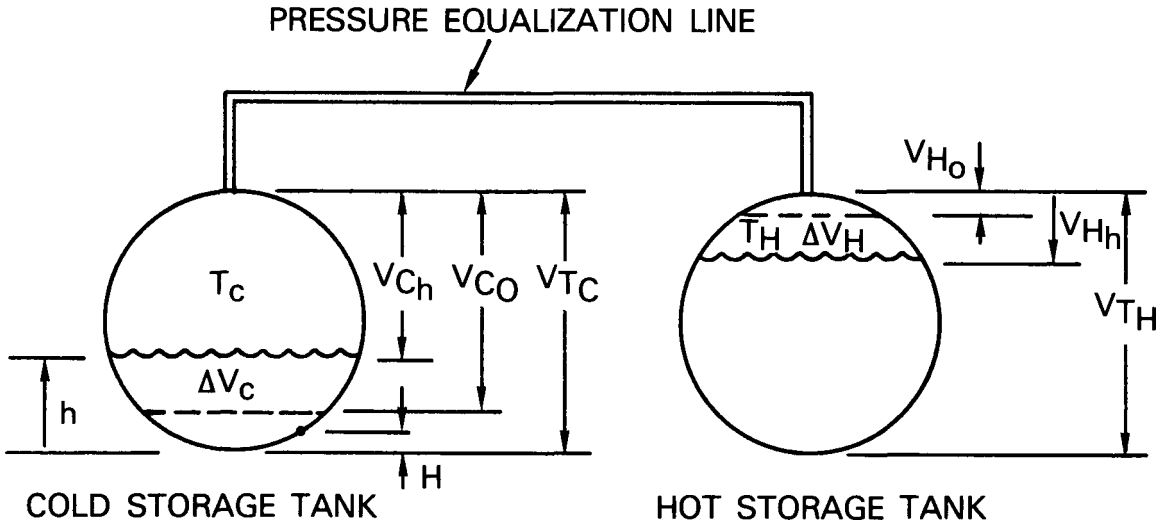

Figure 5.3-24. Analytical Model Used in Establishing Storage Tank Pressures

$$Pg = RW_T/[(V_{CO} - \Delta V_c)/T_C + (V_{HO} + \Delta V_H)/T_H]$$

$$Pg = (RW_T\, T_c/V_{CO})/\left[\left(1+ \frac{V_{HO}}{V_{CO}}\frac{T_C}{T_H}\right) + \frac{\Delta V_C}{V_{CO}}\left(\frac{\Delta V_H}{\Delta V_C}\frac{T_C}{T_H} - 1\right)\right] \qquad (5.3\text{-}18)$$

Substituting Equation (5.3-16) and Equation (5.3-17) into Equation (5.3-18):

$$Pg = \frac{P_{go}\left(1+ \frac{V_{HO}}{V_{CO}}\frac{T_C}{T_H}\right)}{\left(1+ \frac{V_{HO}}{V_{CO}}\frac{T_C}{T_H}\right) + \frac{\Delta V_c}{V_{CO}}\left(\frac{\rho_{NC}}{\rho_{NH}} - 1\right)}$$

But $\Delta V_c = V_{CO} - V_{ch}$ (see Figure 5.3-24). Thus:

$$\frac{P_g}{P_{go}} = 1/\,1 + \left(1- \frac{V_{ch}}{V_{CO}}\right)\left(\frac{\rho_{NC}}{\rho_{NH}}\frac{T_C}{T_H} - 1\right)/\,1 + \frac{V_{HO}}{V_{CO}}\frac{T_C}{T_H} \qquad (5.3\text{-}19)$$

When cold (86 F), the radius of the cold tank is r_{co} = 61.0/2 = 30.5 feet. When hot (614 F), the cold tank will expand to

$$r_c = 30.5 \times 12\ (1 + \alpha\Delta T) = 366\ (1 + 7.23 \times 10^{-6}\ (614\text{-}86))$$

$$r_c = 30.62 \text{ ft (radius)}$$

The volume of the cold tank (614 F) is

$$V_{TC} = (4/3)\ \pi\ r_c^{\,3} = 120255 \text{ ft}^3$$

The corresponding volume required in the hot tank (1100 F) is

$$V_{TH} = V_{TC}\frac{\rho_{NC}}{\rho_{NH}} = 120255\ \frac{54.6}{50.6} = 129762 \text{ ft}^3$$

The corresponding radius of the hot tank at 1100 F is r_H = 31.41 ft. When cooled to ambient temperature (86 F), the hot tank radius becomes

$$r_{HO} = r_H\ (1 - 10.8 \times 10^{-6}(1100\text{-}86)) = 31.07 \text{ ft}$$

It it is assumed that both tanks will be operated between 5 percent and 95 percent full, then from Figure 5.3-24 it follows that:

$$V_{CO} = 120255 \times .95 = 114242 \text{ ft}^3 \quad (5.3\text{-}20)$$

$$V_{HO} = 129762 \times .05 = 6488 \text{ ft}^3 \quad (5.3\text{-}21)$$

$$\frac{V_{HO}}{V_{CO}} = .056792 \quad (5.3\text{-}22)$$

$$\frac{T_C}{T_H} = \frac{(614 + 460)}{(1100 + 460)} = 0.68846 \quad (5.3\text{-}23)$$

$$\frac{\rho_{NC}}{\rho_{NH}} = \frac{54.6}{50.6} = 1.07905 \quad (5.3\text{-}24)$$

Substituting Equations (5.3-20) through (5.3-24) into (5.3-19) gives:

$$P_g/P_{go} = 1/(0.752558 + 2.16591 \times 10^{-6} V_{ch}) \quad (5.3\text{-}25)$$

The volume V_{ch} corresponding to tank depth h is given by:

$$V_{ch} = V_{TC} - \pi/3h^2 (3r_c - h) \quad (5.3\text{-}26)$$

Equations (5.3-25) and (5.3-26) can be used to determine the gas pressure in the tanks at any tank depth h in the cold tank.

The pressure on the tank wall at any elevation H (see Figure 5.3-24) is obtained from

$$P_H = P_g + (h-H) \rho_{NC}/144 \quad (5.3\text{-}27)$$

The volume in the hot tank can be calculated from noting the conservation of sodium mass between tanks:

$$V_{CN} \rho_{NC} + V_{HN} \rho_{NH} = V_{TC} \rho_{NC} \quad (5.3\text{-}28)$$

where: V_{CN} = volume of sodium in cold tank
V_{HN} = volume of sodium in hot tank

The total tank volumes in each case are

$$V_{TC} = V_{CN} + V_{ch} \text{ and } V_{TH} = V_{HN} + V_{Hh} \quad (5.3\text{-}29)$$

From Equations (5.3-28) and (5.3-29):

$$V_{ch} = V_{TH} \frac{\rho_{NH}}{\rho_{NC}} - V_{Hh} \frac{\rho_{NH}}{\rho_{NC}} \quad (5.3\text{-}30)$$

Substituting Equation (5.3-30) into (5.3-25):

$$P_g/P_{go} = 1/(1.01302 - 2.00724 \times 10^{-6} V_{Hh}) \qquad (5.3\text{-}31)$$

The gas pressure in both tanks should always be greater than atmospheric. Therefore the following minimum gas pressure corresponding to an empty cold tank (5 percent full) was established:

$$P_{go} = 17.2 \pm 1.0 \text{ psia}$$

Using the high tolerance value P_{go} = 18.2 psia and a full cold tank (95 percent full) was established:

$$P_g = 23.76 \text{ psia or } 9.06 \text{ psig}$$

The ASME Pressure Vessel and Piping Code requires that all vessels be protected against overpressure conditions. A safety valve on a sodium system is impractical because the sodium vapor in the argon wets the valve and any leakage of argon or any operation of the valve will let oxygen react with the sodium resulting in severe corrosion. Since the corrosion could lead to a nonfunctioning safety valve, it is necessary to use rupture discs on the tanks instead of safety valves. In the design of the rupture disc, there must be an allowance between the elastic limit and rupture stress in setting the design and rupture pressures to avoid creep type failure in the disc. The highest operating gas pressure in the tank occurs when the cold tank is full (95 percent) and the +1 psi high side tolerance is applied. For this condition equations (5.3-25) and (5.3-26) give a maximum operating gas pressure of 23.773 psia or 9.06 psig. The burst disc pressure was set 30 percent above this highest operating pressure:

$$P_B = 9.06\ (1 + .30) = 11.778 \text{ (use 12.0 psig)}$$

Rupture discs have a tolerance on burst pressure due to manufacturing tolerances; therefore a manufacting tolerance of ± 1 psi was applied. The rupture disc will burst in the range:

$$P_B = 13.0 \pm 1 \text{ psig}$$

Tables 5.3-7 and 5.3-8 show pressure characteristics for the cold and hot tanks respectively. The pressures shown are operating pressures. Note that the maximum tank pressure at the maximum burst pressure for the rupture disc (14 psig) is:

$$P_{Hmax} = P_{design} = P_H + (14 - P_g) \qquad (5.3\text{-}32)$$

This becomes the design pressure for the tank. Table 5.3-9 shows the operating and design pressures calculated for the top and bottom halves of the hot and cold tank using the maximum pressure data from Tables 5.3-7 and 5.3-8.

These design pressures were used to design the storage tanks where the wall thickness on the bottom half of the tank was made thicker than the wall thickness on the top half corresponding to the top half and bottom half design pressures given in Table 5.3-9.

Table 5.3-7

COLD STORAGE TANK PRESSURES

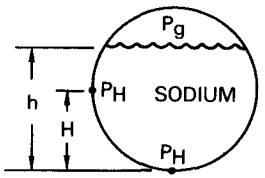

h	H	V	V/V_T	Minimum		Nominal		Maximum	
(ft)	(ft)	(ft^3)	(% full)	P_g(psig)	P_H(psig)	P_g(psig)	P_H(psig)	P_g(psig)	P_H(psig)
0	0.0	0	0	1.292	1.292	2.279	2.279	3.266	3.266
4	0.0	1472	0.01224	1.342	2.859	2.333	3.849	3.323	4.839
8	0.0	5620	0.04674	1.486	4.520	2.485	5.519	3.484	6.518
8.288	0.0	6011	0.05000	1.5000	4.642	2.5000	5.642	3.5000	6.642
12	0.0	12043	0.10014	1.714	6.264	2.727	7.277	3.741	8.291
20	0.0	30101	0.2503	2.391	9.974	3.446	11.029	4.501	12.084
30.62	0.0	60128	0.5000	3.648	15.258	4.781	16.391	5.914	17.524
40	0.0	86892	0.7226	4.936	20.102	6.148	21.314	7.360	22.526
48	0.0	105823	0.8800	5.960	24.160	7.235	25.435	8.510	26.710
52.951	0.0	114242	0.9500	6.450	26.527	7.755	27.833	9.061	29.138
56	0.0	117765	0.9793	6.661	27.895	7.980	29.213	9.299	30.532
61.24	0.0	120255	1.0000	6.812	30.032	8.140	31.360	9.468	32.688
30.62	30.62	60128	0.5000	3.648	3.648	4.781	4.781	5.914	5.914
40.0	30.62	86892	0.7226	4.936	8.492	6.148	9.704	7.360	10.916
48.0	30.62	105823	0.8800	5.960	12.55	7.235	13.825	8.510	15.100
52.951	30.62	114242	0.9500	6.450	14.917	7.755	16.223	9.061	17.528
56	30.62	117765	0.9793	6.661	16.285	7.990	17.603	9.299	18.922
61.24	30.62	120255	1.0000	6.812	18.422	8.140	19.750	9.468	21.078

Table 5.3-8

HOT STORAGE TANK PRESSURES

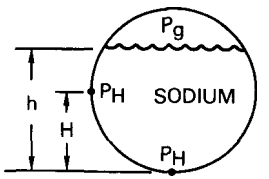

h	H	V	V/V_T	Minimum		Nominal		Maximum	
(ft)	(ft)	(ft^3)	(% full)	P_g(psig)	P_H(psig)	P_g(psig)	P_H(psig)	P_g(psig)	P_H(psig)
0	0	0	0	6.827	6.827	8.155	8.155	9.484	9.484
4	0	1512	0.01165	6.740	8.146	8.064	9.469	9.387	10.793
8	0	5779	0.04454	6.500	9.311	7.808	10.620	9.117	11.928
8.501	0	6488	0.05000	6.460	9.448	7.767	10.754	9.073	12.060
12	0	12400	0.09556	6.137	10.354	7.424	11.640	8.710	12.927
20	0	31093	0.2396	5.178	12.206	6.405	13.433	7.632	14.660
31.41	0	64903	0.5000	3.650	14.687	4.783	15.820	5.915	16.953
40	0	90863	0.7002	2.627	16.683	3.697	17.752	4.766	18.822
48	0	111541	0.8596	1.891	18.757	2.915	19.782	3.939	20.806
54.289	0	123274	0.9500	1.500	20.577	2.500	21.577	3.500	22.577
58	0	127630	0.9836	1.360	21.740	2.351	22.732	3.342	23.723
62.82	0	129806	1.0000	1.290	23.365	2.277	24.352	3.265	25.339
31.41	31.41	64903	0.5000	3.650	3.650	4.783	4.783	5.915	5.915
40	31.41	90863	0.7002	2.627	5.646	3.697	6.715	4.766	7.785
48	31.41	111541	0.8596	1.891	7.720	2.915	8.744	3.939	9.769
54.289	31.41	123274	0.9500	1.500	9.539	2.500	10.539	3.500	11.539
58	31.41	127630	0.9836	1.360	10.703	2.351	11.694	3.342	12.686
62.82	31.41	129806	1.0000	1.290	12.328	2.277	13.315	3.265	14.302

Table 5.3-9

TANK DESIGN PRESSURES

	Top Half		Bottom Half	
	Maximum Operating Pressure(psig)	Tank Design Pressure(psig)	Maximum Operating Pressure(psig)	Tank Design Pressure(psig)
Hot Tank	14.3	25.0	25.3	36.1
Cold Tank	21.1	25.6	32.7	37.2

Figure 5.3-25 shows a plot of tank pressure characteristics for both the hot and cold storage tanks.

Figure 5.3-26 gives the operating time remaining at levels beyond the normal cutoff levels for the case where full receiver flow is assumed into the tank with no flow on the steam generator side. This shows that there is adequate time for alarms to alert the operator.

Steam Generator Subsystem Pressure

Figure 5.3-27 illustrates the analytical model used to calculate the system pressures in the steam generator subsystem. Shown are pipe sizes, flow rates, and elevations of key points in the system. The following equation was used to calculate the pressure differential between two points, A and B, in the system where the flow convention used is flow from B to A.

$$P_B - P_A = \frac{0.02517}{\rho}\left[\frac{W_A^2}{d_A^4} - \frac{W_B^2}{d_B^4}\right]\frac{1}{144} + (Z_A - Z_B)\frac{\rho}{144} + \Delta P_{friction} \qquad (5.3\text{-}33)$$

where: P = pressure (psi)
ρ = fluid density (lb/ft^3)
W = mass flow rate (lb/hr)
d = pipe ID (in.)
Z = elevation

The friction pressure loss $\Delta P_{friction}$ was calculated from:

$$\Delta P_{friction} = f\frac{L_{eq}}{D}\frac{V^2}{2g}\frac{\rho}{144} \qquad (5.3\text{-}34)$$

where: L_{eq} = equivalent length
D = pipe ID
V = flow speed (ft/sec)
g = a constant

The value for L_{eq} is the total length of pipe between points A and B plus additional equivalent length for any valves, tees, elbows, etc., that may be contained in that segment of pipe. Expansions, contractions and side flow from tees were also computed using the equivalent length approach where the equivalent length was always based on the line with the smaller diameter.

The results of the pressure loss calculation are contained in Table 5.3-10 for full design flow rates. The values of P_A and P_B listed correspond to a system configuration where the hot tank is empty (5 percent full) and the lower limit gas pressure is present. Thus the cover gas pressure at point 1 in the system model is 6.460 psig which corresponds to the cover gas pressure shown in Table 5.3-8 for the low limit gas pressure and an empty hot tank (5 percent full).

The solution starts at the cover gas pressure in the hot tank (point 1) and proceeds up to the pump section (point 6) using Equations (5.3-33) and (5.3-34). The solution next moves to the cover gas in the cold tank (point 1)

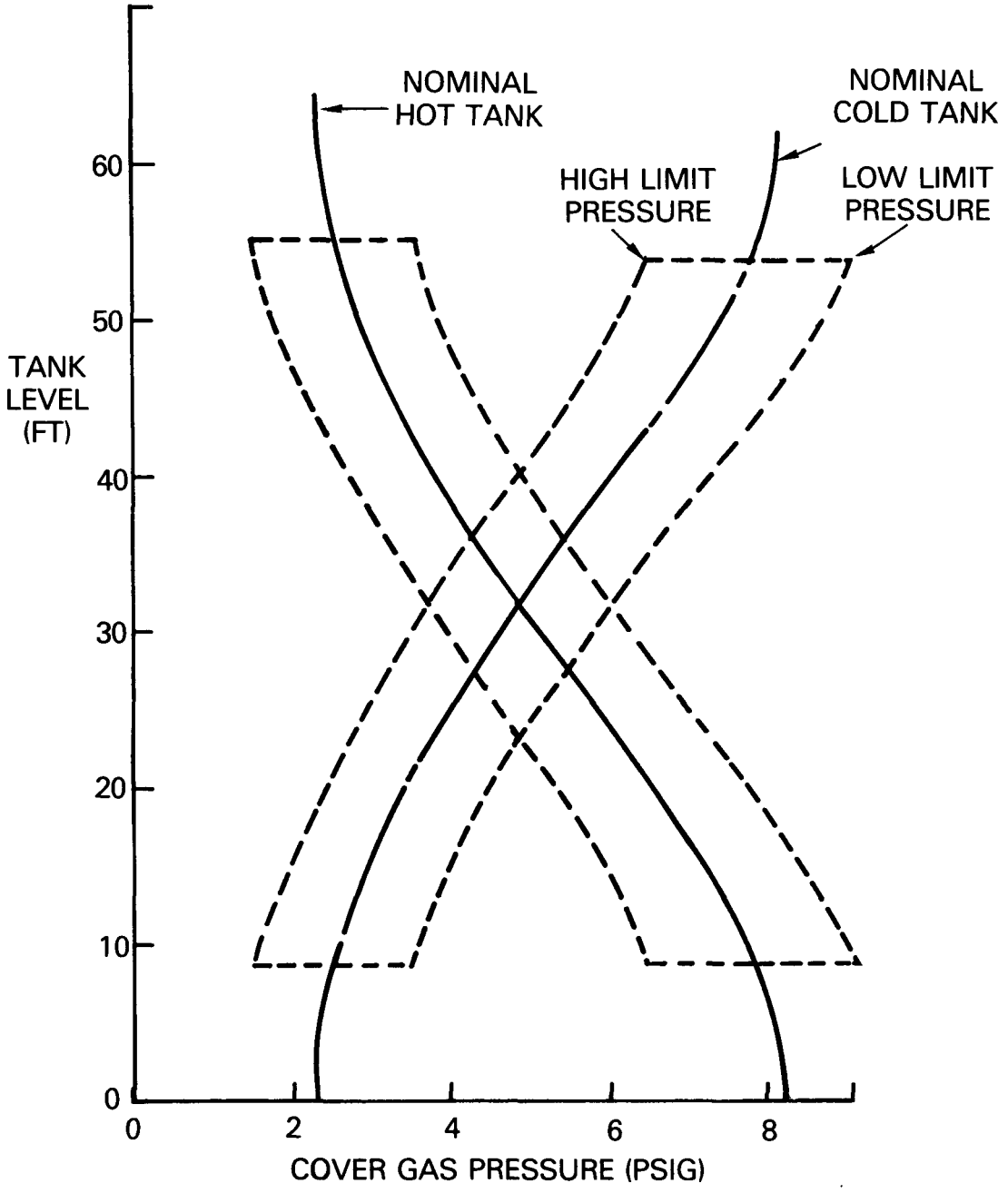

Figure 5.3-25. Cover Gas Pressure Characteristics for Hot and Cold Storage Tanks

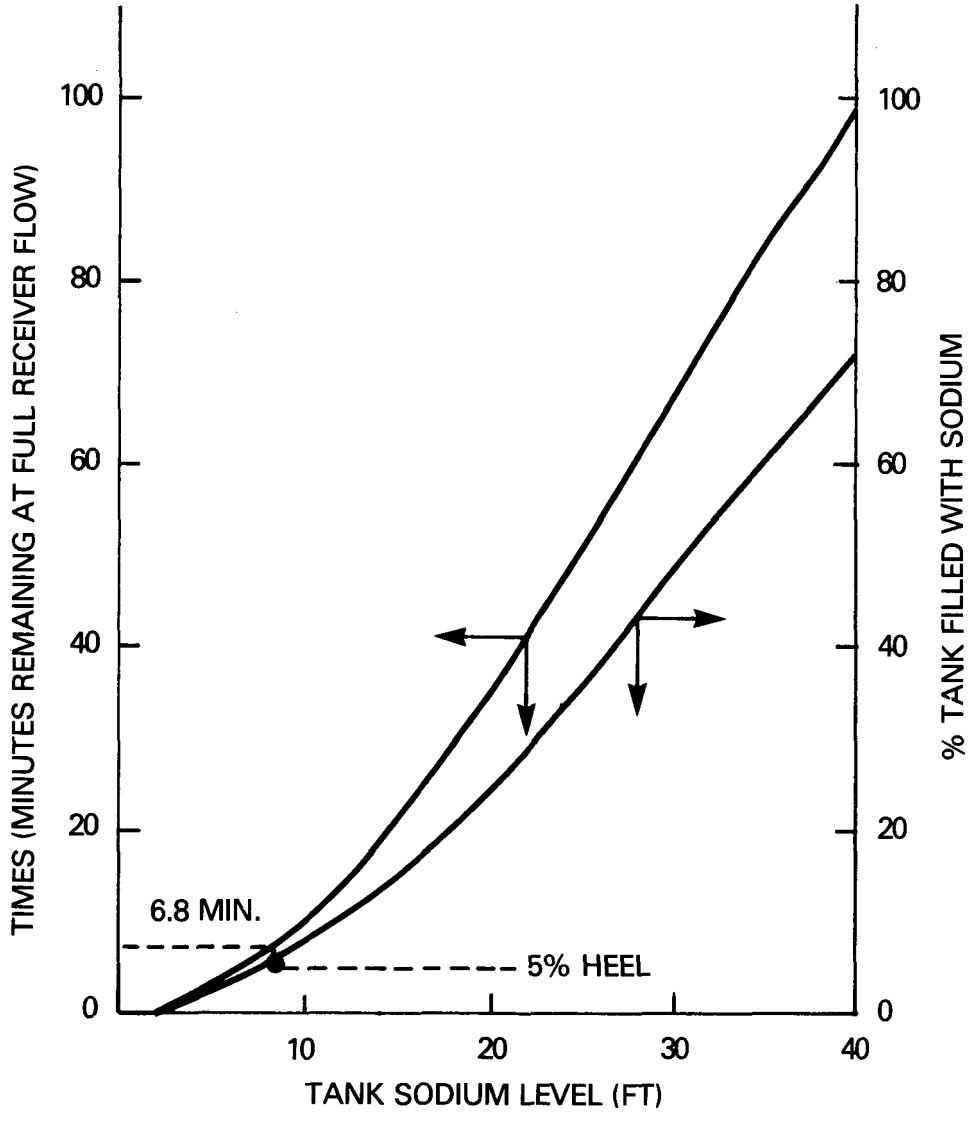

Figure 5.3-26. Storage Tank Fill Characteristics

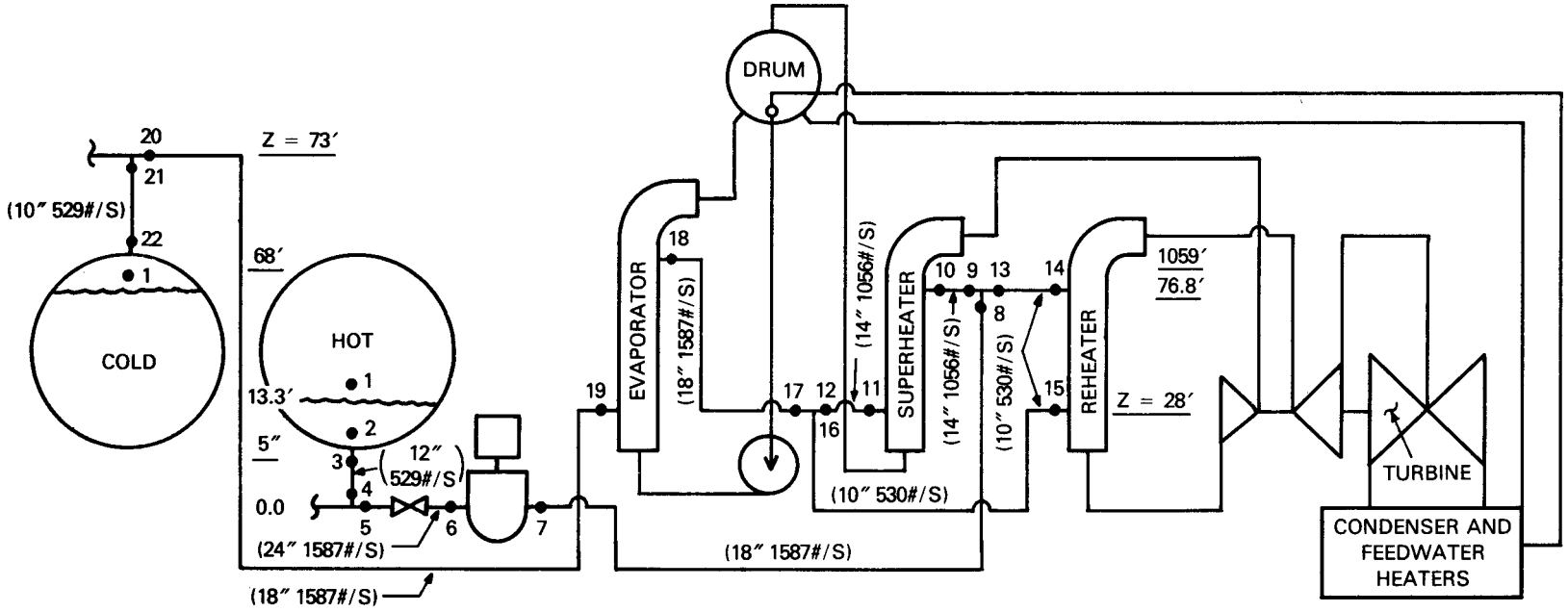

Figure 5.3-27. Steam Generator Subsystem Model Used to Establish System Pressures

Table 5.3-10

STEAM GENERATOR SUBSYSTEM PRESSURE CALCULATIONS - CASE A

Segment A	Segment B	d_A ID (in.)	d_B ID (in.)	W_A lb/hr x 10^{-6}	W_B lb/hr x 10^{-6}	L_{eq} (ft)	Z_A (ft)	Z_B (ft)	ΔP_{vel} (psid)	ΔP_Z (psid)	$\Delta P_{frict.}$ (psid)	$P_B - P_A$ (psid)	P_A (psig)	P_B (psig)
2	1	36	72	1.909	1.909	8.3	5	13.3	0.011	-2.917	0.00	-2.905	9.365	6.460
3	2	12.25	12.25	1.909	1.909	10.0	5	5	0.00	0.00	0.095	0.095	9.270	9.365
4	3	12.25	12.25	1.909	1.909	50.0	3	5	0.00	-0.703	0.476	-0.227	9.497	9.270
5	4	23.00	12.25	5.712	1.909	55.0	3	3	-0.250	0.00	0.523	0.273	9.224	9.497
6	5	23.00	23.00	5.712	5.712	298.0	0	3	0.00	-1.054	1.010	-0.044	9.268	9.224
1	22	72.0	10.25	1.909	1.909	25.0	68	68	-1.690	0.00	0.495	-1.195	6.460	5.265
22	21	10.25	10.25	1.909	1.909	83.0	68	73	0.00	-1.896	1.644	-0.252	5.265	5.013
21	20	10.25	17.25	1.909	5.712	55.0	73	73	-0.196	0.00	1.090	0.894	5.013	5.907
20	19	17.25	17.25	5.712	5.712	410.0	73	28	0.00	17.063	5.590	22.653	5.907	28.560
19	18	17.25	17.25	5.712	5.712	EVAP ΔP	28	105.9	0.00	-29.537	13.000	-16.537	28.560	12.023
18	17	17.25	17.25	5.712	5.712	177	105.9	28	0.00	29.537	2.410	31.947	12.023	43.970
17	16	17.25	10.25	5.712	1.909	42	28	28	0.204	0.00	0.940	1.144	43.970	45.114
16	15	10.25	10.25	1.909	1.909	167	28	28	0.00	0.00	9.310*	9.310*	45.114	54.424
15	14	10.25	10.25	1.909	1.909	R/H ΔP	28	76.8	0.00	-17.470	4.00	-13.470	54.424	40.954
14	13	10.25	10.25	1.909	1.909	132	76.8	76.8	0.00	0.00	2.240	2.240	40.954	43.194
13	8	10.25	17.25	1.909	5.712	10	76.8	76.8	-0.212	0.00	0.230	0.018	43.194	43.212
17	12	17.25	13.376	5.712	3.803	50	28	28	-0.443	0.00	1.015	0.572	43.970	44.542
12	11	13.376	13.376	3.803	3.803	159	28	28	0.00	0.00	2.230	2.230	44.542	46.772
11	10	13.376	13.376	3.803	3.803	S/H ΔP	28	76.8	0.00	-17.470	10.000	-7.470	46.772	39.302
10	9	13.376	13.376	3.803	3.803	119	76.8	76.8	0.00	0.00	2.090	2.090	39.302	41.392
9	8	13.376	17.25	3.803	5.712	75	76.8	76.8	0.460	0.00	1.360	1.820	41.392	43.212
8	7	17.25	17.25	5.712	5.712	365	76.8	0.0	0.00	26.987	4.980	31.967	43.212	75.179

*9.310 Includes control valve ΔP = 6.620 psi

and progressively solves each pressure point moving backward numerically from point 22 to point 7. There are two branches to this path: one through the superheater and one through the reheater.

To balance the pressure drop in both branches, a resistance (ΔP = 6.62 psid) must be added to the reheater branch. This will be provided for by adding a throttle valve between points 15 and 16 as indicated in Figures 5.3-28 through 5.3-31. This throttle valve will be used during operation to control the superheater to reheater heat split to that required by the steam turbine.

When the calculations are completed, points 6 and 7 provide the required data for calculating the pump head. Other key operating configurations were evaluated in the same manner always starting the solution with the cover gas pressure in the storage tanks as given by Tables 5.3-7 and 5.3-8. Table 5.3-11 tabulates the pressures at all 22 points for four key operating conditions identified as Cases A through D. Each case provides data with respect to the steam generator subsystem design as indicated in the footnotes of Table 5.3-11.

Receiver Subsystem Pressures

Figure 5.3-28 illustrates the analytical model used to calculate the system pressures in the receiver subsystem. Shown are pipe diameters, flow rates, and elevations of key points in the system. The analytical technique employed is very similar to that used for calculating system pressures in the steam generator subsystem. Equations (5.3-33) and (5.3-34) were employed as described earlier to calculate the pressures at the various points in the system.

Table 5.3-12 gives details of the calculations which determined the pressure in all 37 points in the receiver subsystem. The values of P_A and P_B shown in Table 5.3-12 correspond to the lowest suction head pressure case for the pump. Under this condition, assurance must be provided that all system pressures are higher than atmospheric pressure. Therefore point 15 in the receiver at the top of the tower, which is the lowest pressure point in the receiver subsystem, was intentionally set equal to zero to start the solution. From point 15, the solution proceeds down paths 15, 14, 24, and 25. The control system uses the throttle valve to hold P_{25} equal to P_{37} therefore the first steps arrived at P_{25}. By starting at point 14, the solution then moves backward with respect to flow arriving at the hot panel central header (point 8). The panel flow shown in Table 5.3-12 corresponds to a single tube in the hot panel. The flows and pressure losses through all 108 tubes are assumed to be equal.

The solution next proceeds in the direction of flow through the bottom branch of the hot panel (points 16 through 20) and on into the collection header, arriving at point 25. The flows in the top and bottom halves of the hot panel were assumed to be equal. It was found that this flow path gave a pressure P_{25} which was 1.761 psi too high to match the value obtained in the first step where P_{25} was calculated. Therefore, a restriction was added (ΔP = 1.761 psid)

Table 5.3-11

STEAM GENERATOR SUBSYSTEM SODIUM PRESSURE DATA - KEY DESIGN CASES
(Pressures in psig)

Point No.	A Full Flow P_g = Low Limit Hot Tank Empty	B Full Flow P_g = Nominal Tanks Half Full[a]	C Full Flow P_g = High Limit Hot Tank Full	D Full Flow P_g = Low Limit Hot Tank Full
1	6.460	4.783	3.500	1.500
2	9.365	15.737	22.494[b]	20.494
3	9.270	15.642	22.399	20.399
4	9.497	15.869	22.626	20.626
5	9.224	15.596	22.353	20.353
6	9.268	15.640	22.397	20.397
Pump ΔP	65.911[c]	57.862	49.822	49.822
7	75.179[d]	73.502	72.219	70.219
8	43.212	41.535	40.252	38.252
9	41.392	39.715	38.432	36.432
10	39.302	37.625	36.342	34.342
11	46.772	45.095	43.812	41.812
12	44.542	42.865	41.582	39.582
13	43.194	41.517	40.234	38.234
14	40.954	39.277	37.994	35.994
15	54.424	52.747	51.464	49.464
Valve ΔP	6.620	6.620	6.62	6.62
16	45.114	43.437	42.154	40.154
17	43.970	42.293	41.010	39.010
18	12.023	10.346	9.063	7.063
19	28.560	26.883	25.600	23.600
20	5.907	4.230	2.947	0.947
21	5.013	3.336	2.053	0.053[e]
22	5.265	3.588	2.305	0.305

[a] Design case (noon)

[b] Maximum pressure case - pump suction side

[c] Maximum pump head

[d] Maximum pressure case - pump discharge side

[e] Minimum system pressure > 0 psig

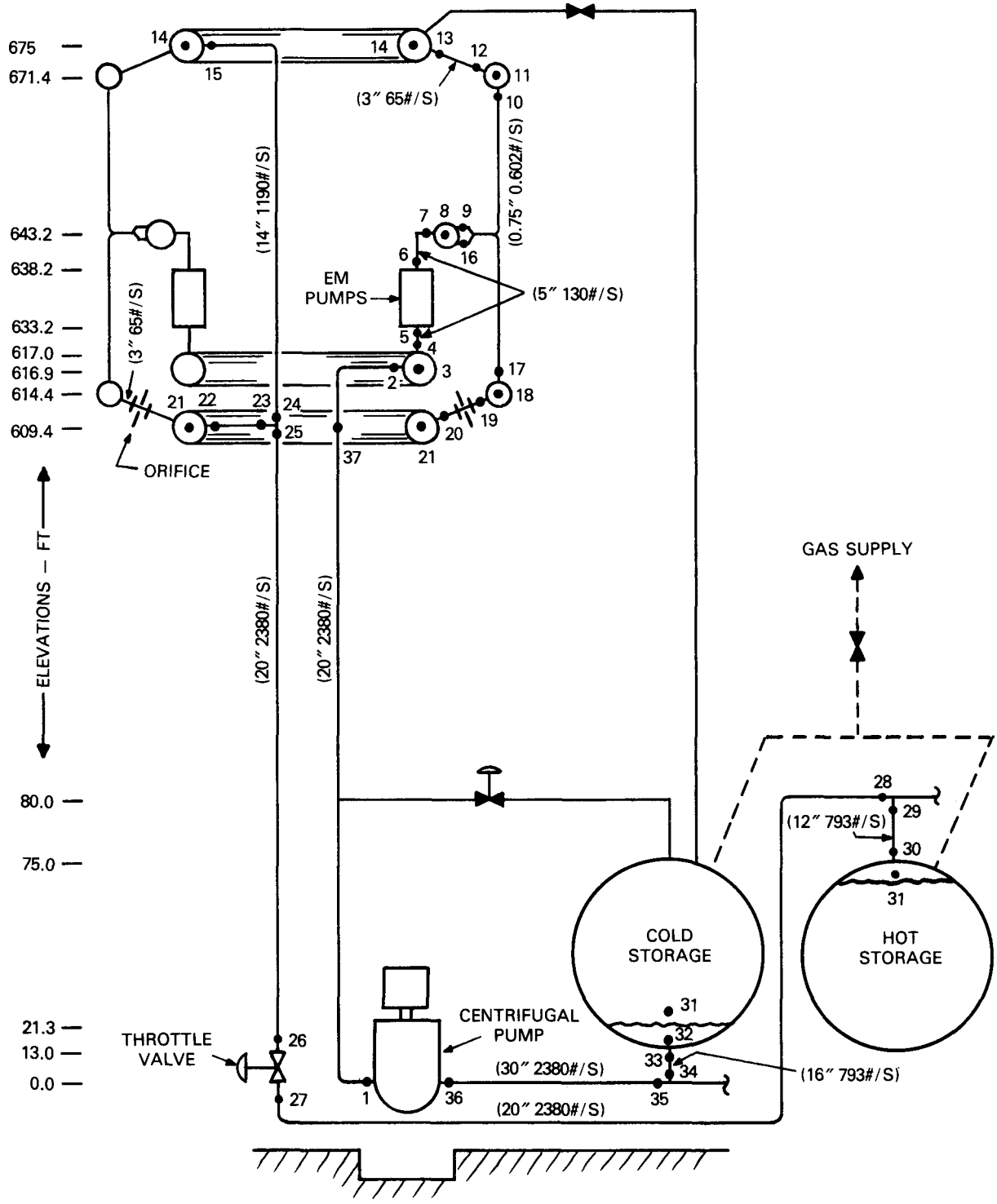

Figure 5.3-28. Receiver Subsystem Model Used to Establish System Pressures

Table 5.3-12

RECEIVER SUBSYSTEM PRESSURE CALCULATIONS

Segment A	Segment B	d_A ID (in.)	d_B ID (in.)	W_A (lb/hr x 10^{-6})	W_B (lb/hr x 10^{-6})	L_{eq} (ft)	Z_A (ft)	Z_B (ft)	ΔP_{vel} (psid)	ΔP_Z (psid)	$\Delta P_{frict.}$ (psid)	$P_B - P_A$ (psid)	P_A (psig)	P_B (psig)
15	14	13.375	17.376	4.284	4.284	23	675	675	2.057	0.00	0.610	2.667	0	2.667
24	15	13.375	13.375	4.284	4.284	112	609.4	675	0.00	-23.051	2.950	-20.101	20.101	0
25	24	19.00	13.375	8.568	4.284	83	609.4	609.4	-0.056	0.00	2.190	2.134	17.967	20.101
14	13	17.376	3.250	4.284	0.2341	8	675	675	-1.602	0.00	0.930	-0.6722	2.667	1.995
13	12	3.250	3.250	0.2341	0.2341	15.2	675	671.4	0.00	1.265	1.770	3.035	1.995	5.030
12	11	3.250	12.25	0.2341	0.2341	2.8	671.4	671.4	2.702	0.00	0.330	3.032	5.030	8.062
11	10	12.25	0.65	0.2341	.002168	3.0	671.4	671.4	-0.132	0.00	0.080	-0.052	8.062	8.010
10	9	0.65	0.65	.002168	.002168	32.4	671.4	643.15	0.00	10.319	1.632	11.951	8.010	19.961
9	8	0.65	15.376	.002168	.4681	0.8	643.15	643.15	+0.115	0.00	0.020	0.135	19.961	20.096
16	8	0.65	15.376	.002168	.4681	0.8	643.15	643.15	+0.115	0.00	0.020	0.135	19.961	20.096
17	16	0.65	0.65	.002168	.002168	32.4	614.4	643.15	0.00	-10.500	1.632	-8.868	28.829	19.961
18	17	12.25	0.65	.2341	.002168	3.0	614.4	614.4	-0.132	0.00	0.080	-0.052	28.881	28.829
19	18	3.250	12.25	.2341	.2341	2.8	614.4	614.4	2.702	0.00	0.330	3.032	25.849	28.881
20	19	3.250	3.250	.2341	.2341	15.2	609.4	614.4	0.00	-1.757	3.531*	1.774	24.075	25.849
21	20	17.376	3.250	4.284	.2341	8.0	609.4	609.4	-1.602	0.00	0.930	-0.672	24.747	24.075
22	21	13.375	17.376	4.284	4.284	23.0	609.4	609.4	2.057	0.00	0.610	2.667	22.080	24.747
23	22	13.375	13.375	4.284	4.284	75.0	609.4	609.4	0.00	0.00	1.980	1.980	20.100	22.080
25	23	19.00	13.375	8.568	4.284	83.0	609.4	609.4	-0.0563	0.00	2.190	2.134	17.967	20.100
26	25	19.00	19.00	8.568	8.568	847	10.0	609.4	0.00	-210.62	14.73	-195.89	213.857	17.967
8	7	15.376	5.295	0.4681	0.4681	4.5	643.2	643.2	-1.408	0.00	0.160	-1.248	20.096	18.848
7	6	5.295	5.295	0.4681	0.4681	33.0	643.2	638.2	0.00	1.896	1.20	3.096	18.848	21.944
37	1	19.25	19.25	8.568	8.568	1233	609.2	10.2	0.00	227.2	19.07	246.27	17.967	264.237
2	37	19.25	19.25	8.568	8.568	20.0	616.9	609.2	0.00	2.92	0.310	3.230	14.737	17.967
3	2	23.25	19.25	8.568	8.568	12.0	616.9	616.9	-1.452	0.00	0.190	-1.262	15.999	14.737
4	3	5.295	23.25	0.4681	8.568	5.0	617.0	616.9	0.141	0.038	0.190	0.369	15.639	15.999
5	4	5.295	5.295	0.4681	0.4681	54.0	633.2	617.0	0.00	6.143	1.970	8.113	7.517	15.630
32	31	72.0	732.0	2.853	2.853	8.6	5.0	13.29	0.0016	-3.143	0.00	-3.142	4.642	1.500
33	32	15.25	72.0	2.853	2.853	17.0	5.0	5.0	0.769	0.00	0.117	0.8863	3.756	4.642
34	33	15.25	15.25	2.853	2.853	60.0	3.0	5.0	0.00	-0.758	0.411	-0.347	4.103	3.756
35	34	29.0	15.25	8.568	2.853	65.0	3.0	3.0	-0.239	0.00	0.446	0.207	3.896	4.103
36	35	29.0	29.0	8.568	8.568	270.0	0.0	3.0	0.00	-1.138	0.624	-0.514	4.410	3.896
31	30	732.0	12.25	2.853	2.853	76.0	67.82	67.82	-1.998	0.00	2.000	+0.002	1.500	1.502
30	29	12.25	12.25	2.853	2.853	92.0	67.82	72.82	0.00	-1.896	1.900	+0.004	1.502	1.506
29	28	12.25	19.00	2.853	8.568	65.0	72.82	72.82	-1.034	0.00	1.210	+0.176	1.506	1.682
28	27	19.00	19.00	8.568	8.568	383.0	72.82	10.0	0.00	23.819	6.660	+30.479	1.682	32.161

*Friction loss includes $\Delta P = 1.761$ across orifice

to balance the system. If this were not done, the flow in the lower half of the hot panel would be greater than that in the top half.

The orifice is required to balance out the difference in static heads in the two panel halves; see Appendix M for a description of this orifice. The up-flow in the top half is resisted by the gravity head and the down flow in the lower half is aided by gravity.

The next step in the solution starts at the center header (point 8) in the panel and works back against the flow to pump discharge (point 6). As stated earlier, the control system is designed to maintain $P_{37} = P_{25}$; therefore the solution for the suction side of the pump starts at point 37 where the pressure is set equal to the pressure at point 25. Proceeding in the direction of flow, the pressures up to and including pump suction were calculated. The EM pump head is then determined from $P_6 - P_5$. From Table 5.3-12 it is possible to derive an expression for EM pump head consisting of the three components: velocity head, static head, and friction head.

$$P_6 - P_5 = 0.365\left(\frac{W}{W_R}\right)^2 - 0.470 + 14.532\left(\frac{W}{W_R}\right)^{1.8} \qquad (5.3\text{-}35)$$

where: W = flow in panels other than the hot panel (lb/hr)
W_R = reference flow in the hot panel (lb/hr)

Equation (5.3-35) was used to calculate the pumping power requirements for all 24 EM pumps.

From points 37 and 25 the pressures down the tower to the control valve inlet (point 26) and the centrifugal pump discharge (point 1) were calculated. The remaining solution starts with the known cover gas pressures in the storage tanks and works out the pressures back to pump suction and control valve outlet. The tank pressures shown correspond to an empty cold tank (5 percent full) and the lower limit on cover gas pressure.

The required centrifugal pump head for the tower pump is obtained from $P_1 - P_{36}$ and the pressure drop across the control valve is obtained from $P_{26} - P_{27}$.

Table 5.3-13 shows in the first column the tabulation of pressures directly from the calculations in Table 5.3-12. This case gives the lowest system pressures in the tower and represents the worst case of net positive suction head (point 36) for the centrifugal pump. Three other key cases are also shown. The second column is the nominal design case with the tanks half full. The third column, corresponding to a full cold tank and high limit on gas pressure, produces the maximum operating pressures in the line between the tanks and control valve. The last column, which shows maximum operating pressures in the remaining section of pipe results from closing the control valve to produce a zero flow situation in the tower. The pump head increases as flow is reduced, reaching a maximum value when the pump is deadheaded. It was assumed for this case that the pump was bypassing 10 percent flow to the cold tank to avoid overheating.

Table 5.3-13

RECEIVER SUBSYSTEM - SYSTEM PRESSURE DATA - KEY DESIGN CASES
(Pressures in psig)

	Full Flow P_g = Low Limit Cold Tank Empty	Full Flow P_g = Nominal Tanks Half Full	Full Flow P_g = High Limit Full Cold Tank	Zero Flow P_g = High Limit Full Cold Tank
1	264.237	275.986	286.786	327.939
2	14.737	26.486	37.286	97.819
3	15.999	27.748	38.548	97.819
4	15.639	27.388	38.188	97.781
5	7.517	19.266	30.066	91.638
6	21.944	33.693	44.493	89.742
7	18.848	30.597	41.397	87.846
8	20.096	31.845	42.645	87.846
9	19.961	31.710	42.510	87.846
10	8.010	19.759	30.559	77.527
11	8.062	19.811	30.611	77.527
12	5.030	16.779	27.579	77.527
13	1.995	13.744	24.544	76.262
14	2.667	14.416	25.216	76.262
15	0.0	11.749	22.549	76.262
16	19.961	31.710	42.510	87.846
17	28.829	40.578	51.378	98.346
18	28.881	40.630	51.430	98.346
19	25.849	37.598	48.398	98.346
20	24.070	35.819	46.619	99.313
21	24.742	36.491	47.291	99.313
22	22.081	33.830	44.630	99.313
23	20.101	31.850	42.650	99.313
24	20.101	31.850	42.650	99.313
25	17.967	29.716	40.516	99.313
26	213.860	225.609	236.409	309.933
27	32.161	35.442	39.722	30.984
28	1.682	4.963	9.243	7.165
29	1.506	4.797	9.067	7.165
30	1.502	4.783	9.063	9.061
31	1.500	4.781	9.061	9.061
32	4.642	16.391	29.138	29.138
33	3.756	15.505	26.305	29.138
34	4.103	15.852	26.652	29.896
35	3.896	15.645	26.445	29.896
36	4.410	16.159	26.959	31.034
37	17.967	29.716	42.695	99.313
Pump ΔP	259.827	259.827	259.827	296.905

Pump Efficiencies and Performance Calculations

The efficiencies established for the various system pumps, drive motors, and power controls are shown in Table 5.3-14. The required developed heads, flows, and powers are listed in Table 5.3-15 along with other pertinent pump data used in establishing the pump designs for the three large centrifugal pumps. Both the receiver pump and the water recirculation pump are constant speed pumps. The steam generator pump speed is controlled to match plant power load demands. This is accomplished by using a motor generator set which controls the electric AC frequency to the pump drive motor. This speed control on the drive motor also compensates automatically for changes in system pressure caused by the cover gas pressure changes in the two storage tanks.

The only pump which might have a net positive suction head problem with the pump inlet pressures calculated above is the receiver pump. Table 5.3-15 shows a calculated suction specific speed of 9016. Any value above 10,000 would become suspect. However, the value 9016 was calculated for a worst case consisting of full receiver flow with low level in cold tank and with minimum cover gas pressure level. The probability of ever having this condition is extremely remote. This pump, along with the other two, is considered to be free of threats from cavitation.

Mechanical Design of Large Centrifugal Pumps

Centrifugal pumps (Figure 5.3-29) were selected for the high head receiver cold leg pump and the steam generator hot leg pump because considerable design and operating experience exists for large centrifugal pumps in this general performance range. The cold leg pump requirements (20,000 gpm, 233 psi, 650 F) are in the range of the 33,500 gpm, 156 psi, 995 F Clinch River Breeder Reactor Project primary pump designed by Byron Jackson, a prototype of which is to be tested. This Advanced Central Receiver System pump will utilize a constant speed drive, since its principal function is to serve the tower head. A bypass valve located at ground level between the riser and downcomer to allow natural circulation of sodium in the receiver assembly during standby conditions can also be used to prevent overheating of the constant speed pump during low flow system startup and shutdown. The steam generator hot leg pump is much like the 14,500 gpm, 180 psi, 1100 F Fast Flux Test Facility pump designed and manufactured by Westinghouse, which has completed successful testing. The Advanced Central Receiver System pump will be equipped with a variable speed drive and a pony motor to maintain low sodium flow for standby and startup conditions. These pumps will be located at ground level in the sodium pump and auxiliary equipment building.

Both the high head receiver pump and the steam generator pump have been designed to ASME Section VIII, Division 1 rules, which is consistent with this nonnuclear application. Even though the steam generator pump operates at 1100 F, it is not judged to be necessary to use code case 1592 because this pump will experience only limited thermal cycling.

The centrifugal pump required for recirculation of feedwater through the evaporator is shown in Figure 5.3-30. This is a conventional design with an extensive operating history in fossil fueled power plants.

Table 5.3-14

PUMP AND DRIVE LINE EFFICIENCIES

Steam Generator Pump	
M-G Motor Drive	95.0
Fluid Coupling	92.8
Generator (M-G)	95.7
Pump Drive Motor	95.0
Pump Mechanical	80.0
Specific Speed	1847
Receiver Pump	
Pump Drive Motor	95.0
Pump Mechanical	80.0
Specific Speed	1300
Steam Drum Recirculation Pump	
Pump Drive Motor	95.0
Pump Mechanical	83.0
Specific Speed	1138
ALIP Absorber Panel (EM Pumps)	
EM Pump	25.0

Table 5.3-15

CENTRIFUGAL PUMP DATA

	Receiver Pump	Steam Generator Pump Nominal Power	Steam Generator Pump Max. Power	H_2O Recirculation Pump
Flow (lb/hr) (gpm)	8.568×10^6 (19565)	5.712×10^6 (14075)	5.712×10^6 (14075)	0.838×10^6 (2184)
Head (psi) (ft)	259.8 (685.2)	57.86 (164.66)	65.91 (187.57)	100.0 (301.0)
Power (MW_e) (hp)	2.9091 (3900)	0.5526 (741.0)	0.6295 (844.1)	0.1204 (161.4)
Efficiency (%) Mech.	80.0	80.0	80.0	83.0
Efficiency (%) Drive	95.0	95.0	95.0	95.0
Efficiency (%) M-G Set	-	84.4	84.4	-
Specific Speed (μ_S)	1300	1847	1847	1138
Suction Specific Speed (S)	9016	3254	3867	2930
Rotation (rpm)	1760	1012	1116	1760
Design Temperature (°F)	650	1150	1150	600
Design Pressure (psig)	350	80	80	2800
Impeller	Double Flow	Double Flow	Double Flow	Single Flow
Number of Stages	1	1	1	1

LARGE CENTRIFUGAL PUMP DATA

	TOWER PUMP (COLD LEG)	STEAM GEN. PUMP (HOT LEG)
FLOW RATE – lb/h	8.57×10^6	5.71×10^6
FLOW RATE – GPM	20,000	14,000
HORSE POWER (MAX.)	3,900	850
DESIGN TEMP – °F	650	1,150
RPM	1,760	1,116 (VARIABLE SPEED)
PUMP HEAD – ft	685	190
DESIGN PRESS. – psi	350	80
PUMP EFF. – %	78	64 (INCL MG SET)
WEIGHT – lbs.	57,000	48,000

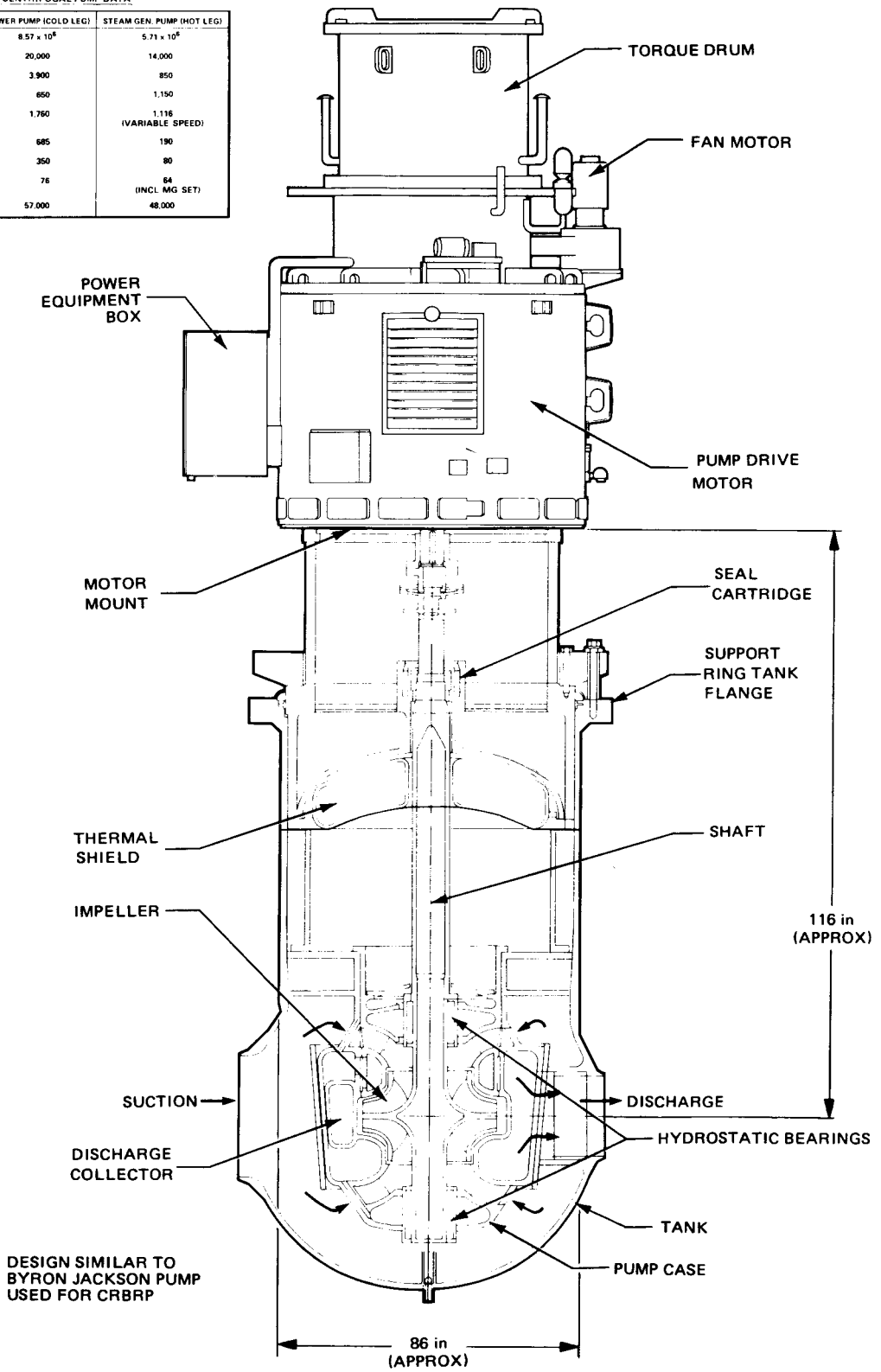

Figure 5.3-29. Sodium Centrifugal Pumps

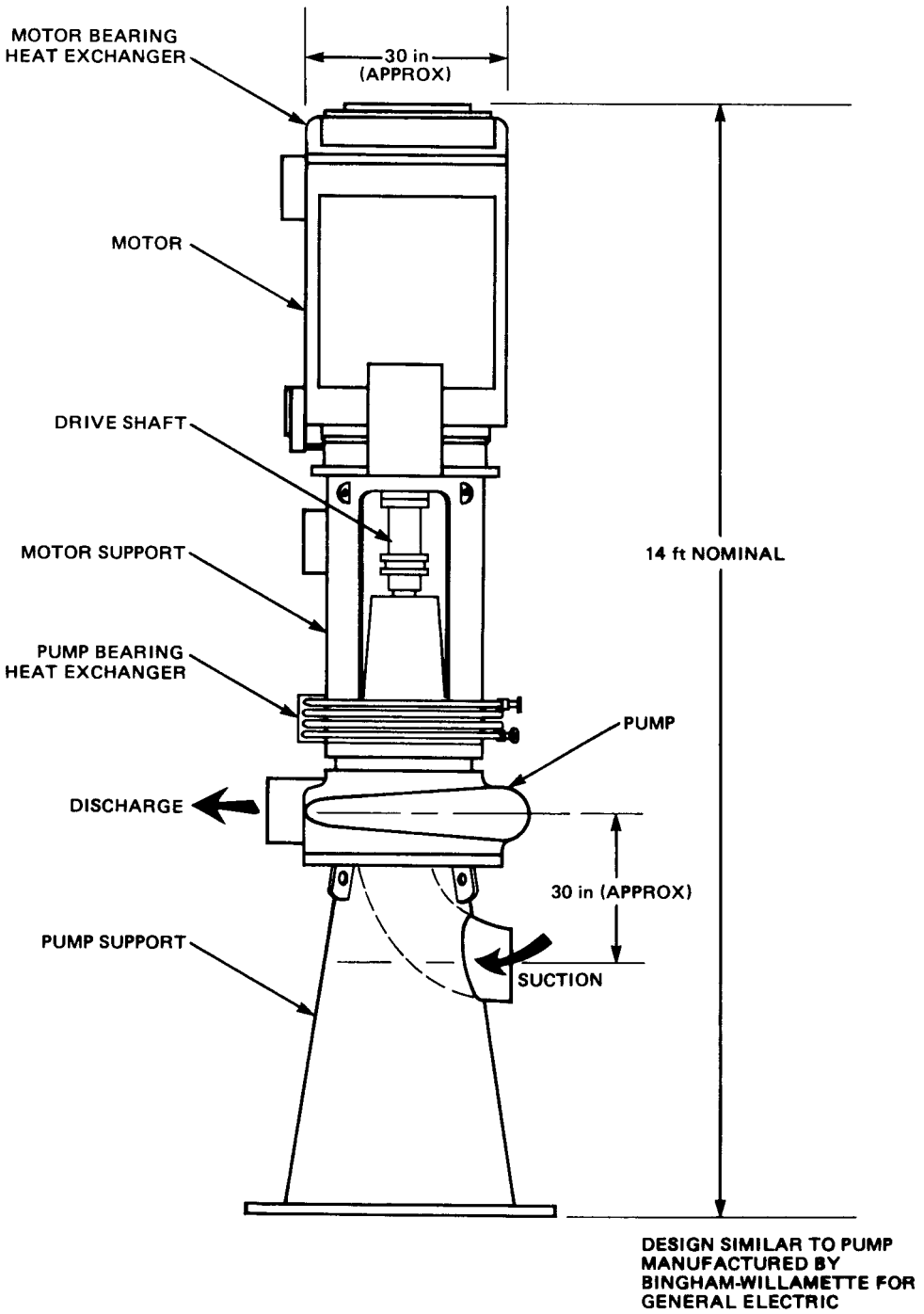

Figure 5.3-30. Recirculation Pump

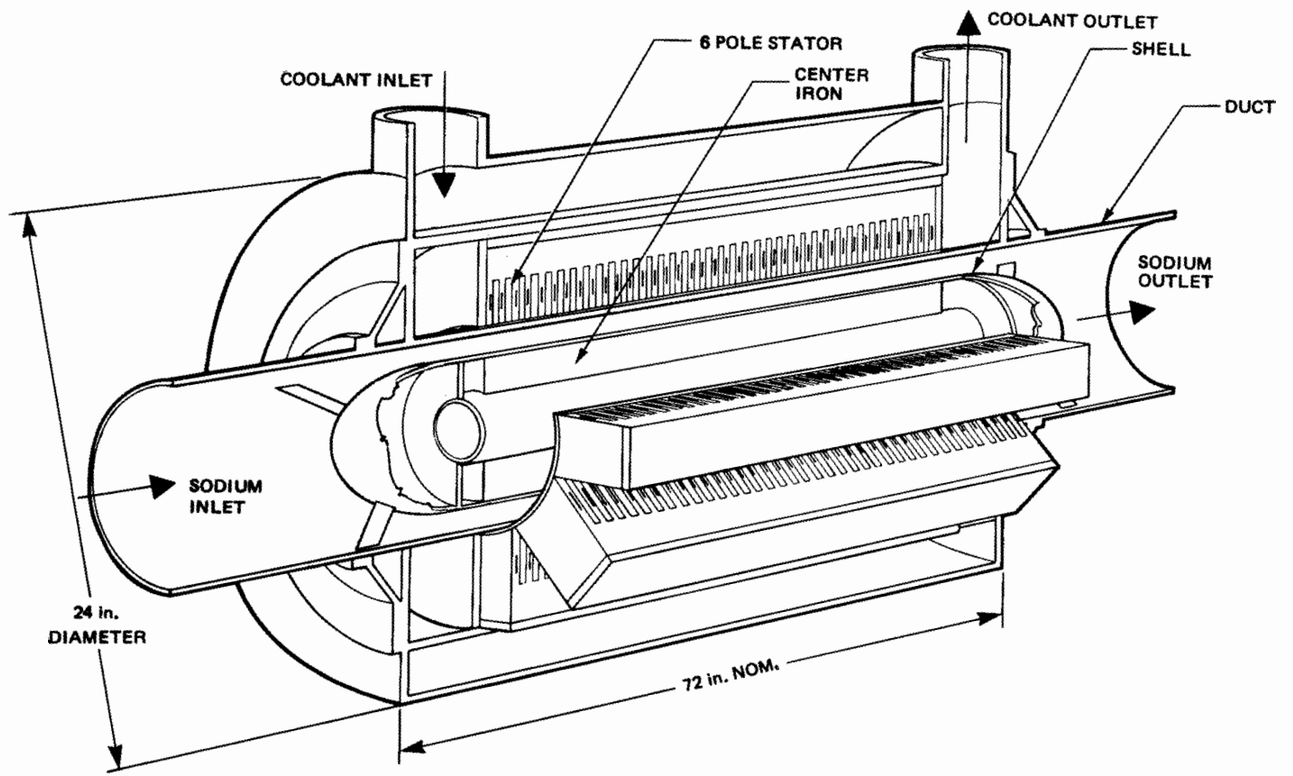

DESIGN SIMILAR TO GENERAL ELECTRIC ALIP PUMP

Figure 5.3-31. Sodium-EM Trim Pump Design

Absorber Panel Pumps

Twenty-four annular linear induction (ALIP) type EM pumps (one per absorber panel) are located in the receiver assembly at the top of the tower to provide sodium flow control to the individual absorber panels to maintain the sodium outlet temperature. These EM pumps (see Figure 5.3-31) were selected over control valves on the basis of their high reliability and good flow control capability over the entire flow range as demonstrated by the successful operation of numerous pumps of this type. These pumps have no moving parts, gas seals, or bearings.

The pump head for each of the 24 panels under full power design conditions can be calculated from Equation (5.3-35) developed earlier. Using the individual panel flow ratio W, established from the solar heat flux inputs and differential temperatures, and the hot panel flow at 100 percent power W_R, the pump head can be calculated. With the head and flow rate established, the pumping power requirements can be calculated. The results are shown in Table 5.3-16.

The ducts in these pumps are designed to ASME Section VIII, Division 1 rules.

Receiver Subsystem Piping

Table 5.3-17 shows the operating pressures and design temperatures for various segments of the receiver subsystem piping along with the pipe selections made for the application. Also shown is the calculated allowable pressure for each pipe and material selection which was made using ASME Section III, Division 1 rules. The pipe diameters were all chosen on the basis that, for reasonable pressure loss in a sodium system, the flow velocity should be less than 25 feet/second. In many instances in Table 5.3-17, the allowable pressures are much higher than required by the design from an operating pressure standpoint. In these cases, the decision was based on good piping practice with respect to welding and handling very thin wall piping. In the future, cost reductions may be realized in the Advanced Central Receiver System plant through the use of thinner wall pipes, if feasibility can be demonstrated.

The operating pressures were taken from the pressure analysis presented above with the exception that all pressures have been rounded off on the high side for operating margin.

Steam Generator Subsystem Piping

Table 5.3-18 shows similar data for the steam generator subsystem. The only new feature added is an addition of 400 psi to all the operating pressures listed to provide design allowance for the occurrence of a large steam-to-sodium leak. The design basis leak is taken to be a full double ended guillotine failure in one tube, which allows sonic water flow out of the severed ends into the sodium. This will produce the worst case acoustic pressure spike of roughly 400 psi in the affected module. With the tube sleeves brazed over the tube to tubesheet welds as described in the steam generator discussion (Section 5.3.5), the assumption of a guillotine failure may prove excessive, and system economies may be possible in the future.

Table 5.3-16

ELECTROMAGNETIC PUMP DATA

PANEL NO.	FLOW (gpm)	HEAD (psi)	HEAD (ft)	POWER (MWe)	POWER (HP)
1	1069	14.43	38.06	0.02684	35.99
2	1022	13.73	34.89	0.02352	31.54
3	976	12.09	31.89	0.02052	27.52
4	930	11.02	29.06	0.01783	23.91
5	884	9.98	26.32	0.01535	20.58
6	838	8.98	23.68	0.01309	17.55
7	792	8.04	21.20	0.01108	14.86
8	746	7.14	18.83	0.00927	12.43
9	701	6.31	16.64	0.00769	10.32
10	654	5.49	14.48	0.00625	8.38
11	608	4.73	12.47	0.00501	6.71
12	562	4.03	10.63	0.00394	5.29

EM Pump Efficiency (%)	= 25.0
Design Temperature (°F)	= 650.0
Design Pressure (psig)	= 120.0
Design Type	= ALIP
Suction Inlet OD (in.)	= 5.563
Discharge Outlet OD (in.)	= 5.563
Total Receiver Pumping Power (MW_e)	= 0.3208
Total Receiver Pumping Power (HP)	= 430.19
Total Receiver Flow (lb/hr)	= 8.568×10^6

Table 5.3-17

SODIUM PIPE SIZE SELECTIONS - RECEIVER SUBSYSTEM

Pipe Segment*	Position	Operating Press (psig)	Design Temp (°F)	Pipe Selection	Material	Allowable Press (psig)**
1-2	Riser	350	630	20 in. SCH. 20	A-106B	549
25-26	Downcomer	325	1150	20 in. SCH. 20	316	359
27-28	Hot Storage	50	1150	20 in. SCH. 20	316	359
35-36	Pump Suction	40	630	30 in. SCH. 20	A-106B	492
33-34	Cold Storage	35	630	16 in. SCH. 20	A-106B	506
29-30	Hot Storage	15	1150	12 in. SCH. 20	316	368
21	Hot Header	120	1150	18 in. SCH. 20	316	328
14	Hot Header	100	1150	18 in. SCH. 20	316	328
3	Cold Header	115	630	24 in. SCH. 20	A-106B	456
19-20	Panel Outlets	120	1150	3 in. SCH. 10	316	608
4-5	EM-Inlet	115	630	5 in. SCH. 10	A-106B	657
6-7	EM-Outlet	115	630	5 in. SCH. 10	A-106B	657

* Defined in Figure 5.3-28
**ASME, Section VIII, Division 1 (C = 0.015, E = 1.0)

Table 5.3-18

ADVANCED CENTRAL RECEIVER
SODIUM PIPE SIZE SELECTION - STEAM GENERATOR SUBSYSTEM

Pipe Segment*	Position	Design Press (psig)**	Design Temp (°F)	Pipe Selection	Material	Allowable Press (psig)†
3-4	Hot Storage	425	1150	12 in. SCH. 40	316	618
5-6	Pump Suction	425	1150	24 in. SCH. 40	316	509
7-8	Pump Discharge	475	1150	18 in. SCH. XS	316	541
9-10	Superheater - in	450	1150	14 in. SCH. 40	316	608
11-12	Superheater - out	450	900	14 in. SCH. 20	316	567
13-14	Reheater - in	450	1150	10 in. SCH. 40	316	657
15-16	Reheater - out	450	900	10 in. SCH. 20	316	585
17-18	Evaporator - in	450	900	18 in. SCH. XS	316	723
19-20	Evaporator - out	425	630	18 in. SCH. 20	A-106B	502
20-21	Cold Storage	400	630	10 in. SCH. 10	A-106B	425

*Defined in Figure 5.3-27
**Operating pressure + 400 psi (allowance for large leak)
†ASME Section VIII, Division 1 (C = 0.015, E = 1.0)

5.3.5 STEAM GENERATOR DESIGNS

The steam generator conceptual designs selected are very close to those used in Task 2 for the 1100 F system (Section 3.4.6). Some of the changes made for Task 4 are outlined below:

1. Elimination of the IHX increased the sodium inlet temperature from 1050 F (Task 2) to 1100 F (Task 4)
2. The turbine heat balance was refined (Section 5.5).
3. Task 2 demonstrated the advantage to be gained from a wide spread between hot and cold leg temperatures in the sodium since it reduces the size of an expensive storage system. Therefore, the evaporator pinch point temperature ΔT was reduced from 40 to 35 F.

Using the turbine steam cycle heat balance, (Section 5.5) as input values on the water side, the procedures outlined in Section 3.4.6 and Appendix H were used to generate the steam generator heat balances shown in Figure 5.3-32.

Sizing Steam Generator Modules

The STMGEN computer code was used to size the evaporator, superheater, and reheater. A summary of the results is presented in Table 5.3-18a. The computer output for all three designs is listed in Appendix P. There is a difference in the value of the active tube lengths between the three tables of computer data and the data given in Table 5.3-18a. The reason for this is that the computer run was made with nominal heat tranfer coefficients and the modules placed in the plant must be capable of meeting possible adverse conditions. The nominal heat transfer correlations used in the design of the steam generators are listed in Table 5.3-19.

Table 5.3-20 shows a final design sizing calculation which was performed in conjunction with the steam generator used as a reference in Appendix I. This illustrates the types of allowances made on tube length for various design uncertainties. Using this as a rough guide for the steam generator designs, the following allowances were made

	Length from STMGEN (ft)	$\Delta L/L$ Correction	Design Length (ft)
Evaporator	69.0	15.8	80
Superheater	33.65	7.0	36.04
Reheater	35.45	7.0	37.96

Thermal Performance

The STMGEN data for the temperature profiles in the three steam generators is plotted in Figure 5.3-33. This illustrates the effect of the pinch point temperature on the required module length. The result of a tight pinch point is an unusually large surface area in the evaporator devoted to preheating the water.

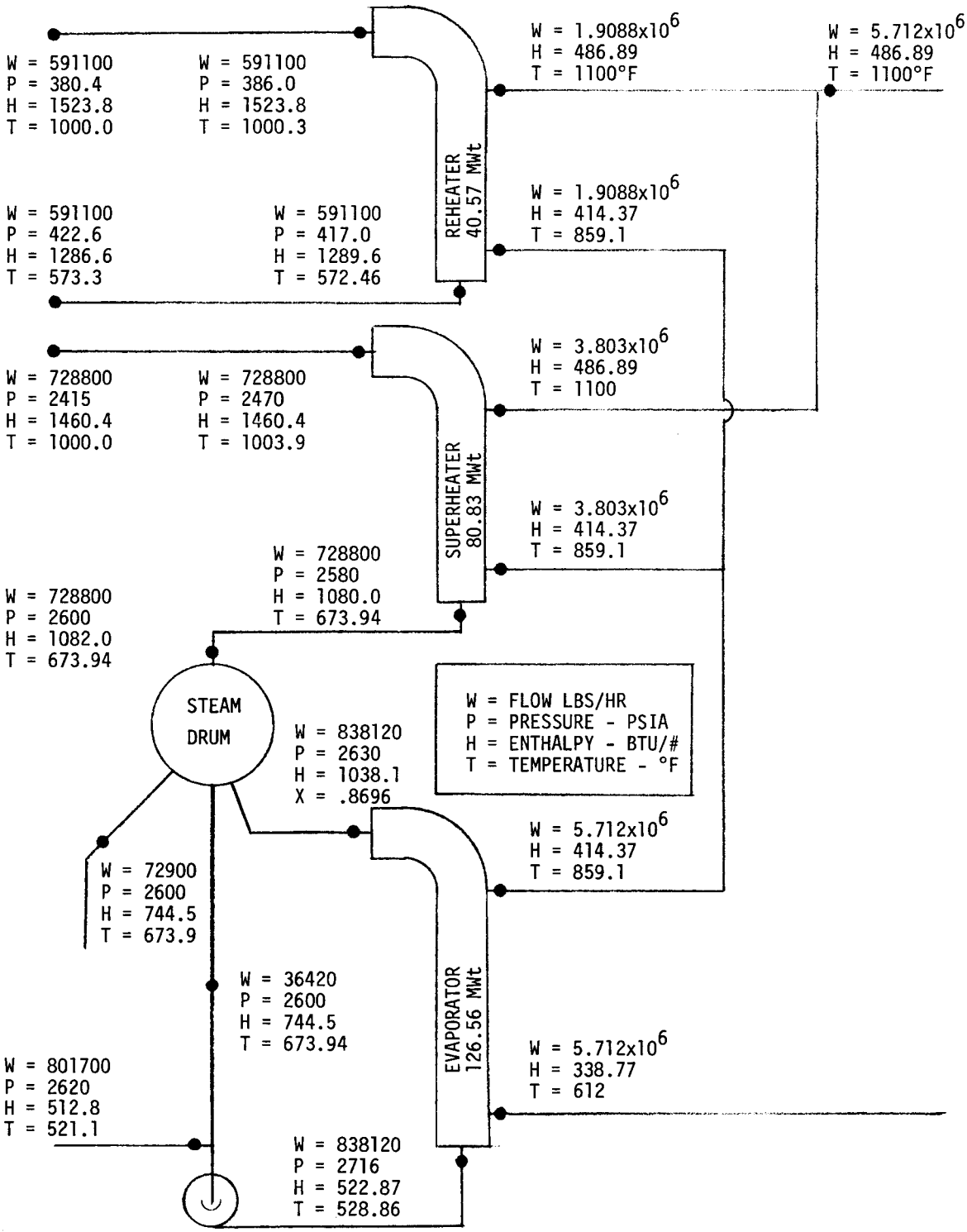

Figure 5.3-32. Steam Generator Heat Balance

Table 5.3-18a

STEAM GENERATOR DESIGN DATA

PERFORMANCE DATA	EVAPORATOR	SUPERHEAT	REHEAT
Power Rating, MWt	126.56	80.83	40.57
Active Heat Transfer Area, Ft^2 (3)	9687.0	3373.2	4251.8
Heat Transfer Uncertainty Factor, %	15.8%	7.0%	7.0%
HEAT TRANSFER COEFFICIENTS (BTU/HR-FT^2-°F)(3)			
Tube I.D. ($x10^{-3}$)	2.3/23.2/2.2(1)	3.2/1.0(2)	0.23/0.25(2)
Tube O.D. ($x10^{-3}$)	6.4/6.3/6.2	5.8/5.4	2.03/1.90
Tube Wall ($x10^{-3}$)	1.8/1.7/1.7	0.88/1.01	1.71/1.92
Overall ($x10^{-3}$)	0.69/0.95/0.68	0.62/0.46	0.19/0.201
SHELL SIDE PARAMETERS			
Sodium Inlet Temp., °F	859.1	1100	1100
Sodium Outlet Temp., °F	612.0	859.1	859.1
Sodium Flow Rate, Lbs/Hr	$5.712x10^6$	$3.803x10^6$	$1.909x10^6$
Vessel O.D./Length, Ft	4.43/97	4.08/54	4.56/54
Tube Pitch/Diam. Ratio	1.95	1.95	1.95
Shell Side Pressure Loss, psi(4)	12.74	9.6	3.95
TUBE SIDE PARAMETERS			
Tube O.D./Thickness, Inches	0.625/0.109	0.625/0.109	1.05/0.05
Number of Tubes	740	572	286
Tube Active Length, Ft	80.00	36.04	37.96
Steam Inlet Temp., °F	528.86(Water)	673.94	572.46
Steam Outlet Temp., °F	87% (Stm.Qual.)	1000	1000
Steam Flow Rate, Lbs/Hr	$8.381x10^5$	$7.288x10^5$	$5.911x10^5$
Tube Side Pressure Loss, psi(4)	65.8	110.2	31.1
MATERIAL OF CONSTRUCTION	2-1/4 Cr-1Mo	Incoloy 800	Incoloy 800

1. Preheat/Nucleate/Film
2. Inlet Value/Outlet Value
3. Based on Tube O.D.
4. Friction Loss - No Static Head Included

Table 5.3-19

HEAT TRANSFER CORRELATIONS USED IN STEAM GENERATOR SIZING CALCULATIONS

REGION	CORRELATIONS USED	AUTHORS	REFERENCE
Sodium Side	$Nu = 12.35 + .0555\ (Pe)^{0.753}$	Gräber and Rieger	1
Water Side Preheat	$Nu = .0204\ Re^{0.805}\ Pr^{0.415}$	Engineering Sciences Data Unit - British	2
Subcooled Boiling and Nucleate Boiling	$h = \left[\frac{e^{P/1260}}{0.072}\right](q")^{0.5}\left[\frac{T_w - T_b}{T_w - T_{sat}}\right]$	Thom, et al	3
Water Side DNB	$x_{DNB} = \frac{18.85}{h_{fg}\ (\rho_g/\rho_\ell)\sqrt{G/10^6}}$	Special AI-MSG Formulation	4
Film Boiling	$Nu_f = 0.80\ [0.0193\ Re_f^{0.8} Pr_f^{1.23}]$ $[x + (1-x)(\rho_g/\rho_\ell)]_b^{0.68}\left[\frac{\rho_g}{\rho_\ell}\right]^{0.068}$	Bishop, Sandberg and Tong	5
Superheat	$Nu_f = 0.0133\ Re_f^{0.84} Pr_f^{0.333}$	Heineman	6
Tube Thermal Conductivity	$K = C_1 - C_2T$	Use reference values for C_1 and C_2 from materials data	

Note: Except for subscript f which denotes "average film" parameters are evaluated at "stream bulk" conditions.

1. V.H. Gräber, M. Rieger, Atomikerenergi 19, p. 23, 1972.
2. Engineering Sciences Data Unit Item 67016, "Forced Convection Heat Transfer to Circular Tubes - Part 1: Correlation for Fully Developed Turbulent Flow - Their Scope and Limitations," Inst. Mech. Engrs., London, 1967.
3. J.R.S. Thom, W.M. Walker, T.A. Fallon, and G.F.S. Reising, "Boiling in Subcooled Water During Flow Up Heated Tubes or Annuli," Symposium on Boiling Heat Transfer in Steam Generating Units and Heat Exchangers, Inst. Mech. Engrs., Manchester, 1965.
4. R.B. Harty, Atomic International Document TR-097-330-008, "MSG Test Report - Steady-State Heat Transfer," May 28, 1974.
5. A.A. Bishop, P.O. Sandberg, and L.S. Tong, "Forced Convection Heat Transfer at High Pressure After the Critical Heat Flux," ASME 65 HT-31, 1965.
6. J.B. Heineman, "An Experimental Investigation of Heat Transfer to Superheated Steam In Round and Rectangular Channels," ANL 6213, 1960.

Table 5.3-20

STEAM GENERATOR MODULE SIZING CALCULATION

Note: All tabulations are shown in feet

			SUPERHEATER	EVAPORATOR (80% Bishop)
CLEAN TUBES			33.4	30.0
TUBE PLUGGING ALLOWANCE - 5%			1.6	1.6
SUPPORT PLATE CORRECTION			0.8	0.8
BLOWDOWN CORRECTION			-0.9	0.3
THERMAL UNBALANCES			0.5	1.0
PLENUM CREDIT			-1.0	-1.0
REQUIRED CLEAN TUBE LENGTH-NOMINAL COEFF.			34.4(2)	32.7(2)
FOULING ALLOWANCE (2 YEAR CLEANING CYCLE)(1)			5.4	6.7
HEAT TRANSFER COEFFICIENT UNCERTAINTIES	99.9% 3σ	95%(3) 1.64σ		
PREHEAT	25%	13.7%	--	0.4
NUCLEATE BOILING	25%	13.7%	--	0.2
DNB	63%	34.6%	--	4.4
FILM BOILING	35%	19.2%	--	2.4
SUPERHEAT	25%	13.7%	2.8	--
TUBE WALL CONDUCTIVITY	15%	8.2%	0.9	1.1
TUBE WALL THICKNESS	5%	2.7%	~0.0	0.5
SODIUM SIDE COEFFICIENT	25%	13.7%	0.4	0.6
FOULING	100%	55.0%	3.0	3.6
TOTAL UNCERTAINTY $[\sqrt{\Sigma\sigma^2}]$			4.2	6.3
TOTAL TUBE LENGTH REQUIRED			44.0(2)	45.7(2)

(1) HFOUL = 5700 BTU/hr-ft^2-°F

(2) Measured ℄ plenum window to ℄ plenum window

(3) 95% uncertainty lengths are tabulated

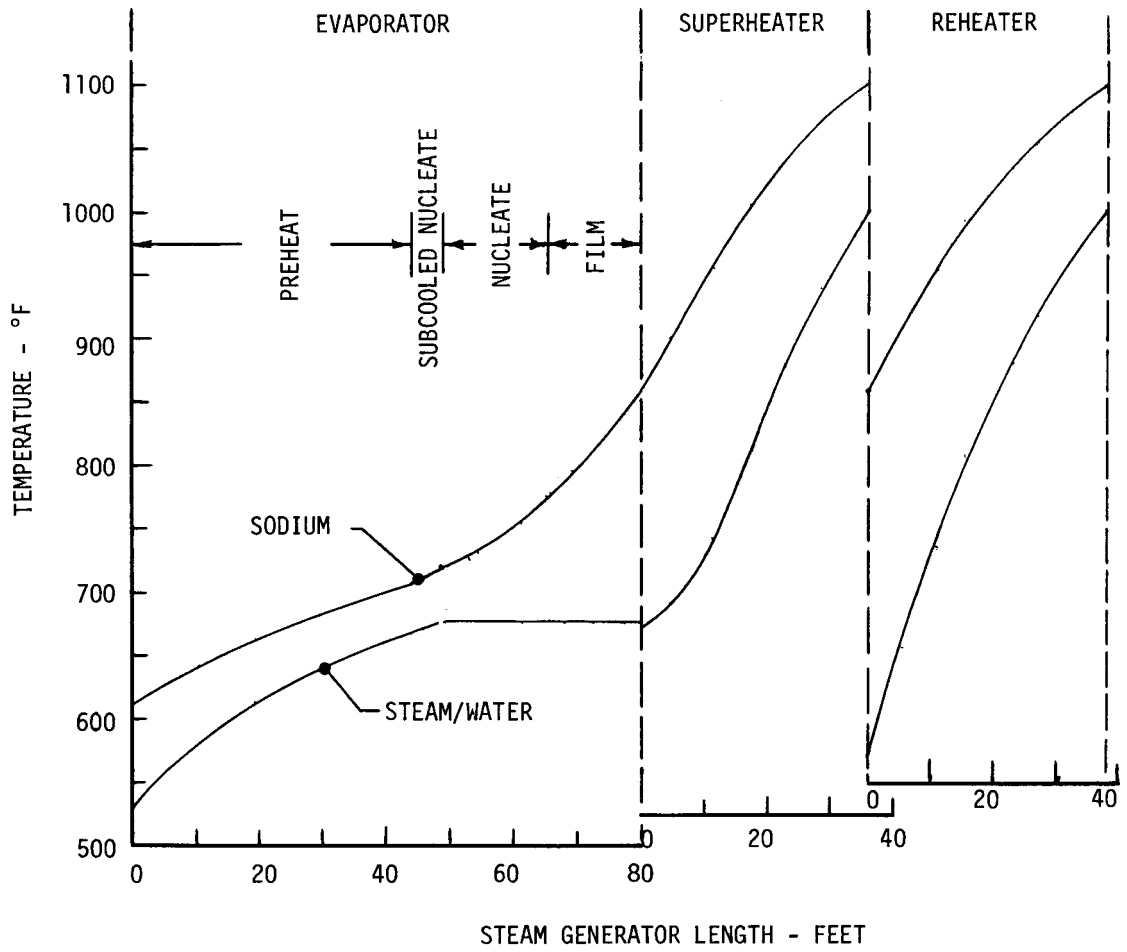

Figure 5.3-33. Steam Generator Temperature Profiles

Figure 5.3-33 also shows the transition point between nucleate and film boiling which is by definition the departure from nucleate boiling point (DNB). Although DNB can cause cyclic strain fatigue problems, the consequences in this design are negligible. A DNB experiment performed in Russia (Ref. 5.3-12) with a 0.630-inch OD by 0.118-inch wall at 2160 psia steam pressure showed a maximum temperature oscillation in the tube wall of roughly 7.2 F. This compares to other results with essentially the same size tube but with a lower steam pressure (1600 psia) which oscillated roughly 35 F (Ref. 5.3-13). The reason that the DNB oscillations reduce at higher pressure levels is the smaller difference in density between steam (film boiling) and water (nucleate boiling) on the tube surface. As an extreme, operation at the critical point for steam, where the density of steam and water are equal, totally elliminates DNB temperature oscillation. Therefore operation of the evaporator at 2700 psia poses no problems with DNB cyclic strain fatigue.

Mechanical Design of Steam Generators

The overall dimensions of the steam generators are illustrated in Figure 5.3-34. A detailed section of the steam generator is shown in Figure 5.3-35; the inset shows how extra sleeves will be brazed over the tube-tubesheet welds to insure high reliability. The overall design of these steam generators is based on ASME Section VIII, Division 1 rules; however, additional analysis and quality assurance procedures have been specified due to the hazard of potential sodium/water reactions. These additional requirements are roughly equivalent to the ASME Section III, Class 3 procedures.

The evaporator module is equipped with an external water recirculation loop as shown in Figure 5.3-32. The pump in this loop is described in Section 5.3.4; the steam drum is shown in Figure 5.3-36.

Steam Generator Operating Limits

Table 5.3-21 shows the various specifications on the operating limits for the three steam generator modules. An explanation is given below for each line item:

Nominal Operating Temperature at Power. Steady-state operation of the modules above or below the nominal temperature is acceptable within the limits specified.

Maximum Operating Temperature. The highest allowable operating temperature.

Maximum Ramp Changes - Heatup and Cooldown from Ambient. These are the permissible rates of temperature rise for the modules. A normal value here is usually 25 F/hour up to 50/F hour for a plant which is shut down and brought on power infrequently. A value of 75 F/hour was set for the steam generators because of the frequent swings in power. This will impose a small penalty on the cyclic strain accumulations over the life of the modules.

Maximum Transient Temperature Change Ramped Up or Down in 60 Minutes or Less (Including Step Changes in Temperature. This is a grossly simplified attempt to point out a general level of acceptability for system thermal

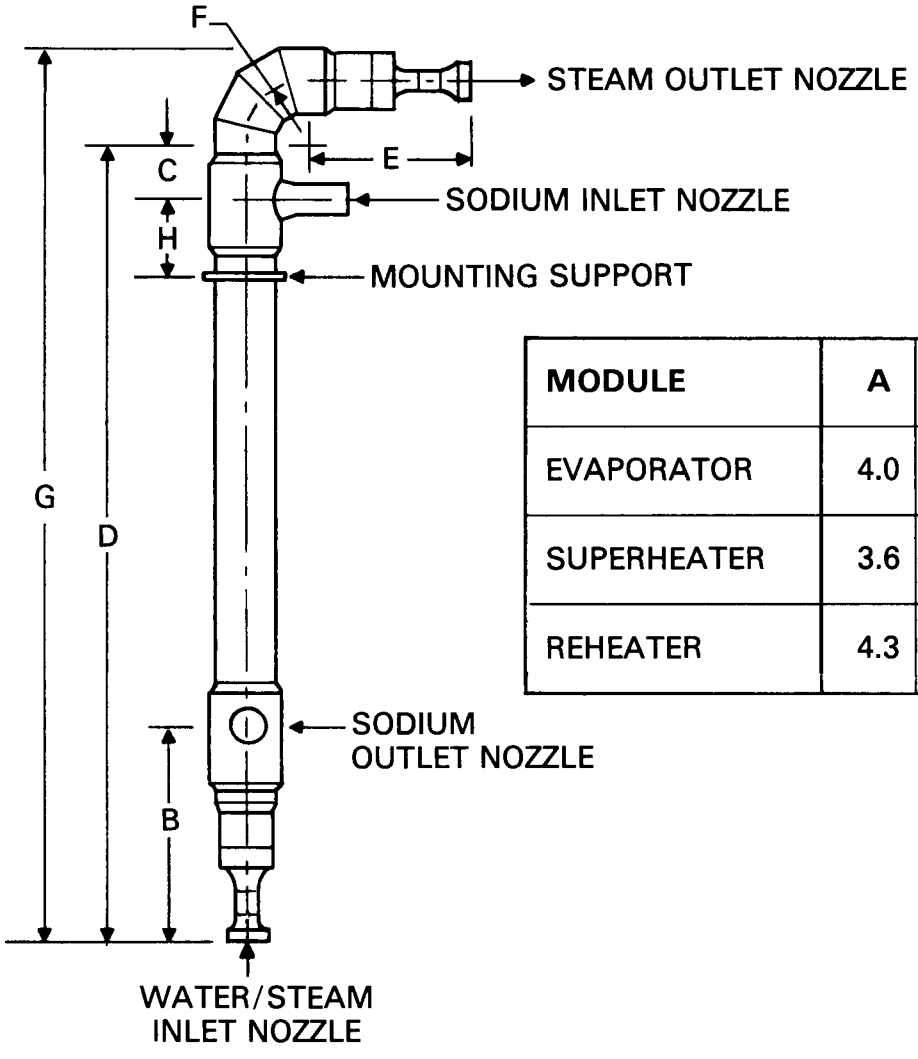

MODULE	A	B	C	D	E	F	G	H
EVAPORATOR	4.0	14.6	4.5	97	11.3	4.0	97	4.0
SUPERHEATER	3.6	13.1	4.1	66	10.2	3.6	66	3.6
REHEATER	4.3	15.7	4.8	69.4	12.2	4.3	69.4	4.3

Figure 5.3-34. Steam Generator Configurations

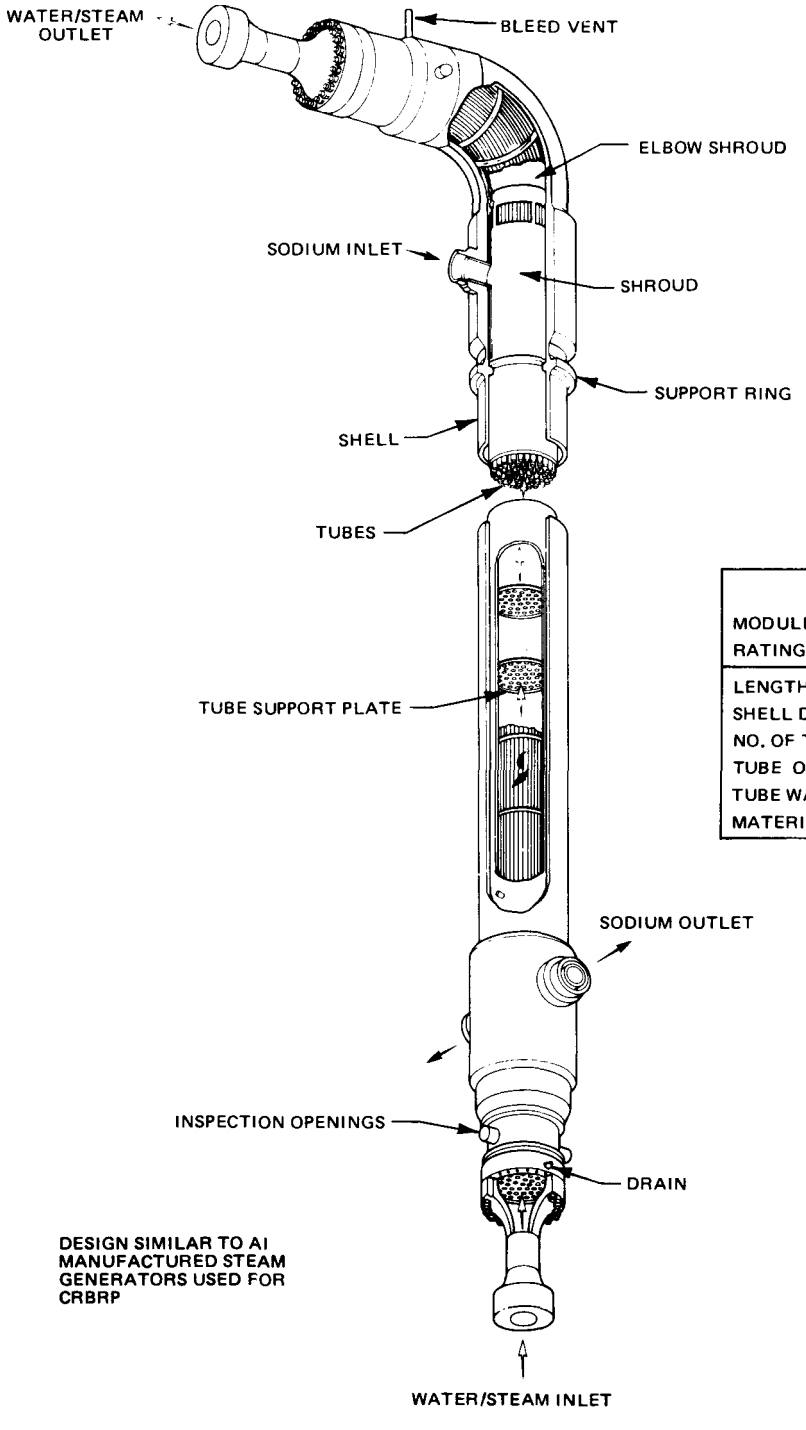

MODULE RATING (MWt)	EV 127	SH 81	RH 41
LENGTH (ft)	97	54	54
SHELL DIA. (ft)	4.43	4.08	4.56
NO. OF TUBES	740	572	286
TUBE O.D. (in.)	0.625	0.625	1.05
TUBE WALL (in.)	0.109	0.109	0.05
MATERIAL	2¼Cr	1800	1800

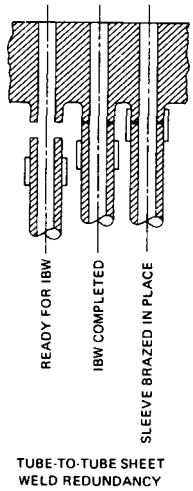

Figure 5.3-35. Steam Generator Module

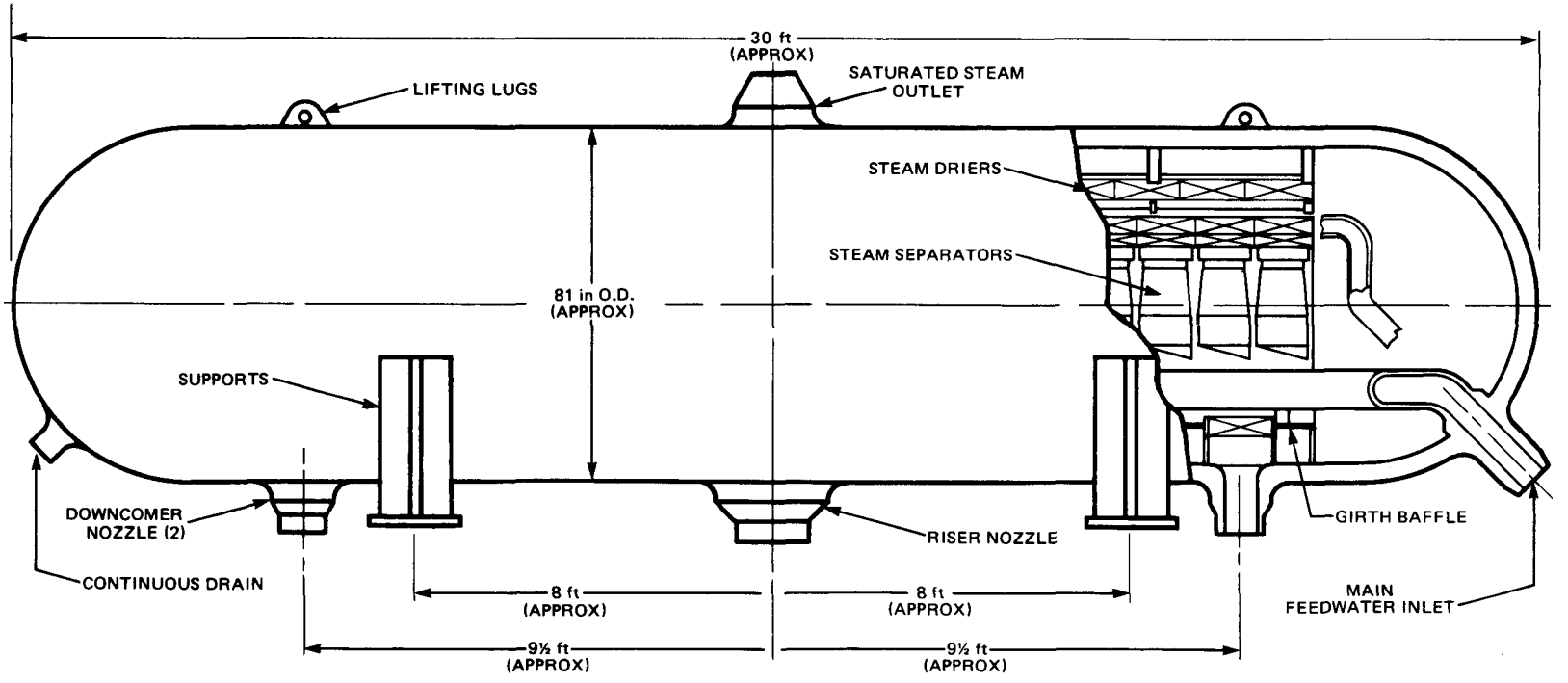

OUTLET STEAM FLOW	728,800 lb/h
STEAM QUALITY	0.87
DESIGN PRESS.	3,100 psi
OPER. PRESS.	2,600 psi
DESIGN TEMP	700°F
OPER. TEMP	674°F
MATERIAL	HS CARB STEEL

DESIGN SIMILAR TO
BABCOCK AND WILCOX CO. STEAM DRUM

Figure 5.3-36. Steam Drum Design

Table 5.3-21
STEAM GENERATOR OPERATING LIMITS

	Sodium		Steam	
	Inlet	Outlet	Inlet	Outlet
Reheater				
(a) Nominal Operating Temperature at Power (°F)	1100±100	859±50	572±50	1000±100
(b) Maximum Operating Temperature (°F)	—	1200	—	1200
(c) Maximum Ramp Changes-Heatup and Cooldown from Ambient (°F/hr)	75	75	75	75
(d) Maximum Transient Temperature Change Ramped Up or Down in 60 Minutes or Less (includes step change)-(°F)	180 (upset) 250 (emergency)	— —	180 (upset) 250 (emergency)	— —
(e) Maximum Differential Temperature Between Sodium and Steam at any Point (effective for fill and operation)-(°F)	~300	~300	~300	~300
(f) Minimum Operating Temperature	None Except for Items (c) and (d)			
Evaporator				
(a) Nominal Operating Temperature at Power (°F)	859±50	612±100	529±100	674±50
(b) Maximum Operating Temperature (°F)	—	950	—	950
(c) Maximum Ramp Changes-Heatup and Cooldown from Ambient (°F/hr)	75	75	75	75
(d) Maximum Transient Temperature Change Ramped Up or Down in 60 Minutes or Less (includes step change)-(°F)	180 (upset) 250 (emergency)	— —	180 (upset) 250 (emergency)	— —
(e) Maximum Differential Temperature Between Sodium and Steam at any Point (effective for fill and operation)-(°F)	~300	~300	~300	~300
(f) Minimum Operating Temperature	None Except for Items (c) and (d)			
Superheater				
(a) Nominal Operating Temperatue at Power (°F)	1100±100	859±50	674±50	1000±100
(b) Maximum Operating Temperature (°F)	—	1200	—	1200
(c) Maximum Ramp Changes-Heatup and Cooldown from Ambient (°F/hr)	75	75	75	75
(d) Maximum Transient Temperature Change Ramped Up or Down in 60 Minutes or Less (includes step change)-(°F)	180 (upset) 250 (emergency)	— —	180 (upset) 250 (emergency)	— —
(e) Maximum Differential Temperature Between Sodium and Steam at any Point (effective for fill and operation)-(°F)	~300	~300	~300	~300
(f) Minimum Operating Temperature	None Except for Items (c) and (d)			

transients in the sodium or water. The upset condition allows continued operation whereas the emergency condition requires shutdown and requalification of the module.

The handling of thermal transients is an extremely complex design problem and requires major expenditures in analysis. Offered here is a ballpark estimate of the type of transients that have caused concern in past steam generator designs.

Maximum Differential Temperature Between Sodium and Steam at Any Point. Steady-state differential temperatures larger than 300 F across a metal part like a tube, shroud, tubesheet, or vessel when the heat transfer is high (e.g., sodium or boiling steam) can raise the stress level to the yield point. The yield point can be exceeded if the differential temperature is applied suddenly as described above. When filling the module for the first time, it is difficult to maintain the metal, sodium and water at thermal equilibrium throughout the process at all points in the module. Therefore the numbers given provide an absolute upper limit on the allowable nonequilibrium.

Minimum Operating Temperature. If required for matching low power or other turbine temperature requirements, the steam generators can be operated at low temperature levels as long as the above conditions are met.

REFERENCES FOR SECTION 5.3

5.3-1. G.D. Gupta, et al., "Thermoelastic Analysis of Nonaxisymmetrically Heated Thick Cylindrical Shells," Journal of Pressure Vessel Technology, Transactions of the ASME, Vol. 100, No. 1, February 1978, pp. 107-111.

5.3-2. M.S.M. Rao, T.V. Narayanan, and G.D. Gupta, "Inelastic Analysis of Nonaxisymmetrically Heated Thick Cylindrical Shells," submitted for publication in the Journal of Pressure Vessel Technology, Transactions of the ASME.

5.3-3. T.V. Narayanan, G.D. Gupta, M.S.M. Rao, "Structural Design of a Superheater for a Central Solar Receiver," accepted for publication in the Journal of Pressure Vessel Technology, Transactions of the ASME.

5.3-4. "Incoloy Alloys," Huntington Alloys, International Nickel Company, Inc., 1973.

5.3-5. R.N. Lyon, "Liquid Metal Heat Transfer Coefficients," Chemical Engineering Progress, Vol. 47, No. 2, February 1951.

5.3-6. "Thermophysical Properties of Sodium-Recommended Values," Reactor and Fuel Processing Technology, Vol. II, No. 1, Winter 1967-1968.

5.3-7. E. Achenbach, "Evaluation of Measurements of the Local and Total Heat Transfer from Smooth and Rough Surface Cylinders in Cross Flow," Heat and Mass Transfer Source Book, Fifth All Union Conference, Minsk, John Wiley and Sons, 1976.

5.3-8. Churchill, Ward, and Usagi, AIChE Journal, Vol. 18, No. 6, November 1972, pp. 1121-1128.

5.3-9. Central Receiver Solar Thermal Power System, Phase I, Pilot Plant Preliminary Design Report, McDonnell Douglass Aeronautics Company, Huntington Beach, California, 1977.

5.3-10. J.I. Gittleman, B. Abeles, P. Zanzucchi, and Y. Arie, "Optical Properties and Selective Solar Absorption of Composite Material Films," Thin Solid Films, Vol. 45 (1977), pp. 9-18.

5.3-11. L.L. Oden, "Method for Preparing Solar Collectors," serial no. 817,886, Department of Interior, Washington, DC, July 1977.

5.3-12. O.V. Remizov, V.A. Vorob'ev, and E.F. Gal'chenko, "Investigation of the Boundaries of the Onset of Dry-Out and Variation of Tube Wall Temperature in This Zone," Risley Translation 2900 - Translated from Proc. Anglo Soviet Sem., Obninsk, Paper No. 3, 17 pages (May 1975).

5.3-13. C.L. Chu, J.M. Roberts, A.W. Dalcher, "DHB Oscillatory Temperature and Thermal Stress Responses for Evaporator Tubes Based on Rivulet Model," Engineering for Power, Vol. 100, No. 3, July 1978.

5.4 STORAGE SUBSYSTEM

The storage subsystem for the commercial plant uses sensible heat stored in sodium and is sized to provide three hours of EPGS operation. The basic requirements of the subsystem are listed in Table 5.4-1.

As conceptually designed, the storage subsystem consists of six spherical sodium storage tanks, three of which are used for storage of sodium at the cold leg temperature of 612 F and three store sodium as it exits the receiver/tower at the hot leg temperature of 1100 F. The storage of hot and cold sodium in separate tankage provides decoupling of the steam generator sodium loop from short term transients originating in the receiver due to cloud cover.

The storage tanks have been sized to provide three hours of continuous EPGS operation after making deductions for turbine startup and thermal losses through tank and piping insulation.

Steam Generators:	3 hr x 247.86 MW_t	= 743.58
Turbine Start :	2% x 247.86 MW_t x 0.5 hr	= 2.48
Losses :	0.815 MW_t x 24 hr	= 19.56
Storage Capacity		765.62 MW_th

Using the storage temperatures shown in Table 5.4-1, this translates into 17.67×10^6 pounds of sodium. However, 5 percent more sodium is required since the tanks are never completely empty (ullage) even at the lowest point. Thus the actual inventory in the tanks is 18.55×10^6 pounds.

Stainless steel (316) can be used in the hot vessel design because it is compatible with sodium and there is no water present as in the steam generators where Incoloy 800 is used. The cold tanks are carbon steel. SA 515 carbon steel has been specified in this study for costing purposes; further study is required to determine whether this is the optimum choice. See Appendix L for a more detailed discussion of the materials selection.

Because of the difference in sodium density between 612 F and 1100 F, the hot and cold tanks must be of different volumes. The volume of the tanks is five percent larger than the liquid volume to provide adequate cover gas space for the sodium flow distributor to operate.

To reduce tank costs, the top and bottom halves have been designed for different pressures as discussed in Sections 5.3.4 and 5.4.1. The tanks are not designed to withstand a hard vacuum because subatmospheric pressures do not occur during normal operation, and the tanks will be protected by burst discs against an accident which could pull a vacuum. During the initial filling with sodium, the tank will be purged with argon, rather than evacuated, to remove oxygen and water vapor. Four to five pressurizations to 20 psig with argon followed by venting should reduce the oxygen level to less than 20 ppm in the sodium after filling, at a cost of less than $30,000 for argon expended.

Table 5.4-1

STORAGE SYSTEM DESIGN REQUIREMENTS

• Storage Capacity ($MW_t h$)	∿766
($MW_e h$)	300
• Storage Temperature (°F)	1100 Hot Leg 612 Cold Leg
• Storage Medium	sodium 18.55×10^6 lb
• Storage Tank Materials	316SS Hot Leg SA515 Carbon Steel Cold Leg
• Storage Tank Total Volume (ft^3) (includes ∿5% additional sodium and 5% additional for cover gas)	384,000 Hot Leg 357,000 Cold Leg
• Tank Design Pressure * (psi)	Top: 25 nominal Bottom: 37 nominal
• Sodium Charge Rate (Hot Leg) (lb/hr)	8.57×10^6
(Cold Leg) (lb/hr)	5.71×10^6
• Sodium Discharge Rate (Hot Leg) (lb/hr)	5.71×10^6
(Cold Leg) (lb/hr)	8.57×10^6
• Minimum Storage Temp (°F)	350
• Insulation Requirement/Temperature Loss	2%/24 hr

*See Section 5.3.4 for determination of design pressures.

The design charge and discharge rates have been selected to be consistent with the Advanced Central Receiver Specifications issued by Sandia Laboratories, which required charging at the peak receiver output rate and discharging at the steam generator input rate.

The storage temperature must be maintained above 350 F to prevent sodium from freezing.

The storage vessels are heavily insulated to reduce losses to about one percent of the maximum storage capacity per day. Additional losses in liquid metal piping increase this to about 2.5 percent per day.

Besides tanks, the storage subsystem also includes the necessary sodium piping and valves, and sodium purification, cover gas, drainage and relief system components. An isometric view of the major sodium storage and steam generation components is shown in Figure 5.4-1.

5.4.1 STORAGE VESSELS DESIGN

Hot and cold storage vessels were designed to a spherical configuration to minimize material requirements compared to cylindrical tanks.* The vessels were designed per Section VIII, Division I, "Pressure Vessels," of the ASME Boiler and Pressure Vessel Code, 1977 Edition (Part UG - General Requirements, p. 27 - Hemispherical Heads).

The following criteria were used in design of the vessels:

1. All welds will receive 100% radiography; welds are full penetration type; code formula "E"; (joint efficiency) = 1.0.

2. No corrosion allowances were made, but wall thicknesses were rounded off to the next highest one-sixteenth inch.

3. No allowance was made for manufacturing tolerance in wall thickness.

4. Vessels designed for 1100 F will be fabricated with SA 240, GR 316 stainless steel, and vessels designed for 630 F will be fabricated with carbon steel.**

5. Each vessel is designed as two individual hemispheres accordinging to Table 5.4-2. This design using two thickness hemisphere reduces material requirements by about 30 percent over a single thickness sphere. Further reduction of about 30 percent could be achieved by using the Hortonsphere construction (Chicago Bridge and Iron design) with continuously graded walls. This design was not used because the complexity of the analysis required is beyond the scope of the present study.

*Cylindrical tanks designed to ASME Section VIII were shown to be more expensive than spherical tanks in Task 2. Cylindrical tanks designed like oil tanks to ASME Section III were also found to be more expensive than spherical tanks; see Appendix Q.

**For cost estimating SA515-GR70 is used. See Appendix L.

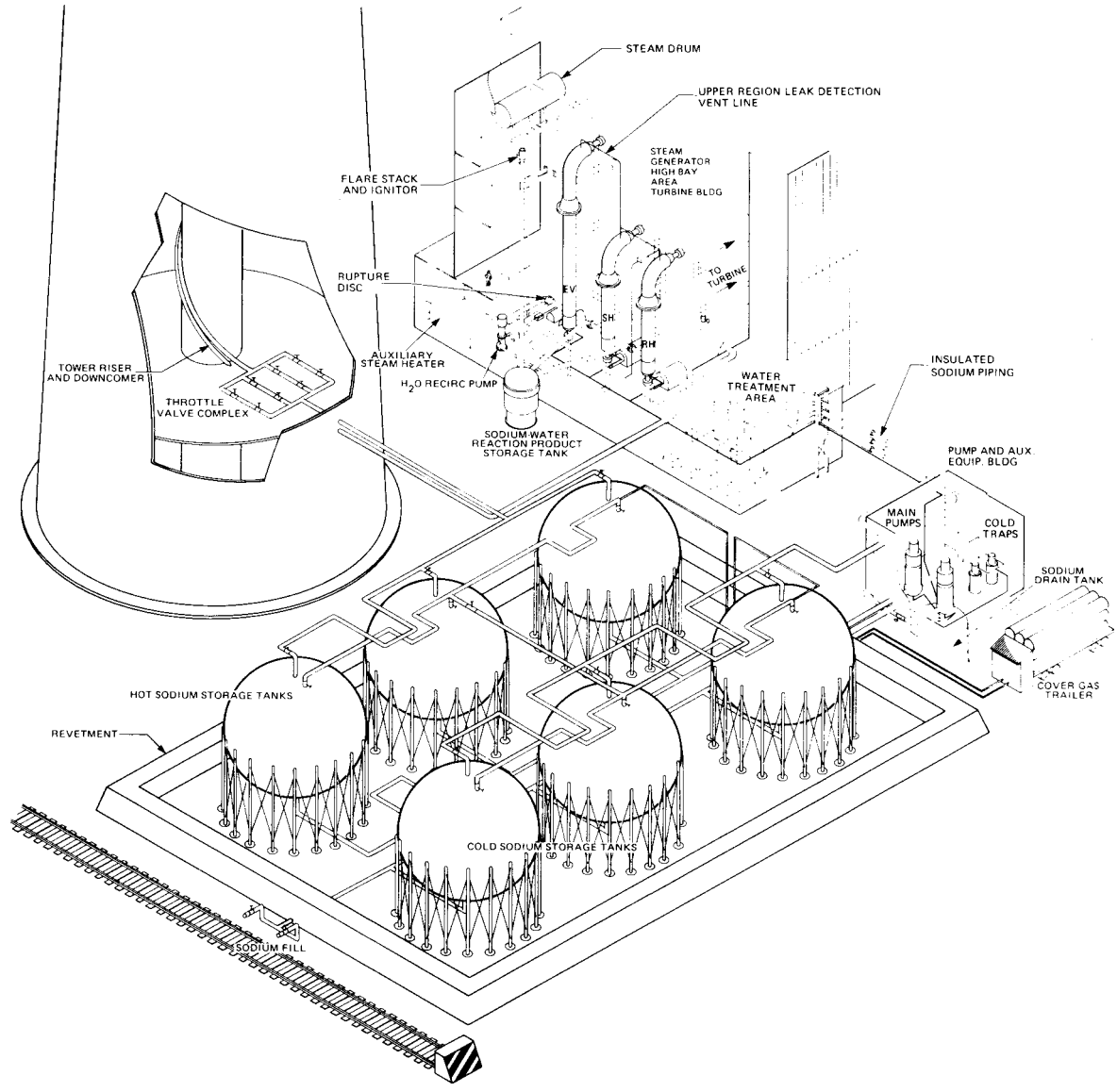

Figure 5.4-1. Plant Sodium Storage Pump and Steam Generator Complex

Table 5.4-2

VESSEL HEMISPHERE PRESSURES

	Top Half		Lower Half	
Vessels	Max. Operating Pressure (psig)	Design Pressure (psig)	Max. Operating Pressure (psig)	Design Pressure (psig)
HOT	14.3	25.0	25.3	36.1
COLD	21.1	25.6	32.7	37.2

Results of the calculations are summarized in Figure 5.4-2. Hot sodium is introduced into the tanks through the thermal sleeve at the top of the tank. An impingement baffle is installed below the thermal sleeve to enable sodium to be smoothly distributed to reduce thermal shock effects. Pipe support legs for the tank will be cold sprung such that, in the heated condition, the legs will straighten as the tank expands. Material for the legs is as specified in Figure 5.4-2. Legs are welded to the tank through a reinforced plate to ensure sufficient strength in the attachment region.

The tanks will be heated by one-half-inch tubular electric resistance heaters with stainless steel sheaths, 30 watts/square inch with four-foot spacing at the top and bottom of the vessel.

Insulation for the hot tanks consists of two four-inch thick layers of Babcock and Wilcox Kaowool (4 pounds/cubic foot) plus five three-inch thick layers of Owens Corning Thermal Insulating Wool Type II, plus an external aluminum jacket. Insulation for cold tanks will be eight three-inch thick layers of Owens Corning Thermal Insulating Wool Type II plus an external aluminum jacket. This insulation selection is based upon a trade-off between insulation costs and the cost of thermal losses. Each MWh of energy lost from storage per year requires about $80 in additional receiver and collector equipment. For the types of insulation considered here, this justifies thicknesses of 1.5 to 2.5 feet.

Spherical Storage Vessels - Manufacturing and Field Fabrication

Fabrication begins in the manufacturer's shop where the plate is cut into pieces of varying sizes. Large plate pieces typically may be 30 feet long and 10 feet wide. Smaller plate pieces would also be cut. The pieces are individually cold pressed to shape in large 3000 ton presses. Edges are beveled and prepared in the shop. Pieces are then shipped to the job site.

The support structure for the tank is fabricated first as a field welded structure. A large crane or derrick is used to lift individual pieces into location. A horizontal ring of plates is first welded to the supports and to each other. Then the tank is expanded in horizontal layers by working up and down from the middle ring of plates.

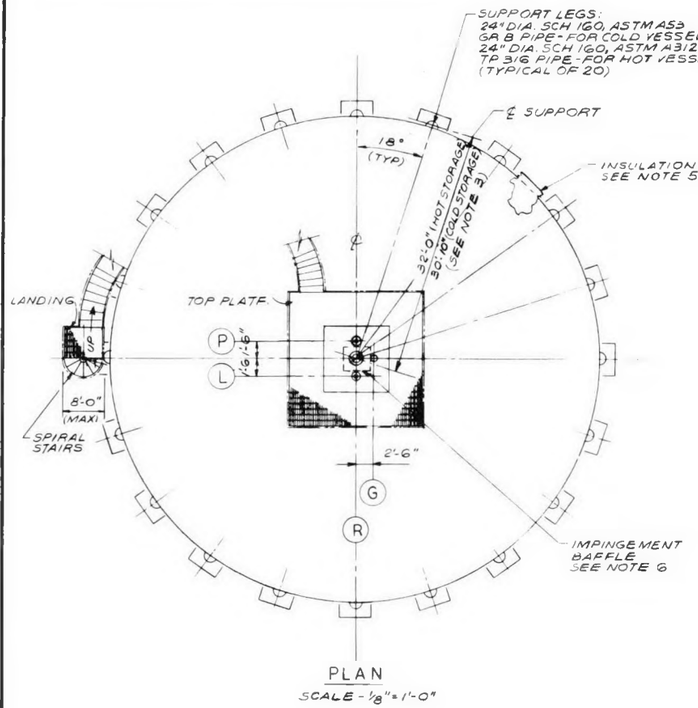

PLAN

SCALE - 1/8" = 1'-0"

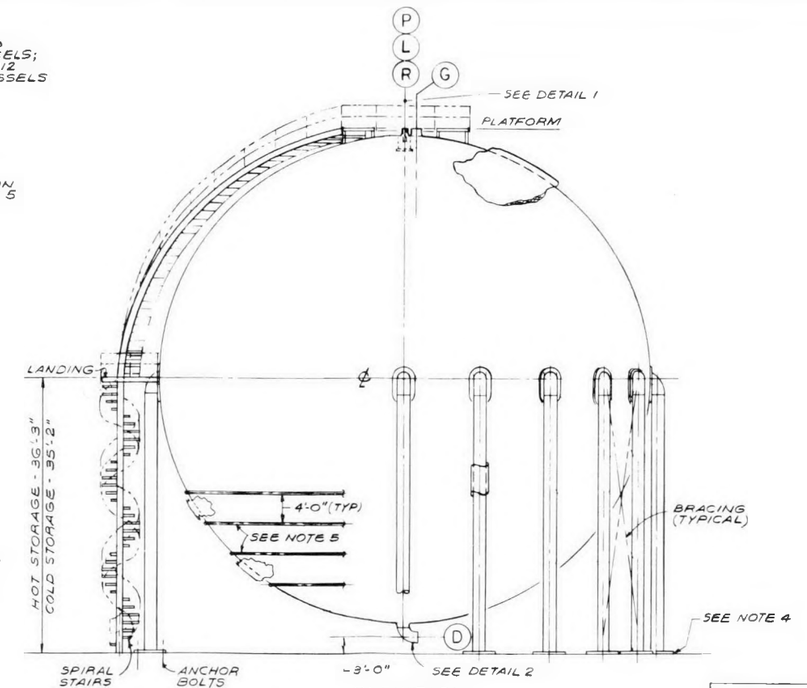

ELEVATION

SCALE - 1/8" = 1'-0"

NOTES

1. VESSELS SHALL BE DESIGNED AND FABRICATED PER ASME BOILER AND PRESSURE VESSEL CODE, SECTION VIII, DIVISION 1, "PRESSURE VESSELS".
2. TEMPERATURE MEASUREMENT SHALL BE BY THERMOCOUPLE WELDED TO OUTSIDE OF VESSEL.
3. PIPE SUPPORT LEGS SHALL BE "COLD SPRUNG".
4. 1/2" THICK ASBESTOS PAD BETWEEN BOTTOM OF SUPPORT LEG PLATE AND CONCRETE FOOTING.
5. 1/2" TUBULAR ELECTRIC RESISTANCE HEATERS, WITH STAINLESS STEEL SHEATH, 30 WATTS / SQ. IN., AT FOUR FOOT SPACINGS TOP AND BOTTOM OF VESSEL. INSULATION FOR HOT STORAGE: TWO-4" THICK LAYERS OF BABCOCK & WILCOX "KAOWOOL" (4 LBS/CU.FT.) PLUS FIVE - 3" THICK LAYERS OF OWENS-CORNING THERMAL INSULATING WOOL, TYPE II, PLUS EXTERNAL ALUMINUM JACKET. PIPE SUPPORT LEGS SHALL HAVE 2" THICK CALCIUM SILICATE INSULATION PLUS EXTERNAL ALUMINUM JACKET. INSULATION FOR COLD STORAGE: EIGHT-3" THICK LAYERS OF OWENS-CORNING THERMAL INSULATING WOOL, TYPE II, PLUS EXTERNAL ALUMINUM JACKET. SUPPORT LEG INSULATION SAME AS INSULATION FOR HOT STORAGE TANK.
6. IMPINGEMENT BAFFLE IS 2'-0" X 2'-0" LG X 1" THICK, SUPPORT OFF TOP.
7. HOT STORAGE TANK FITTING SHALL BE ASTM A312 TYPE 316; FORGINGS SHALL BE ASTM A182 F316.
   COLD STORAGE TANK FITTING SHALL BE ASTM A234. FORGING SHALL BE ASTM A181 GR 2
8. PIPE SUPPORT LEGS SHALL BE ASTM A53 GR.B

NOZZLE SCHEDULE (SEE NOTE 4)

MARK	SERVICE	NOMINAL SIZE OF CONNECTING PIPING (INCHES)	THERMAL SLEEVE (SEE DET. 1)	REMARKS
D	CROSS CONN. TO OTHER TANKS	HOT STORAGE-10 COLD STORAGE-12	NO	SEE DETAIL 2
G	COVER GAS	4	NO	
L	LEVEL INSTRUMENT	2	NO	
P	PRESSURE INSTRUMENT	2	NO	
R	FILL	HOT STORAGE-12 COLD STORAGE-10	YES	SEE DETAIL 1

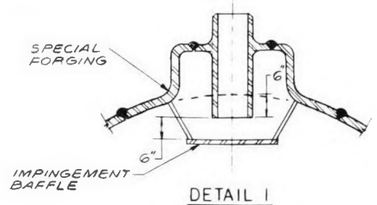

DETAIL 1

THERMAL SLEEVE

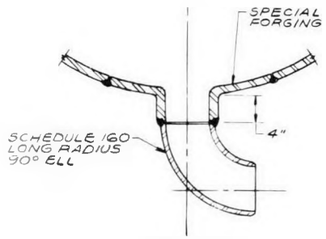

DETAIL 2

(SEE NOTE 7)

	NO. REQ'D	DESIGN PR PSIG TOP HALF	DESIGN PR PSIG BOTTOM HALF	DESIGN TEMPERATURE °F	VESSEL WALL MATERIAL	INSIDE DIAMETER FEET	OUTSIDE DIA W/O INSUL FT TOP HALF	OUTSIDE DIA W/O INSUL FT BOTTOM HALF	WALL THICKNESS-IN TOP HALF	WALL THICKNESS-IN BOTTOM HALF	INTERNAL VOLUME CU.FT.	EXTERNAL SURFACE AREA - SQ.FT.	WT. OF EMPTY VESSEL - LBS TOP HALF	WT. OF EMPTY VESSEL - LBS BOTTOM HALF
HOT STORAGE VESSELS	3	25.08	36.11	1110	SA 240 GR 316	62.6	62.68	62.71	1/2	11/16	128,000	12,950	126,613	174,815
COLD STORAGE VESSELS	3	25.64	37.24	630	SA-515 GR. 70 C.S.	61.0	61.05	61.07	5/16	7/16	119,000	11,714	74,667	104,555

NOTE - FOR TRUE ORIENTATION SEE PLOT PLAN

1/8" = 1'-0" 5' 0' 5' 10' 15'

NO.	DATE	REVISION	BY	CHK	APP.	APP.
1	12.18.78	TITLE BLOCK				

NOTES

DESCRIPTION — COST ACCOUNT

WORK COVERED BY THIS DRAWING CHARGED TO COST ACCOUNT ABOVE

CONSTRUCTION APPROVAL

APPROVAL — DATE

SCALE: AS NOTED

		DATE
DESIGNED BY	V. SHETH	7-24-78
DRAWN BY	B.C. KAISER	7-27-78
CHECKED BY	S. Copelan	7-27-78
APPROVED BY	V.S. Ekanay	8-10-78
APPROVED BY		8-19-78

PROFESSIONAL SEAL

KAISER ENGINEERS

GE/ACRS SOLAR STUDY

COMMERCIAL PLANT CONCEPTUAL DESIGN
THERMAL ENERGY STORAGE VESSELS

JOB No. 78023 | DWG. No. P-003 | REVISION R-1

Figure 5.4-2. Thermal Energy Storage Vessels

5.4.2 Piping and Valves

The storage loop sodium piping plan and layout is shown schematically Figure 5.4-3. Storage system piping material is 316 stainless steel in the hot leg and carbon steel in the cold leg. Piping expansion is accommodated by U-bends in the ground level piping and with a 60° helical spiral for the riser and downcomer. All sodium piping is trace-heated with tubular electric heaters. Cold leg piping is insulated with thermal Wool Type II insulation (Owens Corning Fiberglass Corporation). Hot leg piping is insulated with two inches of Kaowool insulation (Babcock and Wilcox) plus six inches of Thermal Wool insulation. All pipe insulation is covered with an aluminum outer jacket. Storage subsystem piping runs, fittings, and valves are compiled in Table 5.4-3.

Piping runs are grouped together to minimize use of sodium drip pans and sodium-to-gas leak detectors. Piping runs are designed for drainage to the sodium drain tank located under the pump and auxiliary equipment building. Isolation valves are provided for each sodium storage tank so pipe runs can be drained independently of the tanks. It is also possible to pump sodium from one tank to the other by use of the cover gas so that maintenance can be performed.

A large 20-inch sodium check valve is placed in the riser to prevent a rapid flow reversal should the sodium pumps be taken off-line. An illustration of the type of check valve to be used is shown in Figure 5.4-4.

Several sodium control/throttle valves are included in the loop. One 10-inch valve is used to regulate the flow through the reheater. A complex of 2-inch and 8-inch throttle valves are used to isolate the high pressure resulting from the receiver downcomer static head from the low pressure hot leg storage tanks. Both 2-inch and 8-inch valves are used to provide the wide range of flow required of 200 to 20,000 gpm with a pressure drop of 190 ±10 psi. Redundant valves are provided for high reliability (see Figure 5.4-5). Sodium throttle valves of the type to be used are shown in Figures 5.4-6 and 5.4-7. Isolation valves are included in series with each throttle valve to provide tight shut-off and to assist during maintenance and repair.

There is adequate experience (Table 5.4-4) with sodium valves in this size and temperature range to assure reliable designs for the advanced central receiver application.

5.4.3 Sodium Purification

In the course of startup and operation of the large storage and sodium-heated steam generator loops, various impurities will get into solution in the hot sodium. Impurities will result from the accumulation of oxygen, hydrogen, carbon and other materials on the large surface areas of tankage and piping, and from unplanned leakage of water/steam/air into the loop. The conventional method of removing these impurities from the hot circulating sodium is by use of cold trapping.

It is expected that impurity contamination will be high during initial sodium fill and startup operations. Initial cleanup can be accomplished by use of throwaway filters or possibly a high efficiency sacrificial cold trap.

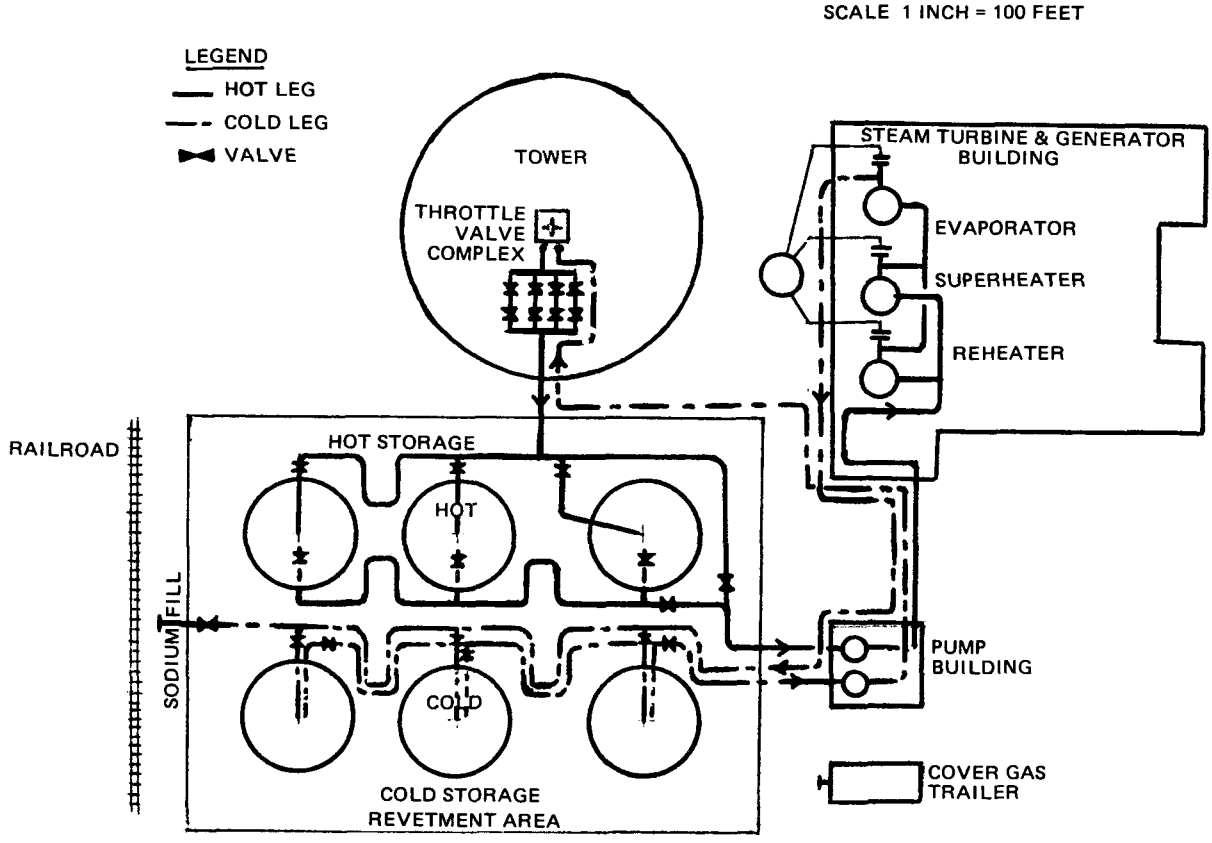

Figure 5.4-3. Sodium Loop Piping Plan

Table 5.4-3

STORAGE SUBSYSTEM PIPING DATA

FROM	TO	MAX. TEMP. °F	DESIGN PRESS. PSIG	MAX. VELOCITY FT/SEC	PIPE SIZE*	RUN LENGTH (FT)	FITTINGS* TEES	FITTINGS* ELBOWS	FITTINGS* VALVES**	COMMENTS
Tower Base	Receiver (Riser)	650	350	21.9	20" Sch 20	750	-	1	-	
Receiver	Throttle Station (Downcomer)	1150	325	24.2	20" .5" Wall	800	-	1	-	
Throttle Station	Hot Storage Tank Inlet Header	1150	35	23.5	20" Sch 20	160	4	2	2-8", 2-2" Cont 2-8", 2-2" S.O.	
Hot Tank Inlet Header	Hot Tank Inlet Nozzle	1150	35	19.4	12" Sch 20	470	3	-	3-12" S.O.	(3) Branch Lines
Hot Tank Outlet Nozzle	Hot Tank Outlet Header	1150	35	19.4	12" Sch 20	275	3	3	3-12" S.O.	(3) Branch Lines
Hot Tank Outlet Header	S.G. Pump Suction	1150	35	10.8	24" Sch 20	140	4	4	-	
S. G. Pump	Steam Gen. (S.G.)	1150	110	19.3	18" Sch 20	350	2	6	-	
Hot S.G. Supply Line	Reheater Inlet	1150	110	18.5	10" Sch 20	30	-	1	-	
Hot S.G. Supply Line	Superheater Inlet	1150	110	21.6	14" Sch 20	80	-	1	-	
Reheater Outlet	Evaporator Inlet Line	860	75	17.6	10" Sch 20	70	-	1	1-10" Cont.	
Superheater Outlet	Evaporator Inlet Line	860	75	20.6	14" Sch 20	40	-	1	-	
Evaporator Inlet Line	Evaporator Inlet Nozzle	860	75	18.3	18" Sch 20	75	2	4	-	
Evaporator Outlet Nozzle	Cold Tank Inlet Line	650	35	17.9	18" Sch 20	500	5	12	-	
Cold Tank Inlet Line	Cold Tank Inlet Nozzle	650	35	17.2	10" Sch 20	290	-	12	3-10" S.O.	(3) Branch Lines
Cold Tank Outlet Nozzle	Cold Tank Outlet Line	650	35	11.4	16" Sch 20	230	-	12	3-12" S.O.	
Cold Tank Outlet Line	Tower Pump Suction	650	35	9.6	30" Sch 20	120	2	4	-	
Tower Pump Discharge	Tower Base	650	300	22.5	20° .5" Wall	400	-	12	-	
Hot Tank Inlet Line	Cold Tank Inlet HDR	650	35	13.5	10" Sch 20	220	-	2	1-10" S.O.	Receiver return to Cold Tanks for Startup & Standby
Cold Tank Outlet Line	Hot Tank Outlet Line	650	35	20.3	10" Sch 20	220	-	2	1-10" S.O.	S.G. Standby and Startup By-Pass
Receiver Downcomer	Cold Tank Inlet Header	650	35	15.9	2" Sch 40	1200	-	6	1-2" S.O.	Receiver Vent Line
Tower Pump Discharge	Cold Tank Inlet	650	300	11.7	4" Sch 80	120	-	4	1-4" S.O.	
Tower Pump Suction	Tower Pump Discharge	650	300	11.7	4" Sch 80	60	4	4	4-4" S.O.	Cold Trap System
S.G. Vent	Evaporator Outlet	1150	75	15.9	2" Sch 40	500	3	6	3-2" Cont.	(3)S.G. Vent Lines
Tower Pump	Dump Tank	650	50	11.7	4" Sch 40	30	-	4	1-4" S.O.	
S.G. Pump	Dump Tank	1150	50	12.6	4" Sch 40	30	-	4	1-4" S.O.	
S.G.'s	Dump Tank	900	50	12.1	4" Sch 40	500	3	4	3-4" S.O.	
Cover Gas Main	Between Storage Tanks	650	50	82.0	10" Sch 40	300	6	-	-	
Cover Gas Branch	Storage Tanks	650	50	45.0	8" Sch 40	290	-	6	6-6" S.O	
Cover Gas Header		100	100	--	4" Sch 40	360	6	-	-	
Cover Gas Supply Lines		100	100	45.0	2" Sch 40	600	-	-	-	6 Total
S.G. Rupture Discs	RP Tank	900	200	15.0	10" Sch 40	225	3	5	-	Carbon Steel
Fill Line		600	100	12.0	4" Sch 40	200	-	4	1-4" S.O.	

*This selection is consistent with the ASME Section VIII, Division 1 code and (or) ANSI B16.34
**S.O. = shutoff valve, Cont. = control valve

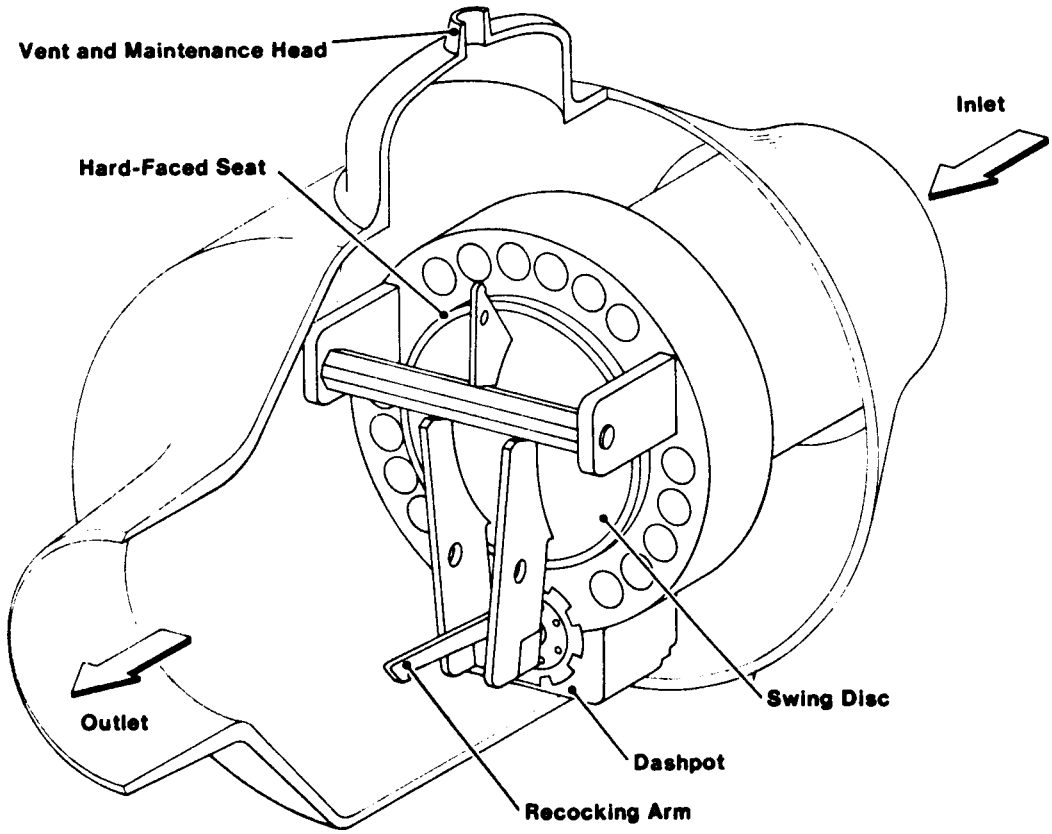

Figure 5.4-4. Large Sodium Check Valve

PURPOSE: ISOLATE HIGH PRESSURE RESULTING FROM RECEIVER DOWNCOMER STATIC HEAD FROM LOW PRESSURE HOT LEG STORAGE TANKS

REQUIREMENTS: DESIGN TEMPERATURE: 1100F
FLOW RANGE: 200 TO 20,000 GPM
CONSTANT PRESSURE DROP: 190 ±10 PSI
TIGHT SHUT OFF
HIGH RELIABILITY — 100% REDUNDANCY

ARRANGEMENT:

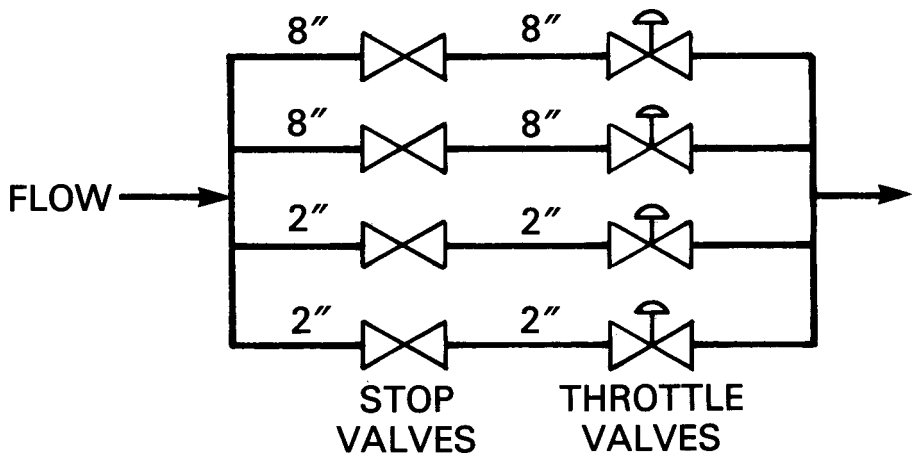

Figure 5.4-5. Downcomer Sodium Throttle Valve Concept

MANUFACTURER	CONTINENTAL FISHER
TYPE	BUTTERFLY
SIZE	8 in PIPE - 300 lb
FULL TRAVEL	3 sec
MATERIAL	S.S.
DESIGN TEMP.	1300°F

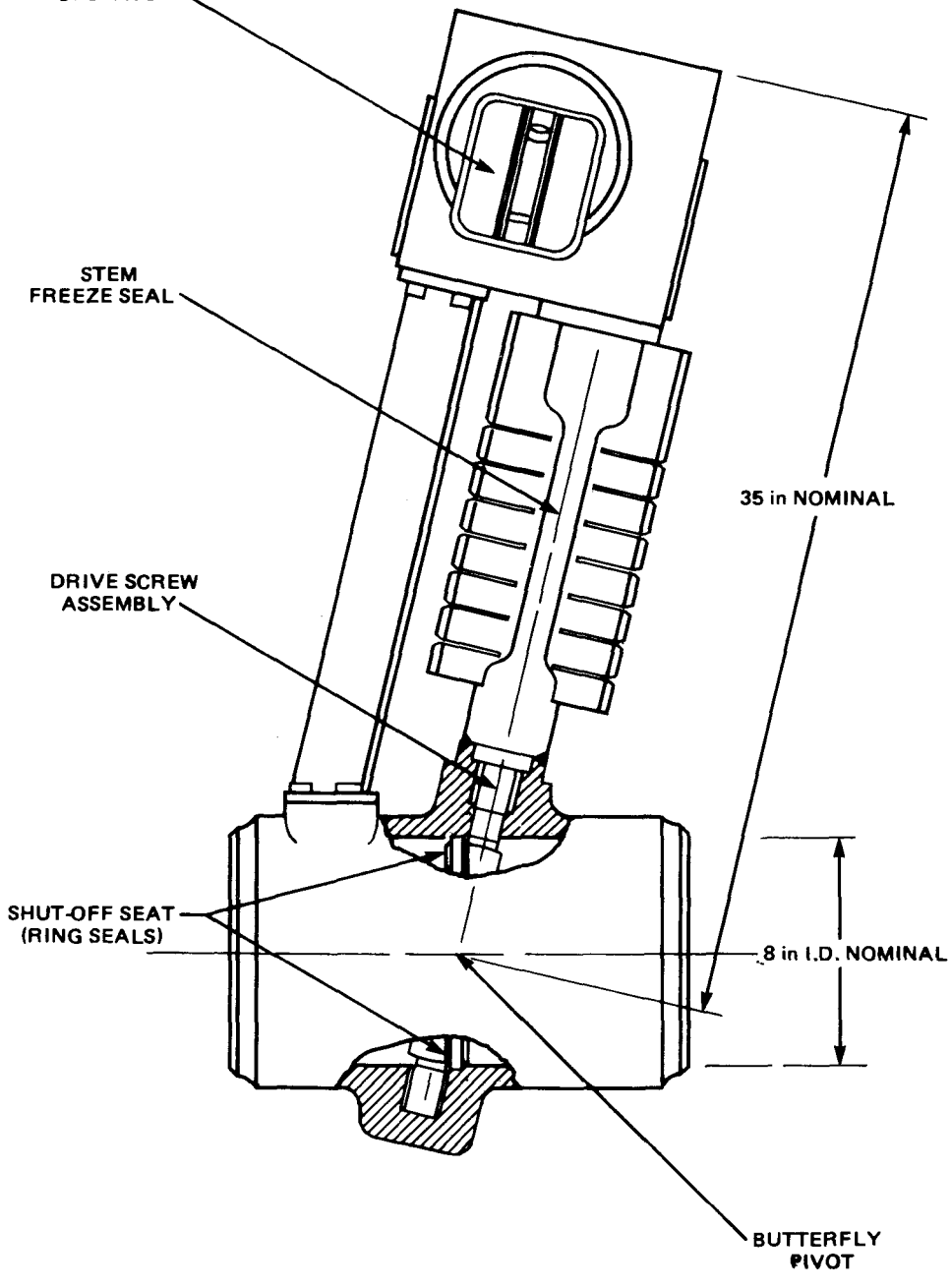

Figure 5.4-6. Eight-Inch Sodium Throttle Valve

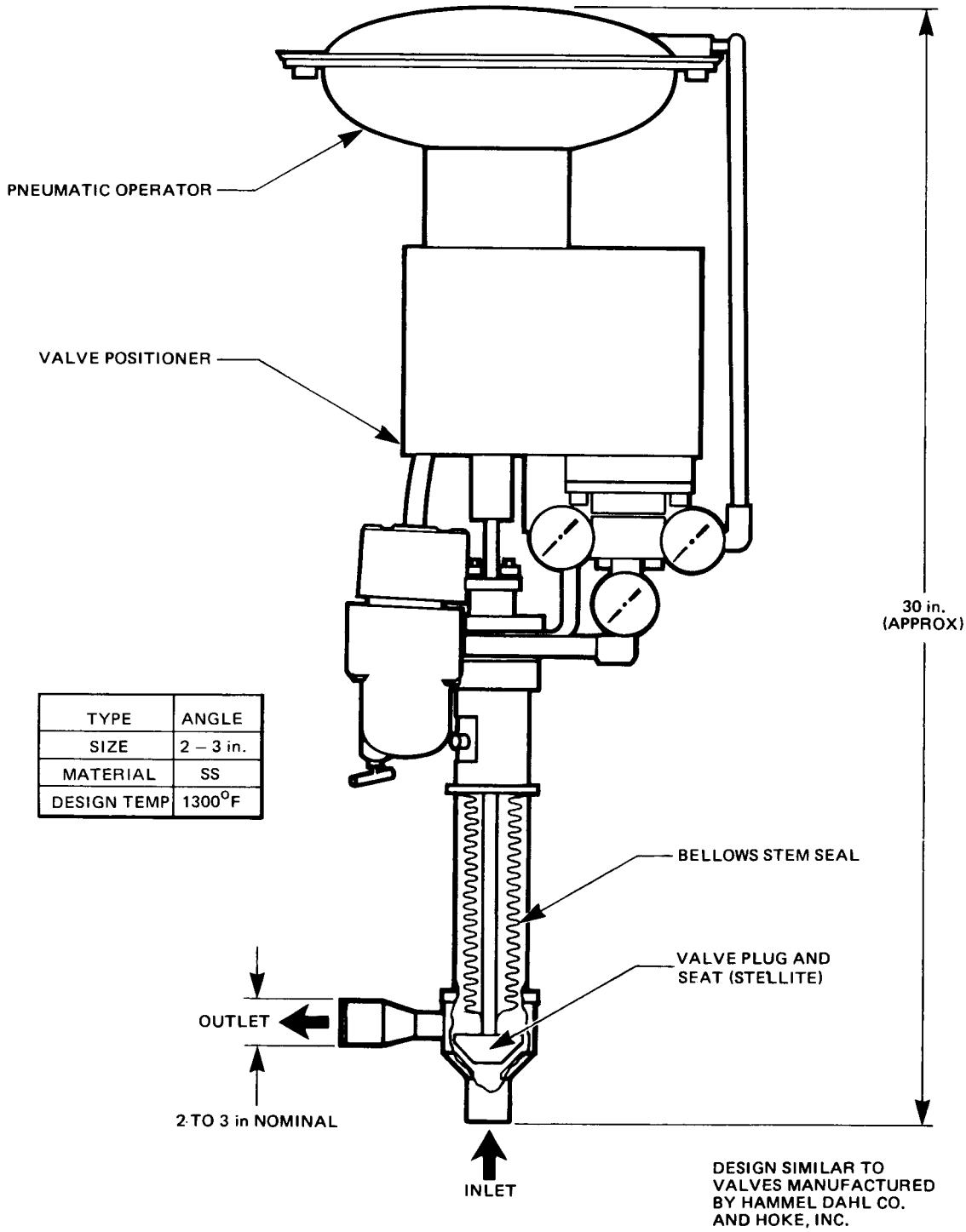

Figure 5.4-7. Two-to-Three-Inch Sodium Throttle Valve

Table 5.4-4

LARGE SODIUM VALVE EXPERIENCE

Throttle Valves:

8-inch Butterfly Throttle Valves (Continental Equipment Company) Successfully Operated Since 1962 in SCTI. Temperatures Up to 1200 F (Similar Valves Up to 10 inches used by Japanese in 50 MW Test Facility.)

2-inch to 4-inch Globe Throttle Valves Successfully Operated at Temperatures Up to 1400 F. (Manufactured by Hammel Dahl, Hoke, Powell.)

Large Stop Valves:

28-inch FFTF* Valves - Rockwell Manufacturing Company

8-inch FFTF Valves - Crane Company

Hallum Valves - Cooper Alloy
Manning Maxwell and Moore

6-inch Valves for GE & Westinghouse Loops - Valcor Company

Check Valves:

24-inch CRBRP** Valve - Foster Wheeler Energy Corporation

16-inch FFTF Valve - Foster Wheeler Energy Corporation

*Fast Flux Test Facility

**Clinch River Breeder Reactor

For normal sodium purification, two large counterflow heat exchanger cold traps will be used (see Figure 5.4-8). The cold traps are installed in parallel in a loop around the cold leg pump. Provision is made for separate or simultaneous operation of the traps, and isolation and replacement when the capacity of the trap is reached. The cold trapping temperature is expected to be ∿250 to 300 F during normal operation with the cold leg sodium temperature at 612 F.

5.4.4 Sodium Loop Relief and Drain

The sodium loop relief system is designed to accommodate the effects of a large sodium-water reaction which could occur either in the evaporator, superheater, or reheater.

During normal plant operation, the relief system remains passive. In the event of a large sodium-water reaction (low probability), the rupture disc associated with the affected module will burst, allowing sodium and reaction products to be ejected into a reaction products tank. Hydrogen gas vented from the reaction is passed through the tank and burned at the exit of a flare stack. The dense reaction products are accumulated in the bottom of the reaction products tank. Following such a sodium-water reaction, sodium remaining in the piping loop and steam generators can be drained into the sodium drain tank to prevent solidification of reaction products within the piping system.

The rupture disk assembly which is close coupled to the sodium outlet of each steam generator is shown in Figure 5.4-9. The assembly consists of a 10-inch reverse buckling Inconel disk which is mounted in front of a knife edge. The disk is designed to collapse against the knife blades when the burst pressure exceeds ∿300 psi.

The reaction products tank (Figure 5.4-10), is designed to accept three inlet pipes coming from the three steam generators. Reaction products are retained in the bottom of the tank.

A sodium drain tank (Figure 5.4-11) is provided at the lowest point in the loop. The 10,700 cubic foot tank is located under the pump and auxiliary equipment building with all sodium piping designed to drain to that point. The tank is trace-heated and insulated. Normally, the tank remains empty. For periods of maintenance, the tank is designed to store the sodium inventory in the piping and steam generators exclusive of that in the energy storage tanks.

5.4.5 Cover Gas Components

An argon cover gas is provided for the maintenance of a positive (<13 psig) inert gas pressure above the sodium in the storage tanks and for purging, filling, and draining operations in all sodium systems. The cover gas is supplied to the storage tanks through interconnected piping from an argon high pressure tank trailer situated near the pump and auxiliary equipment building. Rupture discs are placed in the lines to prevent cover gas pressures from exceeding design values.

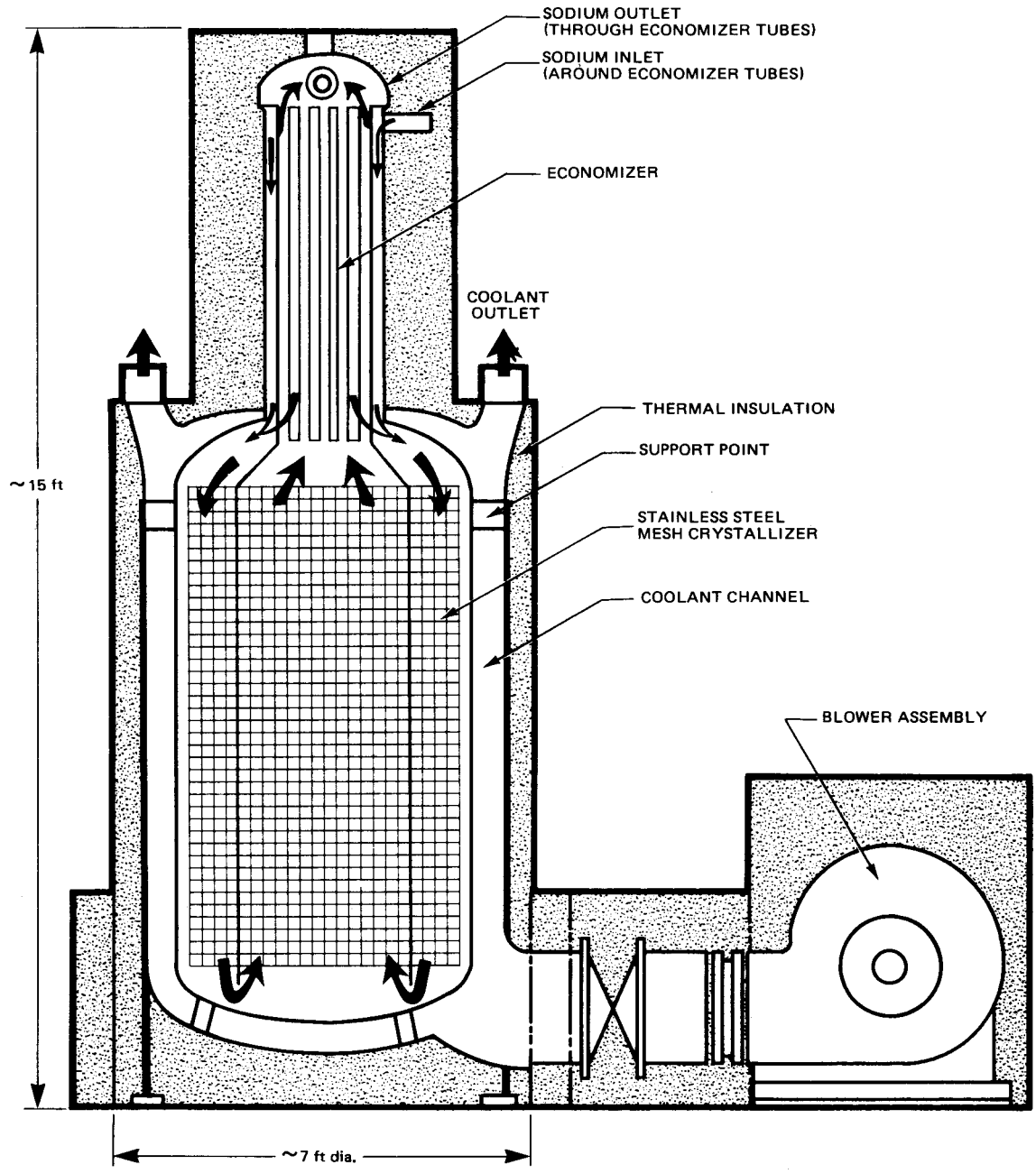

Figure 5.4-8. Cold Trap Design

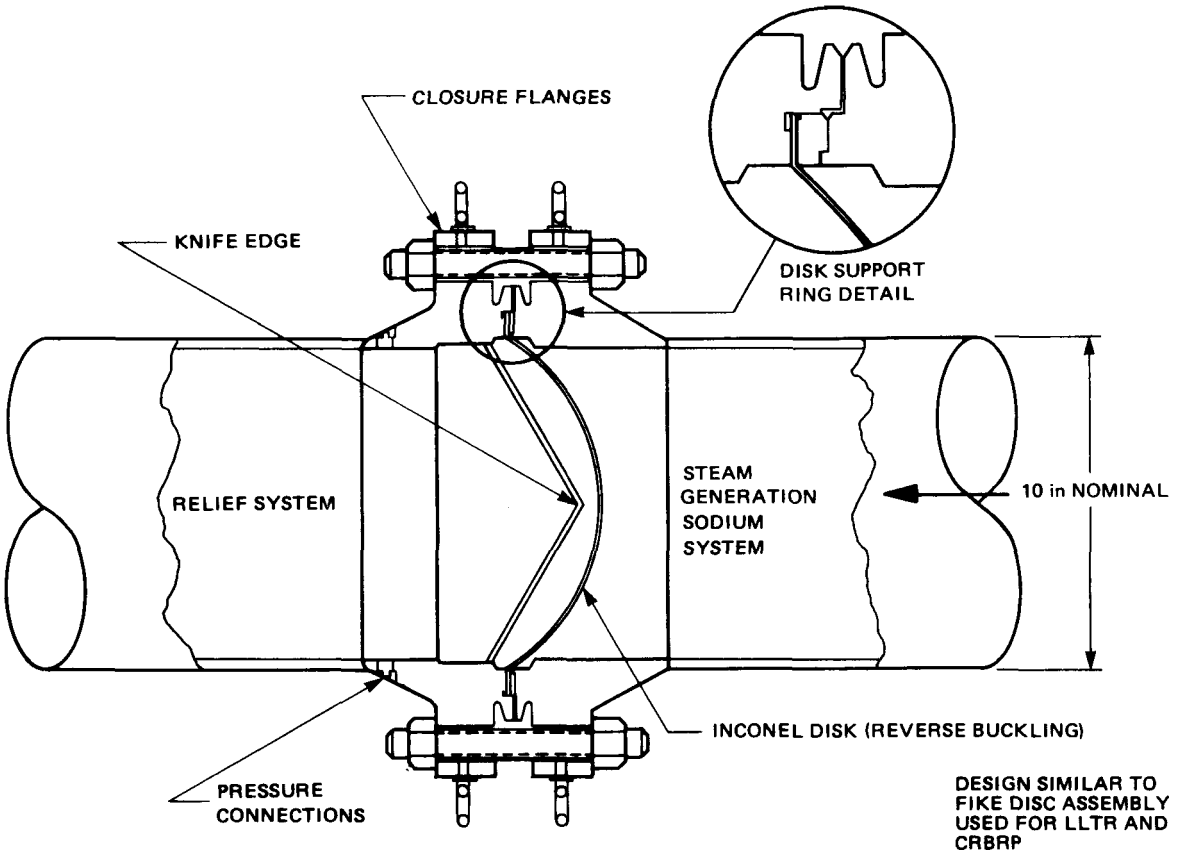

Figure 5.4-9. Sodium-Water Reaction Relief System-
Rupture Disk Assembly

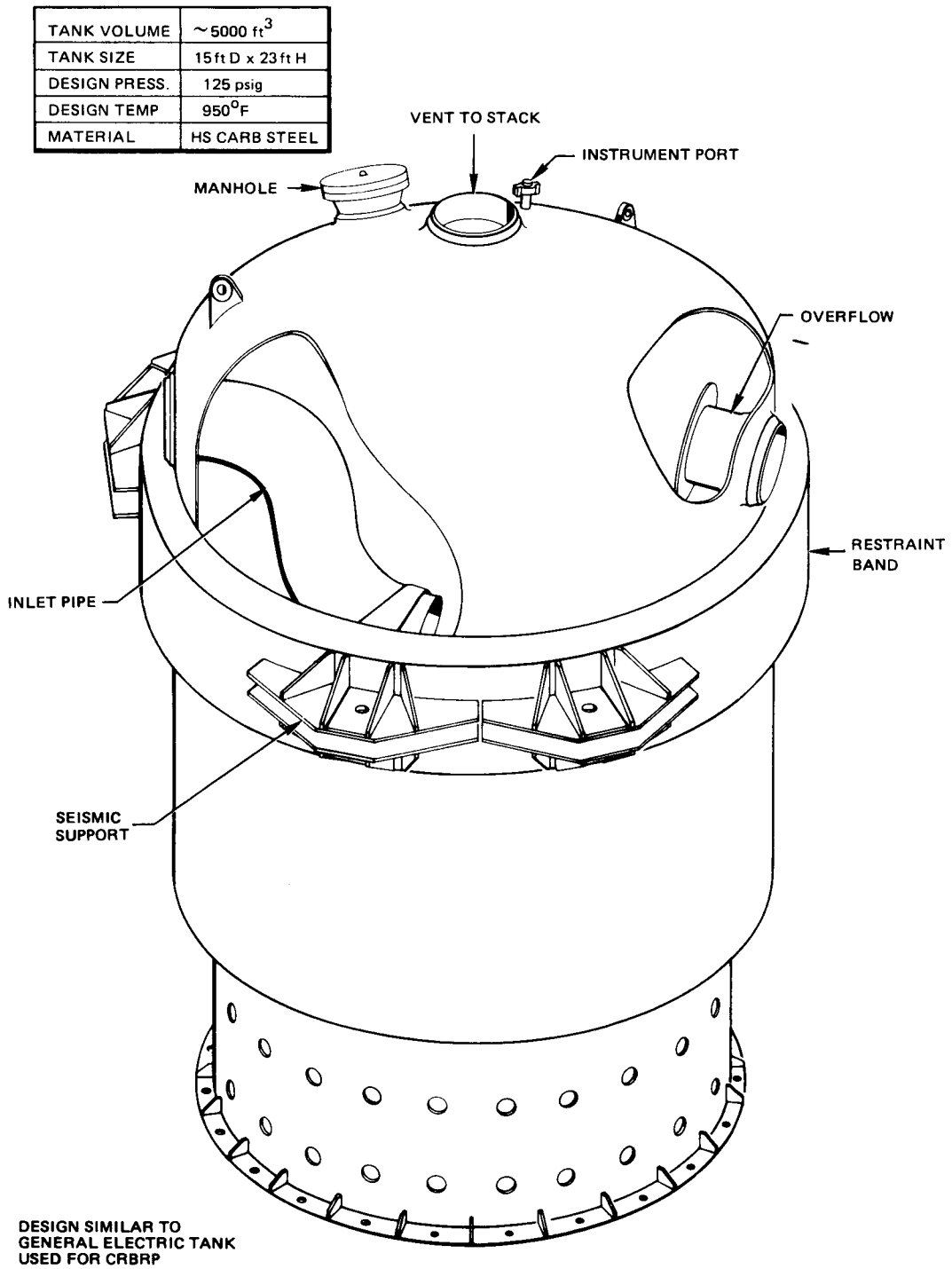

Figure 5.4-10. Reaction Products Separator Tank

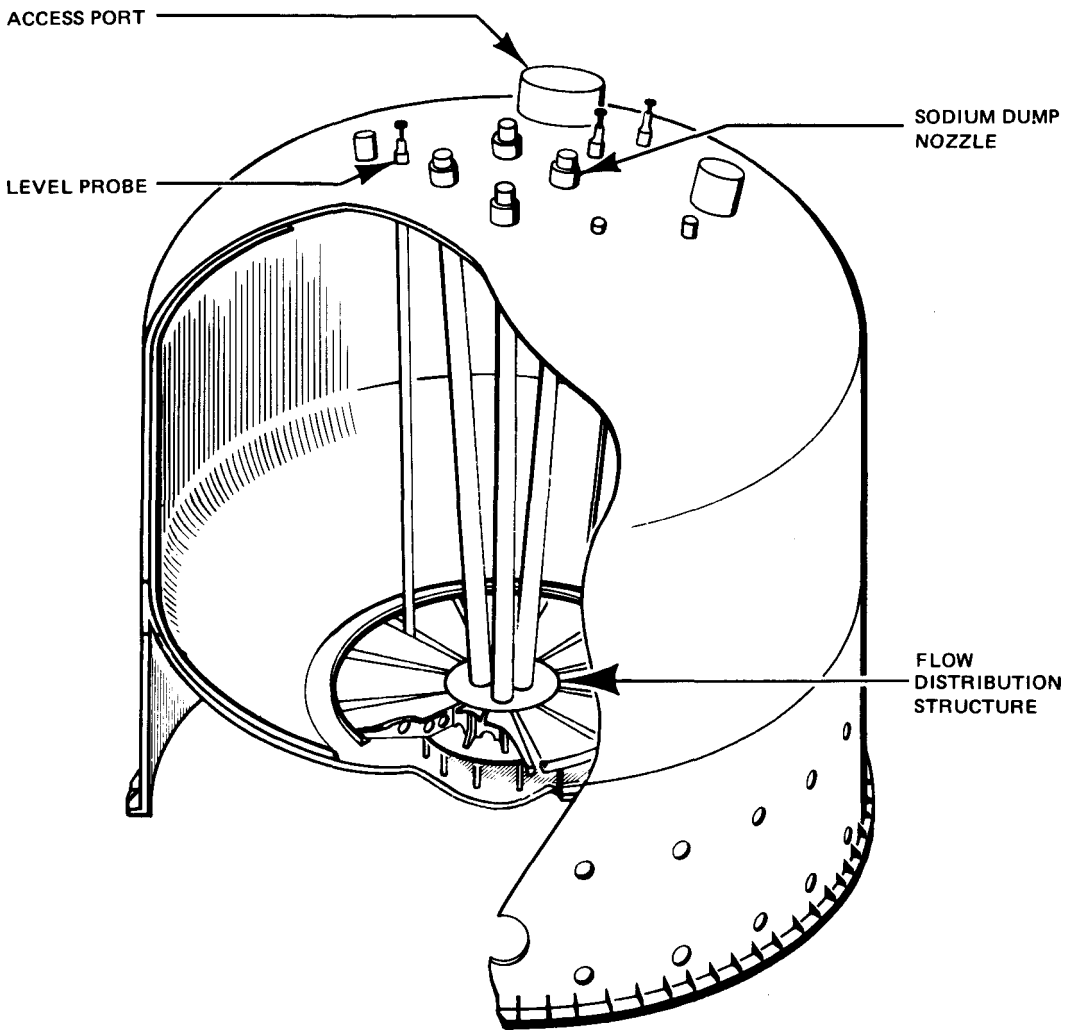

APPROX. SIZE	28 ft dia. x 25 ft HIGH
CAPACITY	10,700 ft^3
MATERIAL	SA515 CS

Figure 5.4-11. Sodium Dump Tank

The storage subsystem will not consume argon other than a small amount due to minor leakage, and purging requirements during maintenance. During regular operation the cover gas moves back and forth between the hot and cold storage vessels. This requires slightly greater thickness in the tank walls to accommodate the resulting pressure variations, but it saves the expense of argon losses or alternately of a compressor and gas storage tank. These options are discussed in more detail in Appendix Q.

5.4.6 Leak Detection and Fire Protection

Three separate systems have been included in this concept to provide the following:

- Detection of water to sodium leaks in the steam generators
- Detection of sodium to air leaks in piping and tankage
- Sodium fire detection, alarming, containment, and extinguishing

A minimum of two oxygen/hydrogen leak detector modules are incorporated in the sodium piping in near proximity to the steam generator outlets. The purpose is to provide sufficient protection against steam/water-to-sodium leaks in the steam generators to ensure that extensive system and steam generator damage would not occur and that plant downtime would be minimized. The leak detector modules, as shown in Figure 5.4-12, are the same design as those being developed for the Clinch River Breader Reactor (CRBR). The module is designed to be attached to loop piping and, with its own pump, extract a small amount of sodium from the loop to continuously measure its hydrogen and oxygen content. Alarms can be set such that manual, semi-automatic, or automatic action can be taken.

Sodium-to-gas/air leak detectors would be installed around vessels and piping where sodium might leak into surrounding and confined gas spaces. These detectors can provide continuous surveillance, leak location, and advanced warning of possible sodium fires. Most effective use of these detectors is made by application to nozzle-tank interfaces, fittings, and valves where gas enclosures can be maintained.

Sodium fire protection design features include means for detecting, alarming, containing, and extinguishing sodium fires. For air-filled cells, sodium spills can be confined and extinguished by use of steel catch pans with suppression decks located above the bottom of the catch pans to permit sodium to flow into the pans but restricting the flow of air/oxygen at the sodium surface. In the event of a spill, the reaction will consume the oxygen below the deck and reaction product gases will displace oxygen in the space to aid in extinguishing the fire.

A massive sodium spill resulting from the rupture of one or more storage tanks will be contained by the earth dikes which are located around the tank complex. Fires in this case would be prevented by dispersing fire suppressing chemicals such as Met-L-X over the surface of the liquid.

5.4.7 Insulation and Trace Heating

Based on the data developed in the parametric analysis (see Section 3.4.5), Kaowool (alumina silicate) and Thermal Wool Type II (fiberglass) insulation was selected for use on tankage, piping, and fittings.

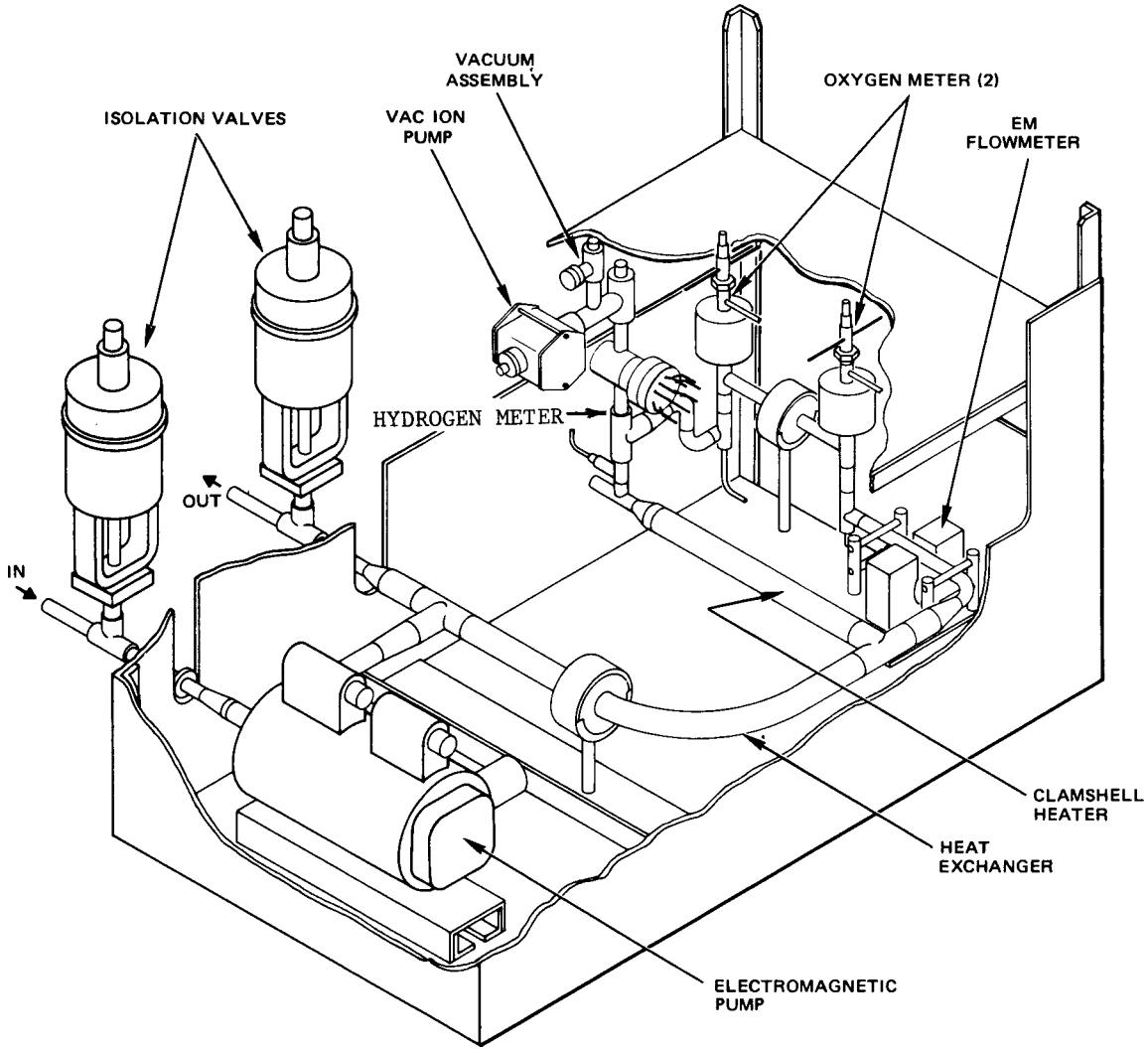

Figure 5.4-12. Oxygen-Hydrogen Detection Module

Insulation thickness on the storage vessels was selected by performing a comparison of the cost of tank insulation and the incremental cost in the receiver/collecter subsystems due to thermal losses. These results are summarized in Figure 5.4-13; they show that the insulation thickness for the hot tanks optimizes at about 1.5 feet, while that on the cold tanks shows lowest cost at about 2.5 feet. Kaowool formed the inner 29 percent of the insulation thickness on the hot tanks, with Thermal Wool as the outer layer; the cold tank used Thermal Wool only. Kaowool is used in the inner layer for hot leg applications since it has low thermal conductivity at high temperatures and the bonding agent in Thermal Wool Type II insulation is limited to 1000 F. Thermal Wool Type II would be used in the hot leg outer layers and throughout the cold leg because its thermal conductivity is low up to 600 F and, as shown in Table 3.4-16, the cost per linear foot is considerably lower than other types.

Costs used in the Figure 5.4-13 comparison were $0.60/cubic foot for Thermal Wool, $7.80/cubic foot for Kaowool, and $0.38/square foot for an aluminum outer jacket. From preliminary collector designs, it was estimated that each MW_t of loss from storage represented 8760 $MW_t h$ of energy lost per year, and that the added collector/receiver required to provide this annual energy would have an incremental cost of $0.671 million.

Based on this optimization, the tank insulation has been specified to be that shown in Figure 5.4-14. Pipe insulation (Figure 5.4-15) was chosen to be similar to that on the tanks but not as thick. No optimization calculation was performed for the pipe insulation.

Thermal losses from the storage vessels have been computed for the concept described above. At the design point these losses are:

	Cold Tanks	Hot Tanks
Insulation Loss (MW)	0.108	0.320
Support Loss (MW)	0.008	0.008
Total (MW)	0.116	0.328

Piping thermal losses were also estimated as shown below:

From	To	MW_t
Outlet of Steam Generator	Inlet of Cold Tanks	0.028
Outlet of Cold Tanks	Inlet of EM Pumps	0.130
Outlet of Absorber	Inlet of Hot Tanks	0.155
Outlet of Hot Tanks	Inlet of Steam Generator	0.058
Total		0.371

The piping loss estimates were made on the basis of preliminary piping diagrams for this concept, and may not correspond exactly with the losses which could be computed from the data in Table 5.4-3.

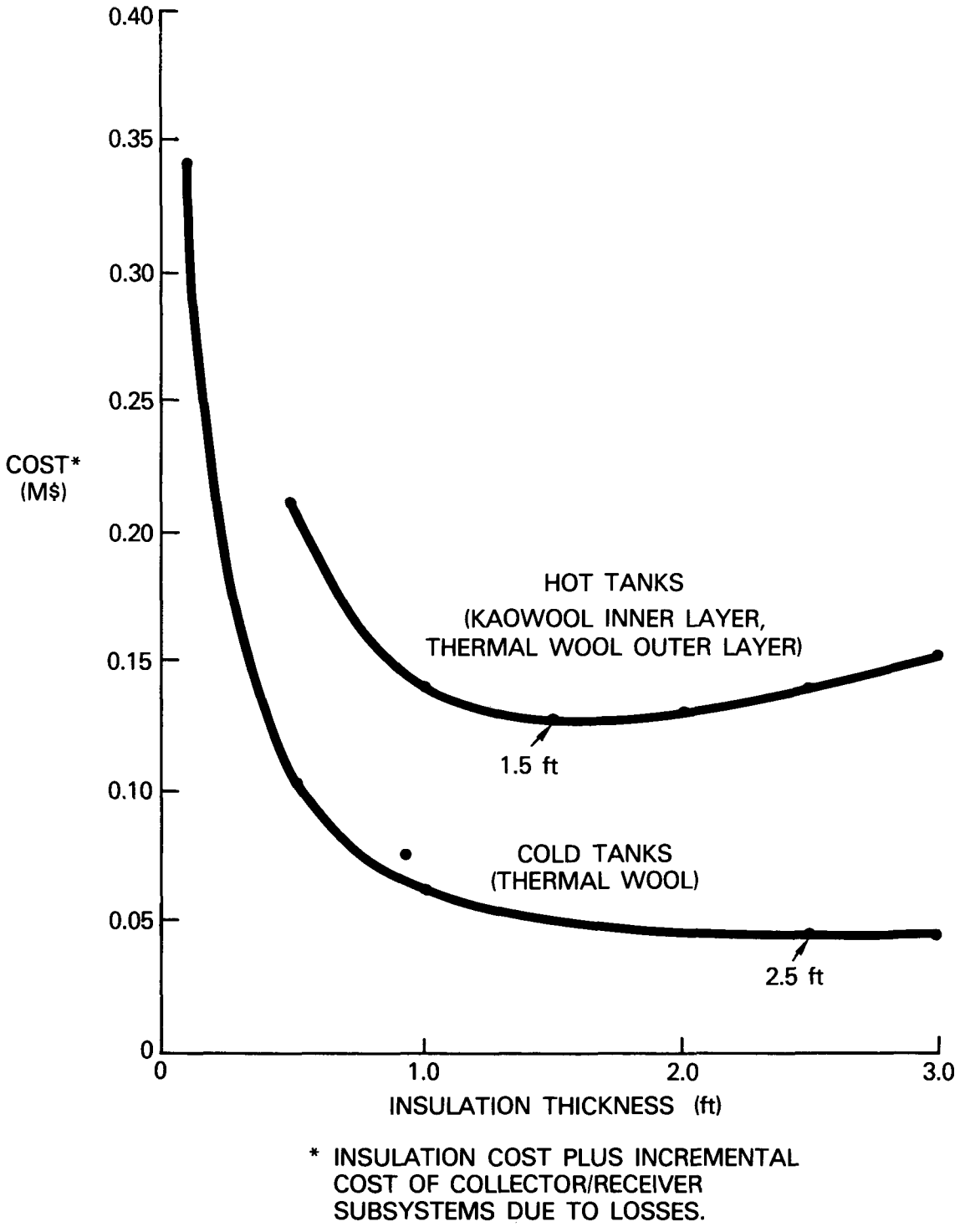

Figure 5.4-13. Storage Vessel Insulation Selection

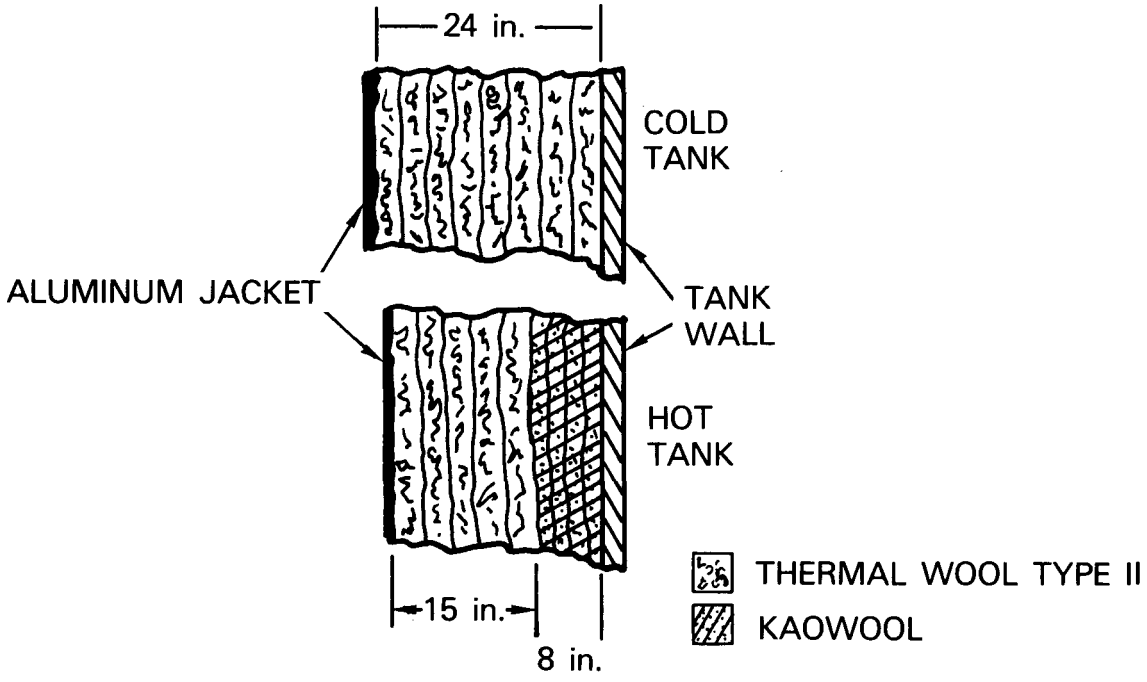

Figure 5.4-14. Storage Tank Insulation Concept

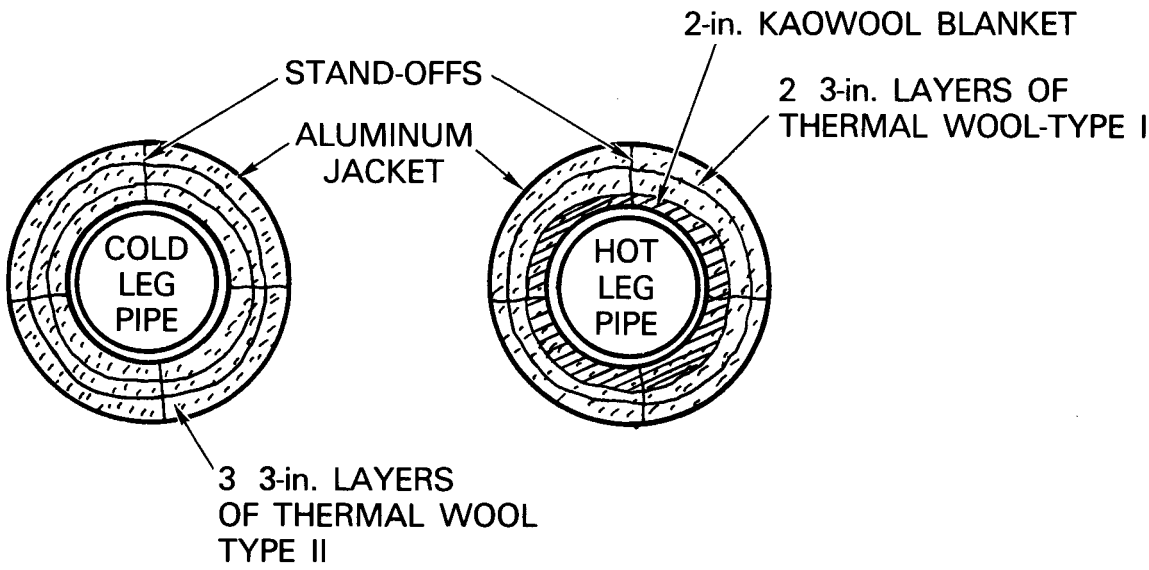

Figure 5.4-15. Piping Insulation Concept

Trace heating requirements and concepts were discussed in Section 3.4.4. Sodium piping, fittings and storage vessels will be heated with tubular resistance heaters designed to maintain a minimum of 350 F. Heaters will be attached to the bottom of horizontal piping with a tack-welded continuous metal strip. A helical mounting of the heater strip is used on vertical piping. Heaters on the storage vessels are installed in horizontal strips spaced about 32 inches apart.

5.5 ELECTRIC POWER GENERATION SUBSYSTEM

In Section 3.5 a steam cycle was selected for this plant concept which has main inlet steam conditions of 2400 psig/1000 F with a single reheat to 1000 F. A detailed heat balance for this cycle is shown in Figure 5.5-1. The turbine has opposed high pressure and intermediate pressure turbines on a common 21-inch diameter shaft. The low pressure turbine is a double flow unit with 23-inch last stage blades exhausting into a condenser at 2 inches of mercury. The feed heating train includes seven heaters, two of which are fed by extractions from the high pressure turbine (heaters above the reheat point-HARP).

Blow-down flow from the steam drum (ten percent) is used to perform feedwater heating before going through a demineralizer and flowing into the condenser. Full flow demineralizers are used in this cycle to protect the steam generators from corrosion.

An initial estimate of total plant auxiliary loads was 10.4 MW_e; therefore, this turbine cycle was sized to provide 110.4 MW_e (gross) or 100 MW_e (net) at a gross efficiency of 44.5 percent (heat rate = 7662 Btu/kW-hr).

Figure 5.5-2 gives an outline description of the turbine/generator, showing casing sizes, weights, and foundation loadings used in establishing installation requirements.

Starting and Loading

Briefly summarizing the starting and loading technique, the goal is to protect the turbine HP-IP rotor against potential cracking due to accumulated strain damage.*

Rotor strain damage depends on the number of thermal cycles encountered and also the severity of the cycles.

The type of transients that can occur are defined as follows:

Transient	Initial First-Stage Shell Metal and First-Stage Reheat Bowl Metal Temperature	Corresponding Downtime Prior to Transient
Cold Start	< 300 F	> 1 week
Warm Start	300 - 700 F	2-5 days
Hot Start	> 700 F	< 1 day
Daily Cycle		
Load Change	ΔT > 75 F	

*"Basic Information For Starting and Loading Reheat Fossil Fired Units," Manual GEK-50804, Medium Steam Turbine Department, General Electric Company, Lynn, Massachusetts.

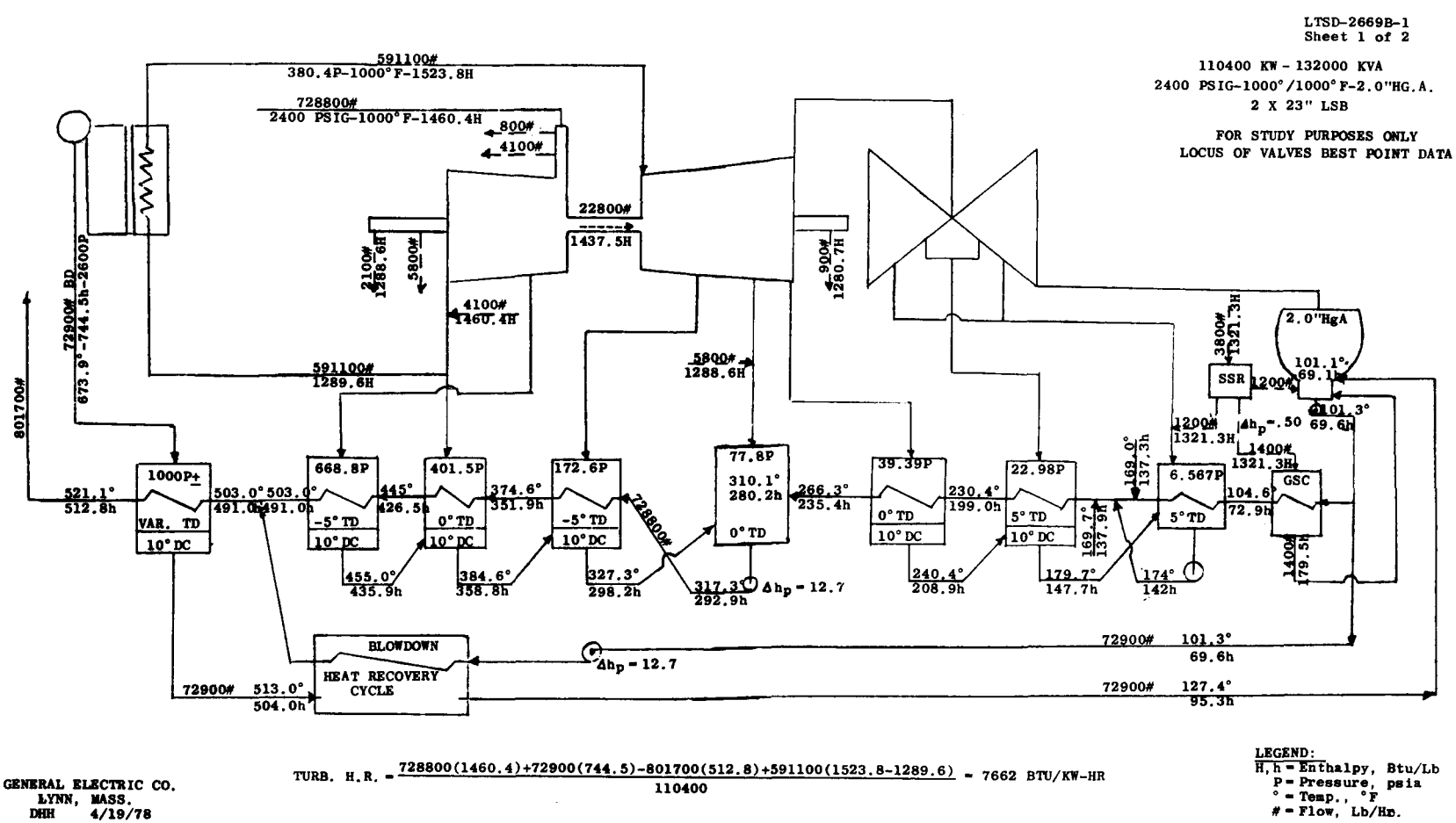

Figure 5.5-1. Steam Cycle Heat Balance

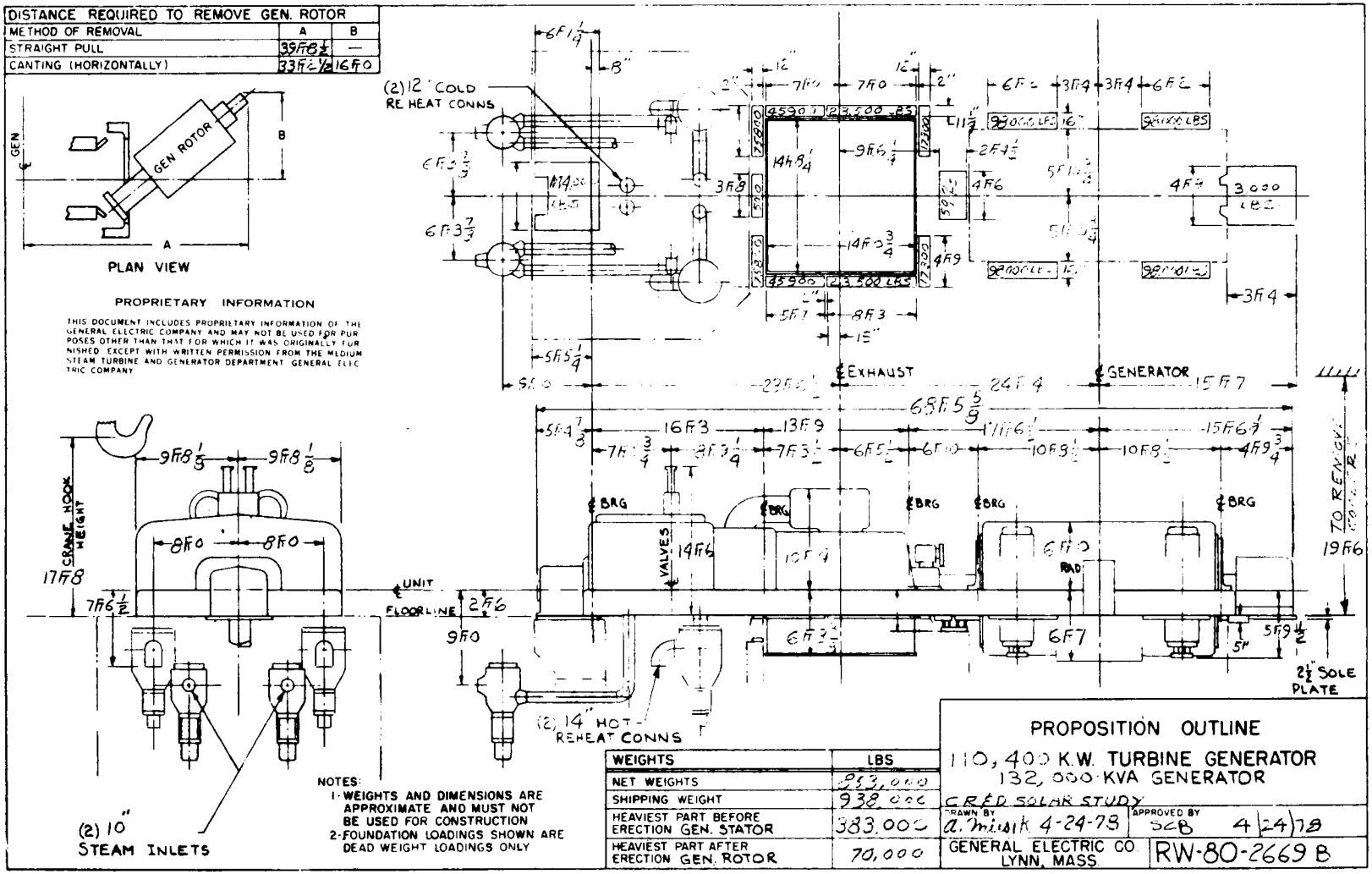

Figure 5.5-2. Turbine Generator Outline Drawing

The solution to maintaining a given life of the turbine, is to control the rate of temperature change of the rotor. Figures 5.5-3 and 5.5-4 define the limits on temperature change and ramp rate needed to achieve the desired life characteristics.

For 30-year life with daily startup and shutdown, this turbine must be operated to achieve at least 10,950 cycles. Table 5.5-1 describes a typical cold start where the turbine temperature is initially at ambient level (75 F). During the prewarm period, the rotor and shell are brought up to 300 F; there is no accumulation of cyclic damage due to this procedure. At the beginning of the start procedure, the mismatch between steam temperature and rotor temperature is 1000-300 = 700 F. If the start and load procedures are carried out as shown, the ramp rate is about 200 F/hour, and Figures 5.5-3 and 5.5-4 show that this procedure could safely be repeated more than 33,333 cycles without seriously damaging the HP/IP rotor.

A warm start procedure which yields a similar long life characteristic is shown in Table 5.5-2. The rotor starts at the temperatures shown and is heated up to 1000 F, so the temperature rise is about 690 F at a ramp rate of about 250 F/hour.

For the solar application, cold starts and warm starts will most likely be infrequent events. The typical event will be a hot start (Table 5.5-3) after an overnight shutdown. Here the high pressure section temperature excursion will be 240 F at a ramp rate of 221 F/hour, while the intermediate pressure section will go through 180 F at 166 F/hour. Again the available life is in excess of 33,333 cycles.

The initial steam conditions and flow rates required for these starting procedures are listed in Table 5.5-4.

These starting procedures are consistent with the daily scheduling of startup and shutdown, and allow ample margin for load following transients should the plant be dispatched in an afternoon load following mode.

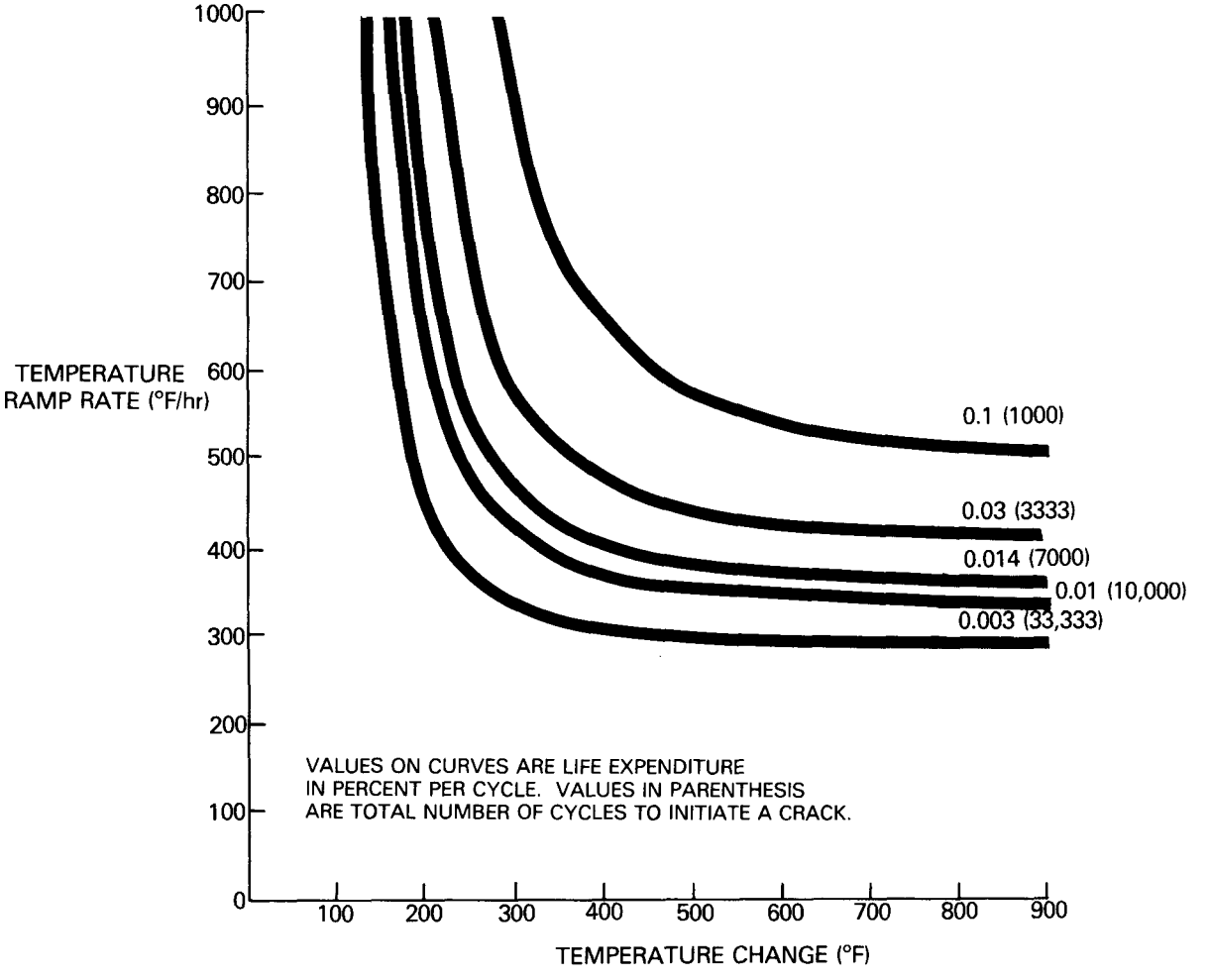

Figure 5.5-3. High Pressure - Cyclic Life Curves (21-inch Diameter Rotor)

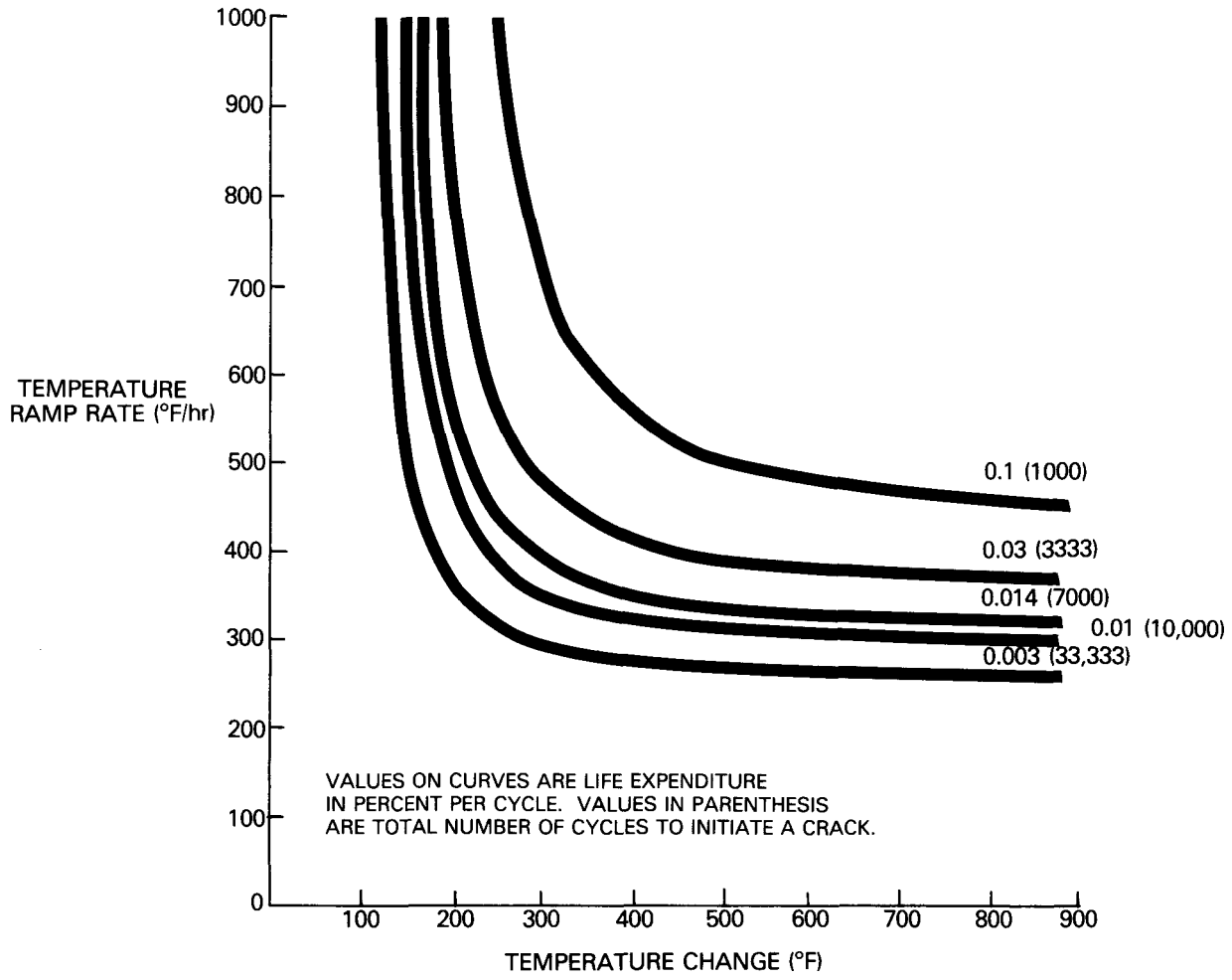

Figure 5.5-4. Reheat - Cyclic Life Curves
(21-inch Diameter Rotor)

Table 5.5-1

STEAM TURBINE TRANSIENTS
(COLD START)

COLD START (First Stage Shell Inner Metal Temperature < 300° F)

Assumed Initial Conditions Before Startup:

1st-Stage Shell Inner Surface Metal Temperature = 75 F
Reheat Bowl Inner Surface Metal Temperature = 75 F
Main Steam Temperature = 600 F
Main Steam Pressure = 1000 psi

Inlet	Time
Prewarm	1 hour
Start	1/2 hour
Load	2 hours and 40 minutes
Total	4 hours and 10 minutes

Cycles Available > 33,333

Table 5.5-2

STEAM TURBINE TRANSIENTS
(WARM START)

WARM START (First Stage Shell Inner Surface Metal Temperature Between 301 F and 700 F)

Assumed Initial Conditions Before Startup:

1st-Stage Shell Inner Surface Metal Temperature = 310 F
Reheat Bowl Inner Surface Metal Temperature = 320 F

Inlet	Time
Start	1/2 hour
Load	2 hours and 15 minutes
Total	2-3/4 hours

Cycles Available > 33,333

Table 5.5-3

STEAM TURBINE TRANSIENTS
(Hot Start)

HOT START (First Stage Shell Inner Surface Metal Temperature Greater Than 700 F)

Assumed Initial Conditions Before Startup:

1st-Stage Shell Inner Surface Metal Temperature = 760 F
Reheat Bowl Inner Surface Metal Temperature = 820 F

Main Steam	Time
Start	30 minutes
Load	35 minutes
Total	65 minutes

Cycles Available > 33,333

Table 5.5-4

STEAM SUPPLY REQUIRED FOR TURBINE START

Inlet Steam:	2400 psi/1000 F
Reheat Steam:	1000 F
Condenser:	2 inches Hga

Flow Rate	Duration
60,000 lb/hr	(10%) initial for seconds (off turning gear)
Then 30,000 lb/hr	(5%) up to and including no load
3,000 lb/hr*	(1/2%) shaft sealing steam required (overnight)

*much lower at full speed

5.6 PLANT CONTROLS

5.6.1 General

The controls for the Advanced Central Receiver System are structured to permit fully automatic operation of the plant under the direction and supervision of the plant master control (Section 5.6.6). Each subsystem will have the capability for operation in a semi-automatic mode (i.e., local control loops operative) under the control of a plant operator from the central control room. This will permit continued operation of the plant should the plant master control be inoperative.

Wherever possible, existing devices and technology have been specified. Conventional power plant control and instrumentation practices will be followed in the design of panels and operator stations.

5.6.2 Collector Subsystem Control

Control of the heliostat field is described in detail in Section 4.0 of the General Electric's Final Technical Report for DoE Contract EG-77-C-03-1468, "Solar Central Receiver Prototype Heliostat, Phase 1." The controls proposed in that report by the GE Energy Systems Programs Department are planned for inclusion in the Advanced Central Receiver power plant. The (minicomputer) controller(s) for the heliostats will interface with the plant master control described in Section 5.6.6 for operation under integrated automatic plant control, but will be provided with a free-standing capability to operate under the direction of a plant operator should the plant master control be out of service.

An extensive discussion of the subsystem control strategy, together with details of equipment components may be found in the cited report and will not be repeated here.

5.6.3 Receiver Subsystem Control

The primary control objective of the receiver controls is to deliver to the hot storage tanks sodium heated to a uniform temperature of 1100 F. The instrumentation and control equipment for this subsystem are illustrated in Figure 5.6-1.

The centrifugal tower pump will be operated at a constant speed to deliver sodium from the cold tanks at approximately atmospheric pressure at the receiver inlet manifold. The motor speed will be set for this condition when the sodium in the cold tanks is at its lowest operating level.

Sodium will be pumped through the receiver panels by the 24 electromagnetic (EM) pumps. Each pump will be separately controlled by terminal voltage variation to set the sodium flow rate at a value which will result in a sodium temperature of 1100 F at exit from that panel. Signals from thermocouples in the top and bottom discharge lines of each panel will be summed and used to generate the control signal for the pump controllers. This control strategy may result in high tube temperatures at low loads (see Section 5.3.2). Infrared scanners will be used to sense this condition and initiate receiver shutdown.

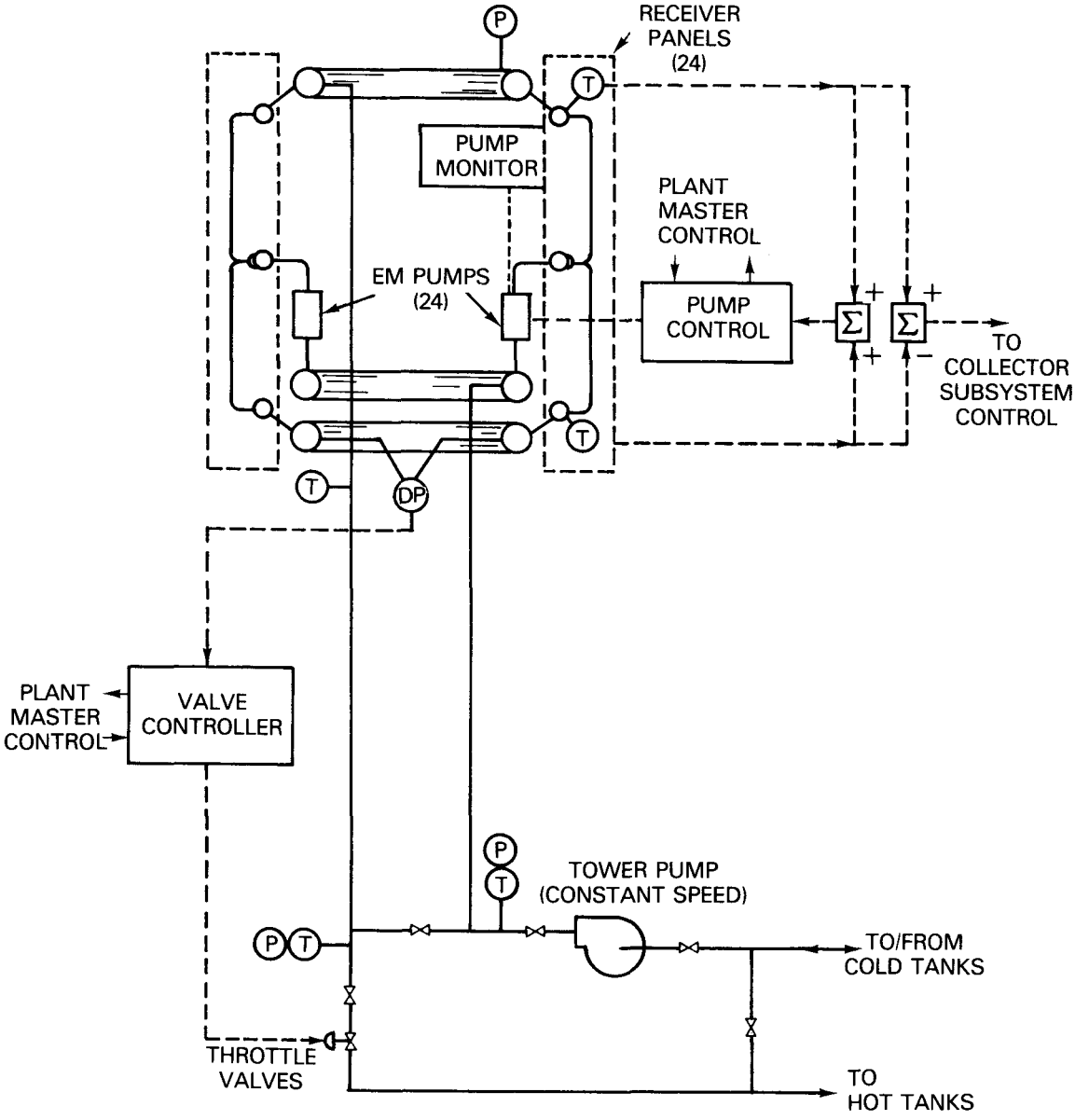

Figure 5.6-1. Receiver Subsystem Controls

The hot sodium flow will be throttled at the base of the tower to reduce the pressure resulting from the head in the downcomer. The throttle valves will be controlled to maintain approximately zero pressure differential between the riser and downcomer at the top of the tower.

For short-term shutdown (e.g., overnight), the receiver's insulating shutter will be closed, the tower lines will be shut off, and the shunting valve at the base of the tower will be opened. Sodium will circulate in the loop by natural convection. Calculations indicate that the sodium will stay above the freezing point for approximately 48 hours under these conditions.

Instrumentation and control equipment for the receiver subsystem is as follows:

Receiver Panel Flow Control

Twenty-four sets of instrumentation and control, one set for each receiver panel, comprised of:

Two type-K thermocouples, 3/16-inch OD, spring-loaded with wells (inlet and outlet flows)

Two millivolts-to-amperes (MV/I) transmitters for thermocouples

Two electronic adder/subtractors

One three-mode electronic controller (contact outputs to raise/lower voltage supply to EM pump) with set-point station

One GE-type AIRT induction voltage regulator motor driven from external raise/lower contact closures to supply controlled voltage to EM pump

One monitor panel with signal transducers for EM pump volts, amperes, and kVA, including necessary pump protective devices

Tower Flow Pumping and Control

One tower pump motor control, 3600 hp induction motor including starter, metering, and necessary protective devices

Three pressure transducers/transmitters, 316SS fittings for operation up to 1200 F sodium, 0-250 psig to be located at:

- tower pump discharge
- receiver discharge header
- receiver return at tower base

One differential pressure transmitter (receiver header ΔP), 0-15 psid full scale at 0-135 psig operating pressure

One three-mode electronic valve controller (tower return flow throttle valves) with setpoint station

Insulating Shutter Control

One insulation shutter drive and control comprised of:

Drive motor

Starter

Protective devices

Dynamic braking

Shaft brake and control

Operator Station

One operator control console for mounting in central control room with control devices, meters, recorders, and annunciators as required to supervise subsystem operation and permit semi-automatic operation by plant operator

5.6.4 Thermal Energy Storage Subsystem Control

The thermal energy storage acts as a buffer between the collector-receiver subsystems and the electric power generation subsystem. Subject to capacity limits, sodium may be charged and withdrawn simultaneously at differing flow rates in either the hot or cold storage tanks. This permits great flexibility in selection of plant operating modes and transition between modes.

Figure 5.6-2 illustrates the instrumentation and control equipment for the thermal energy storage subsystem. On the steam generator side of storage, a variable speed centrifugal pump is controlled to deliver that sodium flow rate which will provide the specified temperature and pressure of steam at exit from the superheater. This operates in conjunction with control of a valve in the reheater line which establishes a flow rate required to produce the specified reheat steam temperature. (Refer also to Section 5.6.5, "Electric Power Generation Subsystem.")

When starting the plant cold or following a shutdown of short duration, it is necessary to mix cold and hot sodium in variable proportions to avoid a thermal shock to the heat exchangers. Control valves responding to sodium temperatures at entry to the heat exchangers will proportion the flows to yield the desired sodium temperature.

Each storage tank will be instrumented to provide measurement of sodium temperature and level, and tank pressure above the sodium. This information will be displayed to the operator with annunciator alarms and monitored continuously by the plant master control. Each tank is also provided with motor-operated valves for tank isolation in the event of a leak, required maintenance on sensors, etc.

Other monitoring and protective devices are shown in Figure 5.6-3.

Instrumentation and control equipment for the thermal energy storage subsystem is as follows:

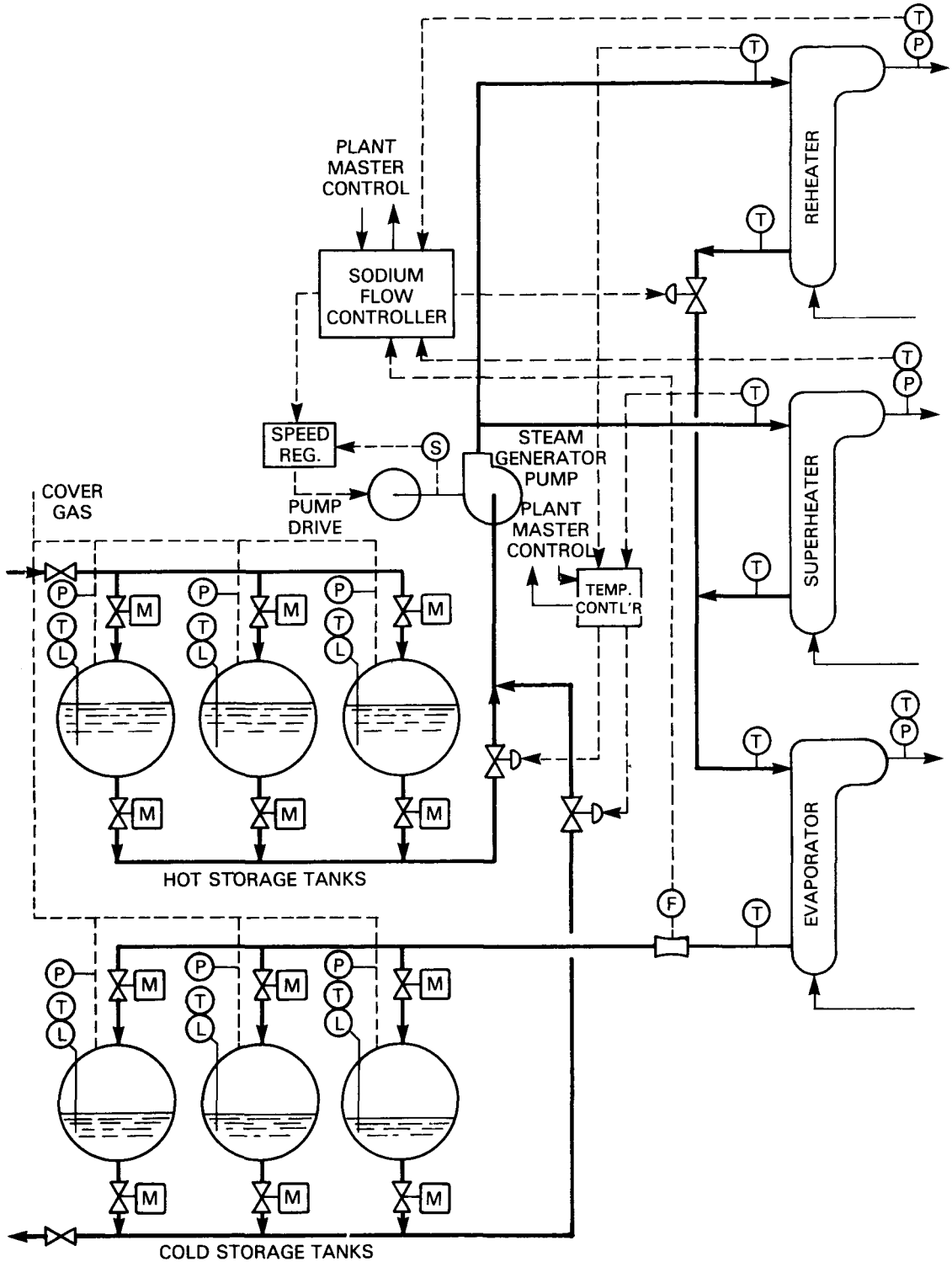

Figure 5.6-2. Thermal Energy Storage Subsystem Controls

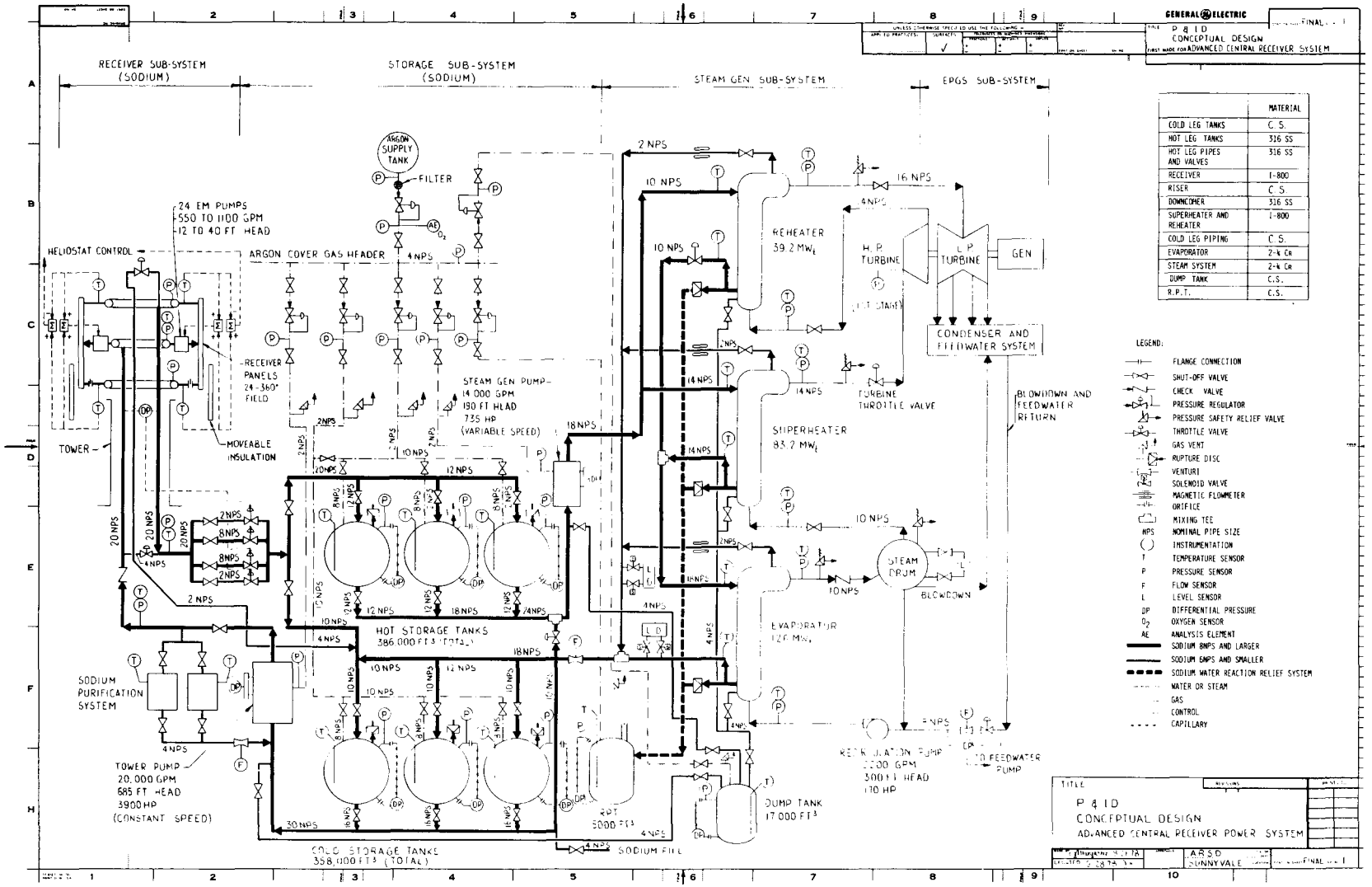

Figure 5.6-3. Piping and Instrumentation Diagram

Sodium Flow Control

One steam generator pump drive and control, including:

One AC-AC motor generator set

- AC induction drive motor
- AC synchronous generator
- Hydraulic slip coupling with controllable range 22-1/2 to 100 percent of top speed
- DC excitation supply for generator
- V/Hz regulator to maintain constant V/Hz output through control of generator excitation over range of 22-1/2 to 100 percent of top speed
- Motor starter, metering, and necessary protective devices

One 850 hp AC induction motor for centrifugal pump drive

- Motor starter, metering, control, and protective devices

One pony motor (for starting pump motor) with starter, metering, control, and protection

One steam generation subsystem controller to provide the following functions:

- Control of steam generator pump flow to regulate superheater steam exit temperature
- Control of throttle valve in reheater sodium flow to control reheater steam exit temperature
- Anticipatory control of sodium flows to superheater and reheater on detection of steam flow transients

One 18-inch carbon steel venturi (cold sodium return flow)

Maximum flow capacity: 1800 lb/sec of sodium at 614 F, 60 psig design pressure

One differential pressure transmitter

Full scale: 1800 lb/sec of sodium at 614 F = 19.29 psid

Nominal flow: 1587 lb/sec of sodium at 614 F = 15.0 psid

Six type-k thermocouples, 3/16-inch OD, spring-loaded with wells (inlet and outlet each heat exchanger)

Six millivolt/ampere (MV/I) transmitters for above thermocouples

Two three-mode throttle valve controllers (for control of temperature of mixed hot and cold sodium flow) with setpoint station

Tank Instrumentation

Six sets of instrumentation, one set per storage tank, comprised of:

One special top-inserted thimble to contain multipoint replaceable probe having six pairs of type-K thermocouples spaced at 10-foot vertical intervals

One differential pressure transmitter (see Figure 5.6-4 for tank level)

Full scale: 21 psid at 30 psig

One process pressure/current transmitter (tank pressure)

Full scale: 30 psig

Twelve MV/I transmitters

Leak Detection and Reaction Products System

Three 2-inch permanent magnet flowmeters, Type 316, Grade SA312, SS

One 0-12 lb/sec of sodium at 1000 F (reheater vent)

One 0-24 lb/sec of sodium at 1000 F (superheater vent)

One 0-36 lb/sec of sodium at 675 F (evaporator vent)

Two leak detection modules, self-contained, with sample pump, heaters and controls, diffusion cell, ionization pump, and Hz concentration meter readout; piping system to supply one-inch root valves capable of remote operation for isolation in case of leak.

One set of instrumentation for reaction products tank comprised of:

One top-inserted thimble assembly with replaceable probe and type-K thermocouples

One MV/I transmitter

One differential pressure transmitter (tank level)

Sodium Purification System

One four-inch carbon steel venturi (sodium purification system flow);

Maximum flow capacity: 730 lb/sec of sodium at 612 F, 50 psig design pressure

One differential pressure transmitter; full scale 730 lb/sec = 15 psid at 50 psig

Two type-K thermocouple assemblies

Two MV/I transmitters

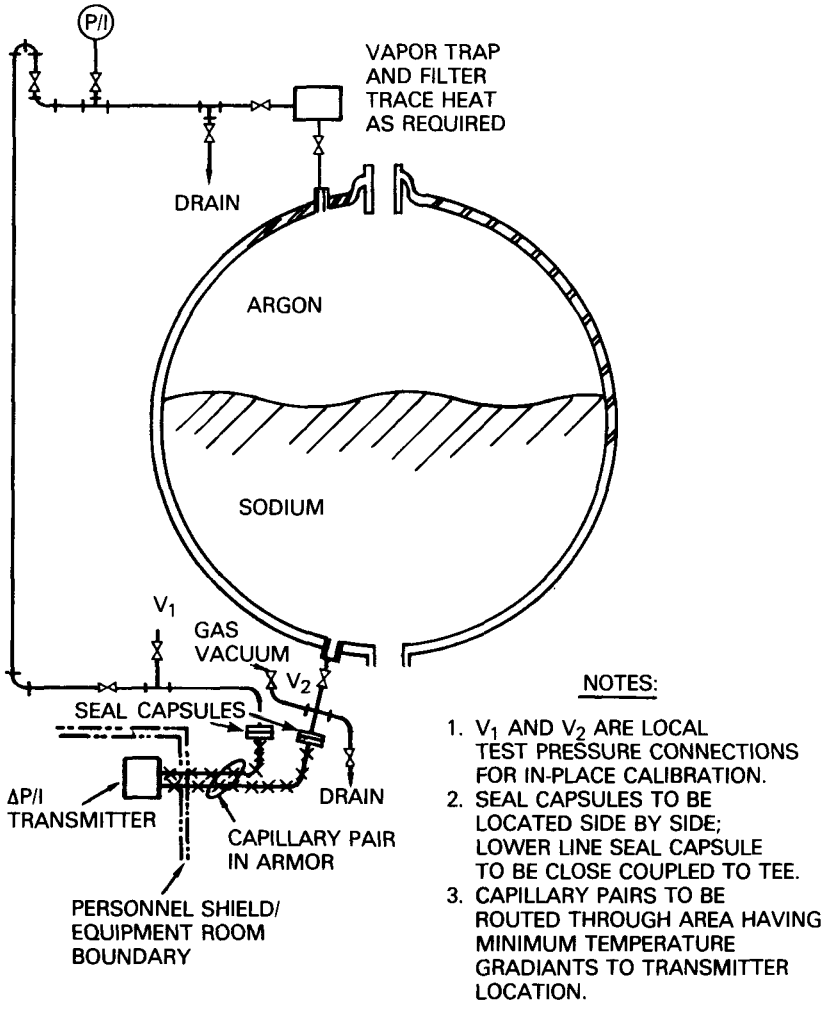

Figure 5.6-4. Tank Level and Pressure Measurement - Installation Details

Operator Station

One operator control console for mounting in central room with control devices, meters, recorders, and annunciators as required to supervise subsystem operation and permit semi-automatic operation by plant operator.

5.6.5 Electric Power Generation Subsystem Control

The overall arrangement of the control for the electric power generation subsystem is shown in Figure 5.6-5. Figure 5.6-6 shows in greater detail the configuration of the electric power generation subsystem (EPGS) with the major sensors, instrumentation, and controls.

The plant master control will direct the operation of an integrated boiler/turbine control which will be a coordinated control scheme. The coordinated control will provide the three well known modes of operation: boiler follow, turbine follow, and combined or coordinated modes. It will provide the unit demand functions, the variable pressure or pressure ramping controls, the operation mode selection, and the auto-manual selections.

The integrated boiler turbine control provides the pressure set point for the main steam pressure control, the turbine bypass control, the unit load demand signal for the sodium control system, and the main steam pressure control. The unit load demand signal also feeds through a transient compensation function to the main steam and reheat steam temperature control, and to the turbine control (electro-hydraulic control) when operating in the boiler follow or coordinated control modes.

The turbine bypass control is used during startup to match the superheat and reheat steam temperatures to the associated turbine metal temperatures (first-stage inner metal and reheat bowl inner metal.) It is also used during major electrical load rejections to bypass steam around the turbine to provide time for an orderly shutdown of the overall plant, or to maintain steam conditions and permit a rapid restart and reloading of the turbine-generator. During the warm-up phase of plant startup, the high pressure turbine bypass system is arranged to control the cold reheat pressure, ramping it as a function of main steam pressure. The low pressure (or reheat) turbine bypass system is set up to control the high pressure turbine bypass flow.

When the turbine-generator is rolled, the bypass system controls are transferred to have the high pressure turbine bypass system control flow and the low pressure turbine bypass system control cold reheat pressure. This permits an automatic, smooth transfer of steam flow from the turbine bypass systems to the turbine at selected steam conditions. As soon as the bypass steam flow is reduced to zero, the bypass systems will be isolated with block valves. A small steam flow will be maintained through the bypass systems to keep them near operating temperature to avoid excessive thermal shock in the event of a load rejection.

The main steam pressure control will be a conventional pressure control system using a three-mode controller. The pressure set point and the unit demand signal will be provided by the integrated boiler turbine control. Its control output will provide reference or demand signals to the sodium temperature and flow control system. Its control action will be limited or cut back by signals from the temperature controls. Three pressure transmitters with automatic two-out-of-three selection will be used to provide a reliable pressure feedback.

The steam temperature controls (superheater and reheater) will make use of attemperation (or desuperheating) to maintain main steam and reheat steam

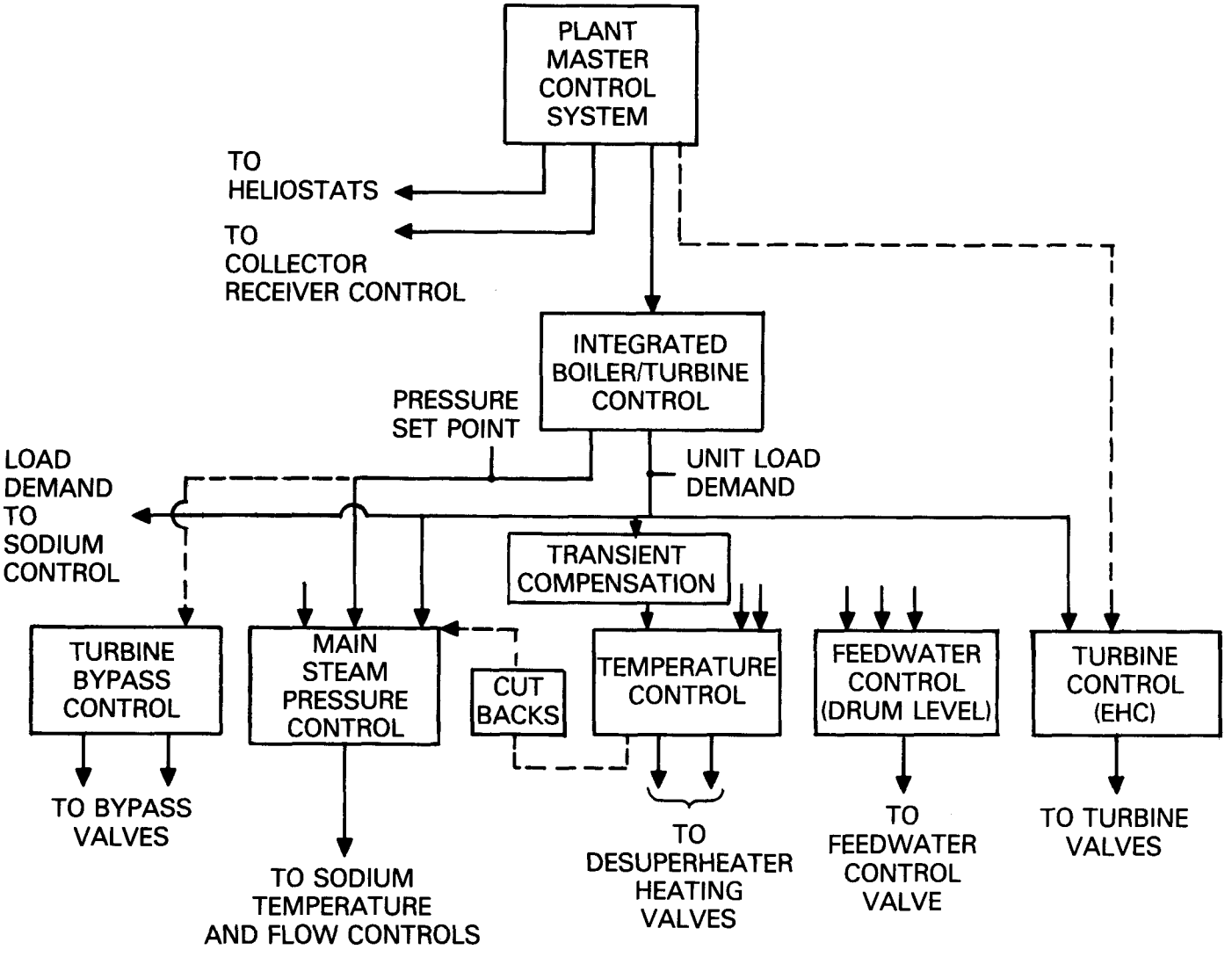

Figure 5.6-5. Overall Control for EPG Subsystem

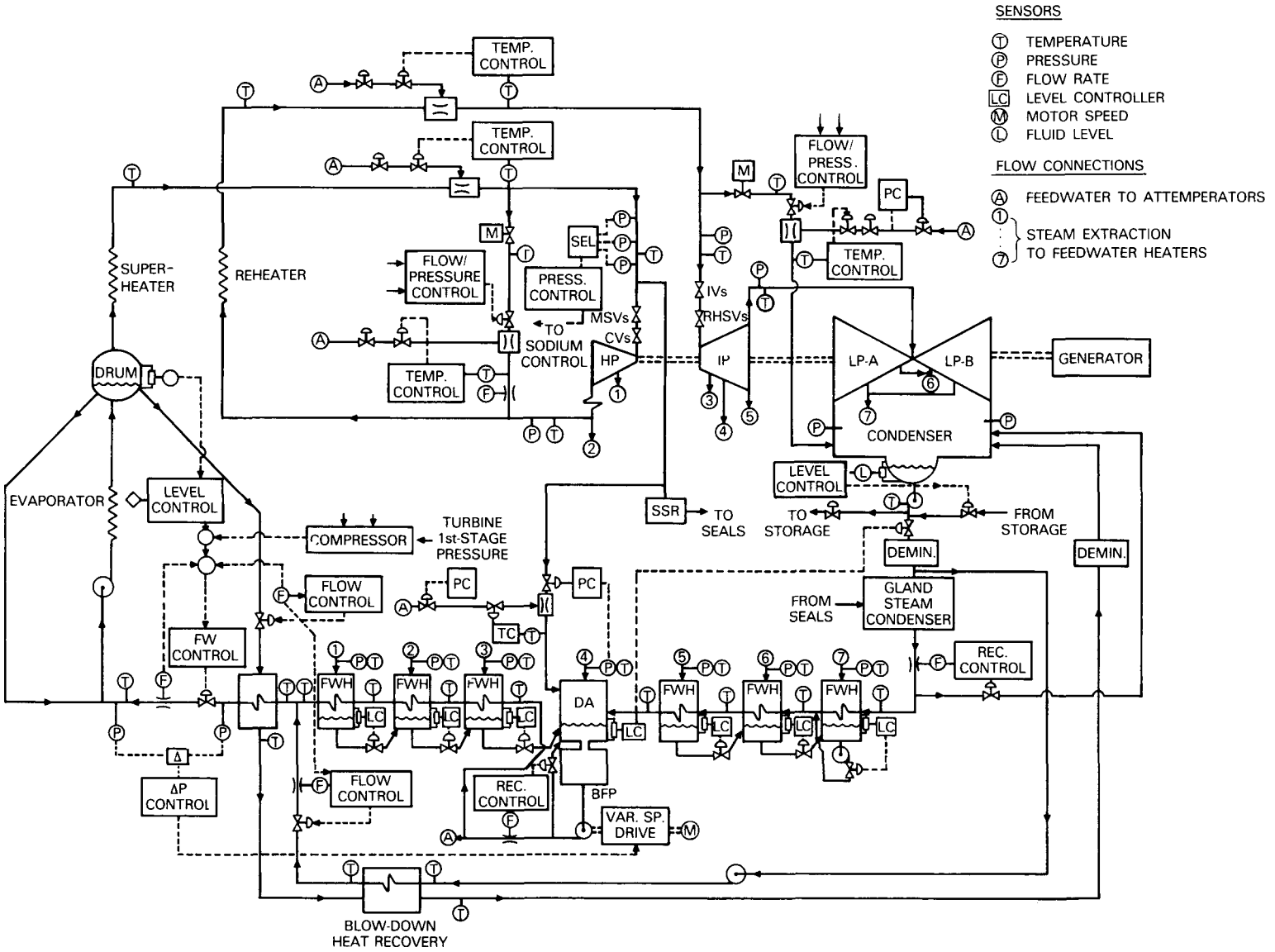

Figure 5.6-6. Electric Power Generation Subsystem

temperatures at the specified values. Transient compensation from the unit demand signal will be used to provide lead during major load changes.

The feedwater control system will be a conventional three element control system using three-mode controllers. It will be arranged with two separate controllers, one for startup (low flow) and one for normal range operation. The transfer to and from one operating condition to the other will be automatic. Associated with the feedwater control, the blow-down flow control and the feedwater differential pressure control are simple control loops.

The turbine control will be a standard electro-hydraulic control (EHC) system which will include automatic startup based on control of turbine rotor stresses. It will be controlled during the startup phase by the plant master control to provide an integrated startup. After the turbine-generator load is above a level which will permit coordinated control from the integrated boiler/turbine control, the EHC will be transferred to that mode.

The condensate and feedwater subsystem controls are all conventional controls. The deaerator level control makes use of two controllers, one for startup and one for normal range operation.

The boiler-turbine-generator (BTG) control board will be a state-of-the-art combination of benchboards and vertical panels arranged in an L or U configuration to facilitate operator access and visability of instrumentation and operating controls. The benchboard sections will contain the general controls (control switches, indicating lights, control and set point stations, etc.). A central section of the benchboard will contain the plant master controls and displays. The vertical panel sections will contain extensive cathode ray tube (CRT) displays as well as adequate conventional instrumentation, miniature recorders (for controlled variables), and annunciators. The intent in the design of the BTG boards will be to make use of techniques proven in operation to avoid major development efforts such as replacement of conventional instrumentation and controls with CRT techniques.

The equipment list for control systems presented below is based on the use of electric analog control elements with pneumatic actuators for the purpose of defining basic functions. However, it should be noted that these functions could also be provided by a distributed digital control system (such as the Honeywell TDC-2000 or equivalent) with a data highway interface to the overall plant master control system (computer). This class of equipment would meet the state-of-the-art criteria mentioned above, providing a conventional operator interface at lower cost and with greater operating flexibility.

All control systems and controller functions will include automatic tracking to provide bumpless transfer to and from the automatic and manual modes. Where specified, the set point stations are to provide for an interface to the plant control computer for overall automatic operation of the plant.

The equipment lists below mention only the specific control valves required for the control functions. Standard practice will be followed and appropriate bypass and isolation valves will be provided as necessary. Subsystem controls for such items as the demineralizer, service water, plant air systems, etc. do not affect the overall plant control strategy and are not covered in the equipment list.

Turbine Controls

A. Basic turbine control (by turbine manufacturer)

Electro-hydraulic control (EHC) or equivalent, to operate either fixed or variable pressure and to include automatic startup based on rotor stress control. To be provided with interface for operation with coordinated boiler control (operation in the turbine follow, boiler follow, or coordinated modes) and with interface for operation with a plant master control system for integrated operation. Main steam pressure limiter to be remotely operated by main steam pressure control in addition to local operation.

B. Steam seal regulator and gland seal condenser (by turbine manufacturer)

C. Lubricating oil temperature control

1. Three-mode controller with three set point levels which can be selected remotely by automatic startup and shutdown control
2. Thermocouple and well in oil from cooler
3. Millivolts/amperes (MV/I) converter
4. Amperes/psi (I/P) converter (to operate valve)
5. Cooling water control valve (pneumatic actuator)

Generator Controls

A. Excitation system (by generator manufacturer)

Static type or equivalent, designed for local and remote operation including suitable interface with a plant control computer for automated startup and shutdown. Includes necessary protective functions such as:

1. Underexcited reactive ampere limit
2. Generator field thermal protection (maximum excitation limit)
3. Generator field ground relay
4. Exciter protective relaying for the specific excitation system
5. Automatic and manual voltage adjusting means compatible with remote operation with circuitry for automatic transfer in case of regulator failure

B. Hydrogen cooling system temperature control

1. Three-mode controller with one set point locally adjusted
2. Thermocouple and well in cold hydrogen path from coolers
3. MV/I converter
4. I/P converter
5. Cooling water control valve (pneumatic actuator)

Steam Supply Related Control Systems

A. Feedwater (drum level) control system (three element control)

1. Steam flow from turbine first-stage pressure compensated for throttle pressure and temperature
   a. Pressure transmitter (first stage pressure): 0-2500 psig
   b. MV/I converter (use main steam thermocouple)
   c. Computational module (XY/Z*)
2. Drum level compensated for drum pressure
   a. Differential pressure transmitter for drum level
   b. Drum pressure transmitter (for compensation)
   c. Two-input summer
   d. Three-input summer
   e. Two-limit units
   f. Computational module (XY/Z)
3. Feedwater flow
   a. Differential pressure transmitter for feedwater flow
   b. Square root extractor
   c. Feedwater flow nozzle
4. Drum level controller (three mode with set point)
5. Two two-input summers
6. Feedwater flow controller (three element)
7. Drum level controller for startup (three element with two set point levels selected remotely by automatic startup and shutdown control)
8. I/P converter
9. Feedwater control valve with pneumatic actuator
10. Four limit units for startup (shutdown) selection of drum level controller and modes
11. Four limit units for high/low alarm and trip

B. Superheater and reheater temperature controls (two single element controls, one for superheater one for reheater)

1. Two thermocouples and wells for steam temperature from de-superheaters (superheater and reheater)
2. Two MV/I converters
3. Two three-mode controllers with set point stations
4. Two I/P converters
5. Two desuperheating water control valves with integral de-superheaters (pneumatic actuators)

*Module multiplies signals X and Y and divides by Z.

6. Two desuperheating water block valves
7. Two limit units to operate motor operated block valves
8. Four limit units for high alarms and trips

C. Main steam pressure control

1. Three main steam pressure transmitters with automatic selection of proper signal to be used for control signal
2. Main stream pressure controller (three mode with local and remotely set set-point station)
3. Automatic pressure ramping controls with local and remote selection of ramping rate
   a. Ramp generator
   b. High and low alarm limit units
   c. Mode and rate selection station
   d. Interface with remote operation pressure
4. Output pressure control signal to interface with steam generator unit controls

D. Drum blow-down flow control

1. Two flow controllers (three mode with local set-point stations)
2. Two flow nozzles for blow-down flow and condensate reinsertion flow
3. Two differential pressure transmitters
4. Two square root extractors
5. Two I/P converters
6. Two flow control valves with pneumatic actuators

E. Feedwater valve differential pressure control

1. Differential pressure controller (three element with local set-point and local programmed set-point)
2. Bias station to balance flows between pumps
3. Two pressure transmitters (0-3000 psig)
4. Two-input summer
5. Two I/P converters
6. Two boiler feed pump speed control actuators (pneumatic)

F. High pressure turbine bypass control

1. Three-mode controller for high pressure bypass flow control (reheater pressure control, operating the high pressure bypass valve) with local and remote set point. The set point will be controlled as a function of the main steam pressure and bypass flow. In the remote mode, it will be controlled by either the master pressure control or the plant control computer.

2. High pressure bypass flow nozzle
3. Differential pressure transmitter (for high pressure bypass flow)
4. Square root extractor
5. High pressure turbine bypass control valve with integral de-superheater (pneumatic actuator)
6. Two thermocouples with wells
7. Two MV/I computers
8. Three-mode controller with local set point station for bypass temperature control
9. I/P converter
10. Attemperator water control valve for temperature control
11. Attemperator water block valve
12. Three dual limit units to operate attemperator water block valve for high alarms and for trips

G. Low pressure turbine bypass control

1. Three-mode controller to operate in cascade with the high pressure bypass control during bypass startup and as a pressure control during bypass shutdown
2. Low pressure turbine bypass control valve with integral de-superheater (pneumatic actuator)
3. Two MV/I converters
4. Three-mode controller with local set point station for bypass temperature control
5. Two I/P converters
6. Attemperator water control valve for temperature control
7. Attemperator water block valve
8. Pressure transmitter
9. Three-mode controller with local set point station
10. Three dual alarm units to operate attemperator water block valve

Condensate and Feedwater Subsystems Controls

A. Hotwell level control

1. Two hotwell level controllers (one for make-up, one for dump) with local set-point stations (three mode)
2. Three hotwell level differential pressure transmitters (two for control, one for instrumentation)
3. Two I/P converters
4. Four hotwell level control valves with pneumatic actuators for split range control

5. Six high level switches for alarm, turbine trip, and dump override
6. Eight low level switches for alarm, pump trip, make-up override, and make-up pump start
7. Absolute backpressure transmitter (0-30 inches of mercury)

B. Vacuum pump automatic start
   1. Two low vacuum switches for automatic start of backup vacuum pump

C. Condensate pump automatic start
   1. Two pump discharge pressure switches for automatic start of backup condensate pump

D. Condensate pump recirculation control
   1. Condensate flow nozzle
   2. Two differential pressure switches
   3. Recirculation flow valve, solenoid actuated

E. Deaerator level control (three-element control)
   1. Deaerator level differential pressure transmitter
   2. Two deaerator level controllers (three mode), one for startup, one for running) with local set-point stations

      Note: Flow signals for condenser and feedwater flow are from condenser pump recirculation control and feedwater control

   3. Deaerator pressure transmitter (0-300 psig)
   4. Computational module (XY/Z)
   5. Three-input summer
   6. Condensate flow controller (three mode)
   7. Automatic transfer switch for startup to running mode
   8. I/P converter
   9. Condensate flow control valve with pneumatic actuator
   10. Solenoid trip valve for condensate flow valve with actuation from emergency hotwell level
   11. Four level switches for deaerator high/low level for alarm, boiler feed pump trip, extraction non-return valves trip, and flow shutoff to deaerator

F. Deaerator pegging steam control
   1. Pegging steam pressure controller (three mode) with local set point station
   2. I/P converter
   3. Pegging steam pressure control valve with integral desuperheater (pneumatic actuator)

4. High/low alarm unit for pegging pressure alarm
5. Pegging steam desuperheating
    a. Spray water pressure transmitter
    b. Spray water pressure controller (two mode)
    c. Two I/P converters
    d. Spray water pressure reducing valve (with pneumatic actuator)
    e. Pegging steam discharge temperature thermocouple and well
    f. Pegging steam temperature controller (two mode)
    g. Pegging steam temperature control valve with pneumatic actuator

G. Boiler feedpump recirculation control
    1. Feedwater flow nozzle
    2. Two differential pressure switches
    3. Recirculation flow valve (solenoid actuated)

H. Feedwater heater level controls (for each of the six closed feedwater heaters)
    1. Level controller (pneumatic)
    2. Level control valve (pneumatic actuator)
    3. Alarm switches

5.6.6 Plant Master Control

The plant master control will be responsible for the overall supervision and coordination of the several subsystem controls in the operation of the plant. It will have as its primary element a stored program process computer of latest design with sufficient capacity and capability to meet the specified requirements.

The master control computer will be interfaced to the several subsystem controllers, operator stations, and plant instrumentation through digital and analog input/output equipment to permit the acquisition of the data required to exercise the specified supervisory and control functions. It will be interfaced to the utility dispatch center via telemetry and/or operator input/output as may be the practice of the operating utility company.

Figure 5.6-7 illustrates the relationship of the plant master control to the other plant controls. Each subsystem will be designed to operate in the absence of the plant master control from operator inputs of the central control room, with the operator(s) providing the supervisory and coordinating functions. Direct communication between subsystem controls will be provided where required to implement this concept.

The plant master control will exercise the requisite logic from the weather and utility load information available to select the appropriate plant operating mode; the six possible modes are illustrated in Figure 5.6-8.

The functions provided by the plant master control will be:

- Utility system interface
  - Predictive generation capability
  - Plant demand/generation control
  - Communication to/from dispatch center
- Automatic plant startup
  - Cold start
  - Warm start
  - Hot start
- Automatic plant operation
  - Selection of plant operating mode (see Figure 5.6-8)
  - Anticipatory control of energy use and generation based upon remote insolation sensing, meteorological data input, etc.
  - Energy storage monitoring and control
  - Direction of subsystem controls
- Automatic plant shutdown
  - For standby (overnight or longer)
  - Load rejection (to house load)

- Plant Supervisory functions
  - Scanning, annunciation, and alarms
  - Protective actions
- Logging and recording
  - Performance calculations
  - Operating records

Equipment for the plant master control function includes:

- Process digital computer comprised of
  - central processor
  - fast access working memory
  - bulk memory
  - analog input/output
  - digital input/output
  - operator input/output
  - video output display
  - peripherals to support software maintenance
- Uninterruptible power supply with automatic transfer and energy storage (battery supply) for three hours of continuous operation

Estimated power requirement for the plant master control is 3 kW.

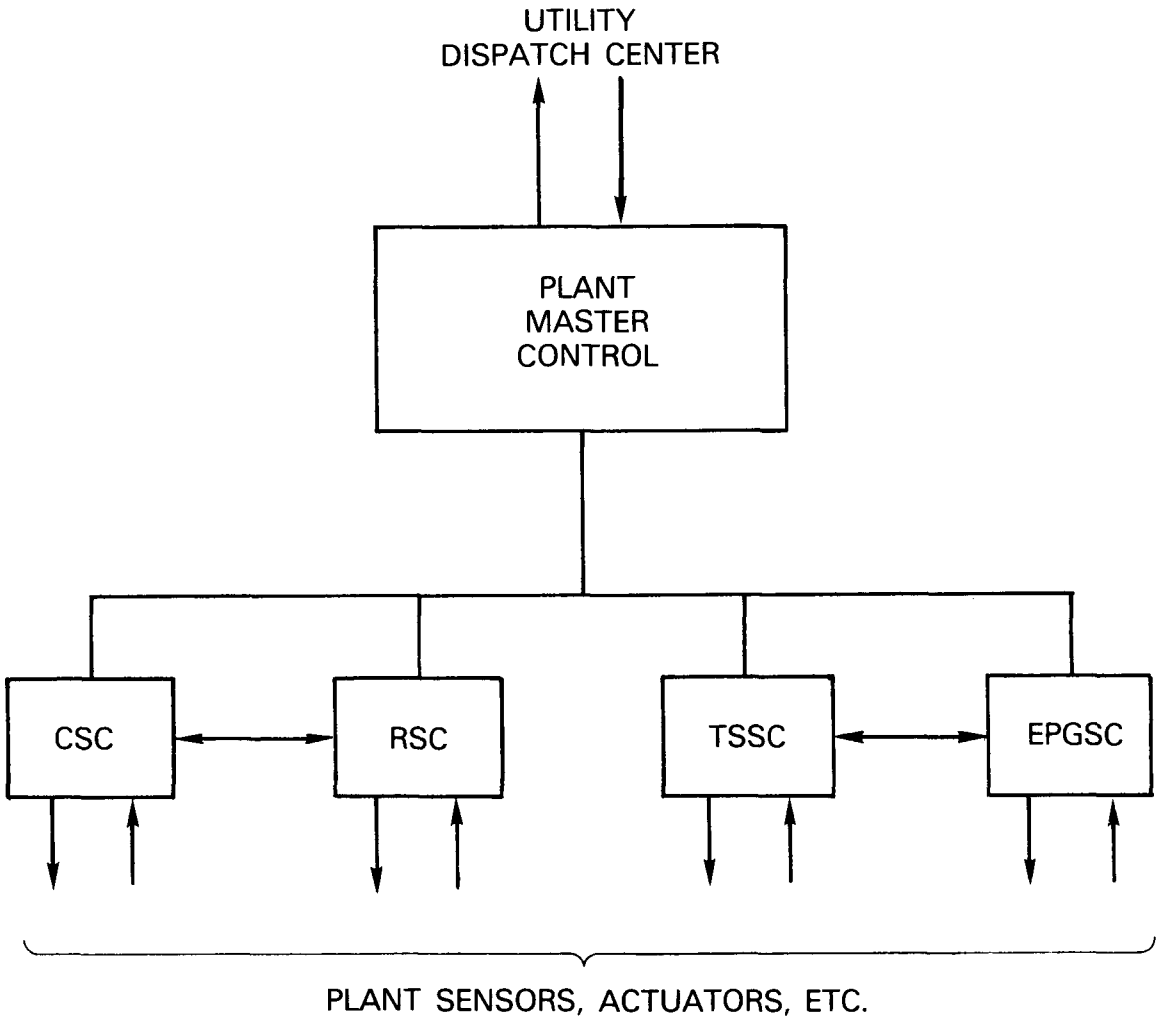

CSC — COLLECTOR SUBSYSTEM CONTROL
RSC — RECEIVER SUBSYSTEM CONTROL
TSSC — THERMAL STORAGE SUBSYSTEM CONTROL
EPGSC — ELECTRIC POWER GENERATION SUBSYSTEM CONTROL

Figure 5.6-7. Relationship of Plant Master Control to Subsystems Controls and Utility Dispatch Center

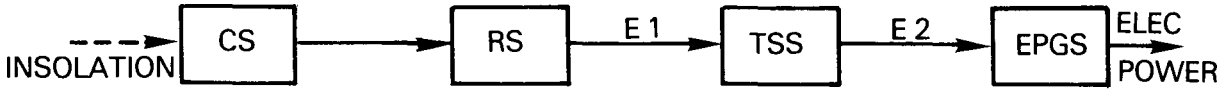

MODE 1 E 1 = E 2 (CONSTANT STORED ENERGY)

MODE 2 E 1 > E 2 (CHARGING ENERGY STORAGE)

MODE 3 E 1 < E 2 (SUPPLEMENTING RECEIVER OUTPUT)

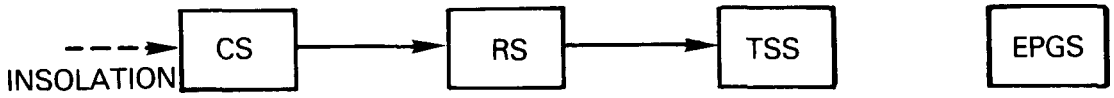

MODE 4: CHARGING ENERGY STORAGE

MODE 5: DISCHARGING ENERGY STORAGE

MODE 6: STANDBY

Figure 5.6-8. Plant Operating Modes

5.7 BALANCE OF PLANT

5.7.1 PLOT PLAN

The plot plan (Figure 5.7-1) was developed to accommodate the following:

- Heliostat field layout and location
- Major equipment installation and maintenance requirements
- Building, structures, and supporting facilities
- Access roads and paved areas
- Utilities

The advanced central receiver power system is assumed to be located near Barstow, California. The plant comprises an approximately elliptical shape heliostat field and supporting facilities located around the receiver tower. Other supporting facilities are located north and south around the perimeter of the heliostat field. The greatest heliostat field dimension is approximately 9000 ft in the west-east direction and approximately 8700 ft in the north-south direction. The area occupied by the receiver tower and the supporting facilities around the tower (exclusion area) is approximately circular in shape and 840 ft in diameter, with the receiver tower in the center of the circle.

The supporting power plant facilities were designed for a maximum daily plant population of 100 employees. The sanitary sewage treatment plant meets the secondary treatment requirements and was designed for 30 years. The water supply system was designed to provide cooling water make-up, domestic water consumption, and a reserve for fire fighting. The cooling water make-up is estimated at 1250 gpm; the fire demand estimate is two hours of fire fighting at 1500 gpm. The domestic water consumption is estimated on an average basis per capita per day at 50 gallons per capita per day (gpcd).

The access road within the internal area as well as the area outside the heliostat field provides sufficient turning radius for maintenance vehicles and delivery trucks. The paved area around the buildings and structures slopes away from the sides of the buildings. The parking facilities were designed with typical 10 foot by 20 foot stalls for approximately 120 parking spaces including maintenance vehicle parking during the day.

The receiver tower, the storage subsystem (hot and cold sodium storage tanks), and the turbine/generator building are the major structures located within the exclusion area. In addition, the maintenance building with adjacent parking for approximately six maintenance vehicles on the left, computer control building, pump house, and inert gas cylinder trailer unit are located in this area. On the opposite or right-hand side of the road entering from the south, there are gates and a security building. The area between the outer and inner access road is proposed to serve for future expansion and equipment storage. Since rail tank cars will be used for the sodium delivery, the railroad spur and its location in relation to the sodium storage tank is important in order to maintain accessible sodium delivery by railroad. Maximum distance from the railroad to one of the cold sodium tanks shall be maintained at 50 feet.

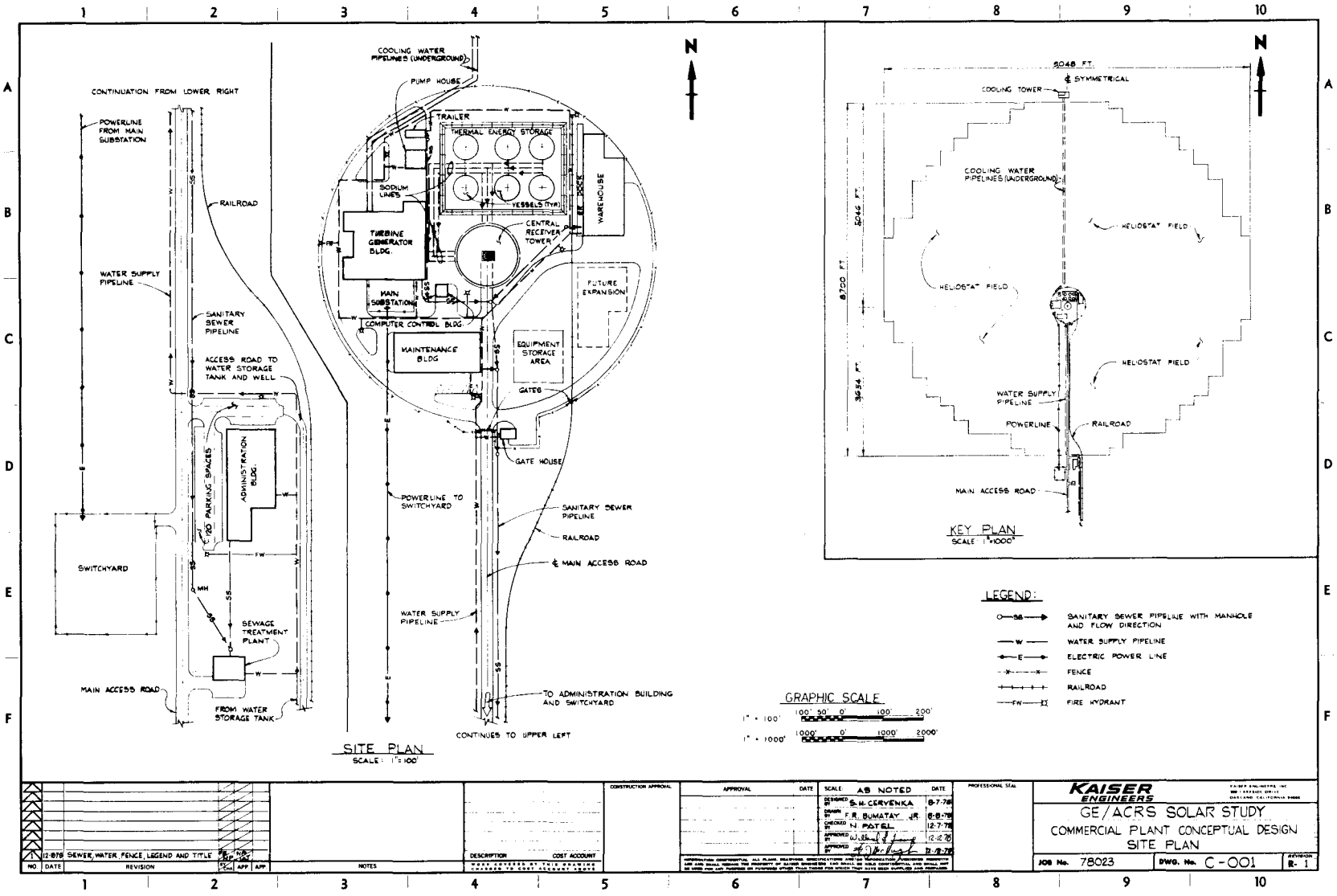

Figure 5.7-1. Plot Plan

Adjacent to the railroad spur is a warehouse. In case the floor area available is found insufficient, there is a possibility of expansion in the southerly direction while maintaining the railroad car capability unloading.

The cooling tower is located approximately 100 feet north from the outer boundary line of the heliostat field. The administration building with the adjacent employee parking, the sewage treatment plant, and the switchyard is located directly south from the main internal supporting area along the main access road approximately 100 feet from the southern boundary of the heliostat field.

The paved area within the exclusion area is sufficient for large truck traffic and minimizes dust pollution. The main access to the central area is from the south and this road also serves as a field access.

The paved area around the turbine/generator building is sufficient to provide vehicle access to the building as indicated, and also required working clearance for possible repair work and/or exchange of the superheater, evaporator, or reheater, which are located along the westerly side of the building.

Water Supply. It is assumed that the power plant water demand will be provided by water from approximately three new wells. Based on information developed by Kaiser Engineers' geologists in conjunction with the Mojava Water Agency, the water quality and quantity varies slightly in the vicinity of the city of Barstow, and groundwater is usually available anywhere at a depth of 60 feet below grade and deeper. The following preliminary water storage estimate is based on the daily consumption rates as previously described above.

a)	Cooling water make-up at 12 hr/day - 1250 gpm	900,000 gal
b)	Fire demand at 2 hr/day - 1500 gpm	180,000 gal
c)	Domestic water consumption 100 people at 50 gpcd	7,500 gal
	Total daily water consumption	1,087,500 gal

Proposed water storage tank capacity is one million gallons.

The water from the wells will be pumped to a water storage tank of one million gallon capacity. Due to the lack of topographical information, Kaiser Engineers is unable to determine more specific location for the water storage tank at present. The water storage tank will be located at highest suitable elevation to provide, if possible, gravity supply to the administration building and also to the internal supporting area around the receiver tower.

Cooling Towers. Based on the direction of the west-to-east prevailing winds at the subject site location, and to eliminate the effect of heliostat shading by the cooling towers, the cooling tower shall be located directly north from the receiver tower. The cooling water line and the cooling water return are 54 inches in diameter each and will be installed underground.

Sanitary Sewer. Based on the estimated population within the plant site and the resulting sanitary waste expected, it is estimated, that an approximately 8 inch sanitary sewer line will be able to carry sanitary waste from the project site, and collect and transport the waste by gravity to the sewage treatment plant located approximately 300 feet south of the administration building. It is expected that the regulatory state environmental agency will require secondary treatment for the sewage treatment plant to meet the effluent criteria. No industrial waste is now expected to be treated at the same location, and mostly domestic waste is expected.

Power Transmission Line. From the main substation, located along the southerly side of the turbine/generator building, the electric power lines run parallel with the main access road and enter the switchyard west from the administration building. At present, we are assuming that an overhead transmission line will be installed from the main substation to the switchyard. Connections from the switchyard to the utility grid are not considered part of the plant and will not be included in the plant cost estimate.

5.7.2 PLANT LAYOUT

Balance of plant equipment is described in the equipment list (Table 5.7-1) and in Figures 5.7-2 and 5.7-3. The steam generators are located in a confined area of the turbine building to isolate the sodium system from the rest of the plant in the event of a leak and subsequent sodium/water reaction. Ease of maintenance and possible replacement of equipment are also considerations in this design. High pressure steam enters the turbine below the operating floor. This will allow sufficient room for turbine rotor removal and lay-down of turbine components during maintenance. The condenser is located below the turbine at the low pressure exhaust. The turbine piping will be compactly tied into the lower half of the turbine. Condenser/heater tube removal can also be accomplished without interference with other equipment. Cooling water (approximately 72,700 gpm at 73°F wet bulb with 10°F approach and range of 13°F) to the condenser will be provided by wet cooling towers. The location of the cooling towers will be outside of the heliostat field on the north perimeter. Preliminary data shows the requirement of four cells 44 feet long by 71 feet wide by 60 feet high, requiring five 200 hp fans (four operating and one spare).

The condensate is heated in six closed feedwater heaters. The location of feedwater heaters No. 1 and No. 2 are in the condenser neck to minimize the larger size piping requirement. Heaters No. 3 to No. 7 are located in one area to facilitate the piping arrangement. Heater No. 4 is an open heater (deaeration tank), where the steam is mixed directly with feedwater. The open heater will liberate some of the noncondensible gases which are vented. The location of the open heater is at a higher elevation than the other heaters in order to meet NPSH requirements for the boiler feed pump. The drain from heater No. 4 is pumped to the remaining closed heaters and finally to the steam drum via a topping heater and the evaporator. Blowdown of the steam drum will be used for heating the feedwater and blowdown return water. The steam exiting from the steam drum passes on to the superheater and reheater.

The turbine lubrication system is isolated in one bay for clean re-use of lubricating oil. Ample space is provided for water treatment, plant air, and boiler. These areas are isolated, yet close enough so piping is not too distant from points of use.

Table 5.7-1

BALANCE-OF-PLANT EQUIPMENT LIST

4100 SITE, STRUCTURES AND MISCELLANEOUS EQUIPMENT

4100 Site

4111 Land

4112 Yard Work

.1 Plant Access Roads and Parking Areas

.2 Field Access Roads

.3 Railroad Spur

.4 Earth Dike (1,060 linear feet)

4120 Buildings

4121 Turbine Generator Building

4122 Administration Building

4123 Warehouse/Maintenance Buildings

.1 Warehouse Building

.2 Maintenance Building

.3 Inert Gas Cylinder Trailer

4124 Computer Control Building

4125 Other

.1 Gate House

.2 Sodium Pump House

4130 Miscellaneous Equipment

4131 Transportation and Lifting Equipment

4132 Communication Equipment

Table 5.7-1 (Cont'd)

4133 Other

.1 Sewage Treatment Plant

.2 Water Supply Wells (3)

.3 Water Storage Tank (Tank- 1 million gal capacity) - one tank

.4 Air Compressor No. 1 (w/diesel unit) 200 SCFM

.5 Air Compressor No. 2

.6 Air Receiver No. 1

.7 Air Receiver No. 2

.8 Plant Air Dryer

.9 Instrument Air Dryer

.10 CO_2 Storage Cylinder (fire protection)

.11 Boiler (building heater) (packaged unit)

.12 Deaerator Tank

.13 Heat Exchanger (heating bldg.)

.14 Blowdown Tank 200 gal

.15 Piping

4200 TURBINE PLANT EQUIPMENT

4210 Turbine Generator and Accessories

.1 Steam Seal System Per heat balance sheet

.2 Turbine Oil Storage Tank (8' dia x 15' long)

.3 Conditioner

.4 Seal Unit

.5 Oil Tank

.6 Generator Auxiliary Equipment

.7 Lube Oil Pump

.8 Generator Lead Cooler

.9 Piping

Table 5.7-1 (Cont'd)

4220	Heat Rejection System		
	.1	Cooling Tower	72,723 GPM 73°F WB 10°F Approach t=13
	.2	Cooling Tower Fans (5 operating, 1 standby)	200 HP each
	.3	Cooling Tower Recirc. Pumps (5 operating, 1 standby)	14,545 GPM 115-ft-TH 600 HP each
	.4	Circulating Water Piping	
4230	Condensing Systems		
	.1	Surface Condenser with Air Removal System	472.7×10^6 BTUH
	.2	Gland Seal Condenser	
	.3	Condensate Polisher	560,500 PPH
4240	Feed Heating or Recuperator System		
	.1	Feed Water Heaters (Nos 1 thru 7)	
4250	Working Fluid Circulation Treatment and Auxiliary Inventory Containment Equipment		
	.1	Topping Heater	17.5×10^6 BTUH
	.2	Blowdown Heat Exchanger	29.8×10^6 BTUH
	.3	Steam and Feedwater Piping	
	.4	Condensate Pump (Operating)	560,500 PPH, 20 PSI, 150 HP
	.5	Condensate Pump (Standby)	As Above
	.6	Feed Water Heater Drain Pump	81,000 PPH, 200 PSI, 25 HP
	.7	HP Feed Water Pump (Operating)	728,800 PPH 3,000 PSI 4,000 HP
	.8	HP Feed Water Pump (Standby)	As Above
	.9	Blowdown Feedwater Pump (operating)	72,900 PPH, 3000 PSI, 400 HP
	.10	Blowdown Feedwater Pump (standby)	As Above

Table 5.7-1 (Cont'd)

4250	Working Fluid Circulation Treatment and Auxiliary Inventory - Continued			
	.11	Conditioner Pump		
	.12	Evaporator Recirculation Pump	200 HP	
	.13	Demineralizer Water Storage Tank	5000 Cal	
	.14	Demineralizer (make-up)	100 GPM	
	.15	Acid Tank	500 GAL	
	.16	Caustic Tank	500 GAL	
	.17	Filter before Demineralizer	100 GAL	
	.18	Filter		
	.19	Demineralizer Water Pump (operating)	Make-up water for main steam cycle plus bldg. blr.	
	.20	Demineralizer Water Pump (standby)	Make-up water for main steam cycle plus bldg. blr.	
	.21	Boiler Feedwater Pump (operating)	Building, Htr. Blr.	
	.22	Boiler Feedwater Pump (standby)	Building Htr. Blr.	
	.23	Steam and Feedwater Piping		
4300	Electric Plant Equipment			
	4310	Switchgear and Transformers		
	.1	Main Power Transformer		
		100/133 MVA 13.8-220 kV, 3Ø, 60 H_z	Each	1
	.2	Power Transformer 15/20 MVA 13.8-4.16 kV, 3Ø, 60 H_z	Each	1
	.3	Power Transformer 15/20 MVA with on- Load Tap Changer 220-4.16 kV, 3Ø, 60 H_z	Each	1
	.4	5- Load Center Type Transformers 1000 kva, 4.16 kV - 480V 3Ø, 60 H_z	Lot	1

Table 5.7-1 (Cont'd)

4300 Electric Plant Equipment - Continued

	Main Tie 7- 1600A Bkrs. Feeders 10- 800A Bkrs.		
.5	Distribution Transformer 45 kva 4.16 kV - 480V 3Ø, 60 H_z Complete with Primary Fusible Disconnect	Each	18
.6	Load Interruptor Switch 13.8 kV 3P, 600 A	Each	1
.7	Distribution transformer and Grounding Resistor for steam Turbine Generator Grounding 50 KVA 8kV - 240V, 1Ø, 60 H_z	Each	1
.8	Isolating Switch 5 kV, 3P, 600A	Each	2
.9	4.16 kV Emergency Switchgear 350 MVA 2000 A, Complete with protective relays	Lot	1
	4.16 kV Main & Tie 3-1200A Bkr. 4.16 kV Feeder 7-1200A Bkr.		
.10	Switch Yard -		
	OCB - 230 kV, 1600 A, 10,000 MVA	Ea	4
	Grounding Grid	Lot	1
	Disconnect Switch 230 kV, 2000A,	Ea	14
	Ring bus - 220 kV, 2000 A	Lot	1
	Towers & Hardwares	Lot	1
	Lightning Arresters	Sets	6
.11	4.16 kV Main Switchgear 350 MVA, 3000A - Complete with protective relays 4.16 kV Main & Tie 3 - 3000A Bkrs. 4.16 kV Feeder 6 - 1200A Bkrs. 4.16 kV Feeder 2 - 2000A Bkrs. Surge Protection 2 - Sets	Lot	1
.12	Two - Load Center Type Transformers 1500 KVA, 4.16 kV - 480V 3Ø, 60 H_z with 480V Switchgear Main & Tie 3-2000A Bkrs Feeder 4- 800 Bkrs		

Table 5.7-1 (Cont'd)

4320	Station Service Equipment		
.1	480 Motor Control Center motor starters for 1/2 to 200 Hp motors	Ea	6
.2	Main Distribution Panel 800A Bus 12 ckt - 3P - 225A Bkr -	Ea	4
.3	Lighting Panel board 100A and 225A Bus 18 and 30-20A Branch Circuits	Lot	1
.4	Lighting System	Lot	1
.5	Emergency Diesel Generator 1500 kw p.f = .8 3p 60 H_z	Ea	1
.6	Communication System	Lot	1
.7	4.16 kV HV starter Line-Ups Complete with protective relays 4.16 kV HV starters with fuse & Magnetic Contactor 4-700A 520 MVA starters Contactor 15-400A 400 MVA starters	Lots	2
4330	Protective Equipment		
.1	Grounding Resistors 400 A, 10 sec. 2400V 300 A, 10 sec. 2400V	 Ea Ea	 2 1
.2	Fire Alarm System	Lot	1
.3	Building Lightning Protection	Lot	1
4340	Power Wiring, Electrical Structures and Wiring Containers		
.1	Wire and Cables, Power, Control Instrumentation	Lot	1
.2	Conduits, Trays, underground duct and manholes, Fittings, hardware and supports	Lot	1

Table 5.7-1 (Cont'd)

4500	Receiver Equipment		
	4510	Receiver Unit	
	4512	Support Structure	
	4513	One EM (sodium) pumps Cooling Blowers (operating)	6000 CFM, 30" H_2O, 50 HP
		One EM (sodium) pumps Cooling Blowers (standby)	6000 CFM, 30" H_2O. 50 HP
	4515	Transportation, Field Erection and Installation	
	4520	Riser, Downcomer and Horizontal Piping	
		.1 Riser	
		.2 Downcomer	
		.3 Horizontal Piping	
	4540	Tower	
		4541 Slip Formed Reinforced Concrete Tower	
	4550	Foundation	
		4551 Ring Foundation	
4600	Thermal Storage Equipment		
	4610	Media Containment	
	4611	Hot Storage Tank 1, 2, 3	62.6 Ft ID Sphere
	4612	Cold Storage Tank 1, 2, 3	61 Ft ID Sphere
	4660	Foundation for Tanks	

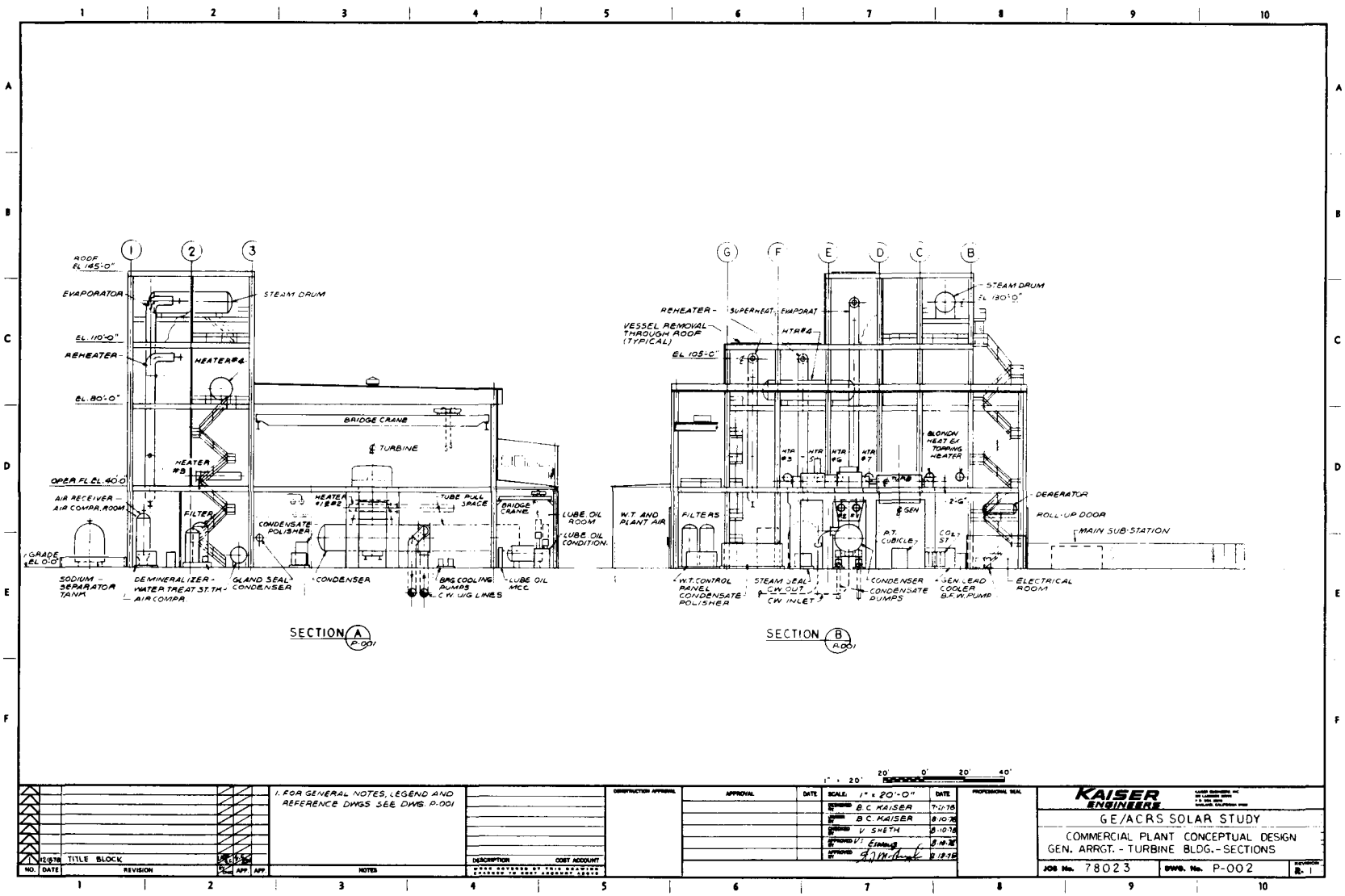

Figure 5.7-2. General Arrangement - Turbine Building Elevation Views

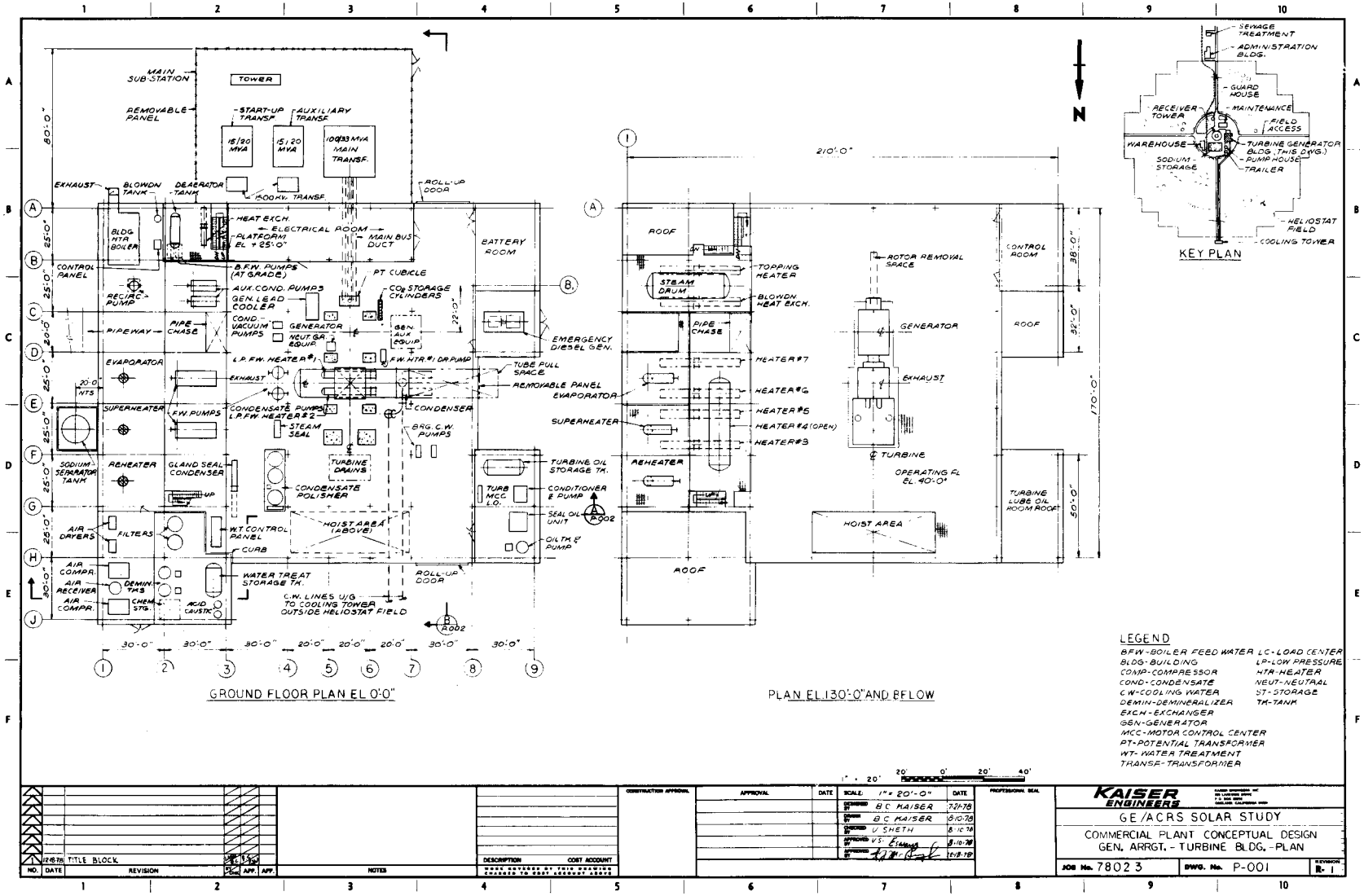

Figure 5.7-3. General Arrangement - Turbine Building Plan Views

The electrical room is conveniently located near the turbine on the main operating floor.

5.7.3 ELECTRICAL ONE LINE DIAGRAM

Figure 5.7-4 shows the electrical one line diagram for the plant. Two 220 kV transmission lines are connected to two 220 kV buses by a "breaker and half" scheme in the main switchyard.

The 4.16 kV switchgear bus is fed via a 220 kV line from the main switchyard and a transformer to bus B. Bus A is fed via a line direct from the generator output segregated phase bus duct through a transformer. Buses A and B are connected by a tie breaker. The 4.16 kV switchgear bus can thus be maintained operational in the event of loss of one of the 220 kV feeds to the bus. Major pumps (greater than 250 horsepower) are connected to 4.16 kV starter buses, bus A and bus B. Loads are distributed between the buses. Small motors and fans are connected to 480 volt switchgear buses A and B which are connected by a tie breaker.

Lighting and a miscellaneous load of 600 kVA is connected to a separate 480 volt switchgear bus. This load comprises lights, air conditioning, and miscellaneous for:

Turbine generator building

Maintenance building

Warehouse

Computer control house

Pump house

Gate house

Sodium storage tank

Tower and yard

Heliostat drives and blowers are supplied from a separate 4.16 kV switchgear bus. A diesel generator supplies the same bus for emergency power which will also supply the 4.16 kV bus. Trace heaters are supplied from a 480 volt switchgear bus which in turn is fed from the 4.16 kV switchgear heliostat bus.

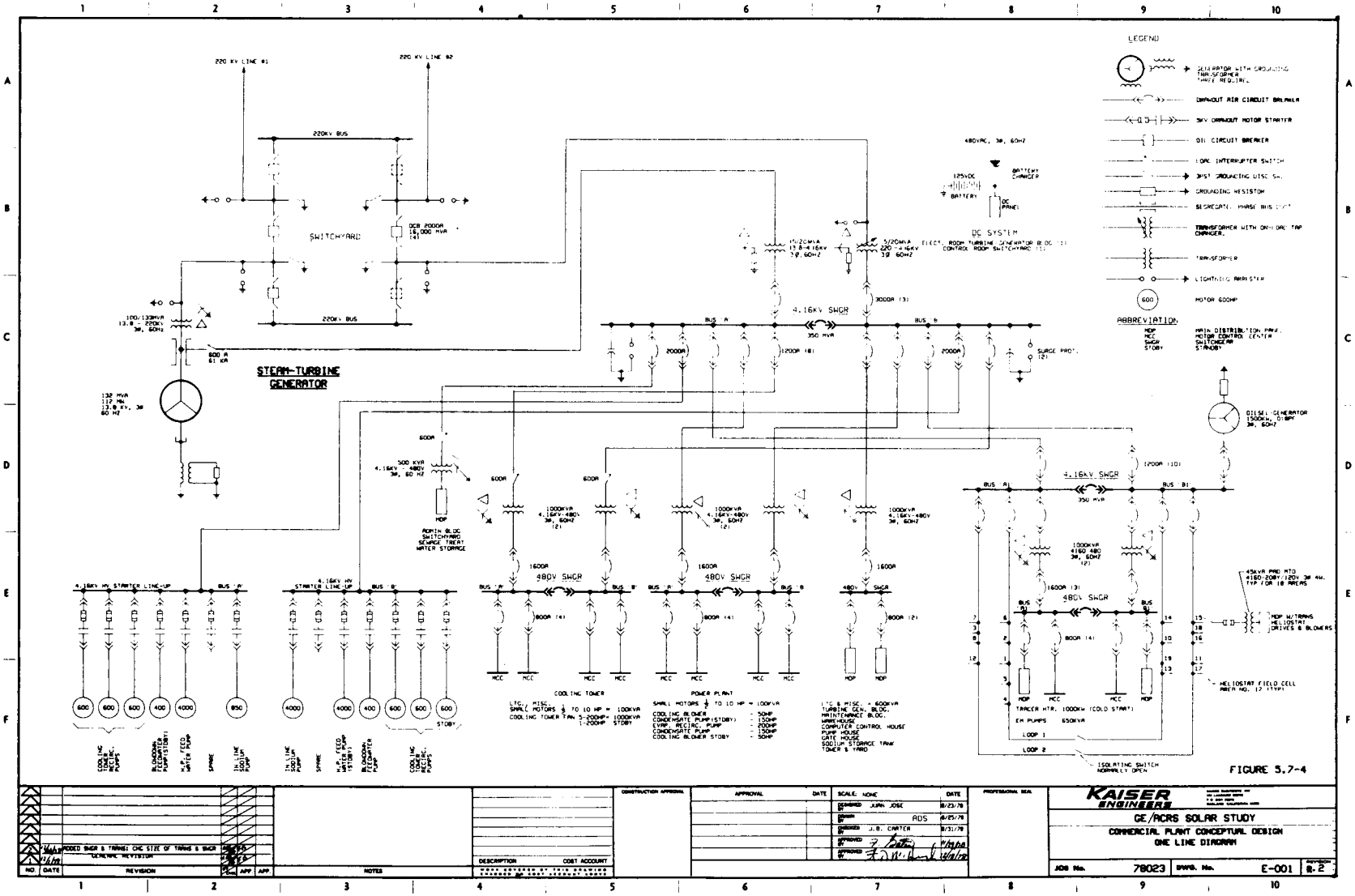

Figure 5.7-4. Electrical One-Line Diagram

5.8 OVERALL PLANT PERFORMANCE

Plant performance has been estimated for the advanced central receiver concept at the design point, during the design point day, and at several other times during the year. These results are summarized below.

Design Point Energy Balance

According to the plant specifications issued by Sandia Laboratories, the design point is that time during the year when the solar angle gives the highest incident power on the receiver. For the surrounding field in the design concept presented here, this time is noon on the summer solstice. The other design point specifications are as follows:

Reference site:		Barstow, California (35° latitude)
Insolation	:	950 watts/m^2
Wind speed	:	3.5 m/sec at 10 m height 5.5 m/sec at 195 m height
Temperature	:	wet bulb 23 °C dry bulb 28 °C

The performance of the General Electric design concept under these conditions is summarized in this section.

Power flows at various points in the plant are shown in Figure 5.8-1, and the corresponding efficiencies are listed in Table 5.8-1.

A detailed listing of the collector/receiver power inputs, outputs, and losses is given in Table 5.8-2. The net power to sodium in the absorber is based on the field performance estimates and absorber loss estimate described in Sections 5.2 and 5.3.2 above. The input from pumps in the tower loop includes all of the power not lost to motor and EM stator cooling. This assumes that all of the pumping input is dissipated in viscous losses between the cold tank outlet and the hot tank inlet. Insulation losses from the tanks and tower piping were derived in Section 5.4.7. Including the tank losses in this way is not strictly correct since these losses should not be charged against the tower flow, but against the total energy stored. However, to summarize all of the losses in one energy balance, the design point is being treated here as a hypothetical steady state in which the storage loss is charged against the tower-base energy, before thermal power is taken off to storage.

Table 5.8-3 completes the energy balance. The power input to the loop from the steam generator pump is a smaller proportion of its electrical input than for the main tower pump because of additional losses in the motor-generator speed control for the steam generator pump. This plant is designed for a solar multiple of 1.5; note that this is measured at the inlets and outlets of the storage tanks.

The EPGS summary is also shown in Table 5.8-3. When auxiliary plant loads are deducted, the net plant output is 98.63 MW_e. A breakdown of the auxiliary loads is given in Table 5.8-4.

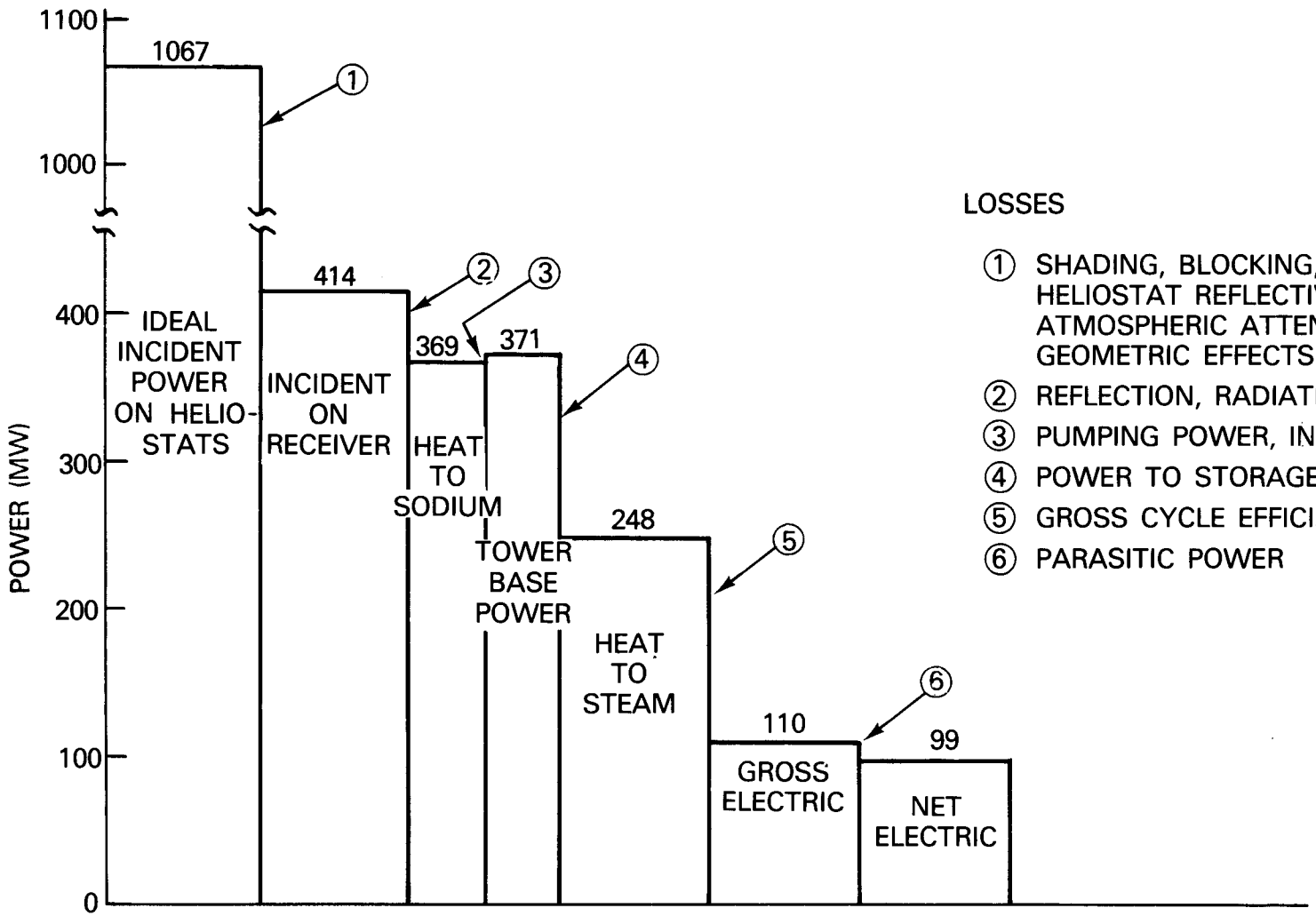

Figure 5.8-1. System Power Flow at Design Point (noon, summer solstice)

Table 5.8-1

OUTPUT SUMMARY
(Design Point)

Power Incident on Receiver:	414.14 MW_t
Power At Tower Base:	371.32 MW_t
Power to Steam:	247.89 MW_t
Net Electric Power:	98.63 MW_t

		Ratio
$\frac{\text{Electricity}}{\text{Steam}}$	$= \frac{98.63}{247.89}$	= 39.8%
$\frac{\text{Electricity}}{\text{Solar Incident-Receiver}}$	$= \frac{98.63}{414.14/1.5}$	= 35.7%
$\frac{\text{Electricity}}{\text{Solar Incident-Helios}}$	$= \frac{98.63}{1066.68/1.5}$	= 13.9%
Solar Multiple	$= \frac{371.32}{247.89}$	= 1.50

Table 5.8-2

PLANT ENERGY BALANCE
(Design Point)

Receiver/Collector Subsystems	MW
Solar Availability (950 W/m^2 x Area)	1066.68
Losses:	
Shading, Blocking, Aiming, Heliostat Reflectivity, Atmospheric Attenuation, Geometric Effects	-652.54
Reflection at Absorber	- 20.71
Radiation	- 19.60
Convection	- 4.83
Net Power to Sodium in Absorber	369.00 MW_t
Power Input From Pumps:	
Main Tower Pump (2.909 MW_e)	+ 2.76
EM Trim Pumps (0.325 MW_e)	+ 0.28
Insulation Losses - Pipes	- 0.28
- Tanks	- 0.44
Net Power Available at Base of Tower*	371.32 MW_t

*Measured at cold tank outlet and hot tank inlet.

Table 5.8-3

PLANT ENERGY BALANCE
(Design Point)

Storage Subsystem	MW
Tower Base Power	371.32
Heat to Storage	-123.78
Gross Heat to Steam Generators	247.54 MW_t
Power Input From Steam Generator Pump (.553 MW_e)	+ 0.44
Piping Heat Loss	- 0.09
Net Heat to Steam Generators	247.89 MW_t
Solar Multiple (371.32/247.89)	1.5
Electric Power Generation Subsystem	
Heat to Steam	247.89
Power Input From Pumps	
Boiler Feed Pumps Main (2.86 MW_e)	+ 2.72
Cleanup (0.29 MW_e)	+ 0.27
Condensate, Recirc. & Feed Htr. Drain (.08,.01,.12MW_e)	+ 0.20
Generator & Mechanical Losses	xx
Reject Heat	xx
Gross Generator Output	110.40 MW_e
Plant Auxilliary Loads	- 11.77 MW_e
Net Plant Output	98.63 MW_e

Table 5.8-4

AUXILIARY LOADS - SUMMARY

Description	Design Point (MW_e)	Hot Hold (MW_e)
Collector Subsystem		
Electronics and Drives	0.40	0
Blowers on Enclosures	0.31	0.31
Receiver Subsystem		
Electromagnetic Pumps (24 units)	0.32	0
EM Pump Cooling Blower	0.03	0
Main Tower Pump	2.91	0
Steam Generator Pump	0.55	
Electric Power Generation Subsystem		
Boiler Feed Pumps - Main	2.86	0
- Blowdown	0.29	0
Condensate Pump	0.08	0
Feed Heater Drain Pump	0.01	0
Evaporator Recirculation Pump	0.12	0
Cooling Tower - Fans (5 units)	0.52	0
- Circulating Water Pumps (5 units)	2.06	0
Hotel Load*	0.76	0.76
Transformer	0.55	0
Total	11.77 MW_e	1.07 MW_e

*Includes lighting, air conditioning, machine shop, and steam turbine auxiliaries using small motors such as lubricating oil pumps and generator cooling blowers.

During a hot hold condition, the collector subsystem requires auxiliary power to keep the heliostat enclosures inflated. In addition, the steam turbine requires lubricating oil, sealing steam, and power to spin the rotor (turning gear). Lighting and other plant facility power requirements also continue during a hold. All other auxiliary equipment can be shutdown as shown in Table 5.8-4.

During a hold, the tower loop will be isolated from storage and a shunt will be opened at the tower base to promote natural circulation of hot sodium through the absorber. The steam generators will be valved off, and the steam generator pump will be shut down. Steam cycle pumps and the cooling towers do not operate during a hold, and the transformer dissipative loss stops as soon as power to the transformer is cut off.

Figure 5.8-2 gives a simplified description of the plant flow circuits, and Table 5.8-5 lists the pressure, temperature, and other thermodynamic variables at various points in the system for the design point condition.

Design Point Day

To study a diurnal cycle, the plant concept was run through a hypothetical day in which the sun moved through the summer solstice path and the solar normal intensity at noon was 950 watt/m^2. Thus at noon the plant performance corresponds exactly to the design point. At other times of the day, the normal insolation and field efficiency were assumed to decrease as shown in Table 5.2-1. This yields the incident power variation listed in Table 5.8-6. To perform a daily energy balance, this incident power function has been divided into roughly one hour segments for numerical integration as shown in Figure 5.8-3.

Incident power Q_{Ii} becomes absorbed power Q_{Ni} as shown in Figure 5.8-4. The receiver efficiency curve is derived from the calculations described in Section 5.3.2, and corresponds to constant ambient temperature and windspeed at the design point values.

In any time period i the heat available at the tower base Q_{Ti} is given by:

$$Q_{Ti} = Q_{Ni} + Q_{TPi} - Q_{TLi} \qquad (5.8\text{-}1)$$

where:

Q_{TPi} = thermal input from tower pumps

$= (2.76 + 0.28)\ (Q_{Ni}/369) \quad MW_t$

Q_{TLi} = insulation loss from piping and receiver

$= 0.28\ MW_t$ (receiver operating)
$= 0.24\ MW_t$ (receiver shut down)

The heat added to (or taken from) storage Q_{si} is given by

$$Q_{si} = Q_{Ti} - \delta i\ (247.54) - Q_{SLi} \qquad (5.8\text{-}2)$$

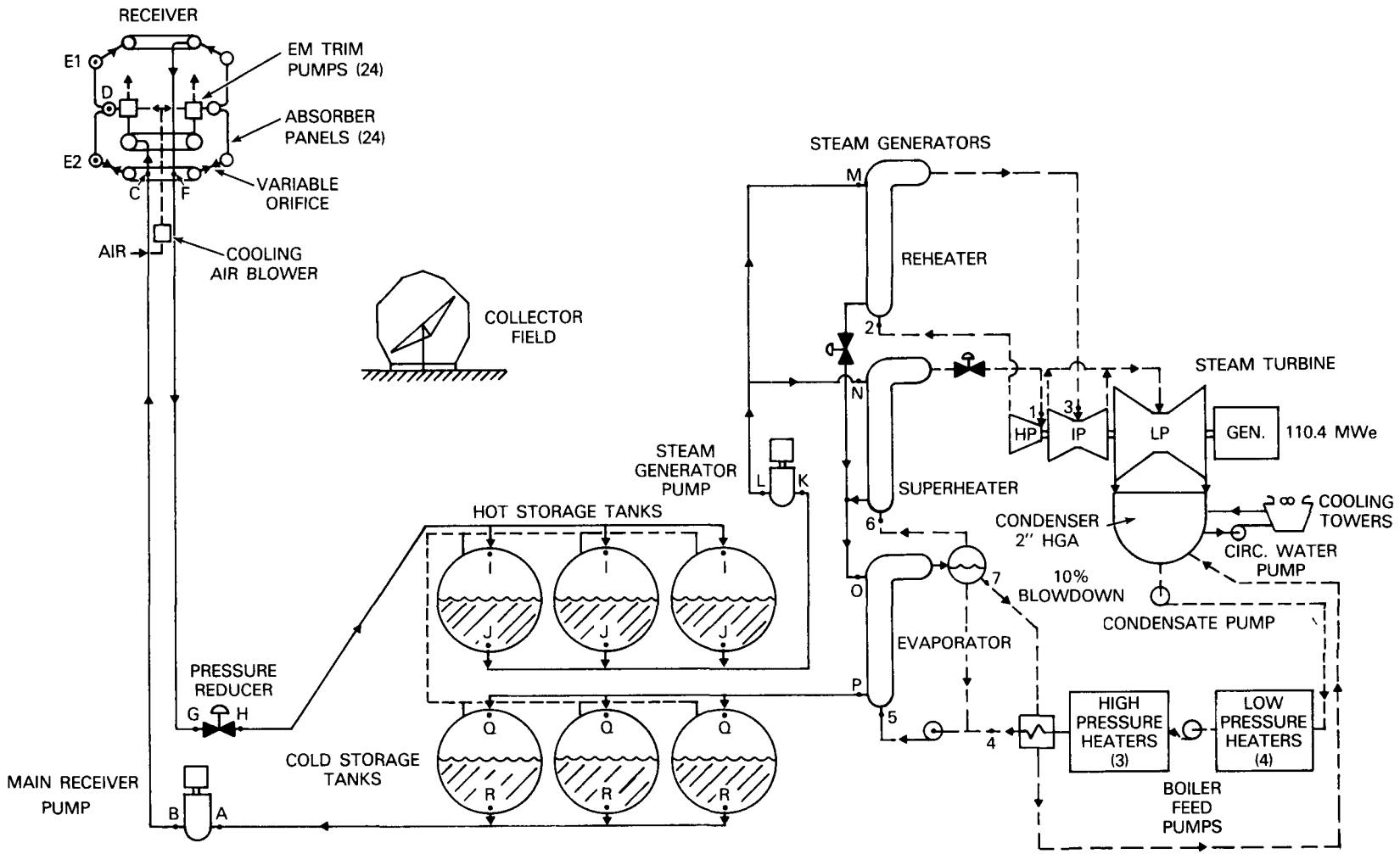

Figure 5.8-2. Guide to Design Point Energy Balance

Table 5.8-5

SYSTEM STATE POINTS

Location	Temperature (°F)	Pressure* (psia)	Flow 10^6 lb/hr	Enthalpy (Btu/lb)	Density (lb/ft^3)
		-Sodium Side-			
A	-	16.2	8.5679	-	54.6
B	-	276.0	8.5679	-	54.6
C	-	29.7	8.5679	-	54.6
D	612.9	31.8	8.5679	339.06	54.6
E1	1097.2	19.8	8.5679	486.05	50.4
E2	1097.2	41.9	8.5679	486.05	50.4
F	-	29.7	8.5679	-	50.4
G	-	225.6	8.5679	-	50.4
H	-	35.4	8.5679	-	50.4
I	1099.2	4.8	8.5679	486.66	50.4
J	1099.2	15.7	5.7120	486.66	50.4
K	-	15.6	5.7120	-	50.4
L	-	73.5	5.7120	-	50.4
M	1100.0	39.3	1.9088	486.89	50.4
N	1100.0	37.6	3.8032	486.89	50.4
O	859.1	10.3	5.7120	414.37	52.5
P	612.0	26.9	5.7120	338.77	54.6
Q	611.9	4.8	5.7120	338.75	54.6
R	611.9	16.4	5.7120	338.75	54.6
		-Steam Side-			
1	1000.0	2415	0.7288	1460.40	-
2	572.5	417	0.5911	1289.60	-
3	1000.0	380	0.5911	1523.80	-
4	521.1	2620	0.8017	512.80	-
5	528.9	2716	0.8381	522.87	47.9
6	673.9	2580	0.7288	1080.00	-
7	673.9	2600	0.0729	744.5	-

*Includes gravity, viscous, and velocity head effects

Table 5.8-6

INSOLATION AND COLLECTOR MODELS-
DESIGN POINT DAY

Hours From Solar Noon	Receiver Incident Power (MW_t)
0	414
1.05	407
2.09	390
3.14	365
4.18	324
5.23	253
6.28*	145

*10° sun elevation

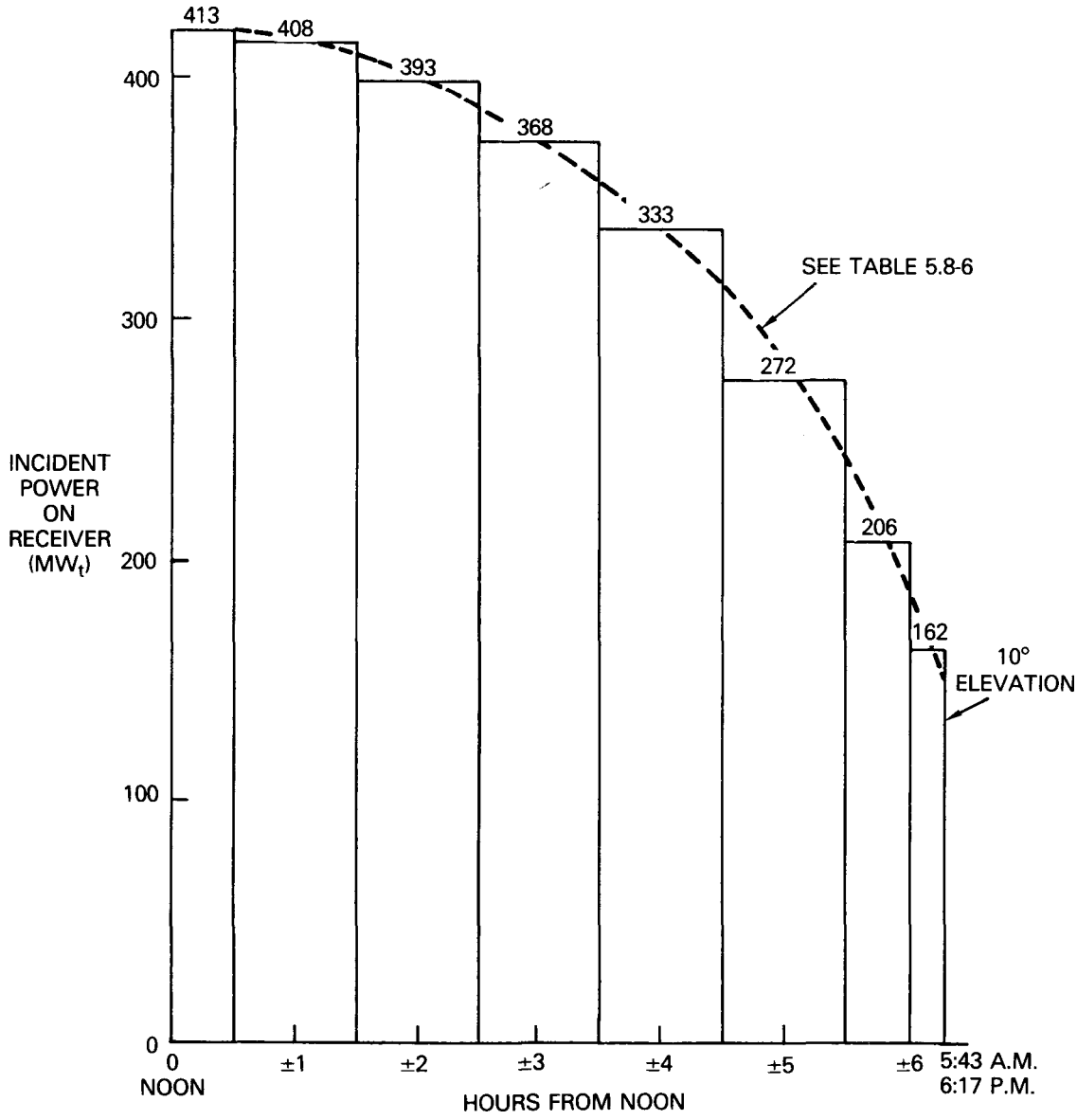

Figure 5.8-3. Design Point Day - Insolation and Collector Models

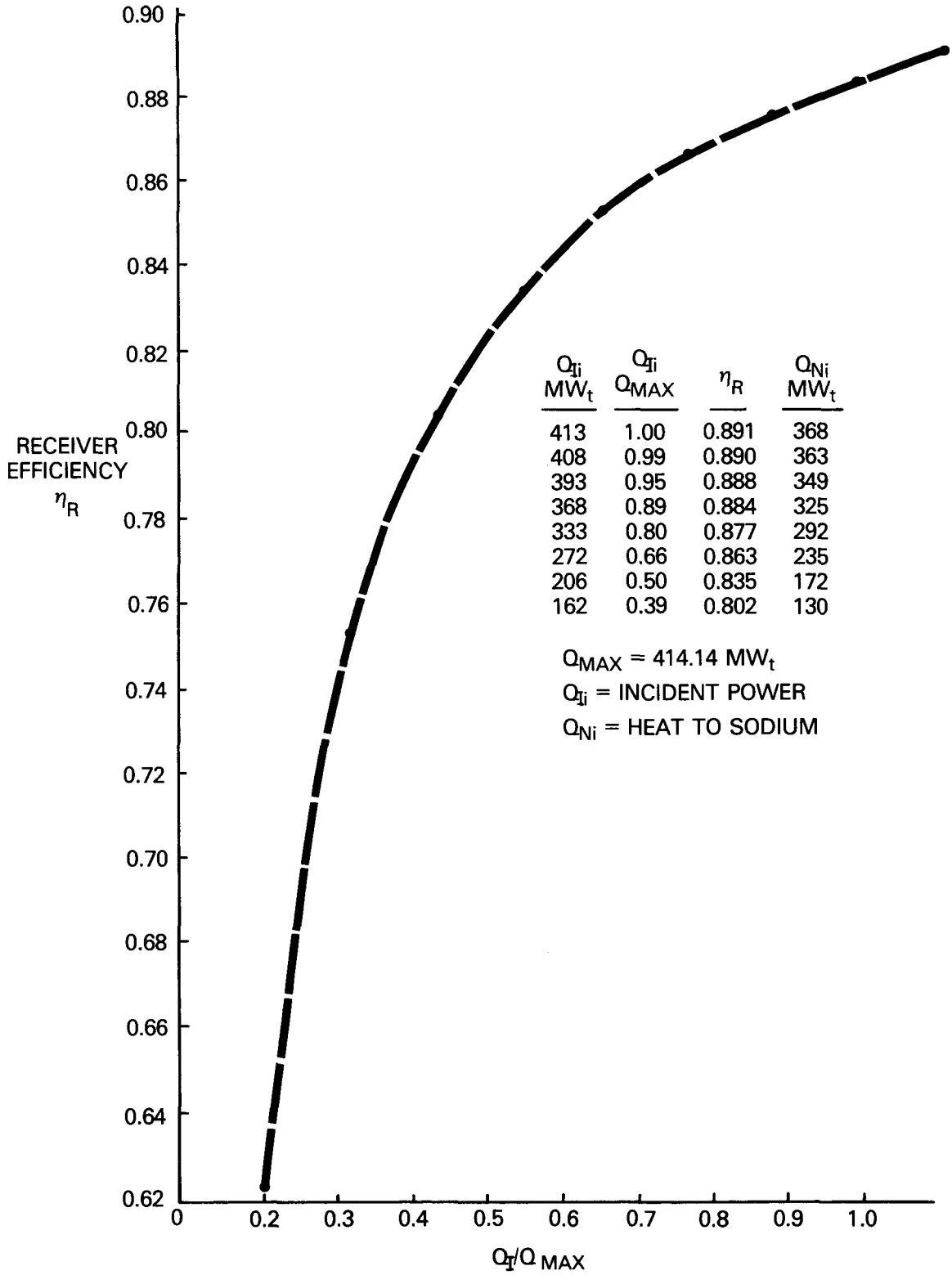

Figure 5.8-4. Design Point Day - Receiver Model

where: δ_i = 1 (turbine operating)
0 (turbine shutdown)

Q_{SLi} = insulation losses from steam generator piping and storage tanks

= 0.53 MW_t

The net electrical output P_{Ei} is given by

$$P_{Ei} = (110.4)\ \delta_i - A_{ci} - A_{Ri} - A_{Ei} \qquad (5.8\text{-}3)$$

where A_{ci} = collector field auxiliary load
= 0.71 MW_e (tracking)
0.31 MW_e (stowed)

A_{Ri} = receiver auxiliary load
= (0.03 + 0.32 + 2.91) $(Q_{Ni}/369)$ + 0.55 δ_i (MW_e)

A_{Ei} = EPGS auxiliary load
= (2.86 + 0.29 + 0.08 + 0.01 + 0.12 + 0.52 + 2.06 + .55) δ_i + 0.76 (MW_e)

The auxiliary load relations are derived from Table 5.8-4.

These models were exercised to simulate plant operation during the day. The operating strategy is shown in Figure 5.8-5. The steam turbine was warmed up and brought to full load just prior to the collector field start (sun elevation = 10°) so that the field and turbine both start together. As shown in Figure 5.8-6, enough energy was left in storage from the previous day to permit full turbine output during the early morning hours.

Storage is drawn down to zero at 6:30 A.M. and then fills up again as excess solar power becomes available. At about 3:00 P.M., the storage tanks would reach their maximum fill levels with a 3-hour design and thermal power would have to be dumped in the collector field. The amount of lost energy is indicated by the cross hatched area in Figure 5.8-6. If this energy could be stored, the day would proceed as shown, with the turbine shutting down at 9:22 P.M. with enough energy left in storage to supply the insulation losses and startup energy for the next morning.

Figure 5.8-7 describes the electrical output profile during this day. The lowest output is at noon when the auxiliary loads are greatest; the highest output is when the EPGS operates out of storage. At night the electrical output is negative, indicating the need to import power to maintain turbine and field auxiliaries.

Table 5.8-7 summarizes the energy balance for this day. The steam turbine ran for 15.65 hours and delivered 1554 $MW_e h$ of electric energy to the utility grid. The average conversion efficiency from sunlight incident on the receiver to electricity was 36.5 percent.

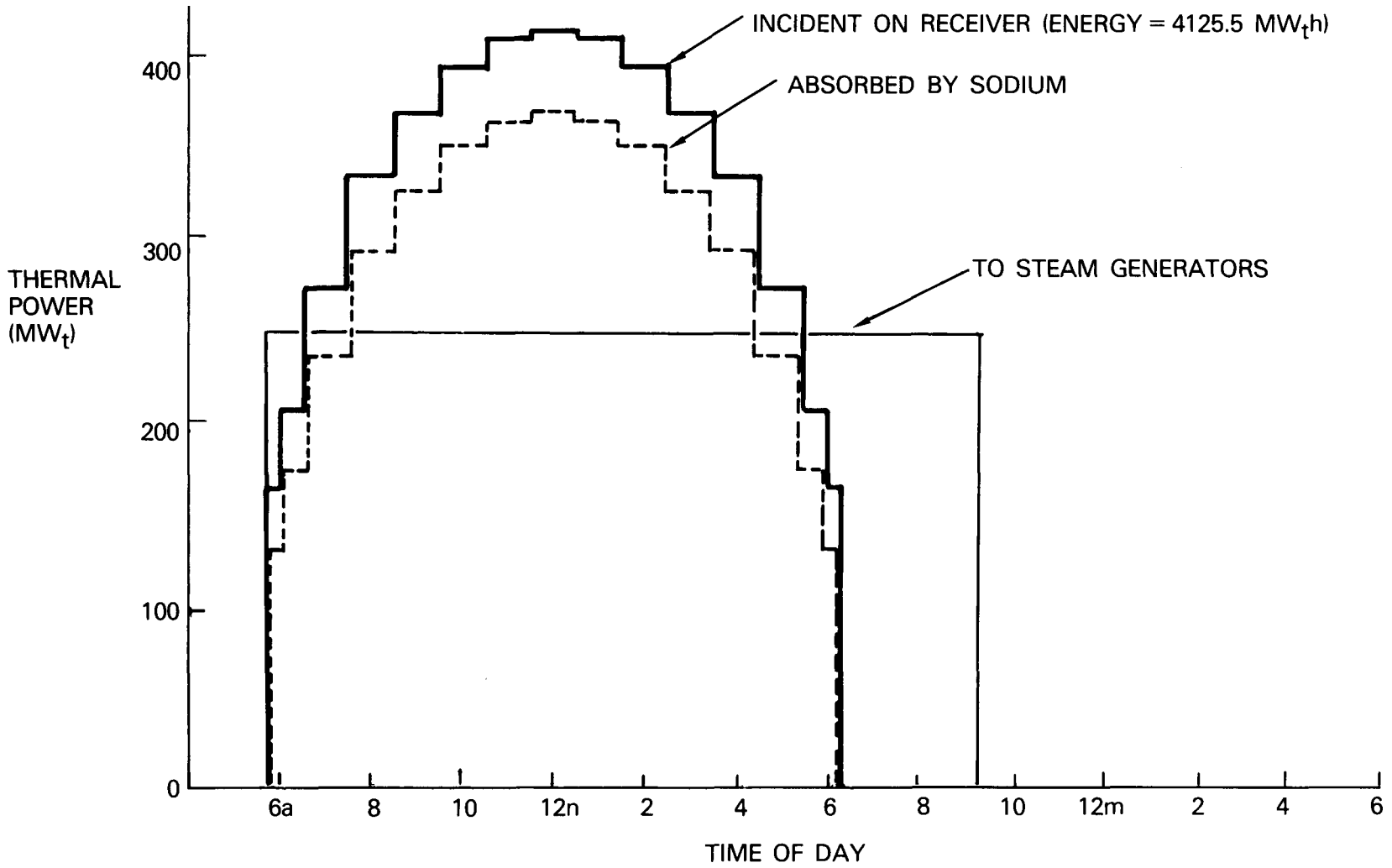

Figure 5.8-5. System Thermal Power Variation During Design Point Day

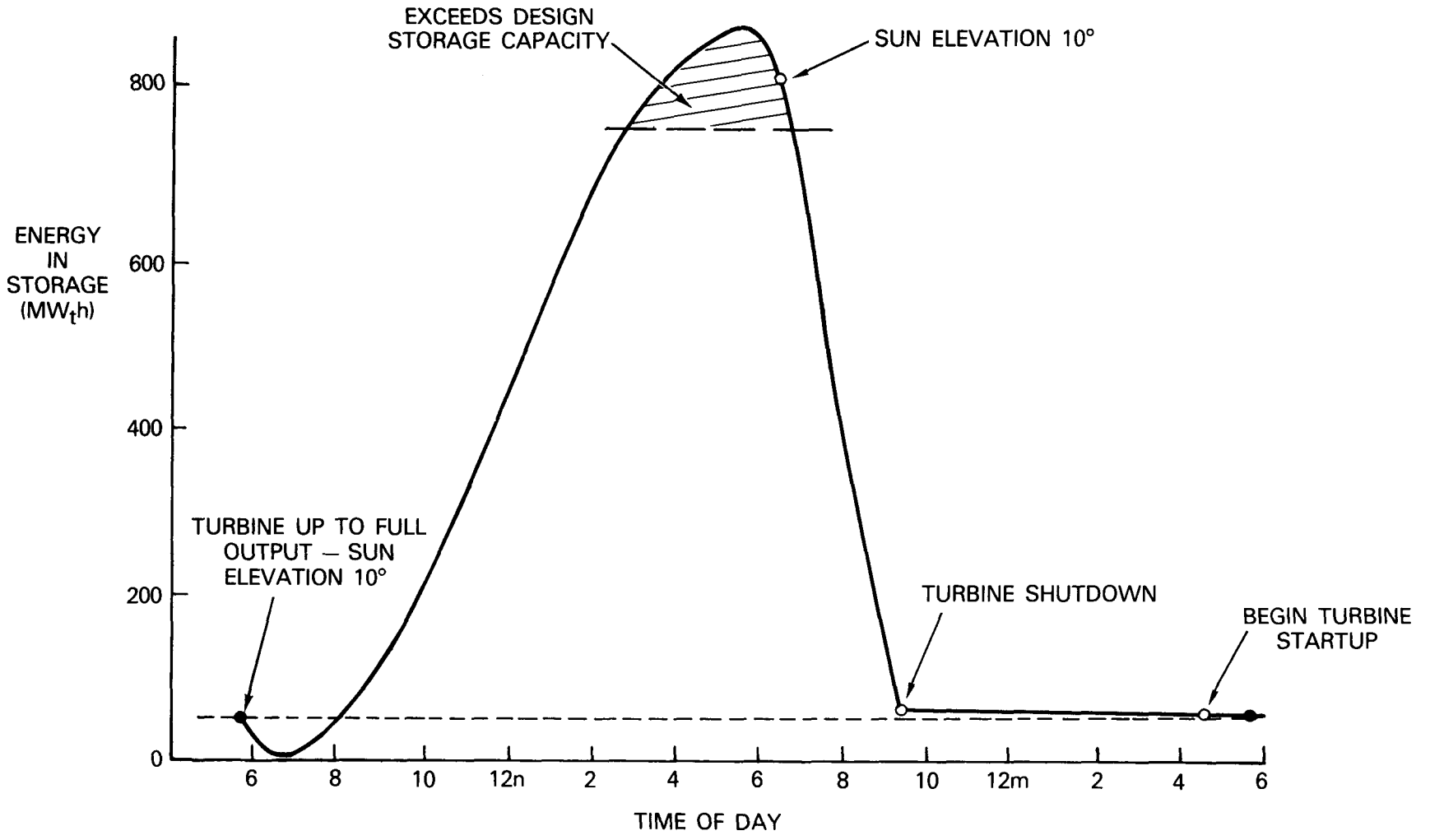

Figure 5.8-6. Storage Energy Balance - Design Point Day

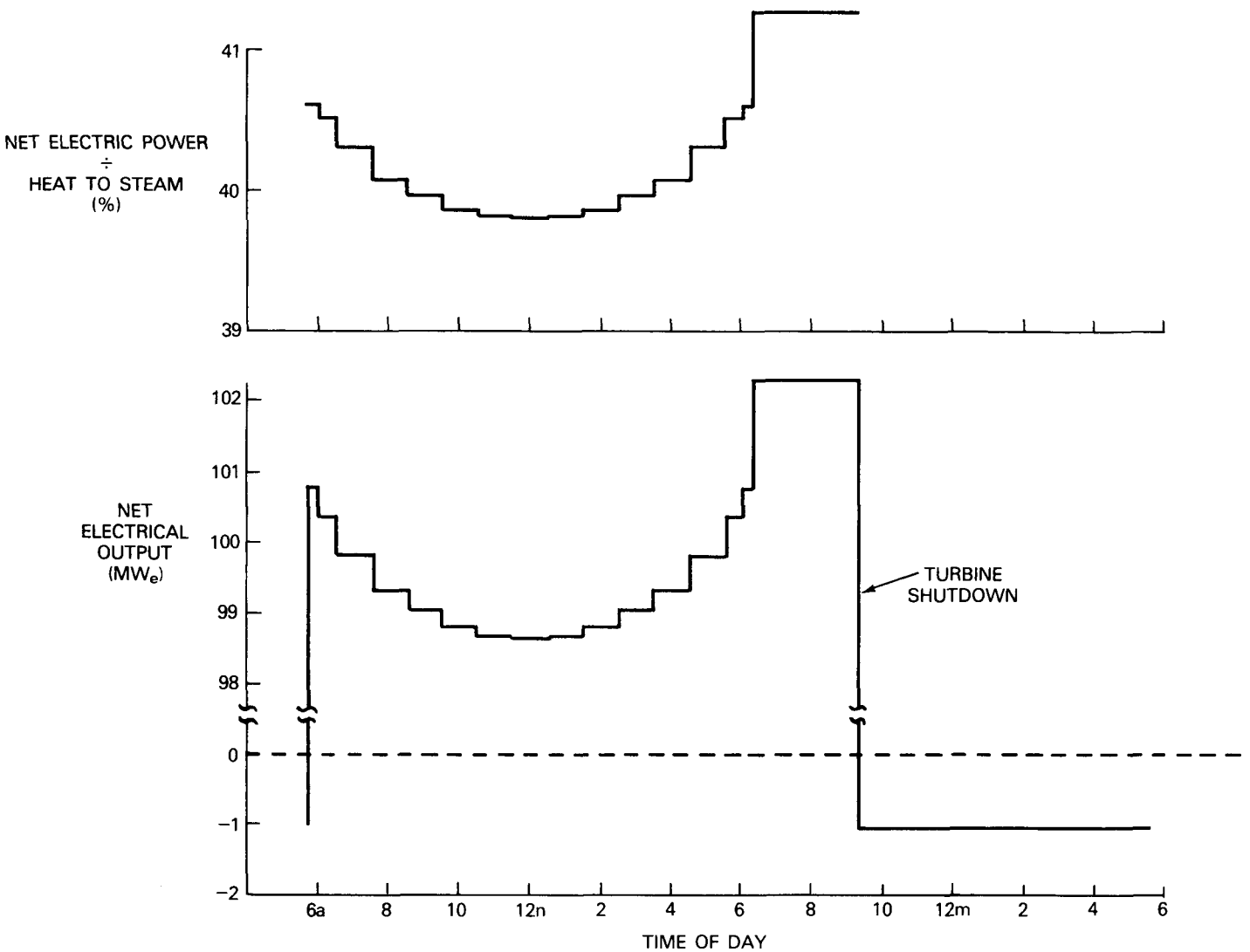

Figure 5.8-7. System Electric Power Variation During Design Point Day

Table 5.8-7

DESIGN POINT DAY
(Output Summary)

Energy Incident on Receiver	:	4258 $MW_t h$
Energy to Storage*	:	823 $MW_t h$
Energy to Steam	:	3880 $MW_t h$
Net Electric Energy	:	1554 $MW_e h$

$$\frac{\text{Electricity}}{\text{Steam}} = \frac{1554}{3880} = 40.1\%$$

$$\frac{\text{Electricity}}{\text{Solar Incident}} \quad \frac{1554}{4258} = 36.5\%$$

$$\frac{\text{Stored Energy}}{\text{Solar Incident}} = \frac{823}{4258} = 19.3\%$$

*Exceeds design storage capacity of 766 $MW_t h$.

Annual Variation of Plant Performance

Collector subsystem performance has been estimated for seven days during the year. These results are detailed in Section 5.2, and a summary is plotted here in Figure 5.8-8. The sun model used corresponds to average observations at 35° latitude, and does not agree exactly with the design point conditions due to the higher insolation level at summer solstice noon (day 92, 1003.24 vs. 950 watts/square meter).

Figure 5.8-8 also shows the daily integral of receiver incident power as well as the annual energy incident on the receiver.

Two things are immediately evident from this figure. First, the peak incident power is greater than the design value of 414 MW_t over as much as half the year. Accepting the additional energy is not a problem for the absorber panels, but would require slightly larger EM pumps on the panels and a larger tower base pump.

Secondly, the daily energy numbers indicate that storage capacities larger than three hours may be appropriate. For instance, if the proportion of stored energy to incident energy were the same as for the design point day (19.3 percent), then the design storage capacity of 766 MW_th would be exceeded from day 92 through day 152. The storage capacity would have to be increased by about 20 percent to accommodate the receiver output on summer solstice.

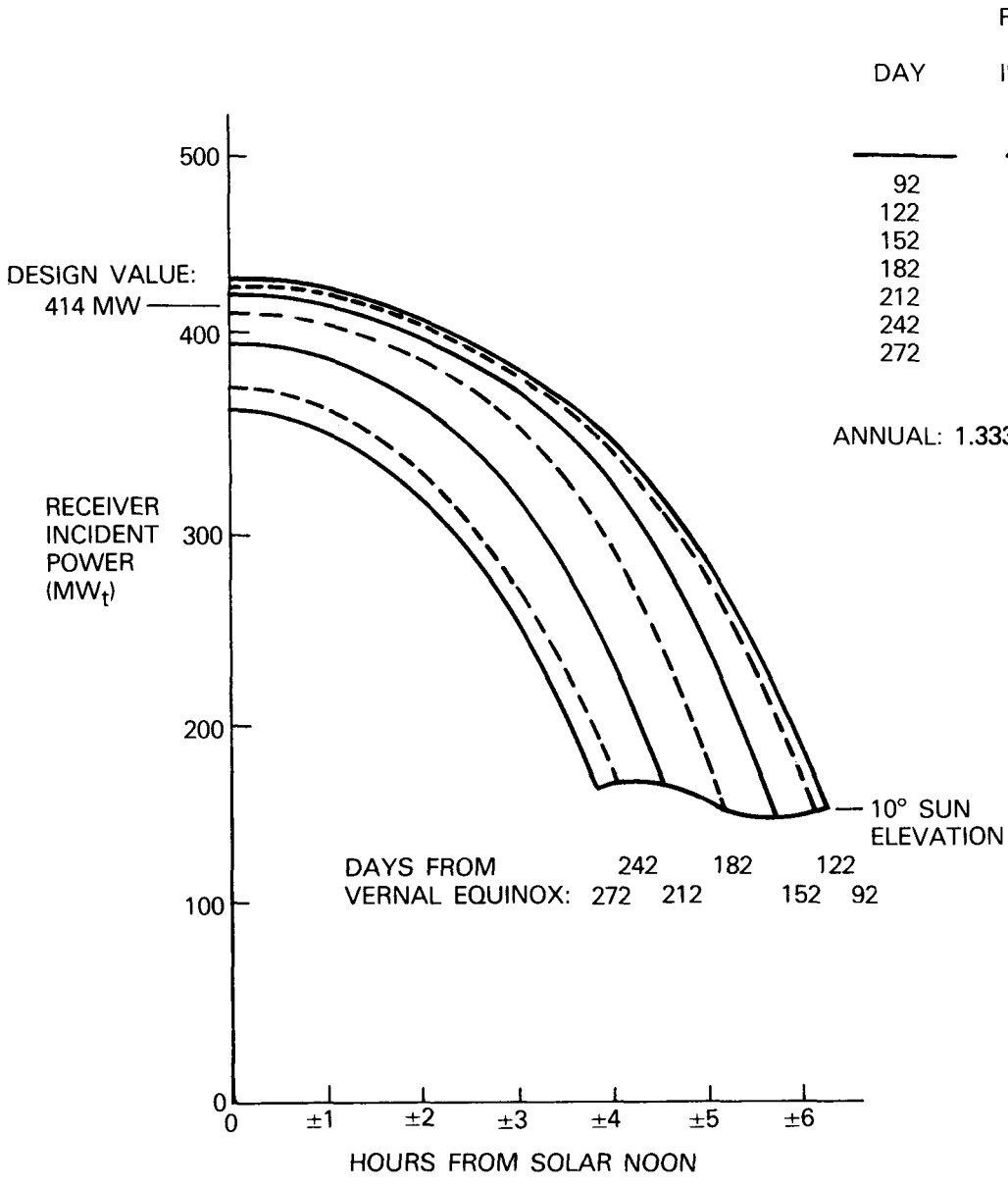

Figure 5.8-8. Annual Variation of Receiver Incident Power and Energy

☆ U.S. GOVERNMENT PRINTING OFFICE: 1980-640-258/2146